OAK RIDGE NATIONAL LABORATORY LIBRARY
3 4456 0017266 7

ORNL-2993
UC-10 - Chemistry-Separation Processes
for Plutonium and Uranium

CHEMICAL TECHNOLOGY DIVISION

ANNUAL PROGRESS REPORT

FOR PERIOD ENDING AUGUST 31, 1960

OAK RIDGE NATIONAL LABORATORY
CENTRAL RESEARCH LIBRARY
CIRCULATION SECTION
4500N ROOM 175
LIBRARY LOAN COPY
DO NOT TRANSFER TO ANOTHER PERSON
If you wish someone else to see this report, send in name with report and the library will arrange a loan.

OAK RIDGE NATIONAL LABORATORY
operated by
UNION CARBIDE CORPORATION
for the
U.S. ATOMIC ENERGY COMMISSION

Printed in USA. Price $3.50. Available from the
Office of Technical Services
Department of Commerce
Washington 25, D. C.

LEGAL NOTICE

This report was prepared as an account of Government sponsored work. Neither the United States, nor the Commission, nor any person acting on behalf of the Commission:

A. Makes any warranty or representation, expressed or implied, with respect to the accuracy, completeness, or usefulness of the information contained in this report, or that the use of any information, apparatus, method, or process disclosed in this report may not infringe privately owned rights; or

B. Assumes any liabilities with respect to the use of, or for damages resulting from the use of any information, apparatus, method, or process disclosed in this report.

As used in the above, "person acting on behalf of the Commission" includes any employee or contractor of the Commission, or employee of such contractor, to the extent that such employee or contractor of the Commission, or employee of such contractor prepares, disseminates, or provides access to, any information pursuant to his employment or contract with the Commission, or his employment with such contractor.

ORNL-2993
UC-10 – Chemistry-Separation Processes
for Plutonium and Uranium
TID-4500 (15th ed.)

Contract No. W-7405-eng-26

CHEMICAL TECHNOLOGY DIVISION

ANNUAL PROGRESS REPORT

for Period Ending August 31, 1960

F. L. Culler – Division Director
D. E. Ferguson – Chemical Development Section A Chief
R. E. Blanco – Chemical Development Section B Chief
K. B. Brown – Chemical Development Section C Chief
M. E. Whatley – Unit Operations Section Chief
H. E. Goeller – Process Design Section Chief
J. C. Bresee – Pilot Plant Section Chief

DATE ISSUED
SEP 26 1960

OAK RIDGE NATIONAL LABORATORY LIBRARY
3 4456 0017266 7

OAK RIDGE NATIONAL LABORATORY
Oak Ridge, Tennessee
operated by
UNION CARBIDE CORPORATION
for the
U.S. ATOMIC ENERGY COMMISSION

SUMMARY

1. HEAD-END AND SOLVENT EXTRACTION PROCESSING

Development of the Sulfex and Darex processes for decladding Consolidated Edison fuel (stainless-steel-clad ThO_2-UO_2 pellets) was continued. Laboratory studies showed that the 20-mil-thick stainless steel cladding dissolved in the Darex reagent, boiling 5 M HNO_3–2 M HCl, in 1 hr; the off-gas was a mixture of nitrogen oxides and NOCl containing less than 0.5 vol % hydrogen. In titanium, the container material for the Darex process, passivation of stainless steel was occasionally encountered. Passivation was readily overcome by increasing the HCl concentration in the reagent to 6 M; in this case the hydrogen content in the off-gas increased to about 2 vol %, which is still below the explosive limit. Soluble uranium and thorium losses in decladding of irradiated prototype fuel, in which the density of the 95% ThO_2–UO_2 pellets was only 80 to 85% of theoretical, were independent of irradiation level up to 575 Mwd/ton. Uranium and thorium losses from intact and partly fragmented pellets were generally 0.05 to 0.5% and 0.03 to 0.9%, respectively; losses from highly fragmented pellets were as high as 9 and 10%.

In the Sulfex decladding process for Consolidated Edison fuel, the stainless steel cladding dissolved in 1 to 3 hr in 200% excess of boiling 4 to 6 M H_2SO_4; the off-gas is hydrogen. Passivation is more serious than in the Darex process, since as little as 0.001 M HNO_3 in the sulfuric acid produced passivation for more than 1 hr; however, traces of nitric acid can be removed by reaction with formic acid. Uranium and thorium losses were slightly lower than in the Darex process. From unfragmented prototype fuel (pellets 80 to 85% of theoretical density, irradiated from 0 to 445 Mwd/ton) uranium and thorium losses varied randomly from 0.07 to 0.44% and 0.04 to 0.33%, respectively. When the fuel pellets shattered, losses were as high as 1.8%.

Consolidated Edison ThO_2-UO_2 fuel pellets can be dissolved in either boiling Thorex dissolvent [13 M HNO_3–0.04 M NaF–0 to 0.1 M $Al(NO_3)_3$] or Darex decladding solution that has been stripped free of chloride and adjusted to 0.04 M NaF, 0 to 0.1 M Al, and 12 to 13 M H^+. The chief variable

in ThO_2-UO_2 dissolution in Thorex dissolvent was pellet density: the initial dissolving rate in 200% excess dissolvent varied from 16 mg min^{-1} cm^{-2} for pellets whose density was 60% of theoretical to 2 mg min^{-1} cm^{-2} for material whose density was 94% of theoretical. For reactor-grade pellets, total dissolution would require 30 to 50 hr. The optimum fluoride concentration is 0.07 M; however, 0.04 M is used in the flowsheet to minimize equipment corrosion. The dissolver solution formerly required evaporation until the temperature reached 155°C to obtain an acid-deficient solvent extraction feed; under this condition corrosion is severe and operations are difficult. To circumvent this problem, the solution is evaporated until its temperature reaches only 135°C, and the residual acid is removed by steam stripping. The use of adjusted decladding solution as core dissolvent eliminates uranium and thorium losses but produces a high-activity-level solvent extraction waste that is not easily volume reduced.

Cyclic Sulfex-Thorex and Darex-Thorex dissolvings, in which a 10 to 20% oxide heel was carried over into subsequent cycles, were found practical with an 8- to 10-hr core dissolution time. Thorium and uranium losses were less than 0.25% in all runs. Heel buildup was more pronounced in Sulfex operation, where a 20% heel remained after four runs, compared with a 10% heel after four Darex cycles.

The Darex process for complete dissolution of UO_2–stainless steel fuels was demonstrated in hot-cell experiments with Yankee Atomic fuel irradiated to 16,000 Mwd/ton; all operations were completely satisfactory. Fuels bonded with sodium or NaK cannot be processed by the Darex process; violent vapor-phase reactions occur between the nitrogen oxides and hydrogen.

The Zirflex process for decladding PWR blanket elements (UO_2 pellets clad in Zircaloy-2) was demonstrated with fuel irradiated up to 1750 Mwd/ton. Uranium and plutonium losses to the 6 M NH_4F–1 M NH_4NO_3 decladding solution increased with increasing burnup. However, losses at maximum burnup were only 0.04 and 0.08%, respectively. Ammonia generated by the decladding reaction must be removed from the system to avoid formation of a $ZrO_2 \cdot H_2O$ sludge.

Uranium-zirconium alloy fuels containing up to 10% uranium may be dissolved in 5.4 M NH_4F–0.33 M NH_4NO_3–0.13 M H_2O_2 (modified Zirflex process). The peroxide promotes uranium solubility and surpresses corrosion of Ni-o-nel by a factor of 3 to 10 except at the solution-vapor interface. Uranium-zirconium alloys may also be processed by the Zircex process, which is based on hydrochlorination of the alloy followed by chlorination of the residue with CCl_4. In the hydrochlorination step at 500 to 600°C, most of the zirconium is volatilized; in the chlorination step, the uranium and residual zirconium are converted to volatile chlorides and are separated by fractional condensation at 300°C. The final uranium chloride product may be decontaminated by conventional solvent extraction processes or by fluorination.

Uranium–3% molybdenum alloy is dissolved in boiling 8 M HNO_3–0.5 M $Fe(NO_3)_3$ to yield a completely stable product solution, containing 1 M uranium, which is suitable as a feed for the Purex solvent extraction process. The disadvantage of this method is the generation of about 1100 gal of first-cycle solvent extraction waste for each ton of uranium processed. An alternative aqueous process, proposed for U–10% Mo alloys, involves dissolution of the alloy in boiling 11 to 13 M HNO_3 and separation of the precipitated molybdic oxide by centrifugation. This process is followed by a low-waste Purex-type solvent extraction procedure but has the disadvantage that the molybdenum oxide solids occupy approximately 30% of the original solution volume and are not easily centrifuged and washed.

The SRE decladding facility in Cell A of Building 3026 was completed and successfully cold tested on unirradiated SRE fuel rods. The facility will be used to declad the SRE Core 1 fuel as soon as building changes for containment are completed.

Experimental tests on the shearing of stainless-steel-clad UO_2 fuel bundles both at ORNL and under two subcontracts were completed. The tests indicated the feasibility of the shear-and-leach approach to mechanical processing of fuels, and a 250-ton shear for hot-cell use was designed and is now being fabricated. A slow-speed shear (~ 5 in./sec) with a stepped-V blade and a vee or semicircular anvil with 3 mils clearance gave the best shearing for subsequent leaching. The major problems in shearing are to

ensure good ferrule–fuel tube separation and to minimize wear and galling by hard braze particles. It is anticipated that a well-designed shear will be able to make 10,000–50,000 cuts between blade replacements.

A new method was developed for processing of uranium-graphite fuels. The fuel is simultaneously disintegrated and leached with 90% nitric acid at either boiling or room temperature. One 4-hr leach at 25°C recovered about 98% of the uranium; recoveries in two leaches were about 99 and 99.5% from fuels containing 1.5 and 13% uranium, respectively. Leaching with boiling acid resulted in slightly higher recoveries. The fuming nitric acid may be recovered for re-use by distillation of the leach solutions. In tests on disintegration of graphite fuels with bromine and interhalogens, bromine, ICl, and IBr caused swelling and disintegration of the fuels. However, uranium recoveries in leaching the residues with boiling 15.8 M HNO_3 were lower than those in the fuming nitric acid process, but higher than those in leaching after mechanical grinding.

In further work on the Hermex process the solubilities of U, Th, Pu, Sm, Nd, and Gd in mercury and of Ru, Pd, Zr, and Mo in uranium-saturated mercury solutions were measured from 25 to 356°C. Ruthenium was more soluble and palladium less soluble in U-Hg solution than in Hg alone. Zr and Mo solubilities in U-Hg were below the limits of detection. A phase diagram for the U-Hg system was prepared from data obtained on Hg vapor pressures for the temperature range 25–431°C. A Hermex flowsheet for UO_2 fuel was also developed in which decontamination factors (DF's) from Ru, Cs, and Sm of > 1000, 220, and 75, respectively, were obtained.

The major development in the solvent extraction subprogram was the development of an acid-salted acid-deficient Thorex process. The advantages of this over the old aluminum-salted process are the production of a waste that contains < 0.1 M Al and may be reduced tenfold or more in volume, the 50% decrease in pulsed column stage heights, and the assurance that U and Th losses and fission product DF's will be equal to or better than those in the older process. The new flowsheet can be used for either a co-decontamination or a partitioning first cycle for U and Th.

Amsco washing of the evaporator feed to prevent carry-over of TBP hydrolysis products produced in intercycle evaporation was evaluated. About

98% of the dissolved and entrained TBP was successfully removed. In solvent recovery tests with filtration after carbonate washing, DF's of 200 from Zr-Nb were obtained. The DF was best with a $CaCO_3$ filter aid and filters with fine (5-μ) pores.

Hot-cell demonstrations of the Yankee and NMSR Darex-Purex flowsheet were made with fuel samples irradiated to 16,000 Mwd/ton. Two-cycle DF's were 7.4×10^5 and 1.2×10^5 for gross beta and gamma, respectively; these are lower than the anticipated values, and more tests are planned.

A flowsheet was developed for recovering enriched uranium from the LAPRE-II fuel which contains 77 g U(IV) per liter in 96.8% H_3PO_4. The 12-fold dilution required for criticality control (to 6 g of U per liter) is sufficient to provide satisfactory feed if the solution is made 1.6 M in $Fe(NO_3)_3$ to ensure complexing of the phosphate.

Engineering-scale tests on unirradiated fuel solutions were made to determine flooding and HETS values for sieve plates, nozzle plates, and nozzle-zebra plates with the interface at top and bottom of the columns. Flooding characteristics in extraction-scrub columns were best with nozzle plates; the scrub section was controlling. Nozzle plates were also less subject to upset by interface "crudding" or particulate matter in the feed. Sieve plates used in either extraction or stripping and with the interface at either top or bottom gave uranium extraction HETS values that were independent of pulse rate.

2. POWER REACTOR FUEL PROCESSING PILOT PLANT

A total of 50.6 tons of natural and depleted irradiated uranium fuel from the BNL, SR, and HW reactors was processed to recover 39.4 kg of plutonium and 37 tons of uranium. Special programs, such as the processing of ANL-CP-2 reactor fuel and MTR irradiated plutonium-aluminum alloy assemblies (containing 30% Pu^{240}), were completed. The raffinate from the MTR plutonium-aluminum program was processed to demonstrate a scheme aimed at recovering the rare earth-americium-curium fraction.

A nonionic (polymeric) species of plutonium, inextractable in TBP and undetectable with normal analytical methods, was formed in three batches of Savannah River dissolver solution, which progressed to conditions of 2.0 M HNO_3 to 0.5 M acid deficiency, causing significant deviations in the

plant material balances. Complexing agents and prolonged digestion in an acid environment (>2 M HNO_3) were required to reconvert the plutonium to the extractable state.

Fission product decontamination was improved by operating the extraction contactors with the organic phase continuous. Two methods of column interface control were developed and demonstrated.

An evaporator explosion on November 20 in Cell 6 of the Hot Pilot Plant, Building 3019, resulted in release of 70 mg of plutonium to nonoperating areas of Building 3019 and of 600 mg to nearby streets and buildings. No one was injured as a result of the explosion and no one received a significant fraction of a lifetime body burden of plutonium either at the time of the incident or during subsequent cleanup operations. The explosion is considered due to the deflagration of nitrated organic compounds in an intercycle evaporator which was being decontaminated and involved nitration by concentrated nitric acid of 14 liters of the proprietary decontaminating agent, Turco 4501.

In the cleanup operation the contamination was bonded to the nearby street and building surfaces with tar, paint, roofing compound, or masonry sealer, as appropriate to the surface. With the exception of the pilot plant section of Building 3019, the Graphite Reactor building, and the road south of these buildings, all areas of the Laboratory were back in service by Monday, November 23. Decontamination of the interior of Building 3019, exclusive of four of the seven processing cells, was 90% complete on August 1, 1960. Decontamination of the processing cells is being delayed pending installation of a temporary secondary containment structure and provision of additional vessel off-gas capacity.

3. FUSED SALT-FLUORIDE VOLATILITY PROCESS

The pilot plant originally designed for volatility processing of fused fluoride fuel was converted (by addition of a dissolver and other equipment) to use with zirconium-containing solid fuels.

In tests on an INOR-8 prototype dissolver, corrosion was not detectable by Vidigage inspection after ten hydrofluorination runs with Zircaloy-2 bars totaling 74.5 hr of exposure to HF-sparged $NaF-LiF-ZrF_4$ melts at 550 to 650°C.

It was observed that Ni, Cr, Sn, and Fe dissolved in the molten-salt solvent as impurities were reduced by reaction with zirconium. Part of the metallic impurities deposited on the fuel specimen being dissolved and tended to retard the dissolution. Some of this finely divided material was also entrained in the off-gas, complicating the off-gas disposal problem. This problem can be minimized by keeping the impurities content of the salt low. This can be accomplished by pretreating the molten-salt solvent with hydrogen and using a mixture of hydrogen and HF as the reactant gas for dissolution.

Hydrogen fluoride dissolution-rate data obtained for a copper-lined dissolver showed a small effect of temperature and a nonlinear effect of ZrF_4 bulk concentration and corroborated the major dependence of dissolution rate on the superficial velocity of gas past fuel surfaces.

Adiabatic differential bed studies of the UF_6 sorption on NaF indicated an initial period when gas-phase diffusion controlled the rate, followed by a longer period in which solid-phase diffusion was the controlling factor.

A series of 12 laboratory-scale tests on the Fused Salt–Fluoride Volatility process with long-decayed Nautilus STR fuel demonstrated good uranium recovery and over-all decontamination from fission product activity but showed the necessity for further work to reduce the amounts of molybdenum, technetium, and neptunium in the UF_6 product.

The feasibility of processing stainless-steel- and niobium-containing fully enriched uranium fuels by the Fused Salt–Fluoride Volatility process was suggested by measurements of acceptable dissolution rates with HF in fused salt mixes.

ThO_2 dissolved rapidly without HF in ZrF_4-bearing salt mixes, by metathesis or the formation of the soluble oxyfluorides.

The feasibility of gaseous transfer of PuF_6 was demonstrated, indicating a possible method of separating UF_6 and PuF_6 based on their relative chemical stabilities. Work on the MoF_6-NaF system proved that a definite chemical complex exists between these compounds, and preliminary vapor pressure data were obtained on the equilibrium between gaseous MoF_6 and the solid complex.

4. MOLTEN-SALT REACTOR FUEL PROCESSING

A study of potential fuel cycle costs as related to conversion ratios for various fuel processing rates indicated that a total fuel cycle cost of $\sim$ 1 mill/kwhr can be achieved, with a minimum at a conversion ratio of slightly less than 1.0, assuming that the volatility process can be extended to apply to fuels decayed only four days. Economically the fluoride volatility process appears to be acceptable for uranium recovery from fuel and blanket salts and the HF dissolution process for Li^7 salt recovery for fuel neutron-poison-level control. However, much experimental work must be accomplished before the volatility process is proved to be technically feasible for molten-salt-breeder application. Scouting chemical investigations for alternative processes indicated that a solution of 5 mole % NO_2 in anhydrous HF might be used as a solvent for the whole fused $LiF-BeF_2-UF_4$ fuel, the components having solubilities of about 50, 50, and 1 g/liter. High-cross-section rare-earth fission product fluorides and ThF_4 are insoluble in this solvent; rare earths are soluble to the extent of $< 10^{-4}$ mole %, only, and ThF_4 to < 0.01 mole %.

5. HOMOGENEOUS REACTOR FUEL PROCESSING

In initial tests with a 13-unit multiple hydroclone unit, solids collection rates averaged 50 to 100% higher than with a single hydroclone. Plugging was eliminated by returning the overflow from the collection hydroclone to the multiclone receiver.

Analysis of samples for I^{135} and measurement of heat generation rates on the low-pressure system iodine trap confirmed previous observations that 80-99% of the iodine in the high-pressure system does not continuously circulate with the fuel, but is retained, probably by adsorption on pipe surfaces, in equilibrium with that in solution. This decreases the effectiveness of the iodine removal system, but xenon poisoning may still be limited to acceptably low levels by iodine removal. The xenon poison fraction at 5 Mw was found, by mass spectrographic analyses of the reactor off-gas downstream of the charcoal beds, to be 0.9%.

6. WASTE TREATMENT

Processes under development to prepare wastes for permanent disposal would convert high-radioactivity-level wastes to solids by evaporation and calcination, solidify intermediate-level chemical decladding wastes with lime, sand, and cement, and decontaminate low-level wastes to dischargeable levels by ion exchange. Evaporation and calcination to 900°C of synthetic high-level wastes was studied in 4-in.-dia, 18-in.-long pots and in 6- and 8-in.-dia, 78-in.-long pots. In the smaller equipment > 98% of the original nitrate in the feed was recovered in the off-gas condensate, and total noncondensible inerts in the off-gas amounted to 0–5 liters/liter of feed, depending on the method of operation and the atmosphere maintained in the system. In the larger equipment, solids deposition in the pot took place either in a radial or vertical direction, depending on the method of operation.

Evaporation and calcination of simulated Purex 1WW to 400°C in the presence of 3 to 300 ml of TBP per liter of waste produced no exothermic and/or violent reaction. Measured thermal conductivities of calcined wastes varied almost linearly with temperature from 0.210 at 90°F to 0.311 Btu hr^{-1} ft^{-1} $(°F)^{-1}$ at 1329°F for calcined Purex waste and from 0.140 at 92°F to 1.52 at 1600°F for a calcined Darex waste. Evaporation and calcination of Purex 1WW in an NO atmosphere decreased the ruthenium in the condensate from about 70 to 0.9–1.5%, without additives, and to 1.9–32%, with additives. The presence of about 2 ml of TBP per liter of waste decreased the amount of ruthenium in the condensate, in an air atmosphere, from about 70 to 4–15%, depending on additives. Decontamination of an air stream bearing a soluble aerosol by a packed scrubber was as much as 1000 times more effective when steam was present in the vapor phase.

Fundamental data on the physical and chemical changes that take place when various components of waste solutions are heated during calcining are being obtained by thermogravimetric analysis.

Based on compression tests, satisfactory methods have been found for solidifying Sulfex and Zirflex decladding wastes by addition of $Ca(OH)_2$, sand, and cement to the waste solutions.

Making typical ORNL low-level process-water waste 0.01 M in NaOH, filtering it, and then passing it through a phenolic cation exchange resin

bed results in over-all decontamination factors of about 10 for ruthenium and cobalt, 100 for rare earths, and 1000 for cesium and strontium. The resin can be regenerated with hydrochloric acid, and the regenerant waste evaporated to about 1/3000th of the original waste-water volume.

A study of the economics of permanent tank storage of power-reactor fuel processing wastes indicates that storage costs should average 0.05–0.23 mill/kwhr (electrical); this cost does not reflect the hazards involved.

7. FUEL CYCLE DEVELOPMENT

Experimental studies of simplified methods for recycle of thorium–uranium-233 fuel to heterogeneous reactors have indicated that high-density oxides can be loaded to acceptably dense oxide fuel cores by vibratory compaction into cladding tubes. Compaction of arc-fused thorium oxide and mixed thorium-uranium oxides by pneumatic vibrators consistently gave bulk densities in stainless steel tubes 87% of theoretical. Compaction was best with a pneumatic vibrator which imparted a sharp impact to the tube on its upstroke but not on the downstroke. The application to fuel element fabrication promises to provide an economically feasible method of recycling uranium-233 and thorium to heterogeneous reactors under shielded conditions.

8. AMEX PROCESS

Uranium was recovered economically from amine extracts as a high-assay product free of sodium, molybdenum, and vanadium by precipitating ammonium uranyl tricarbonate from the solvent phase with a uranium-saturated ammonium carbonate–ammonium sulfate solution and calcining the precipitate. Another stripping method, which recovers uranium from amines as a relatively pure concentrated uranyl nitrate solution rather than as the usual solid concentrate, was demonstrated successfully in continuous equipment.

Favorable results were obtained in solvent extraction recovery of uranium from relatively pure carbonate solutions with a quaternary ammonium extractant, but attempts to treat an actual feed liquor from a Colorado Plateau ore were unsuccessful owing to interference from impurities in the liquor.

9. THORIUM RECOVERY FROM GRANITIC ROCKS

In studies on recovering thorium from Canadian uranium-thorium ores, an inexpensive method was developed for stripping thorium from Primene JM-kerosene by contacting the extract with 2 M NaCl–0.5 M Na_2SO_4 solution and subsequently heating the strip solution to precipitate thorium sulfate.

Studies were initiated to define methods and costs for recovering thorium from granitic rocks in tonnages adequate to satisfy the long-range demands of a nuclear power system based on the Th-U^{233} cycle. In preliminary sulfuric acid leaching tests on twelve granitic rock samples containing 10 to 90 ppm thorium, recoveries ranged from 25 to 80%. Sulfuric acid consumption was high, ranging from 40 to 100 lb per ton of granite. Tentative estimates indicate that thorium might be recoverable from the more easily leached, higher grade granites at costs below $100 per pound.

10. GAS-COOLED REACTOR COOLANT AND EQUIPMENT DECONTAMINATION

Experimental studies on fixed bed oxidation of hydrogen in helium carrier gas were carried out in a 2-in.-dia CuO bed to provide design data for the EGCR gas purification system. The results of these tests were correlated and a design equation obtained which specifies the required bed volume.

A noncorrosive procedure was developed for decontaminating the EGCR charge and service machines which consists in spraying with hot, nonfoaming detergent solution to remove water-soluble fission products and flush off particles. A peroxide–sodium oxalate solution is then used to dissolve residual UO_2 and remove adsorbed fission products.

11. HRP Thoria Blanket Development

Twenty-four experimental batches of specification-grade ThO_2 and 19 batches of thorium-uranium oxide were prepared in the new pilot plant facility. The particles of the mixed oxide lacked integrity, and its preparation was suspended at midyear. The plant was placed in stand-by at the end of FY 1960.

Rounded particles of Th–3 mole % U containing 1.6 wt % Al_2O_3, 1 to 2 μ in diameter, were prepared by flame denitration. In the 100A loop these

gave < 0.1 and 1.3 mpy attack rates and negligible particle degradation when circulated as a slurry at 20 and 40 fps. Yield stresses for the material were a factor of 2 to 4 lower than 1600°C-fired oxide prepared from thorium oxalate.

Spherical ThO_2 particles, 0.5–30 μ in diameter, were prepared by setting 1.3–1.5 M ThO_2 sols to gels in isopropyl alcohol, followed by ammonia-washing, drying, and calcining to 1000°C. Particles with densities up to 8 g/cc were obtained, but they tended to be hollow and to be degraded in jet-abrasion and toroid tests.

Three 4-kg batches of rounded thoria pellets which had good integrity and showed < 1 wt %/hr attrition loss were prepared for studies of the HR pebble-bed blanket. Porous or weak thoria spheres pressed from ceramic-grade powder were strengthened by soaking in thoria sol or dibasic aluminum nitrate solution, followed by firing. Nonspherical thoria bodies, 2 mm in diameter, with high density and strength were prepared by a gel-bead technique.

A palladium catalyst for recombination of radiolytic gases formed in aqueous thoria and urania-thoria slurries had a high specific activity in both out-of-pile and in-pile tests. This activity was not maintained when a large excess of either hydrogen or oxygen was present. Pump-loop experiments under oxygen showed an order of magnitude lower specific activities and an activity half life of several hundred hours. A new apparatus for laboratory studies was developed in which measured amounts of hydrogen and oxygen could be injected at temperature into the autoclave containing the slurry-catalyst system.

The solubilities of hydrogen and oxygen in water and in aqueous 650°C-fired thorium oxide slurries were measured from 27 to 300°C. The presence of the thorium oxide did not affect the hydrogen solubility but resulted in an increase by as much as a factor of 2.3 in the oxygen solubility over what would have dissolved in the water phase alone. With freshly prepared ThO_2 about 2 cc (STP) of oxygen per gram of thorium oxide was irreversibly adsorbed.

Thorium oxide powders fired at 650, 800, 900, 1100, and 1500°C were irradiated for 16 and 22 months in the LITR at a thermal neutron flux of 2×10^{13} neutrons cm^{-2} sec^{-1}. A marked decrease in surface area for all

oxides except the high-fired oxide indicated that irradiation produced about the same sintering effect as firing at 1500°C despite the fact that the temperatures of the powders under irradiation were probably less than 300°C.

12. SURFACE CHEMISTRY

As the first step in studying the adsorption of ions from solution by ThO_2 surfaces, several approaches to producing a suitable sample of ThO_2 were tried. Available theory relates such surface adsorption measurements to the tendency of slurry particles to flocculate and then to cake. In order to interpret adsorption data, the ThO_2 particles should have no internal surface and should be in a certain size range. Such particles were prepared by the breakdown of multicrystalline ThO_2 particles (produced by thermal decomposition of thorium oxalate) by digestion in warm dilute acid. A sample produced this way will be used for the first adsorption measurements.

Several tests have been made to determine the behavior of glass electrodes in ThO_2 suspension systems. The results agree with the theoretical contention that a reversible electrode gives the same reading in a suspension as in a supernatant in chemical equilibrium with the suspension. The tests also indicate that a supernatant can react with the atmosphere to give a change in its pH reading.

13. TRANSURANIUM STUDIES

A solvent-extraction flowsheet was developed on a laboratory scale for recovering plutonium, americium, and curium from highly irradiated Pu-Al alloy. In the pilot plant the first plutonium recovery cycle was successfully demonstrated, and results indicated that the americium-curium recovery cycle was operable although it was terminated because of mechanical difficulties before equilibrium conditions were reached.

A process for separating actinides from lanthanides by anion exchange based on selective chloride complexing was developed and tested on a laboratory scale. The americium, curium, and rare earths were sorbed on Dowex 1-10X resin from a solution of 8 M $LiNO_3$; the rare earths were selectively

eluted with 10 M LiCl, and the americium-curium with 1 M LiCl. In laboratory demonstrations this process gave greater than 99.5% recovery of americium tracer, containing no detectable amounts of rare earths.

Rare earths were separated from americium by selective extraction into 0.5 M mono-2-ethylhexyl orthophosphoric acid from slightly acid 10 M LiCl. Gram amounts of rare earths were extracted from milligram amounts of americium in a countercurrent "mini" mixer-settler with 7 scrub and 8 extraction stages. Extractions of neodymium, cerium, and lanthanum were 99.9, 98, and 90%, respectively, while americium loss by extraction was 0.04%. Complete separation of curium and lanthanum by this extraction system does not appear to be feasible; however, complete separation from all other rare earths can be accomplished. Americium and curium were concentrated by extraction into 100% TBP from concentrated LiCl solution.

Americium chloride solution containing 170 g of americium was successfully converted to pure AmO_2, which assayed at the theoretical value of 88.3% americium.

A program to test the compatability of plutonium and americium oxides in matrixes of aluminum and beryllium was initiated. Preliminary work is being performed with CeO_2.

Conceptual design and cost estimates were completed for the Transuranium Processing Facility; present plans call for construction to begin by September 1961. Equipment design was started.

14. FISSION PRODUCT RECOVERY

A chemical flowsheet is proposed for recovery of strontium and rare earths from Purex wastes. The iron in the waste is first complexed with tartrate, and the pH is adjusted with caustic. Strontium and rare earths are extracted by a solvent comprised of di(2-ethylhexyl) phosphoric acid—tributyl phosphate—Amsco 125-82, and are stripped with nitric acid. Processing the strip product through additional solvent extraction cycles yields separate concentrated strontium and rare-earth fractions.

In preliminary tests, two solvents, sodium tetraphenyl boron in hexone and dinonyl naphthalene sulfonic acid in Amsco 125-82, have shown ability to extract cesium from adjusted Purex waste solutions.

Dowex 50W X-8 (20–50 mesh) resin was used to recover separate strontium and rare-earth products from a synthetic Purex waste solution on a laboratory scale. The solution is diluted by a factor of 10, and oxalic acid is added prior to pumping it through a column of the resin. Strontium is separated from rare earths by eluting with 1 M HNO_3 and passing this product stream through a second resin column. The rare earths are recovered by eluting with 0.5 M monosodium citrate (pH 3.5). Strontium is recovered by eluting with 1 M NaCl and 0.07 M sodium Versenate at pH 6.1.

15. SOLVENT EXTRACTION TECHNOLOGY

Di-sec-butyl phenylphosphonate (DSBPP) showed U/Th separation factors about 34 times greater than those obtained with TBP. An aqueous U^{233} product concentrate, representing the final product in the Thorex process, was treated with 1 M DSBPP in Solvesso 100 in laboratory-batch countercurrent tests, giving complete uranium recovery and a thorium decontamination factor of > 250.

Uranium and thorium complexes of DSBPP were found to be soluble in carbon tetrachloride. Though saturation tests of the DSBPP-plutonium(IV) complex have not been feasible in our laboratory, it has been surmised from the uranium and thorium data that a DSBPP-CCl_4 extractant is a potential alternate for final plutonium purification cycles where the less radiation-stable TBP-CCl_4 system is presently used.

Irradiation tests with 1 M TBP solutions in aliphatic Amsco 125-82 and aromatic Solvesso 100 show the latter to provide radiation protection for the TBP reagent. By measuring the comparative organic acid production the TBP-Solvesso solution was more stable by a factor of 2.5–3 than TBP–Amsco 125-82. DSBPP–Solvesso 100 in similar testing was more radiation stable and showed slightly better uranium–fission product separation than TBP–Solvesso 100 by factors of ~ 1.5 in each case.

A "nitrite-acetone" head-end treatment of the aqueous process feed solution is tentatively suggested as a technique for improving zirconium-niobium and ruthenium decontamination in the Purex co-decontamination cycle. Results of countercurrent tests with TBP and DSBPP indicated that the decontamination factors were improved by an order of magnitude.

Systematic study of plutonium extraction from nitrate solutions continued, including measurement of extremely high Pu(IV) extraction coefficients with dialkylphosphoric acid and usably high coefficients for reduced plutonium from salted solution with tertiary amine. Chemical flowsheet development was completed for scavenging of uranium and plutonium from Sulfex decladding wastes.

Studies on the amine extraction of fission-product and corrosion-product metal nitrates showed that Mo(VI) is extracted in direct competition with nitric acid, its extraction coefficient with 0.1 M amines decreasing from > 100 at ~ 0.1 M HNO_3 to < 10^{-4} at 2–10 M HNO_3. Zirconium extraction coefficients increased with increasing nitric acid, in approximate accordance to the expression

$$E_a^o(Zr) = K(\underline{M}^2_{amine})(\underline{M}^2_{H^+})(M^2_{NO_3^-}) \quad ,$$

with $K \approx 6 \times 10^{-6}$ for trilaurylamine and Primene JM-T in toluene. Extraction coefficients of aged nitrosylruthenium nitrate increased with extraction contact time for several hours. The coefficient measured at 24 hr was 0.08 with 0.4 M trilaurylamine in toluene from 2 M HNO_3, and it varied directly with the amine concentration and inversely with the acidity. Samarium(III) extraction coefficients were all < 10^{-4} with 0.3 M amine in toluene from 2–9 M HNO_3.

A chemical flowsheet for tertiary amine extraction was developed for recovery of the technetium and neptunium that accumulate in some uranium fluorination plant residues, together with recovery of the uranium for recycle. A single-cycle process provides coextraction of these three elements and separation by consecutive stripping, giving good recoveries and relatively high mutual separation. The chemical flowsheet was tested through the stage of continuous countercurrent demonstration in laboratory-scale equipment, using a commercial tertiary amine to process actual plant feed solution.

Americium was extracted preferentially to the light rare earths from concentrated lithium chloride solutions by tributyl phosphate (TBP), giving the most promising separation observed thus far for the transplutonics from fission-product rare earths. A 12-stage batch countercurrent extraction

with 1 M TBP from 10 M LiCl–0.1 N HCl gave a separation factor of 310 between americium and europium. The order of extraction was similar with several phosphonates, with slightly less separation. Americium was extracted between cerium and europium by several amines.

TBP–Amsco 125-82 solutions were degraded chemically with nitric acid and radiolytically by Co^{60} gamma irradiation in order to simulate used radiochemical process extractants. The extent of degradation and the effectiveness of solvent cleanup were assessed by the extraction and stripping of Zr^{95}-Nb^{95} and of Ru^{106}. Products of degradation of both TBP and Amsco 125-82 were strong extractants for Zr^{95}-Nb^{95} but not for Ru^{106}. The usual alkaline washing procedures effectively removed low-molecular-weight acids originating primarily from hydrolysis of TBP and reduced Zr-Nb^{95} extraction by 80–90%. Zirconium-niobium extractants not removed by alkaline washing (with or without alkaline permanganate treatment) were identified as originating primarily from nitration of the diluent, and were sorbed by activated solids, such as alumina.

Measurements of the sulfuric acid transferred to the aqueous phases upon extraction of known quantities of thorium sulfate by di-n-decylamine sulfate–bisulfate mixtures of known bisulfate content indicated an amine sulfate:thorium sulfate ratio of slightly less than three for the complex, in good agreement with the value indicated by isotherm plateaus. These results were in conformity with an equilibrium expression for the extraction which takes into account the effect of varying sulfuric acid activity. An equilibrium constant for this reaction, as well as an independent evaluation of the composition of the complex, has been obtained from a least-squares treatment of extraction data from runs at varying sulfuric acid activity but at constant sulfate ion concentration. At constant composition of the organic phase, but with varying aqueous sulfate ion molarities, the distributions were shown to lead to the following values for the formation constants of the thorium tri- and tetrasulfate complexes, adjusted to zero ionic strength via single-parameter Debye-Hückel ionic

strength corrections:

$$K_{23} = \frac{[Th(SO_4)_3^{--}]}{[Th(SO_4)_2][SO_4^{--}]} = 6 \quad ,$$

$$K_{34} = \frac{[Th(SO_4)_4^{4-}]}{[Th(SO_4)_3^{--}][SO_4^{--}]} = 0.005 \quad .$$

Continued examination of solvent extraction systems for anomalous equilibria due to violence of agitation during equilibration, other than those reported previously for uranium extraction by trioctylamine sulfate and didecylamine sulfate (DDAS), has resulted in definite evidence of such behavior in two additional systems (thorium extraction by DDAS and uranium extraction by 1,3-ethylpentyl-4-ethyloctylamine sulfate).

A vapor-pressure apparatus capable of measurements to within a few microns has been constructed and tested for use in the determination of activity coefficients of solvent extraction reagents in organic solvents.

16. EXTRACTION REAGENT PERFORMANCE

The presence of nitric acid had no significant effect on the yield of acidic degradation products formed by irradiation of TBP—Amsco 125-82 solutions. The G value for nitric acid decomposition was high, being in the range 2.5 to 5.5 instead of 0.03 to 0.2 molecule/100 ev that could be expected under these conditions. The use of an aromatic diluent, Solvesso-100, decreased the yield of acid degradation products from a 1 M TBP solution to about 0.3 molecule/100 ev, which is only 30 to 50% greater than the amount under similar conditions from di-sec-butyl phenylphosphonate, the solvent most resistant to radiation damage so far tested.

Solubilities of a zirconium dibutyl phosphate, uranyl mono- and dibutyl phosphates, and iron(III) dibutyl phosphate in acid aqueous and 1.13 M TBP—Amsco 125-82 solution ranged from 4×10^{-6} M zirconium dibutyl phosphate in water to 0.7 M uranyl dibutyl phosphate in the most acid organic phase tested.

Laboratory tests indicated that low-pressure and molecular distillation are both technically feasible methods for repurifying degraded solutions of TBP in Amsco 125-82.

17. RADIATION EFFECTS ON CATALYSTS

Initial experiments on the effects of radiation on catalysts showed that Co^{60} irradiation to a dose of 1.8×10^{11} ergs/g of a promoted chromia-alumina catalyst increased its effectiveness as a catalyst for the dehydrogenation of methylcyclohexane at 460°C about 30%. The use of S^{35} in $MgSO_4$-Na_2SO_4 catalysts for the dehydration of cyclohexanol doubled the reaction rate at 290°C when 25.9 ml/g of S^{35} was incorporated (as Na_2SO_4) into the catalyst. Irradiation by Co^{60} showed no effect on this catalyst.

18. ION EXCHANGE TECHNOLOGY

Dowex 50W X-12 (100–200 mesh) resin irradiated to 12.5 whr/g of dry resin by sorbed Pm^{147} was analyzed for radiation effects. Moisture content increased from ~ 40% to ~ 70%, corresponding to a decrease in cross-linking from 12% to ~ 4%. The resin acquired some weak acid capacity, in addition to its salt-splitting capacity.

The rate of uranyl sulfate loading on sulfate- and nitrate-equilibrated Dowex 21K anion exchange resin was measured by a single-bead technique. The data were used to calculate apparent uranium diffusion coefficients by considering the process as simple diffusion into a sphere. These apparent coefficients appear to be nearly independent of the loading solution concentration over the range studied but dependent on the particle size of the resin used. The apparent coefficients observed during loading on sulfate-equilibrated 1200-, 960-, and 820-μ Dowex 21K were 1.3×10^{-7}, 0.76×10^{-7}, and 0.49×10^{-7} cm^2 sec^{-1}, respectively. Self-diffusion coefficients for sulfate ions in the resin were $(1.27 \pm 0.25) \times 10^{-6}$, $(0.60 \pm 0.18) \times 10^{-6}$, and $(0.75 \pm 0.17) \times 10^{-6}$ cm^2 sec^{-1} for 1200-, 960-, and 820-μ resin.

A device was designed and constructed for contacting samples containing several beads to eliminate data scatter caused by variation in capacity of individual beads. The uranium self-diffusion coefficient in 1200-μ resin was determined to be 4.4×10^{-8} cm^2 sec^{-1}; the apparent uranium diffusion coefficients observed during nitrate and chloride elution were 1.8×10^{-7} and 2.38×10^{-7} cm^2 sec^{-1}, respectively.

19. CHEMICAL ENGINEERING RESEARCH

A high-speed extraction contactor consisting of hydroclones stacked each above the other was developed to decrease organic extractant holdup time and radiation-induced solvent degradation. In preliminary tests solvent contact times per theoretical stage were 10–50% of those in conventional contacting equipment. Stage efficiencies were 20–75%.

Impedance matching of a mechanical pulser to a pulsed column by a resonant transfer line and air cavity produced pulse volumes in the column 30% greater than those produced by the same mechanical pulser directly coupled to the load. The system was mathematically analyzed and its performance predicted by electrical analog computations.

The steady-state transfer of uranyl nitrate across a quiescent interface between water and tri-n-butyl phosphate in kerosene was studied in an attempt to determine the limiting resistance to mass transfer in solvent extraction operations. No resistance attributable to the interface per se was found, even when surface-active agents were present.

In a fundamental study of thermal diffusion separation of ionic species in liquids, Soret coefficients of $CoSO_4$ and $CuSO_4$ were measured as a function of temperature by a new technique reproducible to 1%.

Transient pressures in the ventilating system of Building 3019 were calculated as a function of time in response to impulse and ramp pressure pertubations in a 10,000-ft^3 cell. For an impulse pertubation of +8.5 in. H_2O the cell would return to atmospheric pressure in 1.5 sec. A ramp pertubation of +3 in. H_2O per sec would raise the steady state cell pressure from the design value of −1.5 in. H_2O to atmospheric pressure.

20. CHEMICAL APPLICATIONS OF NUCLEAR EXPLOSIONS

In order to evaluate the reactions of tritium under the conditions expected from nuclear explosions contained in rock salt, chemical reactions of hydrogen with the impurities found in rock salt were studied. Calcium sulfate is reduced to the sulfide by hydrogen, whereas magnesium sulfate is reduced to the oxide. The reactions proceed at readily measurable rates in the 700–900°C range. The rate was lower by a factor of 1.2 to 1.7 when the calcium sulfate was dissolved in liquid sodium chloride.

Tritium exchanged between water and molecular hydrogen flowing over calcium sulfate to the extent of about 8% at 700°C when the ratio of H_2:HTO was 20. The degree of ionization and enthalpy of argon, hydrogen, and nitrogen were calculated for temperatures up to 20,000°K.

21. OXYGEN-17 SEPARATION PILOT PLANT

A pilot plant facility to separate the natural isotopes of oxygen was designed and is now being built in the deep bay area of Building 4501. The plant is designed to produce about 2 g of 98% O^{18} and 70 mg of 50% O^{17} per day. The process has been developed by and the plant will be operated by the ORNL Chemistry Division; the Chemical Technology Division has assisted in plant equipment design and construction.

22. REACTOR EVALUATION STUDIES

Fuel-material-selection studies indicated that the optimum fuel cycle costs can be estimated for any set of conditions according to the following equation:

optimum cycle cost (mills/kwhr)

$$= A + \frac{B}{\int k d\theta} + C \frac{(\text{fabrication cost, \$/ft of fuel element})^{0.785}}{(\int k d\theta)^{\alpha}}$$

where A, B, C, and α are functions of the fuel uranium density; $\int k d\theta$ in fuel = average over the reactor (cal cm^{-1} sec^{-1}), with k = fuel thermal conductivity, θ = temperature in excess of fuel surface temperature, and the limits of integration are from the surface to the center of the fuel. The effect of diluent poisons in optimum fuel cycle costs was also investigated as a function of fuel density and fabrication cost.

The major problem in the shipment of spent fuels for the civilian power-reactor complex appears to be the dissipation of the fission product decay heat. Preliminary studies indicated that problems associated with criticality and shielding are only secondary.

23. EUROCHEMICAL ASSISTANCE PROGRAM

As part of the USAEC assistance in construction of a fuel processing plant at Mol, Belgium, ORNL provided the loan of one full-time technical consultant, short-term visits of several technical consultants, the full-time assignment of one technical co-ordinator in the United States, and the review and exchange of technical data pertinent to the radiochemical processing of irradiated fuels.

CONTENTS

SUMMARY iii

1. HEAD-END AND SOLVENT EXTRACTION PROCESSING 1
   - 1.1 Chemical Processes for Stainless-Steel-Containing Fuels 1
   - 1.2 Processes for Zirconium-Containing Fuel 19
   - 1.3 Processes for Uranium-Molybdenum Fuels 23
   - 1.4 Mechanical Processing 26
   - 1.5 Processes for Graphite-Containing Fuels 34
   - 1.6 Hermex Process 39
   - 1.7 Solvent Extraction Process Development 42
   - 1.8 Engineering Studies 51

2. POWER REACTOR FUEL PROCESSING PILOT PLANT 58
   - 2.1 Fuel Processing 58
   - 2.2 Equipment Development 61
   - 2.3 Intercycle Evaporator Explosion, Building 3019 64

3. FUSED SALT-FLUORIDE VOLATILITY PROCESS 68
   - 3.1 Pilot Plant 68
   - 3.2 Engineering Studies 69
   - 3.3 Chemical Development 70

4. MOLTEN SALT REACTOR FUEL PROCESSING 75

5. HOMOGENEOUS REACTOR FUEL PROCESSING 77
   - 5.1 Hydroclone Performance and Corrosion Product Studies 77
   - 5.2 Fission Product Studies 80
   - 5.3 Waste Handling 81
   - 5.4 Equipment Decontamination 82

6. WASTE TREATMENT AND DISPOSAL 83
   - 6.1 Pot Calcination of High-Radioactivity-Level Wastes 83
   - 6.2 Solidification of Intermediate-Activity-Level Wastes 91
   - 6.3 Ion Exchange Treatment of Low-Radioactivity-Level Wastes 93
   - 6.4 Economics of Permanent Storage of Liquid Wastes in Tanks 95

7. FUEL CYCLE DEVELOPMENT..... 97
7.1 Fabrication of Fuel Elements..... 97
7.2 Measurement of Densities and Porosities of Fuel Materials..... 101
8. AMEX PROCESS..... 103
8.1 Uranium Recovery..... 103
8.2 Thorium Recovery..... 105
9. THORIUM RECOVERY FROM GRANITIC ROCKS..... 106
9.1 Sample Collection and Source Evaluation..... 106
9.2 Laboratory Processing Studies..... 107
9.3 Cost Studies..... 107
10. GAS COOLED REACTOR COOLANT AND EQUIPMENT DECONTAMINATION..... 108
10.1 Coolant Cleanup Studies..... 108
10.2 Decontamination of Equipment..... 110
11. HRP THORIA BLANKET DEVELOPMENT..... 112
11.1 Oxide Preparation Development..... 112
11.2 Preparation of Thoria Pellets for HR Pebble-Bed Blanket Studies..... 114
11.3 Evaluation of Thoria and Thoria-Urania Powder Preparations for Blanket Slurries..... 118
11.4 Gas-Recombination Catalyst Development..... 120
11.5 Hydrogen and Oxygen Solubility in Aqueous Slurries..... 124
11.6 Thoria Powder Irradiations..... 124
11.7 Thoria Spray Coating..... 128
12. SURFACE CHEMISTRY..... 129
12.1 Preparation of ThO_2 for Surface Adsorption Measurements..... 129
12.2 Use of the Glass Electrode in Measuring pH of Slurries..... 131
13. TRANSURANIUM STUDIES..... 136
13.1 Plutonium-242 and Americium-Curium Recovery Cycles..... 137
13.2 Anion Exchange Separation of Actinides and Lanthanides..... 138
13.3 Rare Earth Extraction into M-2EHPA..... 140

13.4 Oxide Preparation..... 142
13.5 Target Fabrication..... 142
13.6 Transuranium Processing Facility and Equipment..... 143

14. FISSION PRODUCT RECOVERY..... 144
14.1 By Solvent Extraction..... 144
14.2 By Ion Exchange Resin..... 146

15. SOLVENT EXTRACTION TECHNOLOGY..... 149
15.1 Uranium-Thorium Separation..... 149
15.2 Uranium-Plutonium Extraction..... 150
15.3 Metal Nitrate Extractions by Amines..... 156
15.4 Technetium-Neptunium-Uranium Recovery..... 158
15.5 Separation of Transplutonium Elements from Lanthanons..... 164
15.6 Extraction Performance and Cleanup of Degraded Process Extractants..... 166
15.7 Solvent Extraction Equilibria..... 168

16. EXTRACTION REAGENT PERFORMANCE..... 175
16.1 Radiation Damage to Solvents..... 175
16.2 Solubilities of Di- and Monobutyl Phosphates in Process Solutions..... 179
16.3 Purification of Degraded Solvent by Distillation..... 180

17. RADIATION EFFECTS ON CATALYSTS..... 183
17.1 Dehydration of Cyclohexanol on $MgSO_4$-Na_2SO_4 Catalysts..... 183
17.2 Dehydrogenation of Methylcyclohexane on Promoted Chromia-Alumina Catalysts..... 184

18. ION EXCHANGE TECHNOLOGY..... 187
18.1 Radiation Damage to Ion Exchange Resin..... 187
18.2 Kinetics of Uranyl Sulfate Anion Exchange..... 188

19. CHEMICAL ENGINEERING RESEARCH..... 194
19.1 Stacked-Hydroclone Contactor..... 194
19.2 Impedance Matching of a Piston Pulser to a Pulsed Column by a Resonant Transfer Line and Air Cavity.... 196
19.3 Transfer of Uranyl Ion Across a Water-TBP Interface.... 197

19.4 Thermal Diffusion..... 198

19.5 Transient Response of the Cell Ventilation System in Building 3019 to Impulse and Ramp Pressure Perturbations..... 199

19.6 Instrumentation..... 203

20. CHEMICAL APPLICATIONS OF NUCLEAR EXPLOSIONS..... 204

20.1 Hydrogen Isotopic Exchange..... 204

20.2 Reduction of $CaSO_4$ and $MgSO_4$ by H_2..... 204

20.3 Wire Explosions..... 205

20.4 Plasma-Jet Chemistry..... 206

21. OXYGEN-17 SEPARATION PILOT PLANT..... 207

22. REACTOR EVALUATION STUDIES..... 209

22.1 Economic Guides to Fuel Material Selection for Pressurized-Water Reactors..... 209

22.2 Cost and Hazards of Transporting Spent Fuels..... 212

22.3 Miscellaneous IBM-704 Codes..... 215

23. EUROCHEMIC ASSISTANCE PROGRAM..... 217

24. PUBLICATIONS AND ORAL PRESENTATIONS..... 219

ORGANIZATION CHART..... 225

1. HEAD-END AND SOLVENT EXTRACTION PROCESSING

Processes are being developed for uranium, plutonium, and thorium recovery by solvent extraction from first-generation power reactor fuels containing aluminum, stainless steel, and zirconium.[1] Experimental work has shown that stainless-steel-clad ThO_2-UO_2 fuels may be dejacketed by either the Sulfex or Darex process (Sec 1.1). The Darex process is also suitable for the complete dissolution of stainless steel–UO_2 fuels. Fuels containing zirconium may be dissolved by the Zircex, Zirflex, and Perflex processes (Sec 1.2). Fuels containing molybdenum may be dissolved by an aqueous process (Sec 1.3). The jackets may be removed mechanically from some fuel elements, such as those containing sodium or NaK bonding agents, or the whole element may be chopped into short sections and the fertile and fissionable material selectively leached from the jacketing materials (Sec 1.4).

Development of processes for second-generation power reactor fuels was accelerated. New methods for processing graphite-base fuels were evolved (Sec 1.5), and work was started on beryllia and other ceramic and cermet fuels. A new laboratory was provided for the safe handling of beryllium-containing fuels. Further basic data pertinent to the Hermex process (Sec 1.6), a low-temperature solution-refining pyrometallurgical process for uranium, were made.

The chief solvent extraction development (Sec 1.7) was a new acid Thorex flowsheet requiring no aluminum, thereby resulting in a radioactive waste which can be decreased in volume at least tenfold. Satisfactory solvent extraction of adjusted solutions obtained from dissolution of irradiated samples of a variety of power reactor fuels was demonstrated.

Engineering studies (Sec 1.8) included investigation of methods of criticality control and of off-gas disposal.

1.1 CHEMICAL PROCESSES FOR STAINLESS-STEEL-CONTAINING FUELS

Two processes being developed for recovering uranium and thorium from stainless-steel-containing fuels are Darex and Sulfex. The Darex process

[1] Oak Ridge Session of AEC Fuel Processing Symposium at Hanford, Oct. 21 and 22, 1959, p 206–446, TID-7583.

is a total dissolution process for uranium alloy and UO_2 fuels but only a decladding process for ThO_2-UO_2 fuels; Sulfex is a decladding process for either type of fuel. Only Darex is applicable to UO_2–stainless steel cermet fuels (e.g., APPR). The chief Darex and Sulfex effort has been applied to the Consolidated Edison (CETR) fuel, stainless-steel-clad ThO_2-UO_2, which appears to be the most difficult fuel to handle in either process.

The Darex process, which is applicable also to aluminum-containing fuels, involves dissolution of stainless steel, uranium, and UO_2 in boiling 5 M HNO_3–2 M HCl, quantitative distillation of chloride from the dissolver solution after adjustment to 10–12 M HNO_3, and adjustment of the chloride-free distillation heel to correct metal and HNO_3 concentrations for solvent extraction. In the Sulfex process, the stainless steel cladding is dissolved in boiling 4 to 6 M H_2SO_4 and discarded to waste. The undissolved UO_2 is washed free of residual sulfuric acid and dissolved in 8 to 12 M HNO_3. Undissolved ThO_2-UO_2 from either Darex or Sulfex decladding is first washed and then dissolved in Thorex dissolvent [13 M HNO_3–0.04 M NaF–0 to 0.1 M $Al(NO_3)_3$]. In the Darex process, the chloride-free stainless steel cladding solution may be used to dissolve ThO_2-UO_2 by making it 0.04 M in F^-, 0.1 M in Al^{+++}, and 12 to 13 M in H^+.

Darex Dejacketing of CETR Fuel

The 20-mil-thick type 304L stainless steel cladding is dissolved in 1 hr in boiling 5 M HNO_3–2 M HCl (ref 2); the off-gas is a mixture of nitrogen, nitrogen oxides, and NOCl containing less than 0.5 vol % hydrogen (Table 1.1). Mixtures of hydrogen, NOCl, and nitrogen oxides are explosive over wide concentration ranges;[3] however, the hydrogen concentrations measured for Darex are outside these limits and no troubles are anticipated.

---

[2]L. M. Ferris and A. H. Kibbey, Sulfex-Thorex and Darex-Thorex Processes for Dissolution of Consolidated Edison Power Reactor Fuel: Laboratory Development, ORNL-2934 (in press).

[3]K. S. Warren, Survey of Potential Vapor Phase Explosives in Darex and Sulfex Processes, ORNL-2937 (in press).

Table 1.1. Composition of Off-Gases When Type 304 Stainless Steel Is Dissolved in Boiling 5 M HNO_3–2 M HCl

Final solutions contained 50 g of stainless steel per liter

Sample No.	Amount (vol %)									
	N_2O	NO	NO_2	NOCl	HCl	Cl_2	H_2	N_2	H_2O	Total
1	1.0	1.2	8.3	27.2	1.9	3.1	0.2	44.1	3	90.0
2	2.0	2.2	12.2	45.6	2.9	4.4	0.2	27.5	3	100.0
3						3.2	0.1	35.5	3	
4	2.3	3.6	16.3	41.9	3.6	2.5	0.2	28.3	3	101.7
5	2.3	7.2	20.0	36.7	3.6	2.4	0.4	33.1	3	108.7
6	1.2	2.5	19.0	24.2	2.4	2.4	0.4	38.1	3	93.2
7						2.5	0.2	38.0	3	

The hydrogen and nitrous oxide contents of the off-gas from batch Darex dissolutions of type 304L stainless steel were determined for various HCl-HNO_3 mixtures with a total initial H^+ concentration of 7 M. The final stainless steel concentration was 50 g/liter. The average hydrogen content increased from 0.15 vol % in 2 M HCl to 2.0 vol % in 6 M HCl. With 2 M HCl, the hydrogen content increased to a maximum of 0.50 vol % at 30 to 50% dissolution; with 6 M HCl the content was constant in the range 1.5 to 3.5 vol % during dissolution. As the HCl concentration was increased from 2 to 6 M, the NO content of the off-gas increased from 0.7 to 10%. Complete analysis (at Georgia Institute of Technology,[4] under subcontract) of the gases evolved when type 304 stainless steel was dissolved in boiling 5 M HNO_3–2 M HCl to produce a solution containing 50 g of stainless steel per liter showed almost the same hydrogen and NO concentrations obtained in the work at ORNL (Table 1.1). This work also showed the major components to be nitrogen (~40 vol %), NOCl (~35 vol %), and NO_2 (~15 vol %). Nitrogen oxides, NOCl, HCl, and HNO_3 were determined by an infrared method, and the other components by more conventional methods.

[4]Georgia Institute of Technology, final report on subcontract 1373.

Stainless steel in contact with titanium was passive, occasionally, to boiling 5 M HNO_3–2 M HCl for periods up to 2 hr, but the passivation was overcome by increasing the HCl concentration to 6 M.

Uranium and thorium losses to Darex decladding solutions were measured under a variety of conditions. Samples of stainless-steel-clad ThO_2-U_3O_8 pellets (80 to 85% of theoretical density) irradiated for 0 to 575 Mwd/metric ton were declad and then exposed to the boiling cladding solution for up to 4 hr. The uranium and thorium losses for intact and partly fragmented pellets were generally 0.05 to 0.5% and 0.03 to 0.9%, respectively, irrespective of irradiation level (Table 1.2). When the pellets

Table 1.2. Uranium and Thorium Losses in Decladding of Low-Density Consolidated Edison Fuel Specimens with Boiling 5 M HNO_3–2 M HCl

Pellets: 95% ThO_2–5% U_3O_8, 80 to 85% of theoretical density

Run No.	Irradiation Level (Mwd/metric ton core)	Decladding Time (hr)	Losses (%)	
			U	Th
1*	0	1	0.23	0.10
2*	0	2	0.63	0.09
3	58	0.5	0.19	2.3
4**	160	0.67	4.9	5.1
		1.5	4.7	5.0
		2.67	8.0	10.0
		3.67	9.0	8.2
5	169	0.75	0.05	0.03
		1.75	0.03	0.10
		2.75	0.05	0.05
		3.75	0.05	0.06
6*,**	190	1	2.1	1.1
		4	3.7	2.6
7*	275	1	0.06	0.03
		4	0.15	0.06
8	575	0.5	0.10	0.88
		1.5	0.10	0.36
		2.5	0.12	0.18
		3.5	0.14	0.24
		4.5	0.17	0.45

*These experiments conducted at Battelle Memorial Institute under subcontract 1381; see ref 5.

**Core pellets shattered in these runs.

were highly fragmented, the uranium and thorium losses immediately after decladding were as high as 9 and 10%, respectively. The gross beta and gamma activities dissolved from a powdered pellet were 3.0 and 15.1%, respectively, after decladding. In these tests, the decladding off-gas was scrubbed with 1 M NaOH; 0.04% of the total gross gamma and 0.14% of the gross beta activity were absorbed.

Maximum uranium and thorium losses for unirradiated pellets (density, 94% of theoretical) were 0.05 and 0.004%, respectively, for 4-hr decladdings, about an order of magnitude lower than those for the low-density pellets mentioned above. Uranium and thorium losses were unaffected by Co^{60} radiation at an intensity of 1 w/liter. In the presence of atmospheric oxygen, however, the dissolution was accelerated significantly.

Sulfex Dejacketing of CETR Fuel

In the Sulfex process, the stainless steel cladding is removed from UO_2 or UO_2-ThO_2 fuel by dissolution in 200% excess of boiling 4 to 6 M H_2SO_4;[2] the off-gas is hydrogen. Penetration of a 20-mil-thick jacket requires 1 to 3 hr. Passivation of the stainless steel is more serious than in the Darex process. As little as 0.001 M HNO_3 in the dissolvent can cause passivation. Type 304L stainless steel that had been autoclaved at 300°C for 100 hr at 2000 psi was not passive to boiling 6 M H_2SO_4 in the complete absence of HNO_3, and contact of the sample with Ni-o-nel did not induce passivation. Traces of HNO_3 were readily removed by reaction with formic acid; however, with 0.02 M HNO_3 present a tenfold excess of formic acid did not break passivation in less than 1 hr.

Uranium and thorium losses to the decladding solution were generally lower than in the Darex process. Losses from intact CETR fuel (80 to 85% of theoretical density) were independent of irradiation level up to 445 Mwd/metric ton of core. Uranium and thorium losses in 2 to 3 hr decladding for the unfragmented pellets were 0.07 to 0.44% and 0.04 to 0.33%, respectively (Table 1.3). Experiments 1–3 and 5–8 were conducted at Battelle Memorial Institute.[5] When the fuel pellets shattered, losses were

---

[5]R. A. Ewing, H. B. Brugger and D. N. Sunderman, BMI-1427.

Table 1.3. Uranium and Thorium Losses in Decladding of Low-Density Consolidated Edison Fuel Specimens with Boiling 6 M H_2SO_4

Pellets: 95% ThO_2–5% U_3O_8, 80 to 85% of theoretical density

Run No.	Irradiation Level (Mwd/metric ton core)	Decladding Time (hr)	Losses (%)	
			U	Th
1	0	3	0.31	0.05
2	0	4	0.35	0.03
3	0	6	0.39	0.04
4	47	2	0.34	0.33
5	175	3	0.12	0.07
		6	0.30	0.12
6*	195	3	0.77	0.51
		6	0.69	0.43
		8	1.8	1.2
7*	200	3	0.26	0.12
		6	1.6	0.70
8	300	3	0.21	0.10
		6	1.6	0.81
9	318	2	0.44	0.04
10	403	2	0.32	0.24
11	445	2	0.07	0.25

*Core pellets shattered in these runs.

as high as 1.8%. Losses were about an order of magnitude lower from unirradiated pellets whose density was 94% of theoretical. As in the Darex work, unirradiated 93%-dense CETR fuel was exposed to boiling decladding solutions in both the presence and absence of a 1-w/liter Co^{60} gamma-radiation field to determine the effect of radiation on losses. The effect of air inleakage was also determined in the control samples. After 30 hr of contact with the decladding solution with air excluded, the uranium loss was 0.12% for the control and 0.18% for the irradiated sample; corresponding thorium losses were 0.04 and 0.05%, respectively. The uranium loss at 30 hr increased from 0.12% with air excluded to 0.3% with air present; corresponding thorium losses were 0.08 and 0.12%, respectively.

The solubility of stainless steel in H_2SO_4 at 25°C was determined in order to aid in evaluating Sulfex-decladding-waste characteristics. The solubility decreased with increasing H^+ concentration, from 70 g/liter at 8 N H^+ to 40 g/liter at 10 N H^+ (Fig. 1.1).

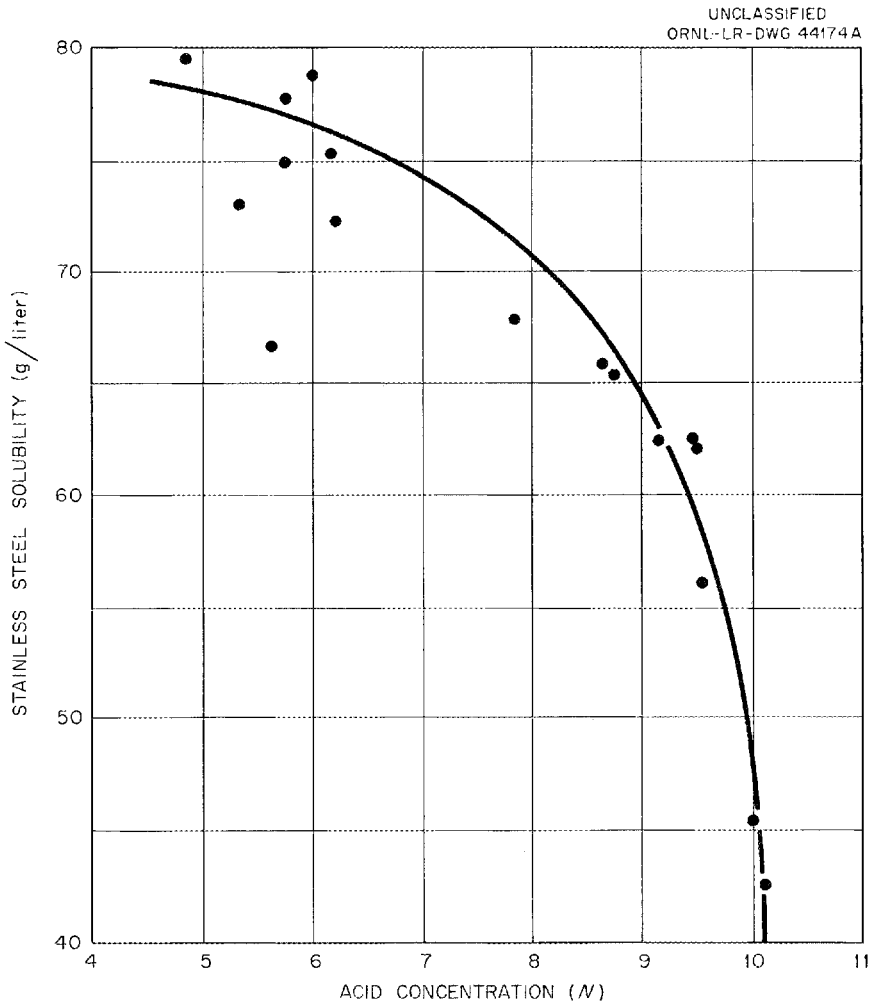

Fig. 1.1. Solubility of Type 304L Stainless Steel in H_2SO_4 at 25°C.

ThO_2-UO_2 Dissolution

The ThO_2-UO_2 fuel pellets can be dissolved in either boiling Thorex dissolvent [13 M HNO_3–0.04 M NaF–0 to 0.1 M $Al(NO_3)_3$] or Darex decladding solution which has been stripped free of chloride and adjusted to 0.04 M NaF–0 to 0.1 M Al^{+++} and 12 to 13 M H^+. The optimum fluoride concentration is 0.07 M, but 0.04 M F^- is used as the flowsheet value to minimize equipment corrosion. Aluminum is added to complex the fluoride ion to

further decrease corrosion; in titanium equipment for Darex, 0.04 M Al^{+++} is sufficient to give adequate protection, but in Ni-o-nel equipment for Sulfex 0.1 M Al^{+++} is necessary. As a result of these aluminum requirements, the ThO_2-UO_2 dissolution rate is slightly lower in the Sulfex process.

The rate of dissolution of ThO_2-UO_2 in Thorex dissolvent [13 M HNO_3–0.04 M NaF–0.1 M $Al(NO_3)_3$] was controlled chiefly by pellet density, the highest rates being achieved with low-density material. The initial (10 min) dissolving rate in 200% excess of dissolvent varied from 16 mg min^{-1} cm^{-2} for pellets whose density was 60% of theoretical to 2 mg min^{-1} cm^{-2} for material whose density was 94% of theoretical (Fig. 1.2). These data

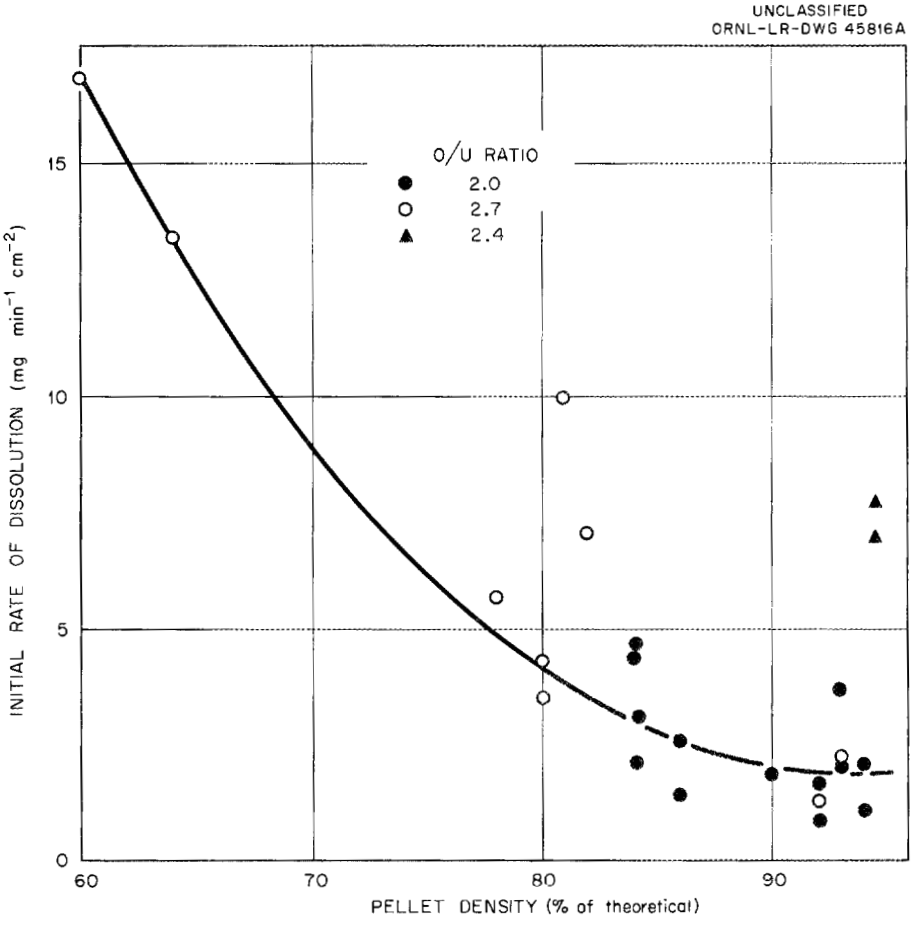

Fig. 1.2. Initial Rate of Dissolution of 95% Thorium Oxide–Uranium Oxide Pellets in 200% Excess of Boiling Thorex Dissolvent. The O/U ratio does not appear to be a major variable affecting the dissolution rate.

indicate a 15-hr dissolution period for CETR fuel 80% of theoretical density and 50 hr for fuel 94% of theoretical density. At constant fuel density the initial dissolution rate was independent of UO_2 content up to 10%.

A series of tests was run to determine the instantaneous dissolution rates of 95.6% ThO_2–UO_2 pellets (~95% of theoretical density) in 8 to 18 $\underline{M}$ HNO_3–0.04 $\underline{M}$ NaF–0.1 $\underline{M}$ $Al(NO_3)_3$ containing 0.02 to 1.0 $\underline{M}$ $Th(NO_3)_4$. These data fit the empirical equation

$$R = 0.627\left(\frac{\underline{M}_{HNO_3}}{10}\right)^3 - 0.336\left(\frac{\underline{M}_{HNO_3}}{10}\right)^4 - 0.12\,\underline{M}_{Th}\left(\frac{\underline{M}_{HNO_3}}{10}\right)^3$$

where R = dissolution rate in mg min^{-1} cm^{-2} and $\underline{M}$ is the molarity of the thorium and the HNO_3. In these tests, 14 $\underline{M}$ HNO_3 gave the highest rates; rates always decreased with increasing thorium concentrations.

In dissolution tests with irradiated CETR fuel samples, the amounts of gross gamma and beta activity in the off-gas were 0.34 and 0.91% of the total activity, respectively; the principal gamma activities were zirconium, niobium, and cesium; no appreciable ruthenium was noted.

The product of CETR fuel dissolution contains 1 $\underline{M}$ $Th(NO_3)_4$ and 9 $\underline{M}$ HNO_3, and it must be adjusted to 1.8 $\underline{M}$ thorium and 0.15 $\underline{M}$ acid deficiency for solvent extraction. This has been done by evaporating the solution until its temperature reached 155°C, but corrosion of the type 309 SNb stainless steel feed adjustment equipment is severe, and operational control is difficult. Satisfactory feed was prepared by evaporating the fuel solution until its temperature reached 135°C (3.3 $\underline{M}$ thorium and 3 $\underline{M}$ HNO_3) and then removing the remaining acid by steam stripping. A quantity of steam equal to 30% of the volume of the original fuel solution was required.

Darex Cyclic Tests on CETR Fuel

Tests conducted in a 1-in.-dia glass tube dissolver showed the feasibility of operating a Darex-Thorex cycle (Fig. 1.3) with about 10% mixed-oxide heel. Results of a four-cycle run (Table 1.4) showed that the Th/U mole ratio in the fuel solution remained constant, and the uranium losses to the decladding solution with a 10% oxide heel from the previous core dissolving were about 0.1%. In four cycles, the accumulated heel did not

Table 1.4. Darex-Thorex Cyclic Dissolution of ThO_2-UO_2 Pellets in 1-in.-dia Glass Dissolver

ThO_2-UO_2 pellet density: 90 to 95% of theoretical
Fuel charged in batches; dissolvent circulated for both decladding and dissolution

Cycle	100 × Ratio of ThO_2-UO_2 Remaining in Dissolver to Amount Charged	ThO_2-UO_2 (%)		Final Product Conc. (g/liter)		Dissolution Rate (mg min^{-1} cm^{-2})	U Loss in Decladding (%)
		Dissolved	Heel	Stainless Steel	Thorium		
1st decladding	110.9			62		17.0	0.11
1st core dissolution	110.9	93.6	6.4		166	2.82	
2nd decladding	106.5			64		17.2	0.09
2nd core dissolution	106.5	92.2	7.8		155	2.67	
3rd decladding	107.7			59		19.4	0.04
3rd core dissolution	107.7	91.0	9.0		156	2.65	
4th core dissolution*	110.2	90.7	9.3		158	2.74	

*Data for the fourth decladding are omitted, since operating difficulties during this cycle resulted in questionable data.

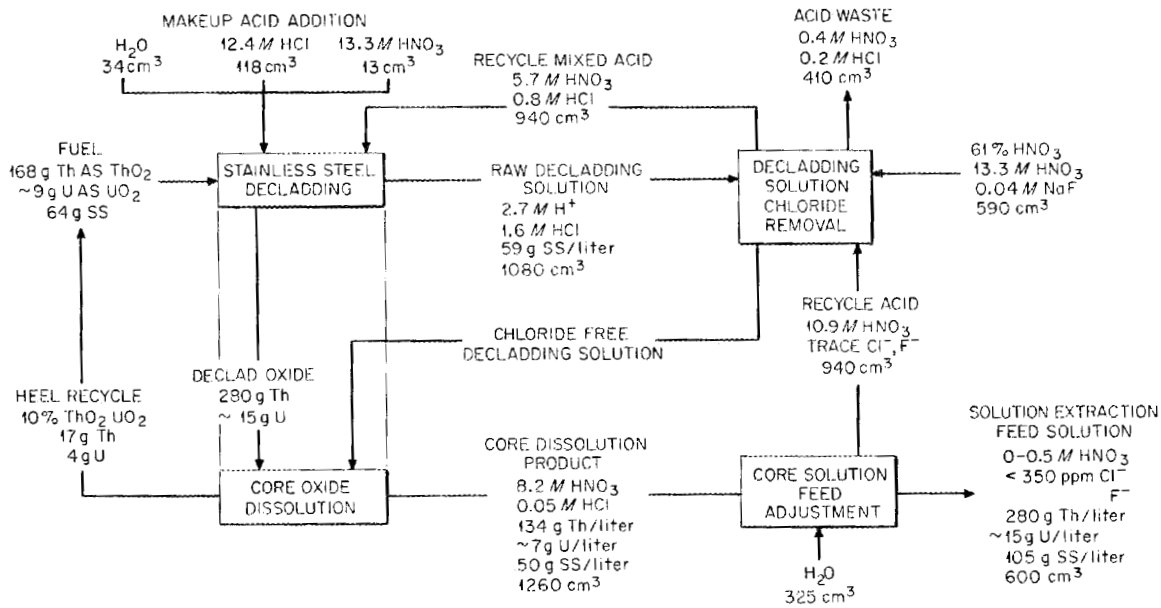

Fig. 1.3. Darex Flowsheet for CETR Fuel.

exceed 10% of the amount of fuel charged per cycle. Each core dissolution period was 8 hr. Although the flowsheet (Fig. 1.3) stipulates chloride-free fluoride-catalyzed decladding solution as the dissolvent, standard Thorex reagent was used so that the data could be compared with those from cyclic Sulfex-Thorex runs. The decladding solution was metered to the dissolver and contacted the cladding only once. All the core dissolvent was added initially and was recirculated around a dissolver-surge tank circuit. However, a plant-scale dissolver would be too small, for criticality reasons, to hold more than a fraction of the dissolvent required.

Sulfex Cyclic Tests on CETR Fuel

Semicontinuous engineering-scale equipment (Fig. 1.4) (4% of proposed ORNL pilot-plant scale) was fabricated from Ni-o-nel, Carpenter 20 stainless steel, and glass and was used to evaluate cyclic operation of the Sulfex-Thorex and Sulfex-Purex head-end flowsheets. The dissolver was a Pyrex pipe, 4 in. in diameter and 19 ft high. Preliminary runs with type 304L stainless steel plate and tubing scrap were followed by runs on unirradiated simulated CETR (ThO_2-UO_2) fuel.

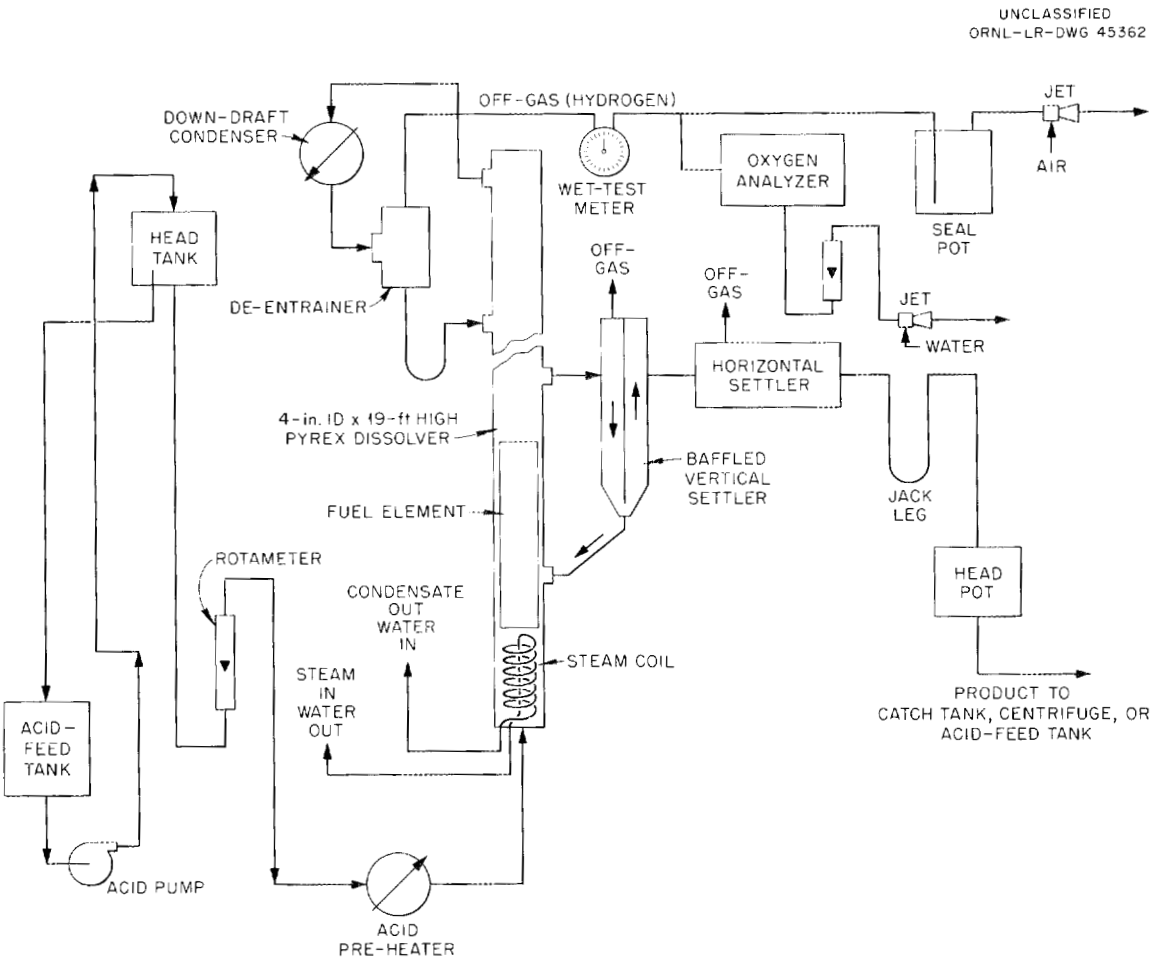

Fig. 1.4. Schematic Diagram of Semicontinuous Sulfex Equipment.

In the preliminary tests with stainless steel and boiling 4 to 6 M H_2SO_4, foaming was vigorous at the aqueous-metal interfaces, but the foam collapsed readily in the space above the reaction zone. The reaction rates for various F/S ratios (dissolvent flow rate/reacting metal surface area) were as follows:

Metal Sample	H_2SO_4 Dissolvent (M)	F/S Ratio (cm/min)	Rate (mg min^{-1} cm^{-2})	Av Stainless Steel Loading (g/liter)
Type 304 stainless steel plate	4	0.021–0.043	1.45–3.0	67
	6	0.014–0.055	0.75–3.1	57
Type 304 stainless steel tubing, 0.5 in. in diameter	4	0.034–0.08	1.1–2.25	29

The reaction rate, particularly with tubing, varied markedly from tube to tube and even in different parts of a single tube, all from the same melt.

Measurement of the hydrogen evolution was a satisfactory way of determining the reaction rate and the reaction completion. The average hydrogen generation rate was 1.1 to 1.2 g-moles/g-mole of stainless steel dissolved, which agrees well with that expected. Although the instantaneous hydrogen evolution rate fluctuated markedly, the cumulative rate was quite even. The dissolution rate decreased throughout the reaction and fell rapidly to zero at completion of the reaction.

The stainless steel dissolution product contained 0.2 to 1.0% insolubles, which were easily attrited by pumping and stirring and could be eliminated by centrifugation. The original solids were essentially all $> 1\ \mu$ in size; after attrition, 20 to 50% were $< 1\ \mu$ in size. The solids were largely composed of silica and iron (Fe_3O_4) but contained ~15% copper, probably from the corrosion of the Ni-o-nel and Carpenter 20 equipment.

A simple pneumatic density indicator was tested and found useful in determining the buildup of fuel oxides in equipment, which is both a criticality and operational control problem. This device permits satisfactory discrimination between highly hydrated silica and fuel oxide present.

In a series of four cyclic Sulfex-Thorex runs, the method of operation was similar to that described above for the Darex-Thorex runs in the 1-in.-dia glass dissolver. The stainless steel was passive to the boiling 4 M H_2SO_4 in the second and third runs, but draining of this acid and admission of fresh acid overcame passivity immediately, presumably by elimination of residual HNO_3. In the fourth run, the H_2SO_4 was made 0.1 M in HCOOH, and dissolution started immediately. Decladding times varied from 3 to 4 hr; stainless steel solution concentrations varied from 26 to 35 g/liter (Table 1.5). Uranium and thorium losses were less than 0.1 and 0.25%, respectively, in each run. Core dissolution times were approximately 10 hr in each run; the core dissolvent was recirculated until the densities of the solutions entering and leaving the dissolver were equal. Unlike the case for Darex experiments, in which the heel remained fairly constant, the amount of heel increased over four cycles to about 20% of

Table 1.5. Data from Sulfex-Thorex Cyclic Runs in 4-in.-dia Engineering-Scale Dissolver

ThO_2-UO_2 pellet density: 90 to 95% of theoretical
Fuel charged in batches; dissolvent circulated for both decladding and dissolution

Cycle	100 × Ratio of ThO_2-UO_2 Remaining in Dissolver to Amount Charged	ThO_2-UO_2 (%)		Final Product Conc. (g/liter)			Dissolution Rate (mg min^{-1} cm^{-2})	Decladding Loss (%)	
		Dissolved	Heel	Stainless Steel	Thorium	Uranium		Thorium	Uranium
1st decladding	100			26.9			2.27	0.022	0.017
1st core dissolution	100	89.5	10.5		83	4.5	1.9		
2nd decladding	110.5			35			1.64	0.08	0.10
2nd core dissolution	110.5	91.2	8.8		141	7.6	2.2		
3rd decladding	108.8			33.3			2.00	0.2	0.02
3rd core dissolution	108.8	86	14		126	6.8	1.9		
4th decladding	114			26			1.70	0.25	0.04
4th core dissolution	114	80	20		137	7.7	2.05		
Heel cleanout (24 hr)	20	99.2	0.02						

the total ThO_2-UO_2 charged per run. At the end of the fourth run, a 24-hr heel cleanout with fresh dissolvent was made; only 0.02% of the ThO_2-UO_2 charged over the four runs remained (Table 1.5).

Darex Processing of UO_2 Fuels

Darex is a total dissolution process for stainless-steel-clad UO_2 fuels such as those used in the Yankee and NSMR reactors and for UO_2-stainless steel cermet fuels of the APPR type. After the fuel is dissolved in 5 M HNO_3–2 M HCl, the chloride is removed by boiling and increasing the HNO_3 concentration to 10–12 M. The chloride-free product is adjusted for solvent extraction. For some fuels centrifugation is necessary to remove siliceous materials.

Engineering-scale demonstrations of the flowsheet,[6] reported last year, were made in titanium equipment on unirradiated NSMR and Yankee Atomic prototype fuel and on Cr-U-Ni fuel. The only flowsheet change required was a slight decrease in the amount of HNO_3 required for chloride removal over APPR conditions; successful chloride removal to < 100 ppm was achieved uniformly. With the Cr-U-Ni fuel, chloride removal was sufficiently improved in the absence of Fe^{+++} to permit omission of the HNO_3 recycle step.

Heat transfer coefficients in a boiling natural-convection titanium steam-heated loop were:

Fuel Solution	ΔT (°F)	U [Btu hr^{-1} ft^{-2} $(°F)^{-1}$]
APPR, NSMR, and Yankee	22–64	170–320
Cr-U-Ni	30–68	310–428
Water	30–68	350–460

In two Darex tests on WACP Yankee fuel samples irradiated to 16,100 and 7500 Mwd/ton and decayed 150 and 480 days, respectively, dissolution was complete in 20 min. In the first test, chloride was removed to 160 ppm and in the second to 490. Chloride removal was limited by the type

[6] Chem. Tech. Ann. Prog. Rep. Aug. 31, 1959, ORNL-2788, Fig. 1.3, p 6.

of equipment used. The distribution of total radioactivity in the three boildown overheads was as follows:

	Radioactivity (% of Total)					
	Test 1				Test 2	
	β-γ	β	γ	Ru	β-γ	Ru
Waste acid cut		0.15	0.24		0.004	
Mixed acid recycle	0.06			0.10	0.02	0.1
Nitric acid recycle	0.02			0.01	0.02	0.4

Since there has been some question about the complete solubility of PuO_2 in the Darex dissolvent, a careful study of this problem was made on the Yankee sample irradiated to 16,100 Mwd/ton. The amount of plutonium at discharge was calculated to be 3400 g/ton in the absence of resonance neutrons and 4200 g/ton with them present. Chemical analysis of the dissolver solution showed a plutonium content of 3430 g/ton, ±10%. This result, plus the absence of any observable solids in the dissolver solution, tends to confirm the complete solubilization of PuO_2 in 5 M HNO_3–2 M HCl.

The removal of insoluble, highly hydrated (97% water) siliceous material (produced during Darex dissolution and chloride removal) from APPR fuel solution by centrifugation at 2180 rpm (800g) in a 12-in.-dia bowl centrifuge was evaluated. Separation, washing, and reslurrying of the solids were all done satisfactorily. Particle size, assuming a density of 2.2 g/cc, was determined by Stokes' settling and neutron activation analysis to be 90 wt % $< 10\ \mu$ and 2 wt % $< 1\ \mu$. Very little attrition was produced by pumping and centrifugation.

Centrifuge cakes up to 3/8 in. in thickness were easily dislodged and mixed with wash water by mechanical braking from 2180 to 0 rpm in 5 sec. Soluble uranium remaining in the cake after successive washes followed the values predicted from simple dilution-decantation theory. Losses after

n washes are represented by

$$\left(\frac{Y_n}{Y_0}\right) = (1 - F)^{n+1} \quad ,$$

where n = total number of washes, Y = weight of uranium, and F = volume fraction skimmed.

Darex Processing of NaK-Bonded Fuels

In four tests to determine the violence of the reaction between 5 M HNO_3–2 M HCl and NaK (or sodium) used as a bond in PRDC blanket and CPPD fuel, only flames were produced. In a fifth test, an explosion completely shattered the 3-in.-dia glass-pipe dissolver. In these tests, stainless steel tubing (0.4-in.-dia, 10-mil-thick wall) was loaded with 5 cc of NaK, and a NaK annulus was produced by inserting a close-fitting glass rod before the upper tube ends were sealed. The rods were then placed beneath 1 ft of dissolvent, behind a blast shield, for the reaction to take place. It has been decided that at ORNL all NaK- or sodium-bonded fuels must be mechanically declad and the NaK reacted with steam or caustic prior to chemical processing.

Darex Corrosion Studies

Titanium is the construction material selected for the Darex-Thorex system. In boiling 13 M HNO_3–0.04 M NaF containing 0.004 M Fe^{+++} and 100 ppm of chloride, titanium was corroded at a rate of 8 mils/month. The addition of ~0.2 M boron, a criticality poison, decreased corrosion to 4 mils/month. Addition of 0.1 M Al^{+++} or Th^{4+} decreased corrosion to 0.5 mil/month, but further addition of either metal resulted in a slight pitting attack not considered serious. At appreciable aluminum or thorium concentrations the corrosion inhibiting effect of borate ion was negated.

In boildown tests of thorium-uranium fuel solutions prepared with the above dissolvent, titanium corrosion was serious at and near the bottom of the condenser at total reflux; however, over 35 boildown cycles, in each of which the volume was decreased by a factor of 3.3, without reflux, attack was negligible after 130 hr of exposure. In order to determine more exactly the conditions of severest condenser corrosion, various

HNO_3-HF mixtures were boiled at total reflux. The corrosion rate at any constant HNO_3 concentration (in the range 3 to 5 M) increased at a rate slightly less than the logarithm of the fluoride ion concentration in the range 0.003 to 0.05 M fluoride. At any constant fluoride concentrations (in the range 0.003 to 0.05 M) corrosion was maximum at 6 M HNO_3. The maximum rate, 1000 mils/month, was with 6 M HNO_3–0.05 M HF; the lowest was 2.2 mils/month with 15 M HNO_3–0.003 M HF. In similar tests with type 309 SNb stainless steel, the maximum rate was 56 mils/month in 15 M HNO_3–0.05 M F^-, and the minimum was 1 mil/month in 3 M HNO_3–0.005 M HF. The maximum corrosion rates to be expected from the above data as applied to actual Darex boildown conditions are < 1 mil/month for titanium at the start of boildown when the condensate is 6 M HNO_3–0.0015 M HF, and 4 mils/month for 309 SNb stainless steel during the period when the condensate is 13.5 M HNO_3 and a maximum of 0.0017 M F^-.

In cyclic tests in boiling the beginning and final Darex-Thorex adjusted cladding solution, the maximum rate of titanium corrosion over 41 cycles was 0.06 mil/month. Each cycle included a 3-hr exposure to beginning solution and a 4-hr exposure to final solution.

Sulfex Corrosion Tests

Ni-o-nel has been selected as the material of construction for the Sulfex-Thorex process equipment. Typical corrosion rates of Ni-o-nel in 4 and 6 M H_2SO_4 were 5.3 and 11.5 mils/month; in the presence of 35 g of dissolved stainless steel per liter the rates were decreased to 1.2 and 1.6 mils/month, respectively.

One method being evaluated for depassivation of stainless-steel-clad fuels is initiation of the reaction with boiling concentrated sulfuric acid. In order to evaluate the corrosion of Ni-o-nel under anticipated conditions, samples were contacted with boiling 8, 10, and 12 M H_2SO_4 for 5 min and then diluted to 4 M H_2SO_4 and boiled at the lower concentration for 3 hr. The maximum corrosion rates for the three concentrations after seven cycles were 3.9, 9.5, and 131 mils/month, respectively. In 12 M H_2SO_4 the rates were higher for welded sections and for couples with type 304L stainless steel than for plate Ni-o-nel; no localized corrosion was noted. These tests indicate that a brief exposure to 8 or 10 M but not

to 12 M H_2SO_4 can be tolerated. Trace chloride in sulfuric acid is also being tested as a depassivating agent. Rates for Ni-o-nel varied from 4.4 to 40 mils/month over the range 4 M H_2SO_4–100 ppm Cl^- to 6 M H_2SO_4–1000 ppm Cl^-.

The best Ni-o-nel heat treatment prior to welding, in order to minimize corrosion in Thorex dissolver solution, is at 1800°C and the worst is at 1725°C. All test samples heated to temperatures between 1500 and 1800°C showed some signs of localized corrosion in the heat-affected zone. Welds annealed for 1 to 2 hr at 1850 to 1950°F and quenched showed the least corrosion. A laboratory dissolver used for 25 Sulfex-Thorex cycles showed an over-all corrosion rate of 2.9 mils/month, but localized attack around welds was considerably more severe.

1.2 PROCESSES FOR ZIRCONIUM-CONTAINING FUEL

Several processes for zirconium-containing fuel are being developed at ORNL. Zirflex, an aqueous head-end process proposed by Hanford for the decladding of zirconium-clad UO_2 fuel with NH_4F-NH_4NO_3, has been modified at ORNL and extended to the complete dissolution of zirconium-clad U-Zr and U-Zr-Nb alloy fuels (modified Zirflex processes). Zircex, a nonaqueous head-end process, involves chlorination or hydrochlorination with Cl_2, HCl, or CCl_4-N_2 of a variety of zirconium-containing fuels at 300 to 600°C; zirconium-clad UO_2 (or ThO_2-UO_2) is declad, whereas zirconium-clad U-Zr or U-Zr-Nb alloys are completely reacted. The reaction with aluminum was also studied.

Zirflex Process

Several studies on decladding of PWR blanket elements, Zircaloy-2-clad UO_2, were made to further refine flowsheet conditions. In a series of cyclic decladdings in 6 M NH_4F–1.0 M NH_4NO_3 and core dissolutions in 10 M HNO_3–0.10 to 0.15 M $Al(NO_3)_3$, the Zircaloy-2 end plugs dissolved very slowly in 15 cycles, indicating that an end plug cleanout would be required at the end of a series of runs.[7] Aluminum nitrate was added to

[7] J. L. Swanson, Proc. UN Intern. Conf. Peaceful Uses Atomic Energy, 2nd, Geneva, 1958 17, p 154 (1959).

the UO_2 dissolvent to complex traces of fluoride carried over from decladding. It was necessary to prevent the return of NH_4OH from the condenser to avoid precipitation of $ZrO_2 \cdot 2H_2O$, and the decladding solution had to be diluted to about 0.1 M zirconium with boiling water in order to prevent the gross precipitation of $(NH_4)_3ZrF_7$.

The uranium loss to the decladding solution in tests on unirradiated samples[8] was less than 0.09% (Table 1.6). Uranium losses in three irradiated PWR blanket sample decladdings were in the range 0.03 to 0.11% and independent of irradiation level. Plutonium losses increased slightly

Table 1.6. Uranium and Plutonium Losses in Zirflex Decladding of PWR Blanket Fuel Elements

Decladding time: about 3 hr

Run No.	Burnup (Mwd/ton)	Soluble Losses (%)	
		U	Pu
1	0	0.01	
2	0	0.08	
3	0	0.02	
4	0	0.04	
5	0	0.05	
6	580	0.03	0.05
7	1270	0.11	0.07
8	1750	0.04	0.08

with irradiation level. In these tests the decladding solutions contained 2.2–8.3% of the gross gamma radiation and 0.1–0.6% of the gross beta radiation in the samples. The activity was mainly due to Zr-Nb. The decladding off-gases contained 0.0001% of the gross gamma activity in the sample, principally due to cesium.

Welded specimens of type 309 SNb stainless steel, Ni-o-nel, and vacuum-melted Hastelloy F were corrosion-tested in cyclic Zirflex operation

[8] L. M. Ferris, Zirflex Process for PWR Blanket Fuel. II. Revised Flowsheet, ORNL-2940 (in press).

alternately in boiling 6 M NH_4F–1 M NH_4NO_3 and 10 M HNO_3–0.1 M $Al(NO_3)_3$. Corrosion was maximum in the vapor phase and was constant throughout the test series. Maximum rates for the three alloys were as follows:

Alloy	Number of Cycles	Corrosion Rate (mils/month)
309SNb	18	3.0
Ni-o-nel	23	4.6–5.1
Hastelloy F	5	3.5–5.0

Some weld decay was noted in the Ni-o-nel specimens.

Addition of 0.03 M H_2O_2 to the decladding reagent decreased corrosion by factors of 3 to 10 for all alloys except at the interface for Ni-o-nel, where the rate was 1 to 5 mils/month. The presence of 0.1 M borate in fresh decladding solution decreased the Ni-o-nel corrosion rate by half, but 0.1 to 0.4 M Zr^{4+} negated this effect. At Zr^{4+} concentrations > 0.4 M, the rate decreased to 0.1–1.2 mils/month.

Modified Zirflex Process

A modified Zirflex process[9] was developed to dissolve U-Zr alloy fuel containing up to 10% U. The dissolvent is 5.4 M NH_4F–0.33 M NH_4NO_3 to which sufficient H_2O_2 is added continuously during dissolution to produce a final solution 0.13 M in H_2O_2. During dissolution the free-fluoride/U(VI) mole ratio must be ≧ 80 or reaction ceases. The off-gas is 98.5% NH_3, 1% H_2, 0.3% O_2, and 0.2% N_2. After dissolution, HNO_3 and $Al(NO_3)_3$ are added to provide a solvent extraction feed containing 0.0075 M U, 0.25 M Zr, 1 M Al^{+++}, 2 M F^-, and 1 M HNO_3 (Fig. 1.5).

Zircex Process

The Zircex process involves reaction with gaseous chlorine or chlorides at temperatures of 300 to 600°C. It has been investigated as a decladding

---

[9]T. A. Gens, Modified Zirflex Process for Dissolution of 1-10% U-Zr Alloy Fuels in Aqueous NH_4F-NH_4NO_3-H_2O_2: Laboratory Development, ORNL-2905 (Mar. 4, 1960).

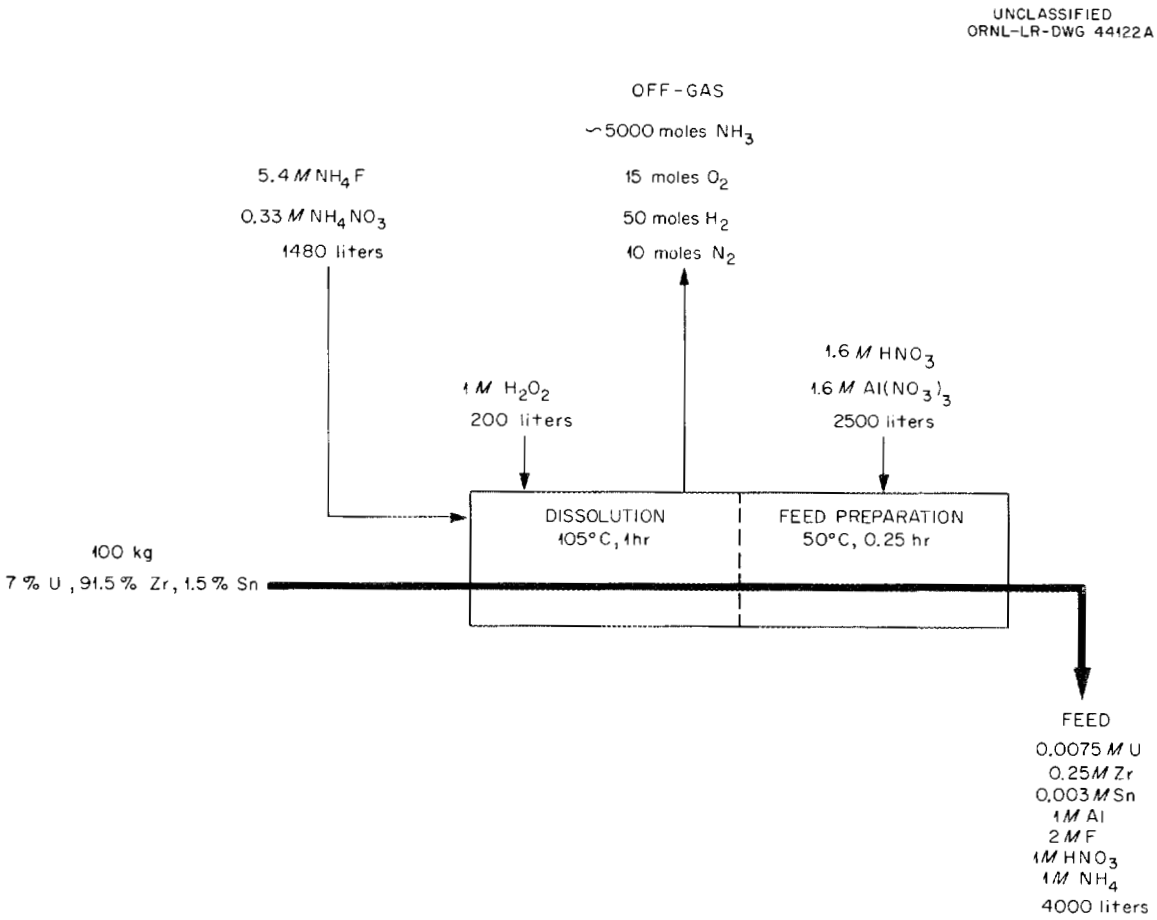

Fig. 1.5. Modified Zirflex Process for Dissolution of 7% Uranium–Zirconium Alloy in NH_4F-H_2O_2.

method for zirconium-clad UO_2 fuels, as a total reaction method for zirconium-clad U-Zr and U-Zr-Nb alloy fuels, and as a reactant for stainless-steel-clad U-Mo fuel previously declad mechanically. A partial or complete gas-phase separation of zirconium, niobium, and molybdenum from the fuel material is effected, thereby avoiding the complicated chemistry encountered in aqueous processes for these fuels. The work on U-Zr and U-Zr-Nb fuel is reviewed below; data on U-Mo fuel are given in Sec 1.3.

Hydrochlorination of STR fuel with HCl at 500 to 600°C to form volatile $ZrCl_4$ and nonvolatile ZrO_2-UO_2-UCl_3 ash, and subsequent chlorination of the ash with CCl_4 vapor at the same temperature to produce volatile $ZrCl_4$ and UCl_4 has been discussed.[10,11] Further work on the similar PWR

[10] Chem. Tech. Ann. Prog. Rep. Aug. 31, 1959, ORNL-2788.

[11] T. A. Gens and R. L. Jolly, New Laboratory Developments in the Zircex Process, ORNL-2992 (in press).

seed (6.3% U–Zr) has shown the feasibility of separating the $ZrCl_4$ and UCl_4 by selective condensation of the latter at 300°C, with a uranium loss of < 0.1%. The $ZrCl_4$ is then desublimed at room temperature. The condensed UCl_4 is either dissolved in HNO_3 and the chloride removed by Darex techniques, or reacted with fluorine at ambient temperature to produce UF_6.

Corrosion tests on 15 possible materials of construction for a cyclic Zircex operation alternating between the use of HCl and CCl_4-N_2 showed that the CCl_4 part of the cycle was the most corrosive and that corrosion rates at 600°C were ≧ 10 times the corrosion rate at 400°C. Rates at 600°C for the better materials – Nichrome V, Inconel, Chloromet-2, and Pyroceram 9608 (a ceramic) – in 1-hr exposure to CCl_4 were 5.5, 18, 32, and 1.0 mils/month, respectively.

Perflex Process Corrosion Studies

The Perflex process[12] involves the dissolution of zirconium-clad U-Zr alloy fuels in HF-H_2O_2 mixtures, which is a very corrosive reagent. Hastelloy C was the best of several alloys evaluated in corrosion tests. In zirconium-free 1 M HF–0.06 M H_2O_2, the corrosion rate was 50 to 55 mils/month, but in the presence of dissolving zirconium the rate decreased to an average of 14 to 18 mils/month during nine dissolution cycles.

1.3 PROCESSES FOR URANIUM-MOLYBDENUM FUELS

The two reactor fuels (CPPD and Detroit-Edison) containing U-Mo alloys are clad in stainless steel and bonded with sodium or NaK. Because of the inherent danger of explosion in direct dissolution of the fuels in acids, plans for processing at ORNL are based on mechanical decladding of the fuels and reaction of the NaK with steam or caustic prior to dissolution. Uranium–3% molybdenum alloy (Detroit-Edison) is dissolved in HNO_3-$Fe(NO_3)_3$ solution, the iron acting as a complexing agent for molybdenum. Fuels containing 10% molybdenum (CPPD) are dissolved in 11 to 13

[12] T. A. Gens and W. E. Clark, Laboratory Development of the Perflex Process for Dissolution of Uranium Alloy Fuels in Hydrofluoric Acid-Hydrogen Peroxide Solutions, ORNL CF-59-11-23 (Nov. 10, 1959).

M HNO_3, and the MoO_3, which is nearly quantitatively precipitated, is removed by centrifugation.

Uranium–3% molybdenum alloy dissolves rapidly in boiling 8 M HNO_3–0.5 M $Fe(NO_3)_3$ (ref 13) to produce a stable dissolver product containing 1 M uranium, 0.074 M molybdenum, 0.5 M Fe^{+++}, and 3.7 M H^+. The molybdenum is solubilized through the complexing action of the iron. The product solution is suitable as a feed for the Purex solvent extraction process for uranium decontamination. However, the first-cycle solvent extraction waste volumes are high because of the low solubility of molybdenum. The solubility of molybdenum vs HNO_3 and Fe^{+++} concentrations is given in Fig. 1.6. By careful adjustment of the acidity to about 0.5 M in a solution containing 0.5 M iron, the molybdenum can be concentrated to 0.25 M. Even then 1100 gal of waste solution will be generated for each ton of uranium processed. The only other means of achieving volume reduction appears to involve neutralizing the waste, centrifuging the precipitated $Fe(OH)_3$ from the soluble molybdates, redissolving the iron in HNO_3, and adjusting the separated iron and molybdenum solutions to 1.5 M Fe^{+++} and 2 M molybdenum, respectively.

The dissolution of U–10% Mo fuel in 11 to 13 M HNO_3 produces a MoO_3 precipitate equivalent in volume to 30% of the dissolver solution volume; it absorbs up to 10% of the soluble uranium and plutonium. The bulk of the uranium and plutonium can be recovered by exhaustive acid washing of the centrifuge cake; alternatively, the cake can be dissolved in sodium hydroxide which also precipitates the uranium and plutonium as hydrous oxides which are recentrifuged, dissolved in nitric acid, and then combined with the dissolver product which contains ~260 g of uranium per liter. The flowsheet as applied to CPPD fuel is given in Fig. 1.7.

---

[13] Oak Ridge Session of AEC Fuel Processing Symposium at Hanford, Oct. 21 and 22, 1959, p 268, TID-7583.

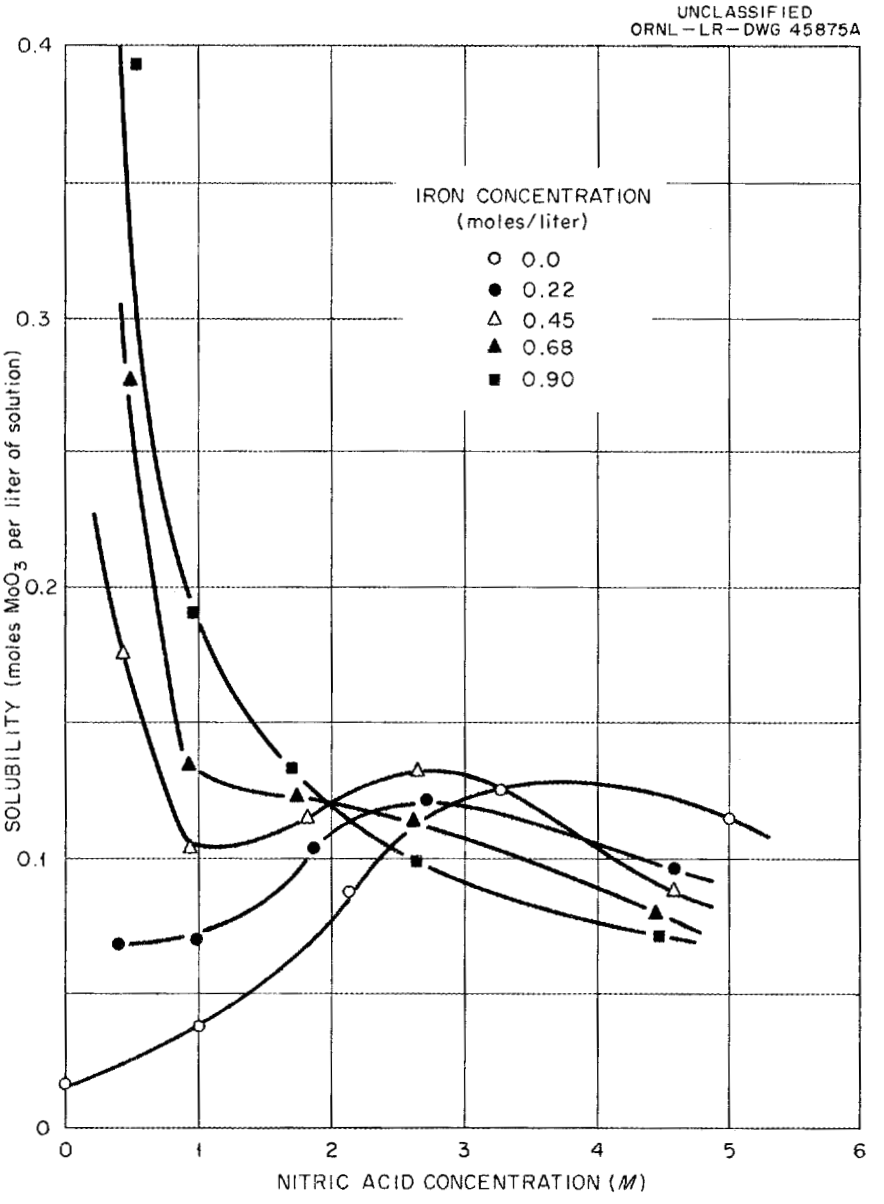

Fig. 1.6. Solubility of $MoO_3 \cdot 2H_2O$ in HNO_3-$Fe(NO_3)_3$ Solutions at 26° C.

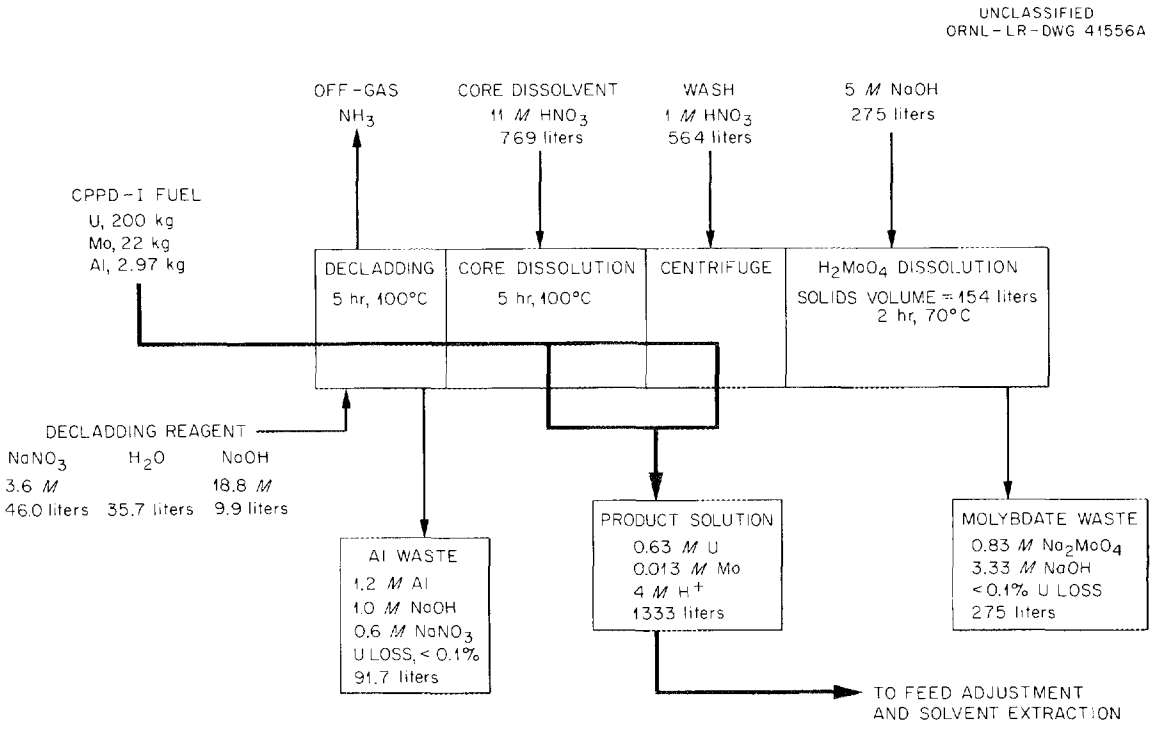

Fig. 1.7. Dissolution of Consumers Public Power Fuel in HNO_3.

1.4 MECHANICAL PROCESSING

Studies on the mechanical dejacketing of NaK-bonded fuels and the shearing and nitric acid leaching of oxide fuels were carried to the non-radioactive pilot plant stage last year.[14] The SRE fuel decladding facility in Cell A of Building 3026 has now been completed and satisfactorily cold-tested. A 250-ton shear for cutting fuel tubes was designed and is being fabricated outside the Laboratory. Several leachers for core material were designed and constructed, and are being cold-tested.

SRE Fuel Decladding

All equipment required for the demonstration of SRE prototype fuel decladding on a scale of ~200 kg of uranium per day for the SRE NaK-bonded Core 1 fuel (~1000 Mwd/t) was installed and cold tested. Layouts were shown in Figs. 1.16 and 1.17 of the last annual report.[14] Major equipment

[14] Chem. Tech. Ann. Prog. Rep. Aug. 31, 1959, ORNL-2788, sec 1.5.

includes two fuel carriers for transport of the fuel from Canoga Park, California, to ORNL; a multipurpose abrasive wheel saw for reduction of the seven-rod assembly to individual rods; a special wire cutter for removing the spiral wire spacer from the rods; roll cutters for opening the fuel tubes; a primary decladder for removing the slugs from the fuel tube (by either hydraulic or mechanical pressure), preparing the fuel slugs for washing, and compacting the residual tubes for discard; a core slug washer; a slug canner; and a NaK reactor. An auxiliary decladder with a longitudinal cutter wheel has also been provided; this device requires the cutting of the fuel rod into 6-in. lengths.

The fuel carriers originally fabricated for transporting PAR loops were modified to carry 10 SRE assemblies. Approval was obtained to use a lattice poisoned with boral (boron-aluminum alloy) for criticality control. The individual assemblies will be canned prior to shipment, and may reach temperatures above 500°F during transit from self-heating. The multipurpose saw alignment and particle collection system worked well, but the hydraulic drive gave trouble; this is being corrected by the vendor. The hydraulic wire cutter worked satisfactorily in remote operation. The 30°-angle roll cutter was tested by making 200 cuts through 10-mil-wall stainless steel tubing; no chipping or scarring of the cutting edges was observed. The primary decladder was also used with only minor difficulties; the collet mechanism was operated over 1000 times and gave no trouble except for a tendency to stick after several days' idleness. Hydraulic expansion of the fuel tubes and removal of slugs were satisfactory at 800–1950 psig; unirradiated 0.79-in.-dia fuel tubes, with a wall thickness of 10 mils, were expanded diametrically 0.5 mil with 800 psig and 365 mils with 1950 psig, the tube bursting pressure. The slugs were easily discharged with a hydraulic pressure of 100 psig. A 100-in.-long screw for use as a slug ramrod if the hydraulic system fails operated moderately well. The tubes, after expansion and slug removal, were easily flattened and rolled into a coil for minimum-volume disposal.

For prevention of NaK fires all operations in the primary decladder are conducted beneath mineral oil. The 100 ml of NaK in each fuel rod is poured from the tube under mineral oil, separated, and reacted, under controlled conditions, with steam in a separate reactor. In laboratory tests

100 ml of NaK contaminated with mineral oil was safely reacted with steam in 23 min. At steam rates of > 3 ml of water equivalent per minute, the NaK began to flash and burn, but at a controllable rate; the reaction was less violent when the NaK was preheated to 100°C. Hydrogen was evolved at a constant rate of 1.86 liters/min for 21 min.

A fuel slug washer is used to steam-clean mineral oil and residual NaK from the declad slugs. The slugs are washed in a basked that rotates to expose all uranium surfaces. The basket is rotated by the steam used for NaK decomposition; 50 psig of steam is required to start rotation but 35 psig maintains it, once established. With 35 psig of steam fed at 182 lb/hr, basket rotation was 1750 rpm; steam was condensed in the 3.27-ft^2 condenser.

Twelve cleaned slugs from each tube are canned in an aluminum can by a commercial canner which has operated satisfactorily. The auxiliary decladder operated satisfactorily, especially after the plow-type tube cutter was replaced with guide rollers and roll cutters.

The facility is ready to test with the SRE Core 1 fuel elements. This will be started as soon as the building alterations required for double containment of all operations are completed in the fall of 1960.

Fuel Shearing

Experimental studies on shearing of multitube stainless steel fuel assemblies, started last year both locally and under subcontract,[15] were concluded. The results of these tests led to the design and fabrication of a 250-ton shear for hot cell use. The shear, now being fabricated by Birdsboro Corporation, will be cold tested in FY 1961, and then installed in Cell A of Building 3026 in FY 1962 for experimental work on a variety of fully irradiated power reactor fuel assemblies.

All cold shear tests were made on the ORNL-designed 36-tube Mark I prototype assemblies, in which the fuel rods are joined with Nicrobrazed ferrules and filled with solid procelain rods to simulate UO_2 and ThO_2-UO_2. The tests were made to determine optimum blade shape, longevity,

---

[15]Subcontracts to Clearing Machine Corporation, Chicago, Illinois, and Birdsboro Corporation, Birdsboro, Pennsylvania.

clearance, wear, velocity, hardness, alloy type, and thrust requirements, and to evaluate production and dislodgement of clad and core fines. Ability to handle brazed ferrules and methods of collecting sheared product were also studied. The two variables that required further evaluation are handling of Kanigan brazed ferrules and means of cutting the last 2–4 in. of the tube bundle. Under optimum conditions the Mark I assemblies can be sheared at a thrust of 80 tons; this is in good agreement with the thrust calculated from Hanford critical shear strength measurements of 9000 psi for porcelain or UO_2 and 57,000 psi for type 347 stainless steel tubing. Extrapolation of these data to stainless-steel-clad UO_2 or ThO_2-UO_2 fuels indicates that a maximum thrust of 270 tons is required for shearing a quarter section of the fuel bundle of the N.S. "Savannah"; 370 tons is required to shear the full N.S. "Savannah" bundle.

The major problems in shearing now appear to be breaking of the tube-ferrule brazed joints and the shear-blade wear and galling caused by fine particles of the hard Nicrobraz alloy. To obtain good tube-ferrule separation the brazed joint must be highly stressed; this occurs only after the blade and anvil are closed and the fuel bundle highly distorted; the separation seems to result mainly from metal tearing rather than shearing.

Shear-blade velocity was varied from 0.5 to 48 ips in cold tests with the prototype fuel. Low blade velocity was superior in all respects except that a slightly smaller amount of oxide fines was formed. Blade wear, galling, and thrust were all minimized at velocities of 0.5–5 ips. At 48 ips wear was excessive after only six cuts, primarily from vastly increased galling which tripled the thrust requirements from ~40 to 110 tons for unferruled Mark I assemblies. Blade-anvil transverse clearances of 1 to 22 mils were tested; low clearances were best, although clearances up to 10 mils appear to be acceptable. Clearances of 1–3 mils are optimum, where Nicrobraz is encountered, to minimize blade galling and chipping. When a blade clearance of 22 mils was used in shearing 35-mil-wall porcelain-filled tubing, excessive wiping of the blades was noted; large clearances cause tearing of metal, which is undesirable. Blade edges, particularly with Nicrobraz present, are easily chipped or broken if kept sharp; rounding to 1/32-in. radius minimizes breakage without significant

loss of performance or efficiency. In the tests performed by Clearing Machine Corporation, a 3% increase in shear power requirement resulted from an increase in blade clearance from 1 to 10 mils, and a 25% increase was noted after rounding of the cutting edges to 1/32-in. radius. In one test with new blades a 7% power increase was noted after 300 cuts. The thrust required at end plug and ferrule cuts was 40 to 100% greater than at other locations. Of the many blade shapes tested, a stepped V blade working against a straight V or semicircular anvil proved optimum. This design ensures minimum thrust (40% less than other designs), minimum wear, maximum dislodgement of core, and best separation of cut tubes from ferrules. With this design a blade life of 10,000–50,000 cuts seems assured.

The amount of porcelain dislodged from 0.5-in. tubes cut to 1-in. lengths varied from 11.9 to 22.6% for the range of conditions tested. Dislodgement was minimum with a 5-mil blade clearance and good gagging of the assembly. About 85% of the dislodged ceramic was < 1700 μ in average diameter and 12–28% was < 100 μ. Under similar shearing operations about 50% of a UO_2 core would be dislodged. About 2.0% of all fines produced were metal fines, of which 18.6% were Nicrobraz particles of Rockwell hardness C 51 or greater. About 0.5% of the Nicrobraz fines were < 3 mils in diameter.

Based on the findings of the many tests made and on the limitations of Cell A of Building 3026, criteria for the fuel shear now being fabricated are:

Type	Hydraulic; horizontal, fabricated of stainless steel, with gag
Tonnage	250 tons
Stroke	Variable, to 9 in.
Number of strokes	1 to 6 per min
Speed	1 to 2 ips
Blade	Stepped punch against vee anvil
Hardness	Rockwell C 56–59
Alloy	Carpenter 610
Clearance	1 to 3 mils
Width	1.5 in.

Leaching

In studies for application to core leaching, the effective surface area of unirradiated UO_2 pellets dissolving in nitric acid was determined as a function of the fraction dissolved by measuring the weight loss of partially dissolved pellets over short periods. The data obtained are expressed by

$$\frac{A}{A_0} = 1 + 47\left(1 - \frac{W}{W_0}\right)^2 - 92\left(1 - \frac{W}{W_0}\right)^3 + 44\left(1 - \frac{W}{W_0}\right)^4$$

in which A and W are the area and weight of pellets at any time, and A_0 and W_0 are the initial superficial area and weight. After a short dissolution time fresh pellets become porous and the effective area is 3–5 times the initial area. The full porosity of a pellet is developed at ~ 35% dissolution. A plot of the data as expressed in the above equation is given in Fig. 1.8. These data are being developed as background for actual chop-leach studies to be performed with the shear now being fabricated; they should not be used to define reaction rates, losses, and other parameters for the chop-leach approach.

Tests were made to evaluate the continuous adjustment of uranium leach solution for solvent extraction by continuous evaporation of excess nitric acid and continuous dilution with water. Evaporation with constant uranium concentration in the still pot was attempted, but operation was difficult when high acid condensate and low H^+/U ratio in the underflow were required (Fig. 1.9). Over-all acid balances checked within 5%.

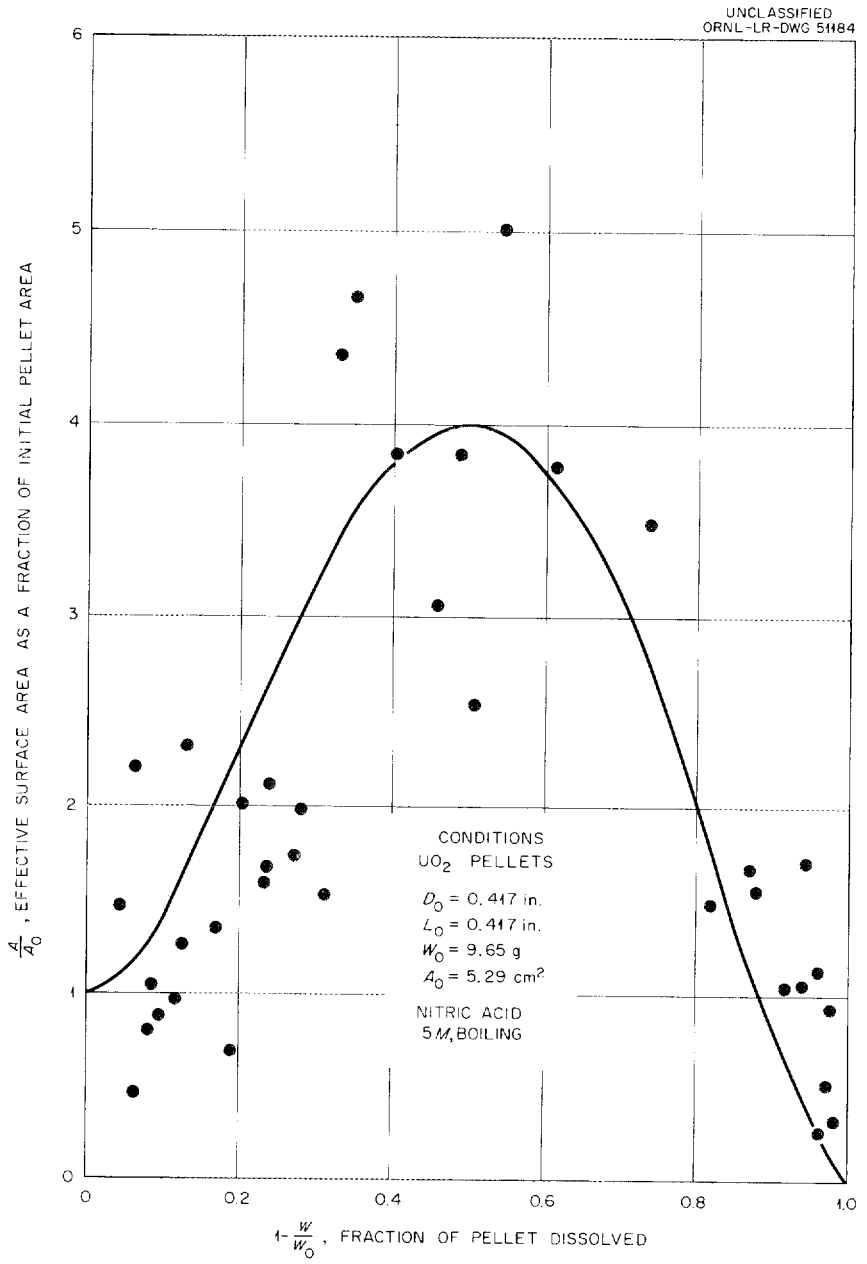

Fig. 1.8. Effective Surface Area of UO_2 Pellets Dissolving in Nitric Acid.

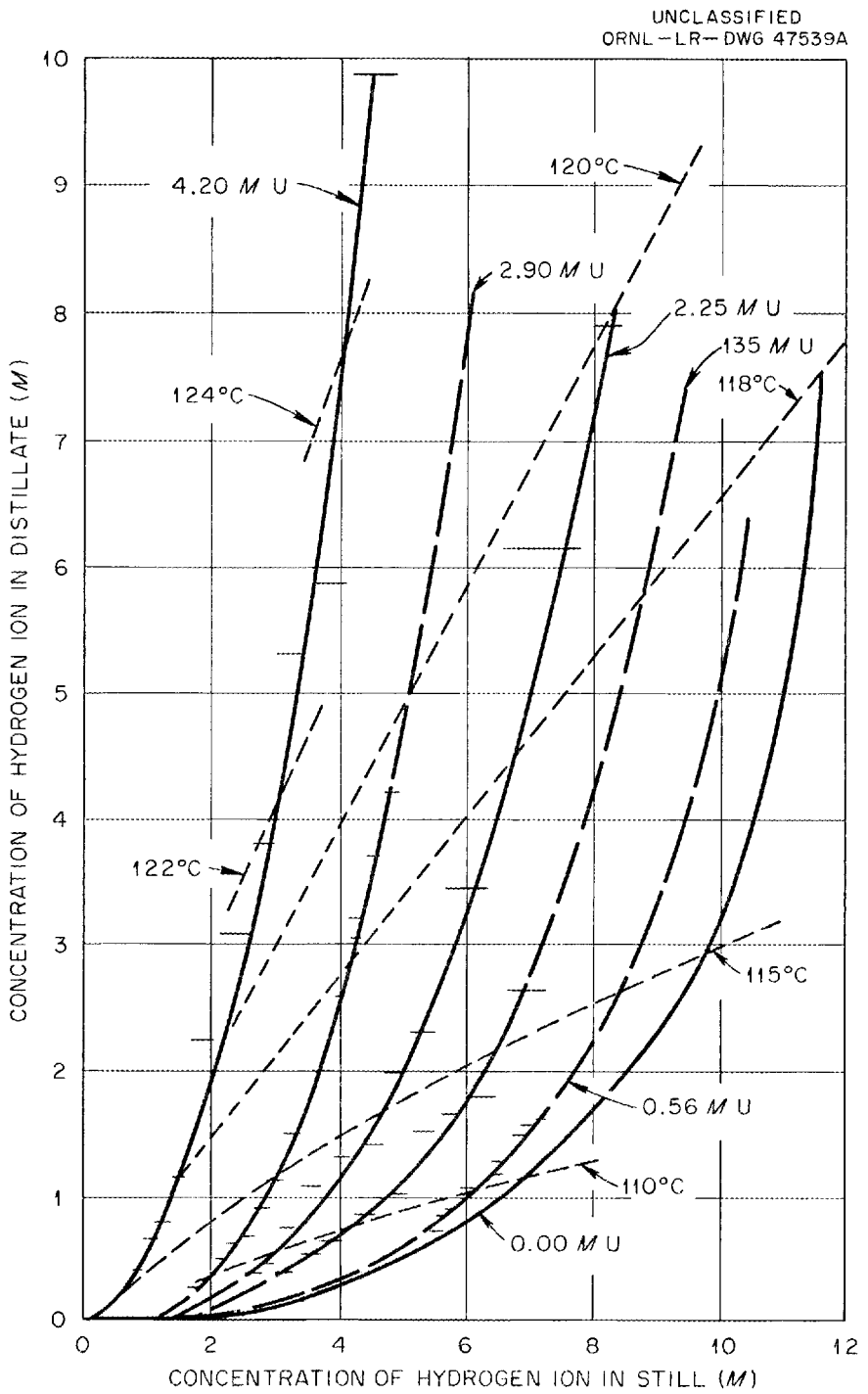

Fig. 1.9. Molarity of Hydrogen Ion in Vapor and Liquid Phases During Distillation of Uranyl Nitrate–Nitric Acid–Water Solutions.

1.5 PROCESSES FOR GRAPHITE-CONTAINING FUELS

Chemical development of processes for uranium-graphite and uranium-thorium-graphite fuels has included investigation of a grind-leach technique, and the use of intercalating agents such as bromine, interhalogens, and fuming nitric acid to disintegrate the fuels prior to acid leaching. Both graphitized and ungraphitized fuels were studied.

The standard grind-leach flowsheet[16,17] includes mechanical reduction of the fuel to −16 mesh, leaching twice with boiling 15.8 M HNO_3, and washing of the graphite residue with water after each leach. Under these conditions the recovery of uranium from graphitized fuels containing ≧ 5% uranium was 99.8%. Fuel with 2–4% uranium had to be ground to −200 mesh to achieve 99% recovery, while losses from fuel with < 2% uranium were > 1% regardless of the fineness of grinding. With ungraphitized fuel, uranium recovery was nearly independent of uranium content and ranged from 99.5 to 99.9% from the −10 +20 mesh Pebble Bed and TREAT fuel samples tested (0.2 to 9% uranium). Leach solutions from ungraphitized fuel were dark red, and in some cases the leaching treatment disintegrated −10 +20 mesh fuel to −100 mesh, probably as a result of nitric acid reaction with the ungraphitized organic binder.

Recovery of thorium and uranium from fuel containing ThO_2 or ThO_2-UO_2 is dependent on the method of preparation. For example, leaching with 15.8 M HNO_3 of ungraphitized −10 +20 mesh Pebble Bed reactor fuel containing high-fired coprecipitated ThO_2-UO_2 (0 to 1% uranium, 6 to 40% thorium) resulted in < 2% uranium and thorium recovery, whereas leaching with Thorex dissolvent [13 M HNO_3–0.04 M NaF–0.1 M $Al(NO_3)_3$] resulted in > 99% uranium and thorium recovery. With graphitized General Atomics HTGR fuel (1.5% uranium, 7% thorium), in which the admixed oxides were converted to the carbides and hydrolyzed gradually in air, leaching in 15.8 M HNO_3 or Thorex dissolvent resulted in recovery of 90% of the uranium and 87% of the thorium from −16 +30 mesh samples. With ThO_2-UO_2 fuels containing admixed UO_2 and

---

[16] M. J. Bradley and L. M. Ferris, Recovery of Uranium and Thorium from Graphite Fuels. I. Laboratory Development of a Grind-Leach Process, ORNL-2761 (Mar. 17, 1960).

[17] M. J. Bradley and L. M. Ferris, Recovery of Uranium and Thorium from Graphite Fuel Elements, ORNL CF-60-1-42 (Jan. 19, 1960).

ThO_2, uranium recovery was independent of ThO_2 concentration, depending only on the uranium concentration in the fuel.

Recent tests with 90% (white fuming) nitric acid showed the chemical feasibility of simultaneous fuel disintegration and leaching of graphitized fuel either at room temperature or the boiling point.[18] For graphitized fuel samples 1.2 cm thick, about 65% of the uranium is recovered in the first step, which is a 4-hr reaction with 90% HNO_3 followed by filtration of the leach solution; another 33% is recovered by three successive cold-water washes (Fig. 1.10). The remainder of the recoverable uranium is

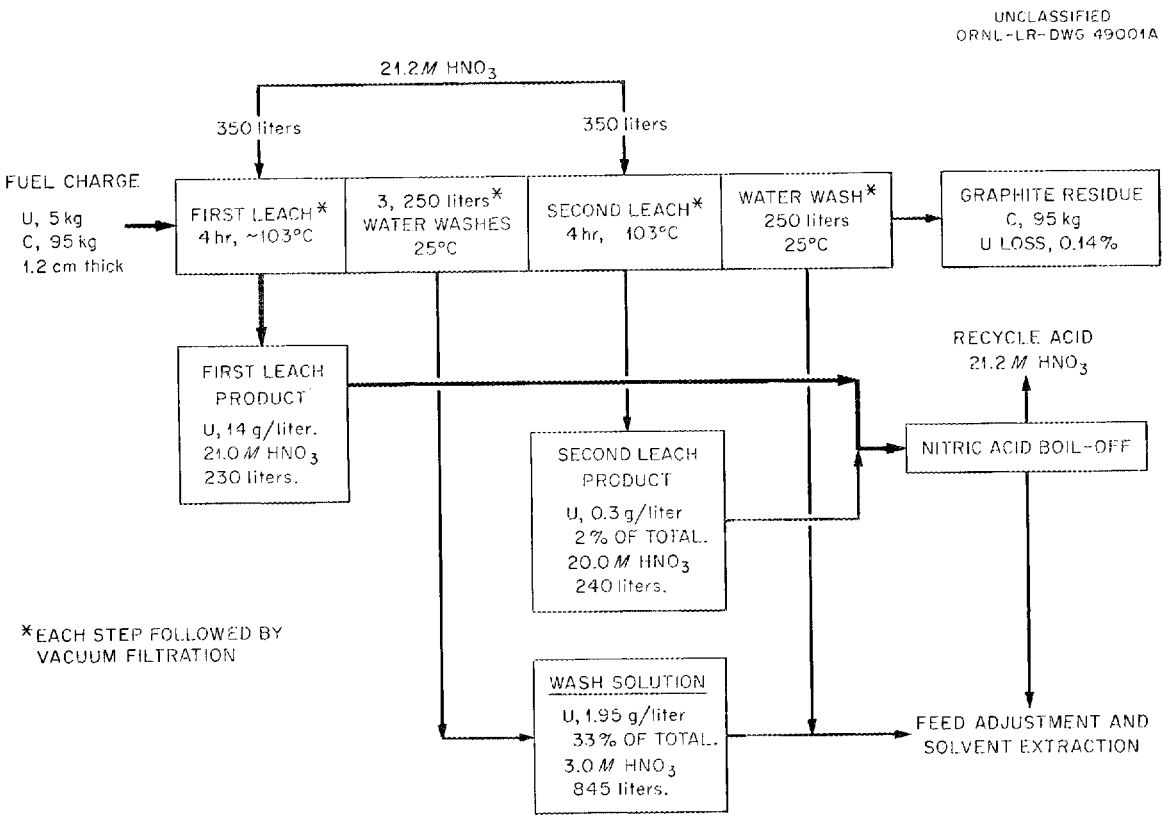

Fig. 1.10. Process for Disintegrating and Leaching Graphitized 5% Uranium–Graphite Fuels with Boiling 90% Nitric Acid.

obtained in a second 90% HNO_3 leach and final water wash. The fuel swells to 3–5 times its original volume, absorbs about 3 ml of acid per gram of fuel, and then crumbles to a powder, 100% −20 mesh and 60% −100 mesh in the first hour of reaction. Longer disintegration times are required for

[18] M. J. Bradley and L. M. Ferris, Recovery of Uranium from Graphite Fuel Elements. III. Disintegration and Leaching with 90% Nitric Acid, ORNL CF-60-3-65 (Mar. 18, 1960).

thicker fuel. The volumes of acid and water used are based solely on the sorptive capacity of the graphite. In order to recover the 90% acid for re-use, the leach solution (which is more concentrated than the 68% azeotrope) is distilled prior to being combined with the wash solutions; when further boildown is required, the condensate is routed to waste.

When fuming nitric acid was used for washing, the first-cycle uranium recovery was slightly less; however, this was compensated for in the second leach, because the acid added to the second cycle was not diluted; recovery of 90% HNO_3 and final feed adjustment are also simplified. Uranium recoveries varied from 99.95% for graphitized fuel containing 13% uranium to ~99% for fuel with 1.5% uranium. With fuel containing ≥ 2% uranium, the uranium recovery was only 0.2% higher at boiling than at 25°C; corrosion at the lower temperature is much less.

Since ungraphitized carbon does not form lamellar compounds, the fuming nitric acid process is not necessarily applicable to ungraphitized fuels. Spheres of admixture ungraphitized Pebble Bed fuel, prepared by National Carbon and Great Lakes Carbon, disintegrated, though at a slower rate than graphitized fuel, but −4 +8 mesh pieces of Si-SiC coated specimens prepared by Minnesota Mining and Manufacturing Company did not.

The major chemical problem with the 90% HNO_3 flowsheet is the possible formation of nitrated organic compounds from the graphite and from organic impurities, which might result in detonations. This is currently being studied.

The use of Br_2, ICl, and IBr as disintegrating agents was studied at 25°C with graphitized fuel specimens in both the intact (0.8 × 4 × 4 cm) and rough ground (−4 +8 mesh) condition (Table 1.7).[19] The interhalogens were better disintegrating agents than Br_2, but subsequent leaching of Br_2-treated samples with 15 M HNO_3 gave superior uranium recovery. The fraction of a 40-g specimen reduced by Br_2 to −20 mesh powder in 4 to 6 hr increased from 0 with electrode graphite to 95% with a sample containing 9% uranium. Bromine and the interhalogens are recovered for recycle either by vacuum distillation before leaching or by fractional distillation of

[19]M. J. Bradley and L. M. Ferris, Recovery of Uranium from Graphite Fuel Elements. II. Disintegration with Bromine and Interhalogens, ORNL CF-60-3-66 (Mar. 18, 1960).

Table 1.7. Comparison of Uranium Recovery from Graphitized Fuels by Grind-Leach, Bromine-Leach, Grind-Bromine-Leach, and 90% HNO_3 Processes

Fuel Composition (%)		Grind-Leach			Bromine-Leach, Samples[d]	Grind-Bromine-Leach, Powder[b]	90% HNO_3, Samples[a]	
U	Th	Samples[a]	Powder[b]	Powder[c]			25°C	Boiling
				Uranium Recovery (%)				
0.7	0	30	80	87	96	97	88	97
2	0		95.8	99.0	99.2	99.2		
2.5	0	28					99.5	99.5
5	0	45	99.77	99.92		99.84	99.53	99.85
9	0		99.82	99.90	99.77	99.84	99.72	99.95
14	0		99.84	99.92		99.80		99.94
1.5	7	78	89	93	95	99		99
				Thorium Recovery (%)				
1.5	7	58	90	90	87	92		93

[a] 1.2 × 1.4 × 4.5 cm.

[b] −4 +8 mesh.

[c] −200 mesh.

[d] 0.7–1.5 cm thick.

the off-gas during leaching. Less than 0.01% of the uranium was solubilized during treatment with Br_2.

In subsequent leaching of Br_2-treated fuel with 15.8 M HNO_3, 99.8% of the uranium was recovered from fuel containing 5–9% uranium (Fig. 1.11). Uranium losses increased sharply with fuels containing < 4% uranium but were consistently lower than grind-leach losses. Uranium losses from ICl-treated fuel containing 10 and 14% uranium were 15 and 3%, respectively.

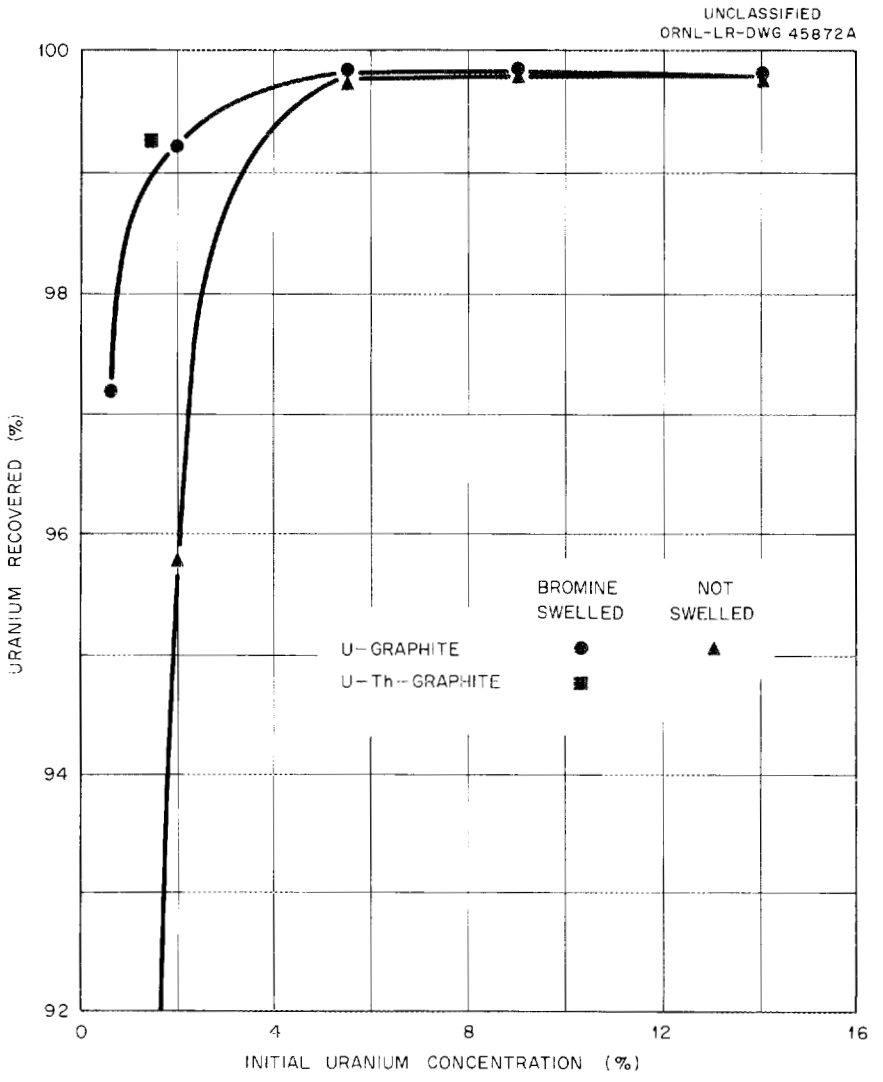

Fig. 1.11. Effect of Bromine Swelling on the Leaching of −4 +8 Mesh Samples of Graphitized Fuel with Two Portions of Boiling 15.8 M HNO_3.

1.6 HERMEX PROCESS

In the Hermex process, irradiated uranium alloys containing > 90% uranium are decontaminated from fission products by extraction with boiling mercury, recrystallization of UHg_4 at 25°C, volatilization of the mercury at 800°C, and subsequent fusion of the uranium.[20-22] The process utilizes the high solubility of uranium relative to that of elements to be separated from it. Solubilities pertinent to the process, thermodynamic properties for the uranium-mercury system, and a corrected phase diagram were determined, and a procedure for application to uranium oxide fuels was studied.

The solubilities of uranium and thorium in mercury from 25 to 356°C were carefully redetermined[23] and compared with that of plutonium as determined by Bowersox and Leary.[24] The solubilities of the rare earths, samarium, neodymium, and gadolinium were also determined. Least-squares plots of the logarithm of solubility (wt %) against the reciprocal of absolute temperature were made; the fitted equations, with standard errors of fit and heats of solution calculated from them, are given in Table 1.8.

The solubilities of several other fission product metals in mercury saturated with uranium were also determined. The solubility of ruthenium varied from 1.2×10^{-3} wt % at 50°C to 1.1×10^{-2} wt % at 356°C, greater by a factor of approximately 10^4 than in uranium-free mercury. Palladium solubility in the same temperature range was 2.1×10^{-5} to 2.4×10^{-4} wt %, about an order of magnitude less than in mercury alone. For zirconium and molybdenum the solubilities were below their limits of detection by the neutron activation method (less than 10^{-5} wt %). The presence of the metals at the above concentrations did not affect the solubility of uranium in mercury.

---

[20] R. E. Blanco, Nuclear Sci. and Eng. 1, 409–19 (1956).

[21] O. C. Dean, Progr. in Nuclear Energy. Ser. III 2, 412–19 (1958).

[22] O. C. Dean et al., Status of the Hermex Process, ORNL-2242 (July 29, 1957).

[23] A. F. Messing and O. C. Dean, Solubilities of Selected Metals in Mercury: Hermex Process, ORNL-2871 (June 15, 1960).

[24] D. F. Bowersox and J. A. Leary, J. Inorg. & Nuclear Chem. 9, 108–12 (1959).

Table 1.8. Solubility Equations and Heats of Solution for Actinides and Lanthanides in Mercury

Element	Solubility Constants*		Heat of Solution** (kcal/g-atom)	Standard Error of Fit
	a	b		
Uranium	2.33	1418.8	6.49	0.01536
Thorium	−0.43	698.5	2.93	0.02046
Plutonium	1.44	954	4.33	
Gadolinium	1.84	1222	5.59	0.03539
Samarium	1.41	1037	4.74	0.07606
Neodymium	1.65	1163	5.36	0.1063

*From solubility equation, $\log (\text{wt } \%) = a - b/T$.

**Calculated from the relation $\frac{d \log \text{wt } \%}{d\ 1/T} = \frac{-\Delta H}{2.303R}$.

Thermodynamic Properties of Uranium Mercurides

The equilibrium vapor pressures of mercury over uranium amalgams as a function of composition were determined for compositions between 50 and 99 at.% mercury and for temperatures from 25 to 431°C. From these data were calculated molal free energies, enthalpies, and entropies of formation of the intermetallic compounds UHg_2, UHg_3, and UHg_4 (ref 25) (see Table 1.9).

Since isothermal vapor pressures were a step function of composition, with sharp discontinuties at the intermetallic compositions, interphase solubilities were considered negligible. A phase diagram (Fig. 1.12) was prepared for the uranium-mercury system at 1 atm, based on the thermodynamic properties presented.

Processing of Uranium Oxide Fuels

A preliminary study was made of a procedure for applying the Hermex process to the decontamination of uranium oxide fuels. Sintered UO_2 pellets

[25] H. C. Forsberg, Thermodynamic Properties of the Uranium Mercurides, ORNL-2885 (Feb. 15, 1960).

Table 1.9. Thermodynamic Properties of Uranium Mercurides

U-Hg Compound	Decomposition Temperature at 1 atm (°C)	ΔF_f Function (kcal/mole)	ΔH_f (kcal/mole)	ΔS_f (kcal/mole)
UHg_2	436	−91.66 − 4.98T	0.0917	4.987
UHg_3	417	−555.47 − 6.31T	0.556	6.311
UHg_4, 25–300°C		−1594.13 − 6.11T	0.1594	6.106
UHg_4, 300–431°C	383	−3777.48 − 2.35T	3.777	2.35

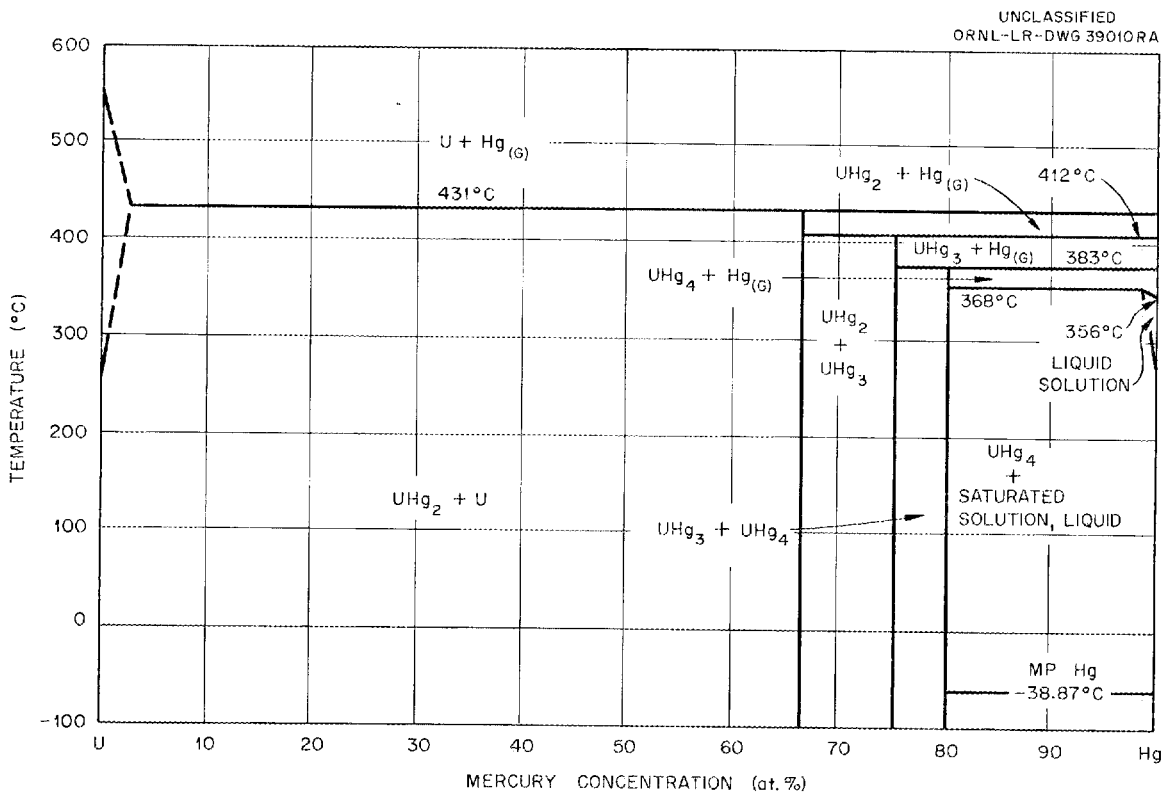

Fig. 1.12. Phase Diagram for the Uranium-Mercury System at 1 atm.

were reduced to uranium by magnesium in the presence of anhydrous magnesium chloride at 1000°C, and the uranium was extracted with mercury. Strontium oxide, rare earth oxides, and magnesium oxide were removed as insoluble dross by filtration at 356°C. The uranium, as UHg_4, was crystallized at 25°C and removed by filtration, leaving the more soluble metals, cesium

and magnesium, in mercury solution. The UHg_4 was converted to UO_2 and mercury by steam at 200°C. Mercury and other volatile impurities were removed from the UO_2 by heating in a stream of hydrogen at 900°C.

In a laboratory test, UO_2 spiked with ruthenium, cesium, and samarium was processed; decontamination factors of > 1000 for ruthenium, 220 for cesium, and 75 for samarium were obtained. Yields from reduction and a single mercury-extraction cycle were as high as 93% of the initial uranium charged.[26]

1.7 SOLVENT EXTRACTION PROCESS DEVELOPMENT

The purpose of this subprogram is to determine the applicability of present solvent extraction processes to the aqueous nitrate feeds prepared by the Darex, Sulfex, Zirflex, and other head-end processes and to develop new processes where required. Parallel work on radiation damage to solvents and the evaluation of new solvents are discussed in Secs 15 and 16, respectively. The major development last year was a new Thorex process for the CETR and other thorium-uranium fuels in which nitric acid is used instead of aluminum as a salting agent. Subsequent waste handling is greatly simplified. High-activity-level flowsheet runs and cold engineering-scale flooding and HETS determinations were made on modified Purex processes for Yankee Atomic and NMSR fuel. The effects of molybdenum for the Detroit Edison blanket and CPPD fuels and of H_3PO_4 from LAPRE-II on solvent extraction performance were evaluated.

CETR Fuel

An improved Thorex process was developed for the CETR and other thorium-uranium fuels (Fig. 1.13). The advantages of the new process over the previous aluminum-salted process are (1) the substitution of nitric acid for aluminum as a salting agent, which permits a tenfold greater volume decrease in the first-cycle waste than was formerly feasible; (2) fission product decontamination factors and thorium and uranium

---

[26]A. F. Messing and O. C. Dean, Processing of High-Fired Uranium Dioxide Fuels by a Reduction–Mercury Extraction–Oxidation Process, ORNL-2909 (July 26, 1960).

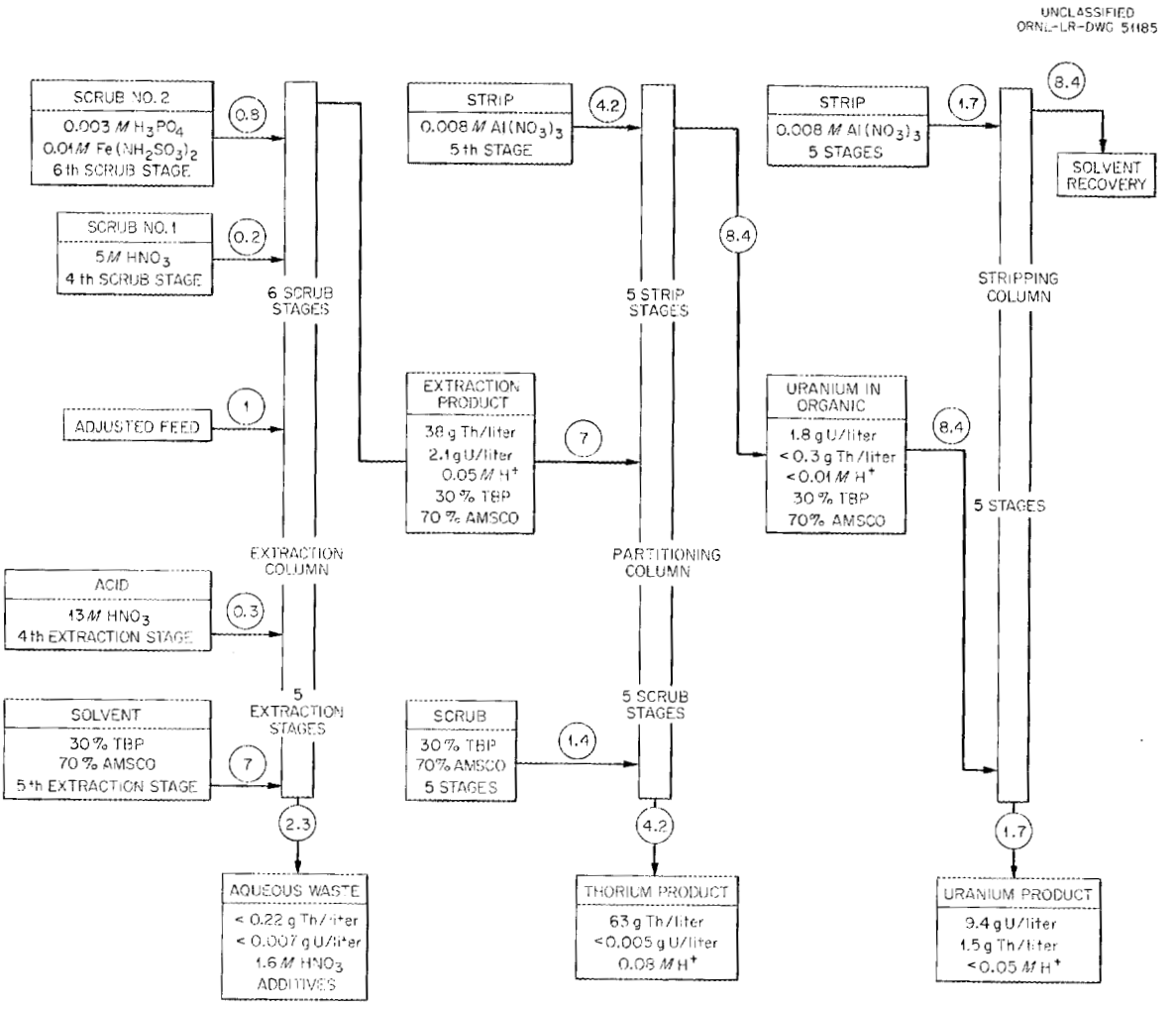

Fig. 1.13. Acid Thorex Flowsheet for Consolidated Edison Fuel.

recoveries equal to or better than those obtained with aluminum salting; and (3) pulsed-column stage heights only 50% of those formerly observed.

In the first cycle, the adjusted feed contains 265 g of thorium and 15 g of uranium per liter, 0.115 M Al^{+++}, 0.046 M F^-, and 0.1 M $NaHSO_3$ and is 0.15 ± 0.05 M acid deficient. The feed is contacted with 30% TBP and scrubbed with nitric acid to co-extract thorium and uranium in the first column. The thorium is partitioned from uranium in the second column with 0.006 M $Al(NO_3)_3$ and the uranium stripped from the solvent with 0.008 M $Al(NO_3)_3$ in the third column. The thorium and uranium are each processed through a second cycle of extraction to achieve sufficient additional cleanup to ensure that the product fission product activities

are ≤ the U^{238} daughter activities. The feed preparation procedure for the new flowsheet was discussed in Sec 1.1.

In the extraction column the use of an acid-deficient feed maintains the fission products as nonextractable species. High distribution coefficients for uranium and thorium are provided at the feed point by thorium salting, and near the bottom of the column, where the thorium concentration is low, by nitric acid addition. The thorium and uranium losses in five extraction stages are < 0.1 and < 0.1%, respectively. Maximum decontamination is obtained with a scrub of 1 M HNO_3; the scrub addition is split to prevent nitric acid carryover to the partitioning column. Under these conditions decontamination factors (DF's) of 10^3, 8×10^3, 10^3, and 2×10^5 were achieved for ruthenium, zirconium-niobium, protactinium, and rare earths, respectively, in countercurrent batch extraction tests.

With an improved thorium-uranium partitioning process it is possible to ensure that < 0.1% of the uranium is lost to the thorium and < 1% of the thorium is lost to the uranium in the partitioning column in 10 theoretical stages by minimizing the volume and the acid in the thorium strip and by decreasing the volume of scrub. Five stages each of scrubbing and stripping are used. The flow capacity of the new Thorex process is governed by flooding in the scrub section of the partitioning column, which occurs at 750 gal ft^{-2} hr^{-1} at 1 in. amplitude and 50 cpm.

In the new Thorex process the uranium is stripped in the third column with 0.008 M $Al(NO_3)_3$ in five theoretical stages. A reflux strip operation was verified in which the uranium product concentration is doubled by refluxing and by withdrawal at a point between the partitioning and strip columns.

Studies were also conducted to develop a co-extraction and stripping first cycle for thorium and uranium from a 30% TBP extraction product in which the HNO_3 concentration varies from 0.02 to 0.2 M. If the maximum stripping loss for uranium is set at 0.1% uranium and stripping with 0.008 M $Al(NO_3)_3$ is to be done in six stages, strip-to-organic ratios of 1.0 and 1.2 are required for organic containing 0.02 and 0.2 M HNO_3, respectively. Uranium is more extractable than thorium and limits the stripping column operation.

The proposed second thorium cycle conditions are similar to the first except that the thorium feed is slightly acid rather than acid deficient. In laboratory tests under these conditions, DF's of 10, 2000, 200, and 2000 were obtained for ruthenium, zirconium-niobium, protactinium, and rare earths, respectively; the thorium loss was 0.02%.

The proposed second uranium cycle is based on the following flowsheet conditions:

Feed	1 volume; 9 g of U per liter, 1 g of Th per liter, 3.5 M HNO_3
Scrub	0.5 volume; 2 M HNO_3
Solvent	1.4 volumes; 5% TBP-Amsco
Extraction stages	6
Scrub stages	4

Under these conditions the uranium loss was 0.02% and the DF's for ruthenium, zirconium-niobium, protactinium, and thorium were 300, 2000, 400, and 10, respectively.

Second-cycle solvent extraction operation has always been complicated by the presence of TBP hydrolysis products produced in intercycle evaporation. These products generally precipitate and decrease decontamination from zirconium-niobium and protactinium. Washing of the first-cycle aqueous product prior to evaporation with 1/50 volume of Amsco in a 5-stage contactor removed 98% of the entrained and dissolved TBP. About 95% of the Amsco and 17% of the TBP were recovered from the used Amsco wash by steam distillation.

Darex-UO_2 Feeds

Two modified Purex runs on irradiated stainless-steel-clad UO_2 fuel solutions prepared by the Darex process were made in "mini" mixer-settler solvent extraction equipment in a hot cell. In the second run a second cycle of solvent extraction was demonstrated in shielded, batch countercurrent extraction equipment. The feed for the first run was a composite of a Darex dissolver solution from the processing of an unirradiated NMSR fuel sample and a Sulfex dissolver solution produced from a Yankee fuel sample irradiated to 1000 Mwd/ton. The Yankee fuel sample had been dissolved in nitric acid 5 months previously. The feed contained, in counts

min^{-1} ml^{-1}, 10^8 gross beta, 6×10^7 gross gamma, and 4×10^5 plutonium alpha. First-cycle uranium and plutonium losses were < 0.01%; DF's for gross beta, gross gamma, zirconium-niobium, ruthenium, and rare earths were 160, 21, 18, and 1700, respectively. The low DF's for all except the rare earths are attributed to the five-month aging of the activity in 2 M HNO_3; the poor rare earth DF is not explained.

The feed for the second run was prepared, using the reference Darex flowsheet, from two WCAP Yankee fuel samples irradiated to 16,100 and 7500 Mwd/ton and decayed 150 and 480 days, respectively. The plutonium valence was adjusted with $NaNO_2$. First-cycle uranium and plutonium losses were < 0.01%. The DF's for gross beta, gross gamma, zirconium-niobium, ruthenium gamma, and total rare earth beta were 9×10^3, 5×10^2, 5×10^2, 8×10^3, and 1.8×10^6, respectively. The low zirconium-niobium DF is attributed to the low saturation (51%) of uranium in the solvent. In the second cycle the uranium loss to the raffinate and plutonium product was < 0.01%; plutonium losses to raffinate and uranium product were 0.5 and 0.4%, respectively. The second-cycle uranium DF's for gross beta and gamma were 81 and 81, respectively; the plutonium DF's were 66 and 6, respectively.

Over-all two-cycle DF's for uranium were 7.4×10^5 and 1.2×10^5 for gross beta and gamma, respectively; the corresponding theoretical values are 3×10^6 and 1.5×10^7.

Since the use of acid-deficient feed and the addition of nitric acid for salting below the feed plate proved so effective in Thorex tests, a similar flowsheet was established and tested for Purex. The conditions were:

Feed	1 volume; 350 g of U per liter, 0.02 M $NaHSO_3$, 0.02 N acid deficient
Scrub	0.7 volume; 1 M HNO_3, 0.004 M H_3PO_4
Acid Salting	1 volume; 13 M HNO_3; added at fourth stage below feed
Extractant	3.5 volumes; 30% TBP Amsco
Extraction stages	5
Scrub stages	8

The uranium DF's for ruthenium and zirconium-niobium were 1.6×10^4 and 2.2×10^4, respectively; plutonium was not extracted. This flowsheet appears best for use in final uranium cleanup after uranium-plutonium partitioning.

Pulsed Column Performance Tests

Engineering-scale pulsed column tests were made with Purex flowsheet conditions for Yankee Atomic or NMSR fuel to obtain comparative performances of sieve, nozzle, and nozzle-zebra plates (alternate plastic and stainless steel sieve plates) operated with the interface either at the top or bottom of the column over a wide range of pulsing conditions. The dimensional data for the plates and the flooding and HETS data obtained are given in Table 1.10.

In the extraction-scrub column the flooding rates are generally limited by the scrub section; only with nozzle plates was an organic-continuous dispersion easily maintained. With sieve plates and a bottom interface, phase inversion to aqueous-continuous occurred in the scrub section at flow rates > 300 gal ft^{-2} hr^{-1}; with a zebra-cartridge scrub section the dispersion was aqueous-continuous in the stainless steel sieve plates and was a double dispersion in the plastic plates. Nozzle plates were less subject to emulsion formation and interface crudding than either zebra or sieve plates when a dilute clay slurry was added to the feed.

In strip column operation the maximum flow capacities were somewhat greater than in extraction columns of equal diameter, and capacities were higher with the interface at the bottom of the column. However, for extraction and stripping columns of equal diameter, the strip column is generally capacity-limiting, since in most flowsheets the total two-phase stripping flow is about twice the total extraction-scrub flow rate.

In both extraction and stripping the HETS values for uranium extraction for sieve plates operated with a bottom interface were unaffected by pulse frequency. In tests with sieve plates operated with a top interface, and with nozzle plates with the interface at either the top or bottom, HETS values decreased with increased pulse frequency.

In other tests the pulsed-column stripping of nitric acid from solvent was used to simulate the scrubbing of fission products from thorium,

Table 1.10. Flooding Capacity and HETS for Pulsed Columns Using Purex-Type Flowsheet

Column	Pulse Frequency (cpm)	Sieve Plate: 0.125-in.-dia Holes, 23% Free Area		Nozzle Plate: 0.125-in.-dia Holes, 10% Free Area		Nozzle Plate: 0.188-in.-dia Holes, 23% Free Area	
		Top Interface	Bottom Interface	Top Interface	Bottom Interface	Top Interface	Bottom Interface
		Flooding (gal ft^{-2} hr^{-1})					
Extraction-scrub	30	890	1130		1160		
	50	790	790		790		1320
	70	470	580		370		1210
Strip	25	1100	1100	1370	1530	1940	1740
	35	920	1100	1120	1370	1740	1940
	50	920	920	550	700	920	1530
		HETS (ft)					
Extraction-scrub	30	2.2	4.5		2.2		3.0
	50	1.8	4.5		2.0		2.6
	70	1.5	4.5				
Strip	25	3.6	1.9	4.5	1.8		
	35	2.9	2.0	2.1	1.5	7.0	4.5
	50	2.1	2.0				

uranium, and plutonium to permit evaluation of the latter under nonradioactive conditions. Studies were made over the aqueous/organic flow range of 1/7 to 1/20; the distribution coefficient for dilute nitric acid vs 30% TBP was ~0.2. Data for the sieve and nozzle plates used in the previous tests (Table 1.10) are:

	Sieve Plates			Nozzle Plates	
Interface	Top	Bottom	Top	Bottom	Bottom
Ratio, A/O	1/7	1/7	1/20	1/7	1/20
HETS, ft	1.3	5.5	3.0	2.4	4.0

These data indicate that nozzle plates are superior to sieve plates in extraction-scrub columns where use of a bottom interface is desired to avoid emulsion and crud formation and carryover.

Uranium Molybdenum Fuels

In order to determine the applicability of the Purex flowsheet to the processing of Detroit Edison blanket (uranium–3% molybdenum) and CPPD (uranium–10% molybdenum) fuel alloys, batch countercurrent solvent extraction tests were run on unirradiated fuel solutions prepared by the two uranium-molybdenum head-end processes described in Sec 1.3. The solutions were spiked with plutonium; the solution concentrations and relative volumes were:

	U–3% Mo	U–10% Mo
Feed	100 volumes; 1.0 M U, 0.074 M Mo, 0.5 M Fe^{+++}, 2.75 M H^+	100 volumes; 0.63 M U, 0.016 M Mo, 3.2 M H^+
Solvent	253 volumes; 30% TBP	155 volumes; 30% TBP
Scrub	51 volumes; 3 M HNO_3	31 volumes; 3 M HNO_3

With both types of fuel solutions, 7 extraction and 5 scrub stages were used. The tests showed no adverse effect of molybdenum on extraction and stage requirements within normal Purex requirements. No molybdenum could be detected analytically at or beyond the fourth scrub stage.

LAPRE-II Fuel

Studies were made at AEC request to establish a flowsheet and to determine the feasibility of processing the Los Alamos LAPRE-II fuel in the Immi hot cell equipment in Building 4507. The fuel contains 77 g of U(IV) per liter in 96.8% H_3PO_4; the reactor core contains 7.27 kg of fully enriched U^{235}. Since the Immi equipment is not geometrically safe, criticality control is achieved by 12-fold dilution of the fuel to 6 g of uranium per liter; at this concentration the H_3PO_4 is 1.4 M. Secondary criticality control is achieved by establishing a batch limit of 300 g of uranium. The solution is then made 0.05 M in $NaNO_2$ and 1.6 M in $Fe(NO_3)_3$ to ensure conversion of uranium to U(VI) and of Pu to Pu(IV); the latter also provides salting strength and ensures the complexing of PO_4^{---} by formation of ferric phosphate complex. Uncomplexed PO_4^{---} blocks uranium extraction by formation of unextractable uranium-phosphate complex.

In batch extraction studies both 2.5% and 6% TBP extracted uranium quantitatively. The latter was chosen for the standard flowsheet because it showed greater compatibility with the Immi equipment. To achieve a uranium extraction loss of $\leq$ 0.01%, seven theoretical stages are required. With a 4 M HNO_3 scrub, uranium internal reflux is only 6%. With a strip of 0.01 M HNO_3, the uranium stripping loss was 0.03% in 4-5 theoretical stages. Because of the complexing action of PO_4^{---} on Pu(IV), only 9% of the plutonium was extracted, scrubbed, and stripped with the uranium. This represents about three times that allowable to achieve a uranium product with 30 ppb of plutonium.

Solvent Recovery Studies

Filtration of used 30% TBP after carbonate washing was very effective in removing activity, which appears to be present as a second phase of very small particle size after carbonate treatment. In tests with solvent containing 8×10^4 gamma counts min^{-1} ml^{-1}, most of which was zirconium-niobium, a filtration DF of 200 was achieved by filtration through a $CaCO_3$ bed on a glass frit with 5-μ pores; without use of $CaCO_3$, the DF was 100. When a glass frit of 40-μ pore size was used, the DF was 20 with $CaCO_3$ filter aid and 1.1 without. In tests with other frits and filter papers the DF was, in general, inversely proportional to pore size.

Immi Facility

The Immi Facility in Cell 1, Building 4507, was completed and tested with unirradiated fuel solutions. It is constructed of Carpenter 20 and type 347 stainless steel, and is a set of batch dissolution, feed preparation, and first-cycle solvent-extraction mixer-settler equipment of intermediate scale size (~100 ml/min of two phases in extraction) for the demonstration of power reactor fuel processing flowsheets at full activity level and on a scale sufficiently large to permit equilibrium testing of crudding problems and other variables difficult to evaluate on a small scale. After leak testing and calibration, the head-end equipment was tested satisfactorily on unirradiated ORR fuel. Operational difficulties experienced with the mixer-settlers are being rectified, and tests are being made on extraction efficiency, hydraulics, and mechanical performance.

1.8 ENGINEERING STUDIES

In preparation for the design and construction of head-end pilot plant systems for the new head-end processes, a number of engineering studies were made on criticality, off-gas handling, solids separations, radiation damage to materials, and other problems peculiar to radiochemical processing.

Criticality Studies

The engineering studies on criticality have included both evaluation of methods to prevent inadvertent criticality and an appraisal of the seriousness of accidents that would result from an accidental excursion. The dissolvers planned for the Darex, Sulfex, and Zirflex processes are to be geometrically or near geometrically safe; in the latter case the addition of soluble neutron poisons to the dissolvents will be required. Equipment downstream from the dissolver will generally not be geometrically safe and will depend on concentration control, use of soluble poisons, or use of fixed poisons such as boron-glass packing to prevent criticality incidents. The use of soluble compounds of the neutron poisons boron, cadmium, and rare earths was found compatible with the proposed head-end

systems.[27] The use of fixed poisons, specifically boron-glass Raschig rings, has now been studied and found practical from both the nuclear and process standpoint. In criticality tests with a 25% packed volume of glass rings containing 6% boron, U^{235}, U^{233}, and Pu^{239} concentrations of 50 g/liter in infinite geometry were proved safe. Calculations have shown that in such a system criticality cannot be reached at any concentration of practical interest; experimental verification of this fact is in progress.

Experiments were performed to determine the mixing and sampling characteristics of a 32-in.-dia 150-gal tank filled with packing. Draft tubes and sparging rings were evaluated to determine their mixing efficiencies compared with nonpacked tanks. The sparge ring was most effective; 90% homogeneity of the solution was achieved in < 4 min at an air flow rate of 0.55 scfm and in 8.5 min at 0.14 scfm.

With regard to nuclear incidents, a study of some 15 accidental prompt-critical excursions in aqueous systems which have occurred indicates that such an incident results in an energy release of approximately 10^{17} fissions in ≤ 0.1 sec. If permanent subcriticality is not achieved by loss of fuel or moderator in the initial burst, the configuration continues to pulse. In one incident a total of 4×10^{19} fissions occurred over 7 min. Enough time elapses between pulses that automatically actuated control devices can shut down the system after the initial burst.

It is quite certain that in such an accident no blast can occur and that the rupturing of a well designed vessel, even with a small vent, is very unlikely because of the long time over which the energy is released. The chief dangers appear to be the exposure of personnel to neutrons and gammas and the spread of activity, particularly I_2, to the environment through the vessel off-gas system. The dose from a single burst of 10^{17} fissions through varying concrete thicknesses is:

Concrete Shield Thickness (ft)	Dose at Outer Face of Shield (rem)
1	520
3	2.3
4	0.19
5	0.014
6	0.0012

[27] Chem. Tech. Ann. Prog. Rep. Aug. 31, 1959, ORNL-2788, chap. 1.

From this it is evident that no danger to personnel exists for exposure through heavy shields but that lethal doses are very likely from unshielded or lightly shielded tail-end process equipment.

If it is assumed that 100% of the xenon and krypton and 0.1% of the bromine and iodine produced in a series of bursts totaling 10^{18} fissions penetrate the off-gas cleanup system, the maximum dose at ground level downwind from a 250-ft stack would be about 0.2 rem. The estimated exposure due to particulates escaping the cleanup system would be about 5 mrem. In the unlikely event of vessel rupture, activity would also be dispersed from the cell off-gas system. Estimated contributions from this source from a 250-ft stack would be 0.65 and 0.006 rem for gaseous and particulate activity, respectively.

Off-Gas Treatment and Disposal

Two problems associated with the dissolution of power reactor fuels are the removal or safe dissipation of Kr^{85} from dissolver off-gas and the handling of the large quantities of H_2 evolved in Sulfex decladding of stainless steel fuels. Although of lesser danger, the removal of NH_3 from Zirflex decladding off-gas must also be evaluated.

Several systems were studied for the removal of Kr^{85} from mixed off-gases. The most desirable from cost and safety aspects uses Freon scrubbing, which was developed at BNL. The use of Freon-12 at −120°C is preferred to higher operating temperatures, because less off-gas compression is required in equipment of the same size, and because rare-gas solubility is considerably greater at the lower temperature.

Studies on the release of Kr^{85} within the ORNL area show that such release, based on the escape of all Kr^{85} from a CETR element over 0.5 hr, would be intolerable from the upset it would cause to instrumentation throughout the area and very dangerous to personnel. Further studies on release at a higher elevation within the Area and at a high point 2 miles away show that both these alternatives are satisfactory. Expected dose rates from the three release sites are tabulated below. The 3039 stack is in the center of the ORNL area, with Haw Ridge on the south edge and

Melton Hill two miles south:

	Dose Rate at Ground Level (mr/hr)		
	3039 Stack	Haw Ridge	Melton Hill
Peak	250	10	1
Maximum over 1 hr	2.5	0.25	0.31
Annual average	< 0.05	< 0.05	< 0.05

Peak rates at the HRT, the TSF, and the EGCR were < 10, < 3, and < 0.7 mr/hr from all the release points.

Hydrogen would be controlled in the Sulfex process by a nitrogen purge to the dissolver before, during, and after decladding, provision of a tight off-gas system, and the use of instrumentation in both the equipment and the cell to shut down the reaction whenever approach to explosive mixture concentrations is noted. If a rare-gas unit were built, the hydrogen would be catalytically combined with oxygen before the off-gases reached the rare gas removal system. If a rare-gas unit were not provided, the off-gas would be diluted with air to below the explosive limit and sent to a stack.

Decladding Solution Activity

In many of the Darex, Sulfex, and Zirflex decladding tests with irradiated fuel samples, the cladding solutions contained considerably more activity than expected from the fuel-loss data. However, radiochemical determination of the nuclides in the solutions and calculations of the exact amount of induced activities in the cladding indicate that the cladding solution will not contain more than 1% of the activity in the first-cycle aqueous raffinates and therefore will not require cooled storage facilities.

The results of these studies show that, except for Co^{60}, all induced activities have half lives considerably less than 1 year and after 6 months' decay will generate little heat in comparison with the long-lived Sr^{90} and Cs^{137}. In a solution of a fuel cladding containing 0.03% cobalt, the Co^{60} activity at 6 months' decay will amount only to 0.5% of the expected gross fission-product activity. Since the biological hazard of Sr^{90} is 10^5 times as serious as that of Co^{60}, the cladding solution hazard is controlled by its fission product content.

Fragmentation of Oxide Fuels

One of the main concerns in decladding processes such as Darex, Sulfex, and Zirflex is the release of uranium oxide fines, which will necessitate a difficult liquid-solids separation to avoid fuel losses. These fines also constitute a criticality hazard with some fuels, because of the increased chance of transport and settling of fines in nongeometrically safe equipment. This problem has been investigated both experimentally and by a literature survey.[28]

Data from PWR, NMSR, and Yankee sources have shown that in samples of solid reactor-grade UO_2 pellets irradiated to 25,000 Mwd/ton at heat fluxes up to 1.5×10^6 Btu hr^{-1} ft^{-2} and at temperatures above the melting point, pellets fracture to > 1-mm particles except for < 1% fines resulting mostly from mechanical attrition. Hollow-core pellets irradiated to 50,000 Mwd/ton behaved similarly. Swaged or vibratory-compacted fuel prepared from 150–800-μ UO_2 was 95% sintered during irradiation, and this fraction also behaved similarly to the reactor-grade pellets. The remaining 5% of the fuel remained unsintered but was not attrited to sizes below those of the original material. Thorium oxide pellets appeared more resistant than UO_2, and fragmentation was only about half as severe. Average fragments were 3/16 in. in diameter and the smallest about 1/16.

Based on these data, criticality control can be achieved with simple sedimentation methods, and separations for control of losses and for accountability by centrifugation at 100 G. Removal of siliceous materials will require centrifugation at about 1000 G.

Radiation Damage Studies

A number of protective coatings, hydraulic fluids, lubricants, plastics, and wood materials were irradiated in a Co^{60} source of 2×10^6 r/hr intensity to total doses of 3×10^9 r to determine their suitability for use in various PRFP applications. The hydraulic fluids and lubricants were studied for use with the SRE decladding equipment, the plastic and wood products for use as fuel shear guides, and the protective coatings

---

[28] A. R. Irvine *et al.*, ORNL CF-60-1-102 (Jan. 13, 1960).

for use in the proposed fuel storage canal. Glass-coated steel was irradiated to assess its suitability for radiochemical process service. The results of these tests are given in Tables 1.11 and 1.12. Since none of the synthetic materials appear suitable for use as shear guides, a metal of high cobalt (57%) and chrome (25%) content, "Stoody No. 1," will be used as a guide for the special stainless steel shear blade.

Table 1.11. Radiation Damage to Formica and Wood Materials from a Co^{60} Source at an Intensity of 2.0×10^6 r/hr and a Temperature of 125–157°F

Material	Total Gamma Irradiation (r)	Hardness Decrease (%)	Remarks
Formica	2.25×10^9	29	Surface powdery, growth ~1%, turned darker
Formica, end grain "C"	2.25×10^9	14	Surface powdery, turned darker, no dimensional change
Ryertex	2.25×10^9	28	Surface powdery and slightly bowed, turned darker, expanded 4%
Ryertex No. 2885	2.25×10^9	25	Material cracked, expanded ~5%, surface powdery and bowed
Gatke	2.25×10^9	20	Surface bowed and powdery, expanded 9%
American Brakelok No. 508	6.3×10^8	4	Material cracked, surface bowed, expanded 2%
Lignum vitae	6.3×10^8	43	Material cracked and charred, expanded 3%
Masonite	2.9×10^8	6	Material cracked, expanded ~0.4%

Table 1.12. Summary of Irradiation Damage Tests at 125–157°F on Coatings, Lubricants and Other Materials

Material	Environment	Total Gamma Dose (r)	Effects
Protective Coatings			
Amercoat 1680 over Dimetcote No. 3	Water	3×10^9	Cover coat 3 mils thick, satisfactory on metal, use on concrete unknown
Amercoat 74 over Fiberglas	Water	1.92×10^9	Failed, at 3×10^9 r only seal coat damaged, body coat still serviceable
Amercoat No. 66	Water	1.92×10^9	Failed, body and seal coat severely damaged, prime coat intact
Phenoline 300	Water	1.92×10^9	
Phenoline 305	Water	1.92×10^9	
Plastite 7144HC	Water	$< 5 \times 10^8$	Failed
Acti-Thane HC-100	Water	$< 5 \times 10^8$	Failed
Polyclad 933-1 DG	Water	$< 5 \times 10^8$	Failed
Ceilerite 6400	Water	4×10^8	Failed
Ceilerite 6400	Air	4×10^8	Failed
Amercoat-66	Air	3×10^9	Satisfactory
Amercoat 1680 over Dimetcote-3	Air	3×10^9	Satisfactory
Acti-Thane HC-100	Air	3×10^9	Satisfactory
Plastite 7144-HC	Air	3×10^9	Satisfactory
Hydraulic Fluids and Lubricants			
Mineral Oil No. 6	Air	1×10^8	Little change, changes in viscosity – up to 1×10^9 r gamma irradiation
UCON-Hydrolube-AC	Air	1×10^9	Serviceable to 5×10^8 r
Hydrolube UCON-150-CP	Air	3.4×10^8	Changes color at 10^6–10^8 r, gels between 1×10^8 and 3.4×10^8 r, with volume increase of 75%
Nyvac-20	Air	3.4×10^8	
Alpha Corp. Type A	Air	3×10^9	Contain MoS_2, good resistance to 6×10^8 r, probably useable to 1×10^9 r
Bemol Co. No. 3	Air	3×10^9	
Andox No. 275	Air	3×10^9	Greases, good to 6×10^8 r and probably to 1×10^9 r , failed between 1×10^9 and 3×10^9 r
Shell Type APL	Air	3×10^9	
Bemol Co. Type 50	Air	3×10^9	Failed at 6×10^8 r
Bemol Co. Type 3A	Air	3×10^9	
Glass Lining			
Pfaudler 53 over Carbon Steel*	Air and Water	1×10^{10}	Satisfactory, no change in stress-strain, corrosion or abrasion resistance
Shear Blade Guides			
Formica	Air and Water	2.25×10^9	Best of 8 materials tested (see Table 1.11)

*Room temperature.

2. POWER REACTOR FUEL PROCESSING PILOT PLANT

The objective of the Power Reactor Fuel Processing Pilot Plant Program is the processing of experimental quantities of power reactor fuels to provide process demonstration and operating and economic data. The former Thorex and Metal Recovery Pilot Plants make up this complex and have been operated both as one unit and as separate units.

2.1 FUEL PROCESSING

A total of 50.6 tons of natural and depleted uranium fuel irradiated at BNL, SR, and HW was processed to recover 39.4 kg of plutonium and 37 tons of uranium; the SR and HW uranium were discharged to waste with AEC approval. Three tons of ANL reactor CP-2 natural uranium fuel that had received negligible irradiation was recovered. Eight MTR-irradiated Pu-Al alloy fuel assemblies were processed to recover 563 g of plutonium, containing 30% Pu^{240}; the raffinates from the plutonium recovery step were processed to recover a rare-earth-americium-curium fraction.

BNL Fuel

The aluminum jackets were codissolved with the core, and the solution was processed by a Purex flowsheet that included one codecontamination cycle, a partitioning cycle, and one additional cycle for uranium and plutonium. The uranium product was evaporated to ~ 400 g/liter and stored, and the plutonium was concentrated and recovered by sorption on cation exchange resin followed by elution with 6 M HNO_3.

The BNL fuel program was completed during a 93-day period of continuous operation with the recovery of 18 kg of plutonium and 37 tons of uranium from 38.2 tons of fuel received from the reactor operator. Measured uranium and plutonium losses totaled 1.3 and 0.8%, respectively; material balances were 101 and 103%. Gross gamma decontamination factors averaged 9.1×10^4 and 1.2×10^6, respectively, for uranium and plutonium. The increase in decontamination by a factor of 5 to 10 previously observed[1] when operating the extraction columns with the organic phase continuous was confirmed.

---

[1] Chem. Tech. Ann. Prog. Rep. Aug. 31, 1959, ORNL-2788, p 35.

SR and HW Fuel

This irradiated uranium, which consisted of two lots, one irradiated at each site, was dissolved in 8 M HNO_3 after aluminum-jacket removal with 5.6 M NaOH–2.5 M HNO_3. The plutonium was recovered by the Purex process, and the uranium was discharged to the chemical waste system with AEC approval.

Gross gamma decontamination factors for the plutonium averaged 3.4×10^6. Measured plutonium losses totaled 2.7%, with a material balance of 83%; a large uncertainty in feed measurements (±12%) accounted for the low balance and reflects the problems associated with the processing of solutions containing nonionic (polymeric) species of plutonium that are inextractable in TBP. These species were formed in three batches of dissolver solution, which progressed to conditions of 0.2 M HNO_3 to 0.5 M acid deficiency. Once formed, the polymeric species required the addition of complexing agents or prolonged digestion in an acid environment (>2 M HNO_3) to reconvert the plutonium to the extractable (ionic) species. Reduction with Fe^{2+} followed by oxidation with nitrite was not effective in destroying the polymeric species.

The analytical method (TTA extraction) normally used in determining plutonium in radioactive solutions does not detect plutonium in the nonionic state. Therefore, in solutions in which neutral or acid-deficient conditions had occurred, the plutonium content of the feed solutions was not accurately measured even though the solutions had been subsequently acidified and digested at 100°C. Consequently, during processing, plutonium was not accurately measured in the feed solution produced from dissolutions to neutral to acid-deficient conditions or in the raffinates produced during the processing of such feeds. The difficulties in measuring the plutonium content of feed solutions were further aggravated by the precipitation of nonionic plutonium from neutral or acid-deficient solution to the extent that representative samples of such solutions could not be obtained. On occasion in samples withdrawn from dissolver solution that had changed to 0.0–0.5 M acid deficiency, 50 to >90% of the plutonium was found in precipitates. In one extreme case the ratio of plutonium to uranium was found to be 150 g/ton when the solids-free supernatants

were analyzed in the conventional manner (TTA extraction) but was determined to be 6300 g/ton when the solids were put into solution by the addition of HF to the sample prior to analysis.

From these preliminary studies of the behavior of plutonium in solutions less than 0.5 molar in HNO_3, it is concluded that dissolving conditions should be set to maintain a minimum of ~ 1 M HNO_3 in the dissolver at all times and that all dissolver solutions should be examined for nonionic plutonium species prior to processing.

ANL Fuel

The CP-2 fuel had received only negligible irradiation and had decayed for >5 years; so, fission-product activity was very low. Adequate decontamination was obtained in processing the fuel through only the Purex partitioning and second uranium cycles.

MTR Fuel

The MTR assemblies were dissolved in 6 M HNO_3–0.05 M Hg^{++} and processed for separation and recovery of plutonium, rare earths, americium, and curium according to a tentative, two-cycle, transuranic flowsheet (Sec 13) summarized as follows:

Feed (100 vol)	Scrub (25 vol)	Extractant (100 vol)	Strip (100 vol)
Al^{+++}, 1.25 M	HNO_3, 1.5 M	TBP, 30%	HNO_3, 0.01 M
HNO_3, 1.5 M			
Hg^{++}, 0.05 M			
Pu^{4+}, ~ 0.4 g/liter			

The raffinate was collected, adjusted, and processed in the second cycle as follows:

Feed (100 vol)	Scrub (50 vol)	Extractant (200 vol)	Strip (133 vol)
pH, >0.2	pH, >1.5	TBP, 30%	HNO_3, 0.25 M
Al^{+++}, ~ 1.5 M	Al^{+++}, 1.0 M		

The rare-earth-americium-curium recovery step was terminated, owing to a leak in the evaporator, after about 35% of the first-cycle raffinate was processed. Although the system was not at equilibrium at shutdown,

analyses of flowing streams indicated that ~ 70% of the rare earths, americium, and curium present in the second cycle feed were being extracted, separated and recovered.

Measured plutonium losses in the first cycle totaled 1%; gross gamma decontamination factors from fission products for the recovered plutonium averaged 20, but those for rare earths were $>10^4$. The plutonium product was diluted with uranyl nitrate solution and further decontaminated by a standard Purex two-cycle flowsheet, the plutonium being isolated by cation exchange. Overall decontamination factors averaged 1×10^7. The rare-earth-americium-curium fraction was evaporated and stored pending development of an americium-curium separation process.

2.2 EQUIPMENT DEVELOPMENT

In an effort to improve decontamination, the first and second uranium cycle extraction columns were modified to operate organic continuous, and two types of interface-control systems were tested.

The 1A extraction column was modified to operate with an external interface (Fig. 2.1). A remote metering valve (A) in the column raffinate line (1AW) was set at a predetermined opening to allow all the aqueous and a small fraction of the organic phase to flow to a phase separator. The aqueous phase was transferred to a waste-raffinate catch tank. The solvent phase (10% of the total solvent fed to the column) cascaded to a surge vessel, from which an automatically controlled pump transferred the liquid back into the contactor via the column pulse leg. The draw-off pump rate was controlled by the liquid level in the surge tank. With this method of control, operation was stable and extraction losses remained normal. In addition to the advantage of increased decontamination of the product, the contactor remained less contaminated even when higher activity-level feeds than previously encountered were processed. Plant decontamination is more rapid since most of the residual contamination in the contactor is located in the phase separator, a small piece of equipment.

The interface control in the second-uranium-cycle extraction column (1D) was maintained by a pneumatic differential-pressure controller. This instrument detected the differential-pressure signal from the liquid-level probes (one in each of the measuring pots attached to the column with small

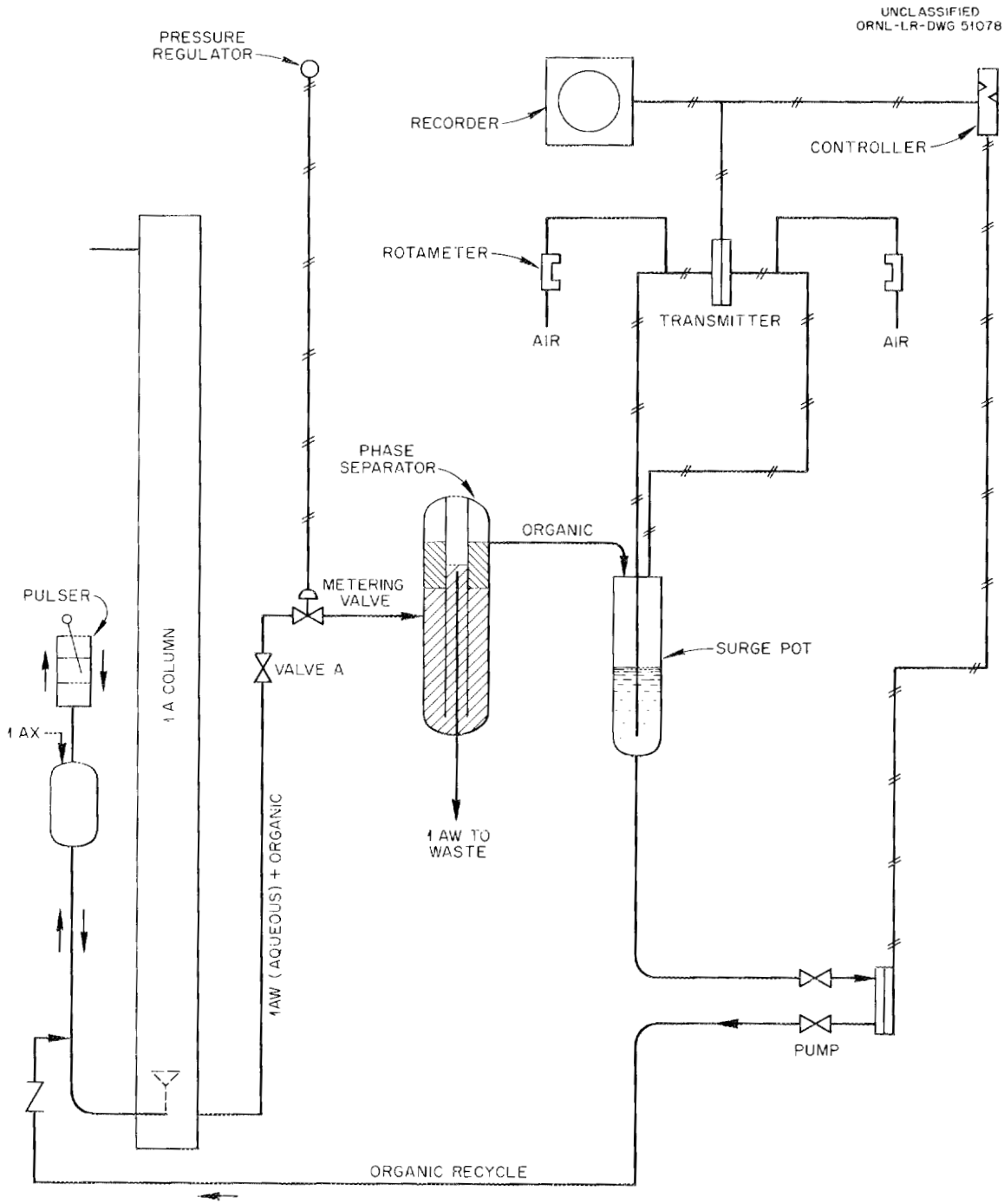

Fig. 2.1. 1A Column Interface Control System.

external pipe at points 10 in. apart, spanning the interface position at the bottom of the contactor) and converted it to a 3- to 15-psig-pressure air signal which operated the column raffinate valve (1DW). The measuring pots were continuously purged with a small stream of fresh solvent to maintain identical solution gravity in each leg. The differential-pressure

transmitter (part of the controller) selected for optimum operation had a range from 0 to 5 in. of water. A 0- to 100-in. transmitter (Fig. 2.2) was also used in this system to detect a change in the over-all column weight.

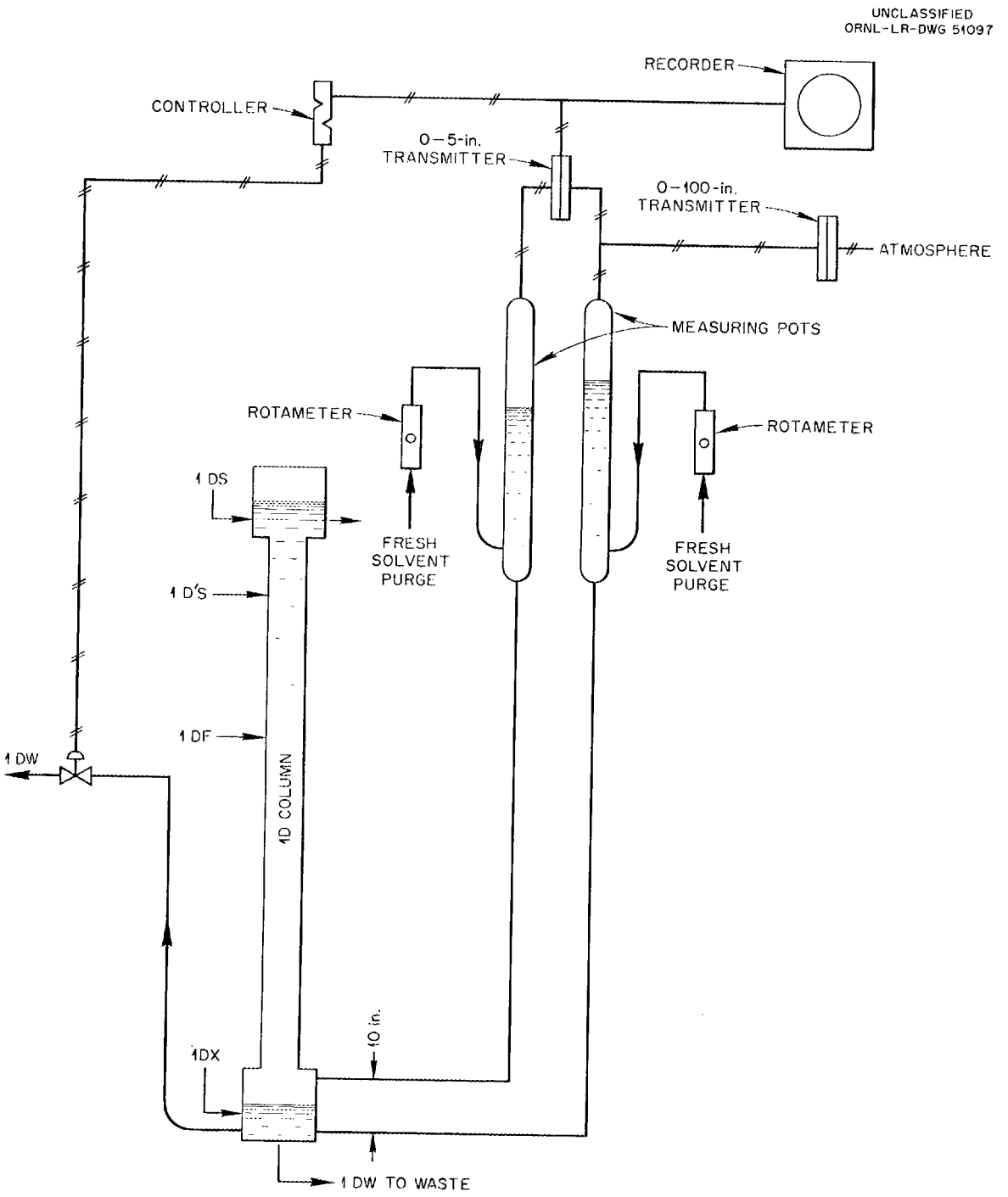

Fig. 2.2. 1D Column Interface Control System.

2.3 INTERCYCLE EVAPORATOR EXPLOSION, BUILDING 3019

On November 20, 1959, during a decontamination program, an explosion occurred in cell 6 of the Hot Pilot Plant, Building 3019 (ref 2). The explosion was due to the deflagration of nitrated organic compounds in an intercycle evaporator and involved nitration by concentrated nitric acid of 14 liters of the proprietary decontaminating agent, Turco 4501. Approximately 15 g of plutonium was released from the subcell that contained the evaporator; about 70 mg was released from cells 6 and 7 to the interior of Building 3019, and about 600 mg was released through the cell-6 door and deposited on nearby streets and building surfaces. No personnel were injured by the explosion and no one received a significant fraction of a lifetime body burden of plutonium either at the time of the incident or during subsequent cleanup operations.

The section of Building 3019 involved contains the high-activity level solvent extraction equipment for the first cycle decontamination of power reactor fuels and the volatility process equipment for recovering uranium from fused salt reactor fuels.[3] The high-activity level analytical facility and control laboratories, in the west portion of the building, were not affected. The solvent extraction processing of highly irradiated uranium had been completed about 1 month preceding the accident and a decontamination program started.

The intercycle evaporator consists of a steam stripper, a vapor separator, a heat exchanger, and connecting piping (Fig. 2.3). The uranium-plutonium-bearing aqueous stream from the stripping column flowed by gravity through the steam stripper, for removal of entrained and dissolved organic phase, to the natural-convection evaporator loop. Over-head vapor from the evaporator was routed from the vapor separator through the packed section of the steam stripper, where it served as the stripping medium, and then to the condensate-collection system.

Two days before the explosion, the evaporator was treated with boiling Turco 4501 (a proprietary decontaminating agent which is a strongly basic

[2]L. J. King, Intercycle Evaporator Explosion, Building 3019, Oak Ridge National Laboratory, ORNL-2989 (in press).

[3]F. L. Culler, et al., Summary Report of Hazards Evaluation, ORNL-2956 (in preparation).

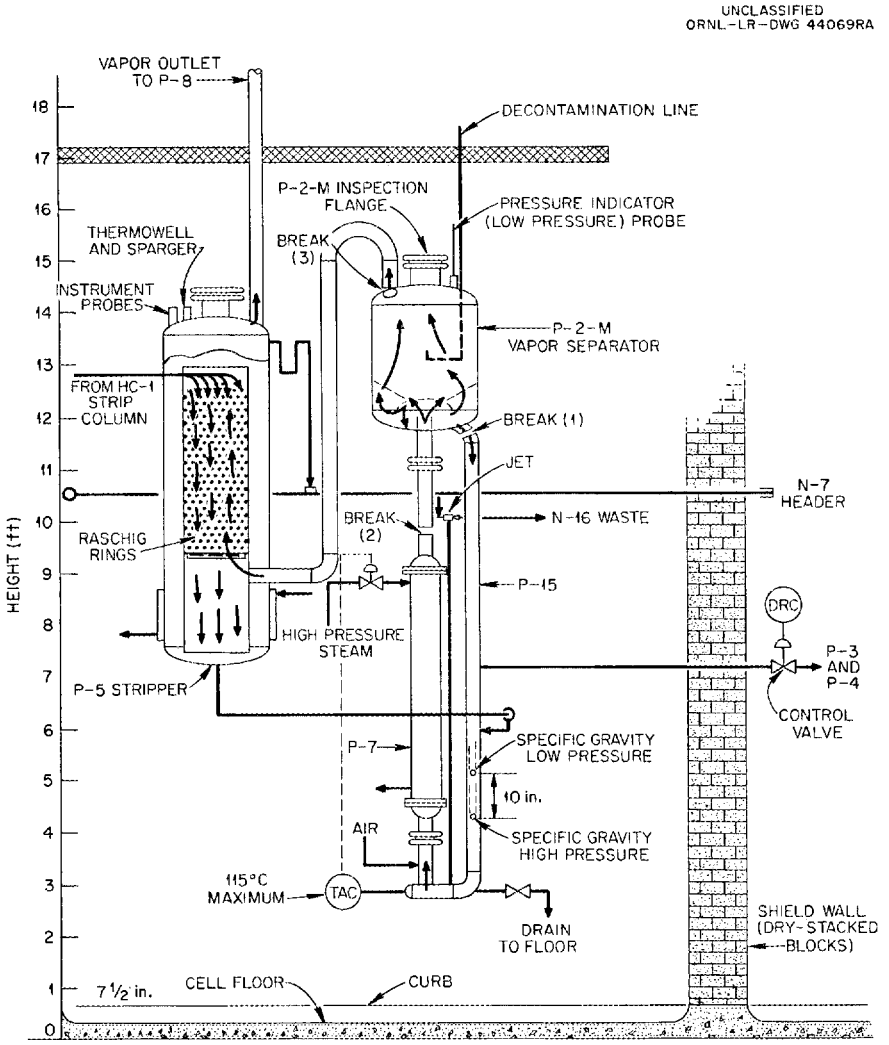

Fig. 2.3. Schematic of P-15 Evaporator System.

solution of the alkali salts of various organic hydroxyacids, various amines, surface active agents, and phenol), a water rinse, hot 30% HNO_3, and a water rinse. There was no change in the radiation levels. The evaporator was flushed through the manually operated drain valve with 200 gal of water, 400 liters of hot 25% NaOH, and 300 gal of water. Again, there was no change in the radiation levels. A solution of 200 liters of Turco 4501 plus steam jet dilution was added to the evaporator and boiled for 2 hr. The evaporator was drained through the remotely operated product outlet valve because the drain valve was located in the 100-r/hr radiation zone. (This left a heel containing 13.9 liters of the organic compounds,

the subsequent nitration of which provided fuel for the deflagration.[4]) The next step was the addition of 270 liters of 4 M HNO_3 to the evaporator, omitting the normal water flush and bringing together the organic compounds and the nitric acid. The heat exchanger steam was turned on, thereby providing sufficient heat to concentrate the nitric acid and allow complete reaction between the acid and the organic compounds. The temperature increased throughout the concentration of the nitric acid until the nitro compounds, just formed, ignited and the evaporator exploded at 10:58 PM on Nov. 20, 1959.

The necessary and sufficient requirements for the explosion were (1) the existence of a drain heel from the Turco 4501 treatment, (2) the omission of a water rinse before the addition of the nitric acid, and (3) the heat supplied by the heat exchanger jacket steam.

Approximately 70 mg of plutonium was released to the penthouse, cold-solution makeup, sampling, and office areas of Building 3019 via pipe passages through the cell walls. The contamination was spread through a connecting tunnel to the Graphite Reactor Building (3001), which had to be evacuated. The door to cell 6 was thrown open, allowing about 600 mg of plutonium to be released to nearby streets and building surfaces.

Building 3019 obviously was not designed to contain the plutonium which was released from the evaporator by the explosion. The cell ventilation filters retained the alpha activity with a high degree of efficiency[5] but, the existence of the cell-6 door, which opened readily, precluded confinement of the plutonium to Building 3019.

Cleanup

The alpha activity on nearby streets and buildings was "fixed" with tar, paint, roofing compound, or masonry sealer, as appropriate to the surface. With the exception of the pilot plant portion of Building 3019, the Graphite Reactor Building, and the road south of these buildings, the affected areas of the Laboratory were back in service by Monday, Nov. 23, 1959.

---

[4]W. Davis, Jr., W. H. Baldwin, and A. B. Meservey, Chemistry of the Intercycle Evaporator Incident of November 20, 1959, ORNL-2979 (in press).

[5]M. H. Lloyd, Radioactivity Collected on Building 3019 Off-Gas Filters, ORNL CF-60-8-38 (in preparation).

The decontamination of the interior of Building 3019, exclusive of processing cells 4 through 7, was 90% complete on Aug. 1, 1960. Areas were cleaned to noncontamination-zone or to painting specifications (Table 2.1), and the surfaces were resurfaced or painted.

Table 2.1. Surface Alpha-Activity Specifications for Building 3019 Decontamination

Final Condition	Maximum Contamination (dis/min per 100 cm^2)			
	Direct Reading		Transferable	
	Average*	Maximum	Average*	Maximum
Clean	30	300	3	30
Painting specifications	300	3000	30	300

*A minimum survey includes one smear and four probes with a gas-purged alpha meter per square meter of projected surface area.

Cleanup effort in cells 6 and 7 was started in April 1960 but was suspended pending installation of a temporary secondary-containment structure and provision of additional vessel off-gas capacity. These were not considered necessary at first because, although material balances[6] had shown 4.6 ± 3.3 kg of plutonium missing, it was thought that no plutonium would be in the evaporator because of the series of decontamination treatments to which it had been subjected. However, flushing of the evaporator with water and with 6 M HNO_3, both containing the neutron poison boron as a precaution against criticality, removed 9 and 100 g of plutonium, respectively. Cell cleanup will be resumed as soon as the new radiation safety requirements are met.

[6]D. A. Gardiner, Measurement of Source and Special Nuclear Materials in the Power Reactor Fuel Processing Plant, ORNL CF-60-3-53 (Mar. 21, 1960).

3. FUSED SALT–FLUORIDE VOLATILITY PROCESS

The Fused Salt–Fluoride Volatility process is of considerable interest in the processing of uranium fuel elements containing the difficultly soluble element zirconium. It consists in hydrofluorinating the fuel components to fluorides in a molten fluoride mixture, fluorinating the UF_4 to the volatile UF_6 and sorbing the volatilized UF_6 on NaF beds (see also Sec 4).

3.1 PILOT PLANT

Modifications to the Volatility Pilot Plant required for processing zirconium-uranium fuel elements are essentially complete. The principal change in the pilot plant was the addition of an INOR-8 hydrofluorinator, the HF supply, recycle, and disposal equipment. A newly designed fluorinator of L nickel, absorbers, and a molten-salt sampler were also installed. A movable combination NaF absorber and complexible-radioactive-products trap was satisfactory in operability tests and will be installed on the fluorinator-gas outlet as an alternative to the fixed-bed absorbers.

A fuel element carrier-charger and more heavily shielded waste-salt removal equipment have been provided, along with an aqueous KOH scrubber, in order to remove HF and F_2 from cell ventilation air both in normal trace amounts and in case of accidental release of larger amounts. A data logger is being installed to determine the feasibility of computer processing of experimental data from a batch-operated high-temperature radiochemical pilot plant.

The flowsheet for initial operation of the plant is the same as that previously presented,[1] except that initial and final dissolution temperature are 650 and 550°C, respectively; the previous flowsheet required 700 and 600°C. These lower temperatures for the hydrofluorination step were achieved by starting with 37.5-37.5-25 mole % NaF-LiF-ZrF_4 instead of 43-57 mole % NaF-LiF. Corrosion of the dissolver is reduced by operation at lower temperatures.

---

[1]Chem. Tech. Ann. Prog. Rep. Aug. 31, 1959, ORNL-2788, Fig. 3.1.

3.2 ENGINEERING STUDIES

Ten hydrofluorination experiments, according to the flowsheet published earlier,[2] in the INOR-8 prototype of the Pilot Plant hydrofluorinator demonstrated satisfactory dissolution rates, of the order of 0.15 lb hr^{-1} ft^{-2}, with initial and final temperatures of 650 and 500–550°C, respectively. General corrosion of the vessel was not detectable by Vidigage inspection after 74.5 hr of HF exposure at 550 to 650°C. A single point at the interface level had corroded at a rate of ~0.04 mil/hr. Complete dissolution of Zircaloy-2 elements was also demonstrated.

Finely divided metallic particles, thought to be the result of the reduction of fluoride impurities (fluorides of less active metals such as Ni, Sn, Cr, Mo, and Fe), are present as a result of corrosion of the dissolver vessel and dissolution of Zircaloy-2. Observations made during the ten runs, as well as for copper-lined equipment, indicated that the initial reaction takes place between metal fluoride salts and metallic zirconium and hydrogen. Some of the metals produced by reduction adhere to the surface of the zirconium, decreasing the exposed surface and thus the dissolution rate. Some of the reduced metal is dispersed into the salt, where it continues to react with HF. As the particle size is decreased, some of the metallic particles become entrained in the off-gas stream and have been identified in the off-gas system. The remaining particles are sometimes found dispersed through the salt melt and sometimes adhering to the structural metals of the dissolver. In the latter case they may protect the base metal against corrosion, but they increase the difficulty of inspecting and measuring corrosion losses. The lower dissolution temperatures used in these runs should decrease the corrosion.

Additional hydrofluorination studies with respect to copper-lined equipment indicated a small effect of temperature and a nonlinear decrease in dissolution rate with increasing concentration of zirconium tetrafluoride in the molten salt. The chief control factor of dissolution rate as well as vessel corrosion is gas velocity. These data contribute to the determining of the absolute rate and the dissolution mechanism.

---

[2] Ibid., p 40.

The rate of sorption of UF_6 from a UF_6-N_2 stream on an NaF bed was studied by noting temperature changes due to heat of sorption in an adiabatic differential bed. Results indicate that the initial rate is controlled by gas-phase diffusion and that solid-phase diffusion becomes controlling as bed loading increases; the initial sorption rate increases with increasing concentration of UF_6 in the gas (UF_6-N_2) stream and decreases with increasing bed temperature. A deep bed and the necessary metering equipment for rate studies by the sorption wave technique are installed and the studies are in progress.

In a test of the movable combination absorber-and-trap unit, 1/8-in. right cylindrical pellets were transferred with reproducible results when the bed was fused together by sorbed material. The advantages of this system are elimination of the radioactive-solids handling problem by dropping the used NaF directly into the fluorinator, virtual elimination of the possibility of plugging the fluorinator off-gas system, and a possibility of decreased uranium loss to spent sorber beds.

3.3 CHEMICAL DEVELOPMENT

The Fused Salt–Fluoride Volatility process (Fig. 3.1) was satisfactorily demonstrated in 12 runs with 650-g batches of spent Nautilus fuel (Zircaloy-2–uranium alloy). The fuel was dissolved by hydrofluorination in 57-43 mole % LiF-NaF at 600–700°C to give a melt of composition 31-24-45 mole % LiF-NaF-ZrF_4 and containing ~0.4% U^{235} as UF_4. The melt was fluorinated at ~500°C to volatilize UF_6, and the volatilized UF_6 was sorbed on NaF at 100°C. Because of the high decontamination from fission product activity in the fluorination, the desorption and transfer through a second NaF bed at 400°C were carried out in the cold laboratory. In 12 dissolution tests with spent Nautilus fuel, total dissolution times, average dissolution rates, and HF efficiencies varied greatly (Table 3.1). The factors involved have not been completely evaluated.

Some of the means used to increase the rates were: (1) prehydriding of the fuel before introduction of the HF, (2) omission of part of the dissolver salt at startup to promote the direct gas-phase reaction (this probably cannot be done in the plant because of the possibility of a runaway reaction), (3) hydrogen sparging of the dissolver salt before introduction of the fuel, and (4) the use of extra H_2 with the HF. Although

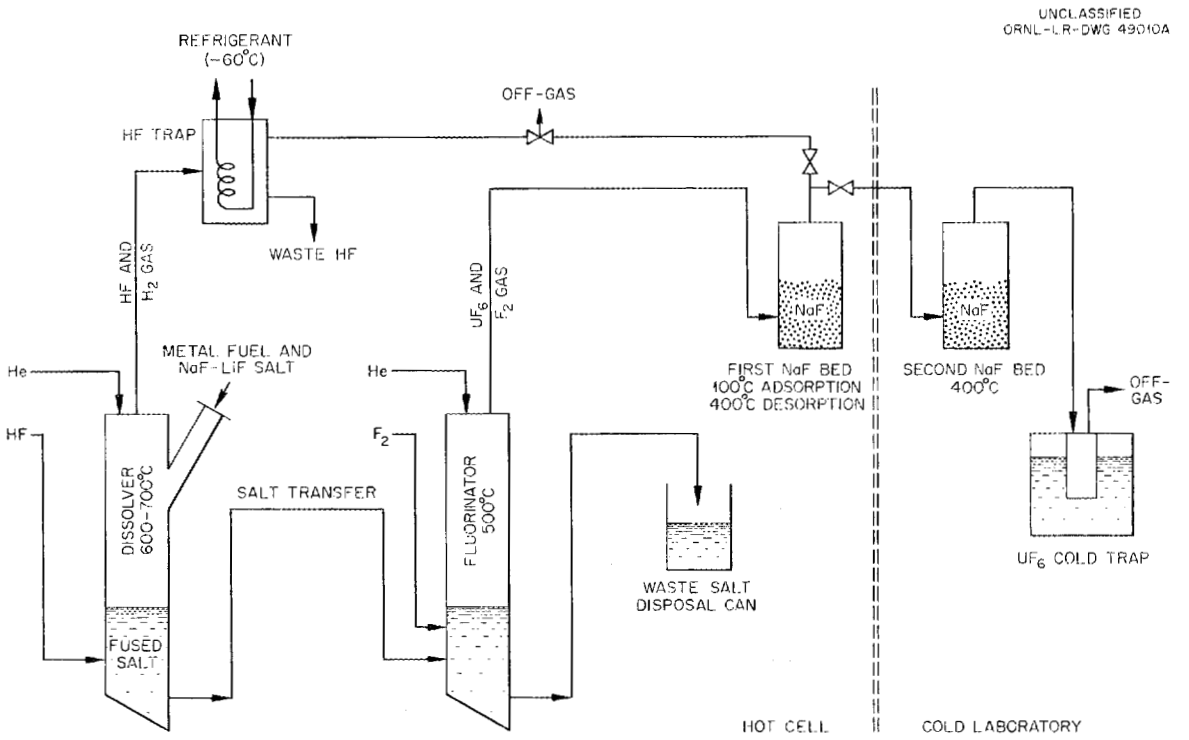

Fig. 3.1. Schematic of Laboratory Process Test Equipment for the Fused Salt–Fluoride Volatility Process.

Table 3.1. Typical Dissolution Rates of Nautilus Fuel

Run	HF Flow Rate (ml/min)	HF Concentration (%)	Average HF Efficiency (%)	Dissolution Time (hr)	Average Dissolution Rate (mg min^{-1} cm^{-2})
1	820	100	20.1	62	0.17
3	1130	100	30.3	34	0.30
10	1200	70 (30 H_2)	27.3	29	0.35
12	1400	100	47.7	16	0.64

no definite conclusions were reached with respect to items 3 and 4, it is believed that prehydriding promotes the subsequent hydrofluorination reaction. Considerable hydriding always occurs in the course of regular hydrofluorination. The use of hydrogen to sparge the dissolver before fuel introduction was to reduce NiF_2 or other fluorides, causing them to precipitate from the salt solution thus preventing them from plating out on the zirconium-uranium fuel and inhibiting the hydrofluorination process.

Entrainment or volatilization of uranium in the waste HF was less than 0.03%. No difficulty should be encountered in the Volatility Pilot Plant with uranium loss in this step. Niobium transfer was high in one run in which the reaction took place in the gas phase.

Although some difficulty was encountered at times in achieving complete volatilization of UF_6 from the process fused salt, recovery was repeatedly better than 99.8%. The fluorination rate was definitely slower at 500 than at 600°C in "cold" laboratory work, but other factors such as configuration of equipment and impurities in the salt are more important in determining the plant fluorination rate.

Over-all decontamination factors for specific fission products were satisfactory (Table 3.2). In all except one run, in which a valve was not operated properly, the activity in the product UF_6 was less than 10 times the activity of unirradiated U^{235}.

Table 3.2. Over-All Decontamination Factors

Activity	Decontamination Factors				
	Run 8	Run 9	Run 10	Run 11	Run 12
Gr β	2×10^6	3×10^6	9×10^6	1×10^6	$> 2 \times 10^9$
Gr γ	$> 1 \times 10^9$	2×10^8	5×10^7	2×10^6	6×10^7
Ru γ	2×10^8	4×10^7	2×10^6	5×10^4	1×10^7
Zr γ	8×10^5	2×10^6	3×10^6	1×10^5	9×10^4
Nb γ	4×10^7	$> 2 \times 10^8$	8×10^7	$> 6 \times 10^7$	8×10^5
Cs γ	3×10^9	1×10^9	1×10^9	2×10^{10}	2×10^9
Sr β	3×10^8	$> 3 \times 10^9$	$> 1 \times 10^{10}$	$> 9 \times 10^9$	$> 5 \times 10^9$
TRE β	5×10^8	$> 1 \times 10^{10}$	$> 7 \times 10^9$	$> 3 \times 10^9$	$> 1 \times 10^{11}$

Molybdenum, technetium, neptunium, and chromium were always present in the product UF_6 from the Nautilus fuel process tests (Table 3.3). The first three are transferred as volatile fluorides, with the UF_6, through the NaF absorption-desorption step (first bed) and pass unaffected through NaF at 400°C (second bed). The chromium probably came from the stainless steel reactor in which the UF_6 was hydrolyzed prior to analysis. The parallelism between the molybdenum and technetium contents suggests similar

Table 3.3. Impurities in UF_6 Products

Run No.	Concentration (ppm, based on uranium)			
	Cr*	Mo	Np	Tc
8	200	10,100	260	1020
9	290	5,200	240	490
10	150	2,200	58	260
11	80	2,500	310	240
12	< 100	1,200	290	60

*Probably from corrosion of the cold trap during the hydrolysis of the product to obtain a representative aqueous sample.

behavior of these two elements in the process by being only partially absorbed with UF_6 on the first NaF bed. The neptunium content of the product is relatively constant, indicating that this element follows uranium in the process. In none of the UF_6 products was any plutonium detected by alpha-energy spectrometry.

The processing of stainless steel- and niobium-containing alloy or dispersion fuels by modification of the Fused Salt–Fluoride Volatility process appears feasible on the basis of dissolution rates. A choice of fused salt systems is available and is being evaluated. For example, niobium dissolved at rates of 1.7 and 0.7 mg cm^{-2} min^{-1} at 500 and 550°C, respectively, in 31-24-45 mole % $LiF-NaF-ZrF_4$. The rates were 1.6 and 3.3 mg cm^{-2} min^{-1} at 550 and 650°C, respectively, in 50-50 mole % $NaF-ZrF_4$ at an HF flow rate of 400 ml/min. Due to analytical problems, poor material balances for niobium have thus far been obtained, but as much as 16% is volatilized (as NbF_5) with the excess HF used. In the case of stainless-steel-containing fuel, either the $NaF-ZrF_4$ and $LiF-NaF-ZrF_4$ systems or flinak (42.0-11.5-46.5 mole % KF-LiF-NaF) may be used, but it is suspected that suitably fast rates will be obtained only with flinak or with the other systems using a low Zr/alkali metal ratio. For example, in 60-40 mole % $NaF-ZrF_4$ dissolution rates for type 347 stainless steel were 0.4 and 1.1 mg cm^{-2} min^{-1} at 600 and 700°C, respectively, while in flinak the rates were 9.7, 8.5, and 5.5 mg cm^{-2} min^{-1} at temperatures of 550, 600,

and 650°C, respectively. Copper would probably be the preferred construction material for stainless steel dissolution because copper has a corrosion rate of 0.0011 mg cm^{-2} min^{-1} in flinak at 600°C.

Thorium oxide fuels dissolved without the use of HF in ZrF_4-containing salts (e.g., 31-24-45 mole % $LiF-NaF-ZrF_4$) but not in non-ZrF_4-bearing salt, as exemplified by flinak. The reaction is either ordinary metathesis or the reaction represented by

$$ThO_2 + ZrF_4 \rightarrow ThOF_2 + ZrOF_2$$

with the oxyfluoride being compatible with the fused salt system. As much as 14 wt % thorium was incorporated into fused salt in one test at 650°C. The dissolution reaction proceeds extremely rapidly even in the case of arc-fused thoria. Comparable tests with flinak at 600–700°C gave slow reaction rates, ~0.3 mg cm^{-2} min^{-1}, with HF sparging. Gas-phase reactions of HF with 1700°C-fired thoria gave similar slow rates. No tests of corrosion due to the introduction of oxygen were made.

When NaF was contacted with MoF_6 at 100°C there was an evolution of a large amount of heat and a weight increase, which indicates the existence of an MoF_6-NaF complex at 100°C. The stoichiometry observed indicates that the formula may be $MoF_6 \cdot 3NaF$, similar to the $UF_6 \cdot 3NaF$ complex. Preliminary vapor pressure data, using the transpiration method in the range of −25 to +60°C, has given the tentative expression of $\log P_{mm} = 9.9 - (2800/T)$. The atmospheric pressure decomposition temperature according to this expression would be 120°C. Operation of the first NaF absorption bed at greater than 120°C in the process will therefore possibly lead to much less molybdenum contamination in the product UF_6 while still giving adequate uranium recovery.

Direct fluorination of uranium metal containing plutonium indicated that the hexafluorides of these elements might be separable through use of a difference in chemical stability. Three cold-trap fractions collected in this experiment contained 69.8, 30.2, and ~0% of the total uranium and 0.32, 57.3, and 25.2% of the total plutonium content, with only 6% of the plutonium remaining in the reactor. It is speculated that the presence of uranium metal or lower fluorides of uranium in the early part of the run prevented formation of the volatile PuF_6.

4. MOLTEN SALT REACTOR FUEL PROCESSING

The method proposed for processing fused Li^7F-BeF_2-UF_4 fuel is fluorination of the UF_4 to volatile UF_6 and separation of fission products from the LiF-BeF_2 carrier by dissolution in HF.[1]

A study of potential fuel cycle costs and poison fractions for various fuel processing rates for a 1000-Mw (electrical) molten-salt breeder reactor indicated a total fuel cycle cost (processing, all inventories, and losses) slightly >1 mill/kwhr for a good breeder with a 10–12 year doubling time, increasing rapidly with breeding ratio. The cost drops to well under 1 mill/kwhr for lower conversion ratios, and appears to be approaching a minimum for a conversion ratio somewhat less than 1. Inventory charges and replacement-salt costs account for over half the net fuel cycle cost. Economically, the fluoride volatility process appears entirely adequate for uranium recovery from both fuel and blanket salts, and the HF dissolution process for Li^7 salt recovery, including replacement of fuel-carrier salt on a long cycle, appears adequate for fuel-salt poison control. Much development work is necessary to adapt technologically these processes to the requirements of the molten salt breeder.

The first required process application will be for uranium recovery from both fuel and blanket salts which, with fuel salt replacement, provides adequate processing for a converter reactor. Decontamination of the fuel-carrier salt will be required only when good breeder reactors are built, but it may offer some advantage with lower-breeding-ratio reactors. Thorium recovery and blanket-salt decontamination will be required eventually, but not for decades.

Preliminary laboratory studies indicated that decontamination of the total fuel in one step may be feasible. A solution of 5 mole % NO_2 in anhydrous HF dissolved LiF, BeF_2, and UF_4 with solubilities of 50, 50, and 1 g/liter, respectively, at 25°C. Rare-earth solubilities were $< 10^{-4}$ mole %; ThF_4 was insoluble, $<<0.01$ mole %. The decontaminated fuel could be recycled after distilling off the NO_2 and HF.

---

[1] Chem. Tech. Ann. Prog. Rep. Aug. 31, 1959, ORNL-2788, sec 4.

A solvent containing ClF_3 in anhydrous HF was not satisfactory because, although the uranium solubility was significant, the LiF and BeF_2 solubilities were substantially lower than in HF solution.

Due to temporary interest in one-region molten salt reactors using fuel salts containing large amounts of ThF_4, solvents for ThF_4 were briefly investigated. Hot aqueous 50 wt % NH_4F solution dissolved ThF_4 to the extent of about 50 g/liter, but the ThF_4 solubility was greatly decreased in the presence of other components of the fuel salt. All the BeF_2 and UF_4 but only 10 to 15% of the LiF and ThF_4 dissolved from a LiF-BeF_2-ThF_4-UF_4 (67-18.5-14-0.5 mole %) fuel salt. Lithium fluoride by itself is soluble to the extent of only 0.5 g/liter in hot aqueous 50% NH_4F. Thorium fluoride is not appreciably soluble in aqueous BeF_2 solutions containing up to 0.77 mg of BeF_2 per milliliter.

5. HOMOGENEOUS REACTOR FUEL PROCESSING

A scheme for processing the uranyl sulfate fuel of the Homogeneous Reactor Test for removal of insoluble fission and corrosion products by continuous centrifugation with a multiple hydroclone system showed promise. The original objective of fuel processing to maintain low nuclear poison levels was easily achieved with a single hydroclone. However, the large inventory of uranium adsorbed, or in other ways permanently fixed, by the corrosion product scales significantly increases the uranium inventory and, for any practical power reactor, introduces an eventual difficult recovery operation. In addition, accumulation of scale on the heat exchanger has lowered the heat transfer coefficient about 20%, which is of little consequence if limited to such magnitude but would be more serious as scaling continued.

5.1 HYDROCLONE PERFORMANCE AND CORROSION PRODUCT STUDIES

Solids Removal in Runs 20 and 21

Studies on increasing the rates of solids removal from the fuel by faster processing with multiple parallel hydroclone units were continued. In previous studies[1] with a single hydroclone, processing the entire fuel volume every 1–2 hr did not prevent accumulation of solids in the reactor piping system. Competing mechanisms, mainly deposition or scaling of pipe surfaces, lowered and maintained circulating solids concentrations around 10 ppm.

Initial operation with a 13-unit multiple hydroclone, or multiclone, in reactor run 20 was reported earlier.[1] Solids were concentrated in the multiclone, from which the underflow stream was routed to the original single hydroclone in the processing cell for solids collection; solids collection and removal were followed by dissolution and sampling. In the first 800 hr of run 20, removal rates averaged 1.4 g/hr, dropping from 5 g/hr during the first 50 hr to 0.5 g/hr at the end of 800 hr. With a single hydroclone in run 17 average removal rates were 0.85 g/hr in a similar period. In the last 800 hr of run 20, solids collection rates

---

[1]Chem. Tech. Div. Ann. Prog. Rep. Aug. 31, 1959, ORNL-2788, p 42.

averaged <0.3 g/hr, the minimum ever obtained with a single hydroclone. Since all previous runs had been less than 1000 hr in length, it was difficult to ascertain if the low removal rates were a result of the continued decrease with time or of some malfunction of the system. The single collection hydroclone was removed, but visual inspection in a hot cell showed no evidence of damage.

A new collection hydroclone was installed prior to run 21, but the removal rate was only 1 g/hr in the first 86 hr, and this was followed three weeks later by a period when only 0.2 g/hr was removed. After the run the multiclone was removed and tested in an underwater installation at the reactor site. The feed ports were found to be partially plugged, which probably decreased the efficiency of the unit nearly to zero. Radiation readings indicated that about 100 g of solids remained in the feed chamber. Approximately half these solids were flushed from the unit during tests made at higher flow rates than used in normal operation, but this did not free the plugged hydroclones. Solids efficiency tests on the extremely radioactive (> 6000 r/hr) unit were not practical.

Revised Multiclone Design

Complete analysis of the multiclone performance indicated that significant improvements could be achieved by increasing the pressure drop across the unit and by returning the overflow from the collection hydroclone to the multiclone underflow receiver. The particle size of solids collected has averaged less than 1 μ, where efficiencies are only about 20%. Thus a significant fraction of solids concentrated by the multiclone was not removed by the collection hydroclone and was returned to the reactor. Some additional gain could be expected by using slightly smaller hydroclones in the multiclone assembly. Therefore, a unit incorporating eighteen 0.4-in. hydroclones was built and installed so as to utilize the full 90-ft head of the reactor circulating pump instead of the 42-ft head available in the previous installation. A screen was placed in the feed stream to remove particles larger than 0.030 in. in an effort to reduce the possibility of again plugging the feed ports.

Solids Material Balance by Radiation Survey

Measurement of activity levels at more than 200 points in the cell with a Victoreen roentgen rate meter (maximum range 6000 r/hr) indicated that probably more than 85% of the solids are deposited on high-pressure system piping. This scale appeared fairly uniform, varying in thickness no more than a factor of 2, with slightly higher values upstream of the heat exchanger than downstream. The fuel dump tank and sediment trap in the line to the fuel feed pump were almost completely free of solids, but an accumulation of solids, estimated at 100 g, had settled out in the multiclone feed chamber.

A survey of the low-pressure system iodine trap 76 days after shutdown showed high activity at the bottom of the silver mesh bed and activity twice as great at a point near the top of the bed. Both sources were decaying with an 8-day half life. Presumably some of the recombiner pellets had broken and sifted down to the silver mesh bed where the platinum on the pellets trapped iodine that was not retained in the silver bed.

Multiclone Development Studies

Parallel hydroclones used industrially are normally operated with relatively high underflow rates and performance is similar to that obtained with single hydroclones. Recent studies have shown that efficiency is a direct function of underflow rate for parallel hydroclone units. A more careful investigation of this effect has been started since there are definite advantages to operating multiclones with induced underflow if efficiencies remain high.

In engineering studies apparent induced underflow ratios and efficiencies were measured for the new HRT multiclone and for a Dorr-Oliver TM stage modified to give 32 hydroclones in parallel on one induced underflow receiver. The apparent induced underflow ratios for the two multiclone units were 2.5 to 5.0 times the experimental and calculated values for single hydroclones of the same dimensions. The efficiencies for ThO_2 particles of about 1.6 μ dia, corrected for the underflow volume, were 80 to 90% for single hydroclones with continuous underflow, 50 to 60% for the multiclone with 5% of the feed flow as continuous underflow, and 16 to 22%

for induced underflow operation of the multiclone. These results are believed due to unequal flows through the underflow ports of the parallel units, although size classification during the tests may have contributed to the apparent reduction in efficiency.

5.2 FISSION PRODUCT STUDIES

Iodine Behavior in the HRT

Iodine contributes a significant fraction of the total biological hazard of aqueous homogeneous reactor fuel, and one isotope, I^{135}, decays to the neutron poison Xe^{135}. Iodine is removed, on a 1-hr processing period, from the HRT fuel solution by volatilization from the letdown stream and is trapped on a silver-plated mesh bed in the vapor stream. Reanalysis of data from past runs and additional information from run 21 showed that only 5 to 20% of the iodine in the reactor circulates with the fuel. The remainder is held, presumably by adsorption on the walls, in equilibrium with that circulating. This decreases the effectiveness of this method of xenon control. While there is evidence that the amount of iodine circulating changes with time, the change is not large.

The effect of the tellurium precursor on sample results and their interpretation was shown to be negligible by analyzing samples a number of times over a period of several days. The I^{133}/I^{131} activity ratio corrected back to sampling time remained constant, indicating no grow-in of I^{131} from the Te^{131} precursor. This was expected since tellurium is very insoluble and less than 1% circulates with the fuel.

Heat generation in the iodine trap was measured carefully over two 5-day periods of constant power operation. From the heat generation rate and from the transient buildup and decay rates, it was evident that there was little heat contribution from the short-lived isotopes. This indicates holdups consistent with that noted above.

Xe^{135} Poison Fraction Measurements

Rather complete removal of the 135 chain from the circulating fuel, coupled with the large negative temperature coefficient of reactivity and continuous uranium transfers in the system, makes measurement of the Xe^{135}

poison level in the HRT by normal transient reactivity measurements inaccurate. A scheme for measuring the xenon poisoning was devised, based on analysis of the off-gas for the Xe^{136}/Xe^{134} ratio. After a suitable time at constant power, the off-gas was routed to a spare charcoal bed for 48 hr. This gas, after decay of the active isotopes, was purged from the bed and was analyzed by mass spectrographic methods for the ratio of the xenon isotopes. The xenon poison fraction, calculated from existing yield data, was 0.009 ± 0.0005 with this precision based on statistical variation between successive samples. Uncertainty in the primary yield data may introduce errors as great as 0.0015 in the measurement. This value was a factor of 2 lower than expected, indicating somewhat less iodine holdup, thus more complete removal, than had been estimated from other means.

5.3 WASTE HANDLING

Shield Water

Decontamination of shield water by precipitation—adsorption techniques continued to prove adequate for handling this low-level liquid waste from the reactor. From July 1959 to July 1960, 1,700,000 gal of water, containing 185 curies, was treated. The total activity released to White Oak Lake was 2.4 curies. The primary treatment consists of adding soluble trisodium phosphate to precipitate calcium, which acts as a scavenger as it settles. In one case, when strontium was the chief activity, dispersal of diatomaceous earth on the pond surface was very effective after limited success with trisodium phosphate.

Off-Gas

Operation of the charcoal adsorber beds for fission gas retention was routine with little attention required. Ineffectiveness of the recombiner resulted in concentrations of deuterium in the off-gas ranging from 1 to 10%. A continuous analyzer was installed on the exit gas stream to monitor this deuterium content. A fire was ignited in one of the beds, presumably due to the heat of recombination of D_2 and O_2 in a fashion similar to that reported previously.[2] The fire was detected immediately by a sharp temperature rise and was quenched by stopping oxygen flow to that bed. No activity

[2] Ibid., p 44.

was released and gas analyses subsequently showed a barely detectable rise in CO_2 content.

5.4 EQUIPMENT DECONTAMINATION

The chromous sulfate descaling method for stainless steel in the HRT was further developed. At the cost of increasing descaling time to several hours, the corrosion rate was reduced to less than 0.1 mil per month on 347 stainless steel, Zircaloy-2, and titanium by monitoring the pH at 1.60 ± 0.05 and the temperature at 85°C while circulating the solution through mossy zinc. The pH was controlled by continuous addition of H_2SO_4 as the zinc was consumed. Although trivalent uranium was an even more effective descaler than divalent chromium, its instability was a severe handicap to its use.

6. WASTE TREATMENT AND DISPOSAL

Safe and economic management of wastes from reactor fuel processing is essential to a sound and mature nuclear power economy. Present methods of disposal do not offer either the degree of permanence required for containment of high-level wastes or efficient means for substantially decreasing the quantity of radioisotopes released to the environment as tighter restrictions are imposed. Processes under development to prepare wastes for permanent disposal are: (1) conversion of high-radioactivity-level wastes to solids by evaporation to dryness and calcination in a portable vessel, or "pot," which would serve as the container for final storage in specially constructed concrete vaults or mined cavities in geologic formations such as salt or limestone; (2) conversion of intermediate-radioactivity-level chemical decladding wastes to solids by mixing at room temperature with sand, cement, and lime; and (3) decontamination of low-radioactivity-level wastes by ion exchange with phenolic resins.

6.1 POT CALCINATION OF HIGH-RADIOACTIVITY-LEVEL WASTES

A process for converting wastes to solids by pot calcination has been investigated on both bench and engineering scales with synthetic wastes at tracer levels of activity in order to obtain chemical and engineering data for design of a pilot plant. It promises to be both simple and versatile, but has not yet been demonstrated with actual high-radioactivity-level wastes.

In this process (Fig. 6.1), waste that has been stored three or more years for decay of short- and intermediate-lived fission products is fed to an evaporator where the volume is decreased by factors of 2 to 4. The overheads from the evaporator go to an acid fractionation column which produces concentrated acid for recycle to the chemical plant and a very dilute low-radioactivity-level waste which can be further decontaminated before disposal as low-level waste. The evaporator bottoms, in the form of a very concentrated solution or slurry, go to an electrically heated cylindrical pot for evaporation to dryness and calcination at temperatures of 700–900°C. The calciner off-gases are first passed through a downdraft condenser where 85–95% of the nitrogen oxides are absorbed in the condensing water and then to the acid still for recovery of the remainder. The condensate is recycled

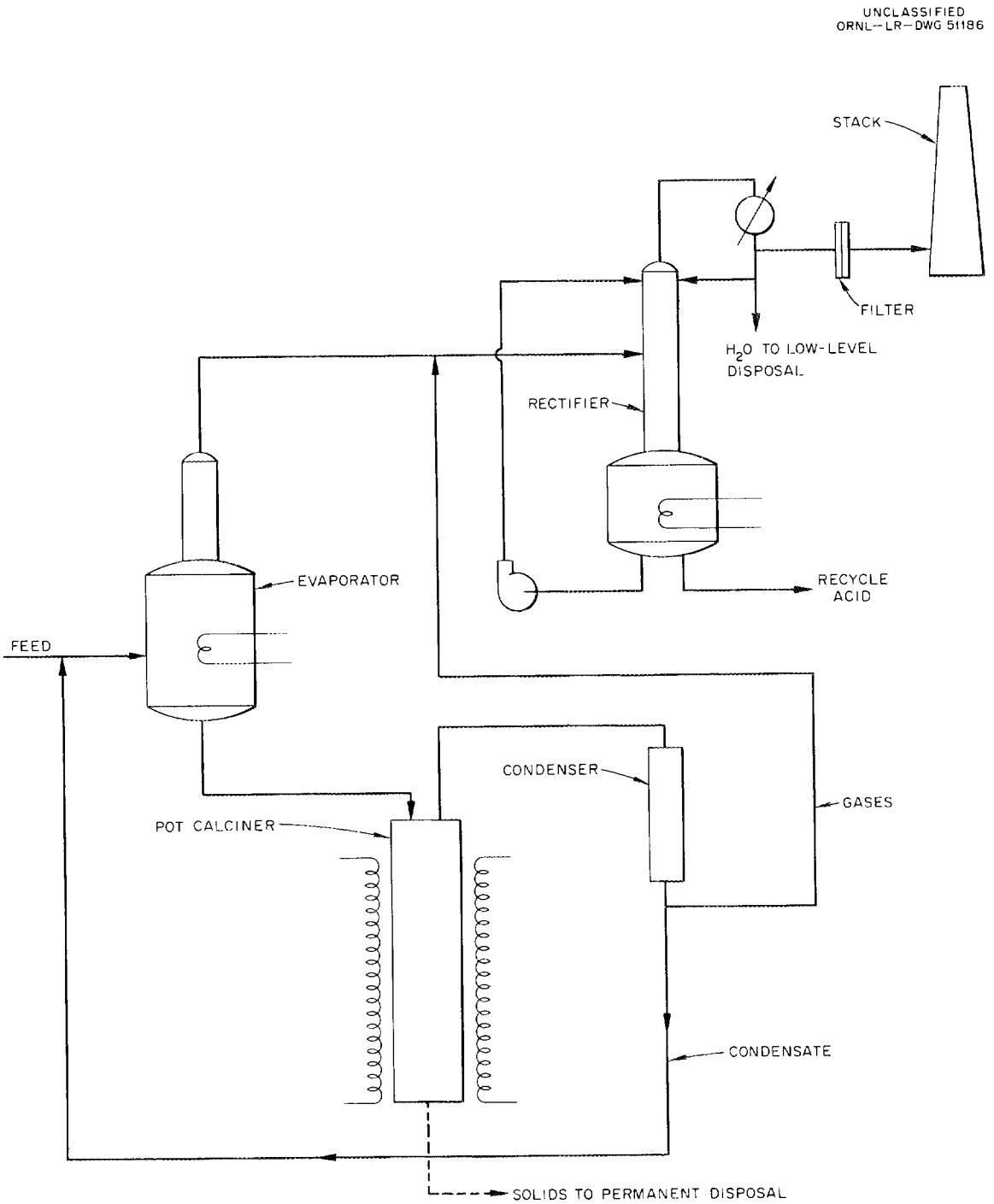

Fig. 6.1. Flowsheet for Converting High-Level Wastes to Solids by Pot Calcination.

to the evaporator, and the gaseous inerts in the system are removed in the reflux condenser of the acid rectifier, filtered, and then released through a stack. When the pot is filled with calcined solids, connecting process lines will be broken and the pot will be sealed, removed from the furnace, and shipped to a permanent storage site.

The feasibility of pot calcination in terms of the rate of calcination and rate of heat dissipation during storage has been established. Tests with Purex waste indicate that the effluent from the processing of 6 tons of uranium could be calcined and contained in one pot, 10 in. in diameter by 6 ft long. Aluminum-bearing wastes from processing of 1 kg of U^{235} in U-Al alloy fuels could be handled with one pot, 12 in. in diameter by 6 ft long. The problems of heat dissipation during permanent storage in various natural environments have been reported,[1] and the diameters of the calciner pots for a practical case have been limited to 12–15 in., which will permit heat dissipation by natural rather than forced cooling.

Bench-scale equipment for calcination studies consisted of a feed reservoir and pump, a calcination pot (4 in. in diameter and 18 in. long), a 5-kw furnace, and an off-gas handling system composed of a downdraft condenser, packed absorber column, polyethylene expansion bag, and gas-recirculation pump (Fig. 6.2). Illustrative of the experiments in this equipment

[1]J. J. Perona and M. E. Whatley, Calculation of Temperature Rise in Deeply Buried Radioactive Cylinders, ORNL-2812 (Feb. 3, 1960).

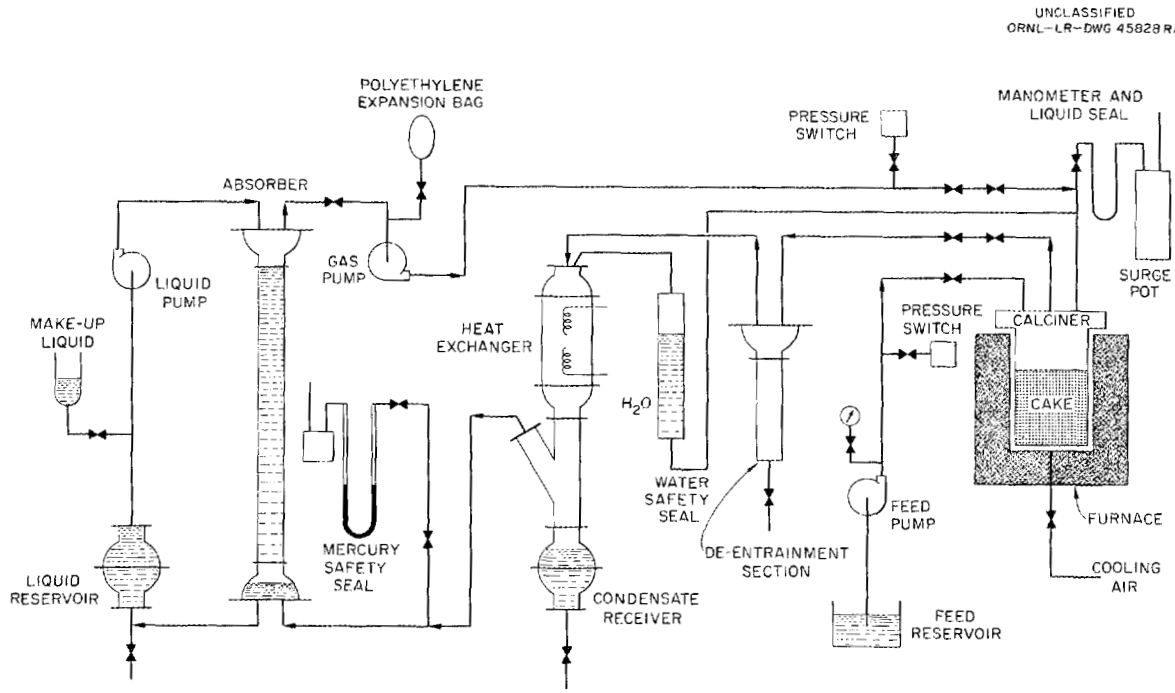

Fig. 6.2. Schematic of Apparatus for Calcining Wastes and Scrubbing Volatile Ruthenium from Off-Gas.

is the evaporation and calcination to 900°C of a synthetic Purex 1WW concentrate (5.6 M H^+, 6.1 M NO_3^-, 1.0 M SO_4^{--}, 0.6 M Na^+, 0.1 M Al^{+++}, 0.5 M Fe^{+++}, 0.01 M Cr^{+++}, 0.01 M Ni^{++}, and 0.002 M Ru ion). Sodium hydroxide (1.2 moles/liter, original concentration) and calcium hydroxide (0.2 mole/liter, original concentration) were added to the waste to reduce sulfate volatility. The feed rate, adjusted to be approximately equal to the boil-off rate, declined throughout the run, from 100 ml/min initially to almost zero at the end of the evaporation, as the can filled with solids and the heat-transfer rate decreased. A volume-reduction factor (volume of feed per bulk volume of solid residue) of 8.4 was obtained. The solid residue had an apparent density of 1.56 g/ml, equivalent to a porosity of about 48%. The condensate, residue, and off-gas contained 87, 11, and 0.5%, respectively, of the initial weight of the feed. The condensate and off-gas contained 98 and 2%, respectively, of the nitrate, and 0.7 and 0.02%, respectively, of the sulfate originally present in the waste. The condensate contained 26% of the ruthenium originally present in the feed when NO was not present in the evaporator; with NO added (NO will be produced in very active wastes by the radiation decomposition of nitrate) the ruthenium concentration in the condensate was decreased to ~1% of that in the feed. Approximately 5 liters of noncondensable off-gas was collected in the expansion bag per liter of waste. Analysis of the gas showed it to be principally oxygen. In similar experiments with NO admitted during the run, added with the intent of decreasing ruthenium volatility, the production of noncondensable off-gas was decreased to almost zero.

Experiments with synthetic Purex 1WW waste and concentrated Darex waste (1.9 M H^+, 2.9 M Fe^{+++}, 0.6 M Cr^{+++}, 0.3 M Ni^{++}, 0.3 M Al^{+++}, 13.9 M NO_3^-) were performed in 6- and 8-in.-dia stainless steel vessels, 78 in. long. The off-gas system (Fig. 6.3) consisted of two 15-ft^2 downdraft shell and tube condensers and a bank of orifices and differential-pressure cells for measuring noncondensable off-gas rates.

The runs with Purex waste were started with the calcination pot partially filled with water in order to avoid violent flashing and entrainment caused when waste solution is pumped into a hot, dry pot, and the liquid level was held constant at the top of the vessel throughout the feeding period. The initial feed rate was 60 liters/hr and decreased during the

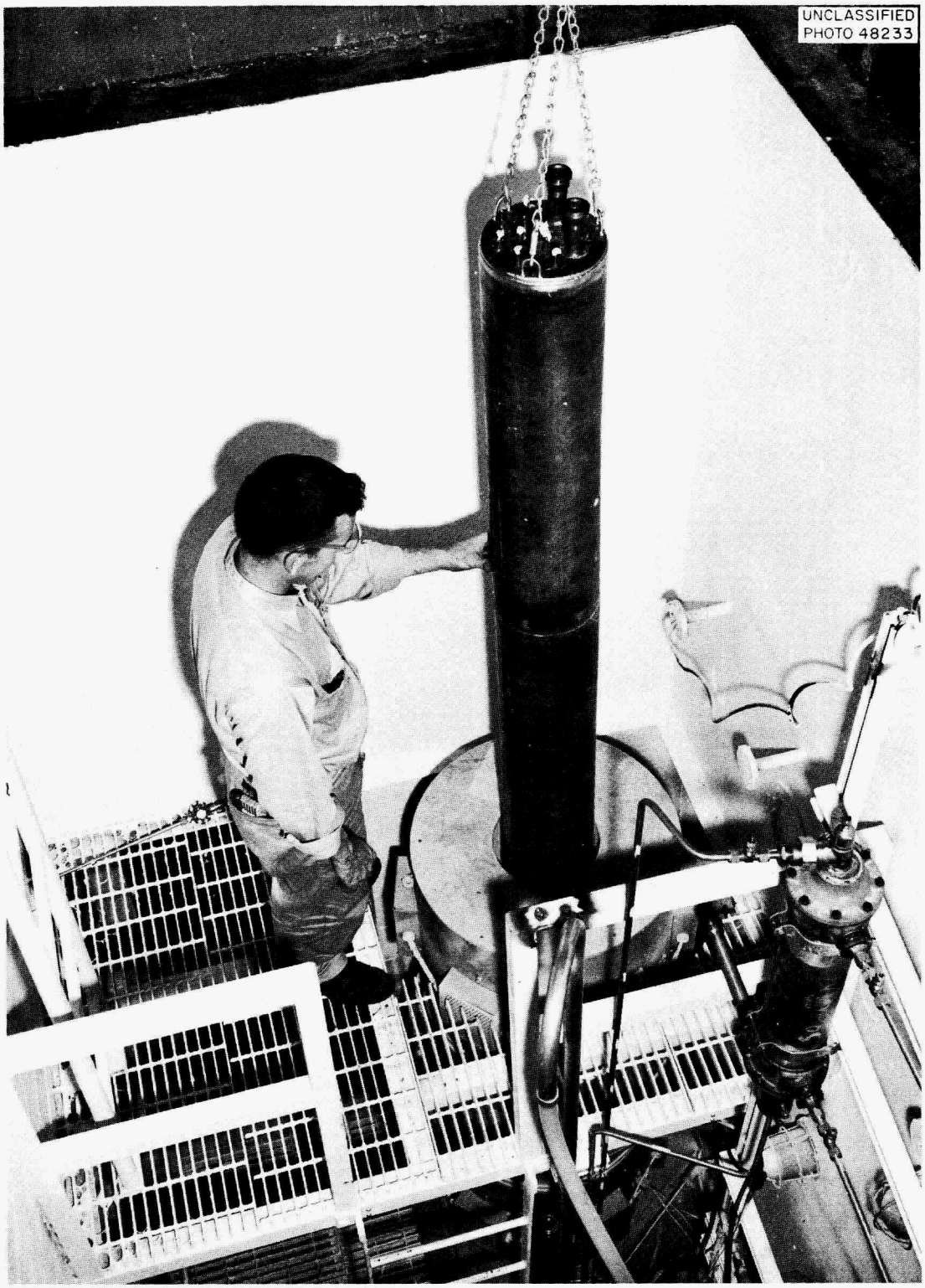

Fig. 6.3. Shell-and-Tube Condensers of Off-Gas System.

run to 1 liter/hr as the heat transfer surface was covered by the deposited solids. After feeding was stopped, heating and calcination continued for about 7 hr until solids temperatures of 700–900°C were reached. The density of the calcined solids was 1.5 g/cm^3 and the NO_3^- content averaged 200 ppm. From 85 to 95% of the nitrate in the feed was recovered in the condensate as HNO_3.

From deposition patterns of radioactive tracers added to the feed and the readings of thermocouples in the calcination vessel, it was established that the deposition of solids occurred mainly in the radial direction, with little deposition in the vertical direction. The data were adequately represented by

$$t = \frac{\alpha\rho\lambda R^2}{4k(\Delta T)} \left[2\left(\frac{r}{R}\right)^2 \ln\left(\frac{r}{R}\right) + 1 - \left(\frac{r}{R}\right)^2 \right] ,$$

where

t = time, hr,

α = volume of condensate per volume of deposited solid,

ρ = density of condensate, lb/ft^3,

λ = heat of vaporization of condensate, Btu/lb,

R = radius of vessel, ft,

k = thermal conductivity of deposited solid, Btu hr^{-1} ft^{-2} (°F)$^{-1}$ ft,

ΔT = difference between temperature of vessel wall and temperature of boiling liquid, °F,

r = distance from axis of vessel to surface of deposited solid, ft.

Calcinations of synthetic Darex waste were performed at constant feed rates ranging from 3 to 23 liters/hr. The density of the calcined solids was 0.8 g/cm^3, and the nitrate content was about 300 ppm. In contrast to the Purex runs, solids deposition took place mainly in the vertical direction, with little radial buildup. A constant height of liquid was maintained above the solid phase, which moved up the vessel as the height of deposited solids increased. The following equation relating the experimental variables was derived:

$$t = \frac{\alpha\rho\lambda R}{2Uh_L(\Delta T)} h_S ,$$

where

U = over-all heat transfer coefficient, Btu hr^{-1} ft^{-2} $(°F)^{-1}$,

h_L = height of liquid phase (constant), ft,

h_S = height of solid phase (variable), ft.

Nitrate-Organic Reactions

Experiments were performed with simulated Purex 1WW and various amounts of tributyl phosphate (TBP) to determine if a buildup of TBP or its degradation products during the evaporation of waste could cause an exothermic or even an explosive reaction. No violent reactions or rapid rises in pot temperature were detected in batch evaporations and calcinations to 400°C of simulated waste containing 3 to 300 ml of TBP per liter.

Thermal Conductivity

Measurements of the thermal conductivity of a calcined Purex waste showed variations from 0.210 Btu hr^{-1} ft^{-1} $(°F)^{-1}$ at 230°F to 0.311 at 1329°F, while the thermal conductivity of a calcined Darex waste varied from 0.140 Btu hr^{-1} ft^{-1} $(°F)^{-1}$ at 92°F to 1.52 at 1600°F. The Purex residue had an apparent density of 1.56 g/cc, which is equivalent to a porosity of about 48%. The Darex residue had an apparent density of 0.591 g/cm^3, which is equivalent to a porosity of about 89%.

The values of thermal conductivity for these wastes increased almost linearly with increasing temperature. This variation of thermal conductivity with temperature is typical of a powder rather than a cellular material (solid phase continuous, gas phase dispersed). However, the calcined wastes had the physical appearance of a cellular material rather than a powder.

Ruthenium Volatility

The limiting activity in the treatment of off-gases from the evaporation and calcination of radioactive wastes is probably ruthenium, since it is volatile under oxidizing conditions even at relatively low temperatures. Since it is desirable to have a means of positively controlling ruthenium volatility, batch evaporations and calcinations of Purex 1WW

concentrate were performed with a reducing atmosphere in the evaporator-calciner vessel. A reducing atmosphere was maintained in the equipment by sweeping NO through it. When simulated Purex 1WW containing no additives was evaporated in air without an NO sweep, the condensate contained about 72% of the feed ruthenium. With the NO sweep, 0.9–1.5% of the ruthenium appeared in the condensate. The use of sodium and calcium additives, to reduce sulfate volatility, increased the ruthenium in the condensate to 17–32%. The substitution of magnesium for calcium (mole for mole) decreased the ruthenium volatilization to 2–15%, depending on the amount of sodium. The presence of about 2 ml of TBP per liter of waste decreased the ruthenium volatility, in the absence of NO sweep gas, from about 70% to 4–15%, depending on additives.

Off-Gas Studies

In order to evaluate the effectiveness of the distillation tower in the plant flowsheet as a scrubber for soluble aerosols, a series of experiments was made by passing an air stream containing a $Cr(NO_3)_3$ aerosol with Cr^{51} tracer through a tower packed with 1/4-in. Raschig rings and operating at total reflux. The $Cr(NO_3)_3$ aerosol, having a lower vapor pressure than the steam in the vapor phase, would be expected to grow in size by diffusion of H_2O into the droplets. Sufficient growth of the particles in a steam atmosphere provided by a reboiler in the scrubber system should result in attenuation of the aerosol by the water in the scrubber tower due to inertia effects as the air stream passes through the tortuous passages of the packing when the aerosol was steam-suspended and passed to the scrubber. Decontamination factors were about 8.8×10^3 for tower vapor-phase compositions of 0.30 to 0.95 mole fraction of steam. When the tower was operated with the reboiler off and no steam in the vapor phase entering the scrubber, the decontamination factor was less than 10 (Table 6.1). The average volumetric mean diameter of the aerosol entering the tower was 10 μ in both cases.

Thermochemical Studies of Waste Components

Fundamental data on the physical and chemical changes of various salts during waste calcination are essential for predicting the effects of both

Table 6.1. Particulate Attenuation in a Packed Distillation Tower

Vapor Composition (Mole Fraction Steam)	Activity of Air (Counts min^{-1} ft^{-3})		Decontamination Factor
	In	Out	
0.30	2.30×10^4	2.63	8.7×10^3
0.47	7.24×10^3	2.20	3.3×10^3
0.64	5.62×10^3	3.55	1.6×10^3
0.95	2.2×10^4	2.57	8.6×10^3
0	2.3×10^4	4.3×10^3	5.4
0	2.4×10^4	3.2×10^3	7.5

major and minor components during calcination on the composition of the off-gas, and the nature of calcined product. One method of obtaining such information is the use of thermogravimetric analysis, in which the sample is weighed continuously while being heated. The data obtained from such measurements on typical components of high-radioactivity-level wastes show the temperature at which certain chemical changes take place, and in many cases the composition of the resulting compound can be calculated from weight loss (Table 6.2).

6.2 SOLIDIFICATION OF INTERMEDIATE-ACTIVITY-LEVEL WASTES

It has been proposed that decladding wastes be converted, by mixing with additives at room temperature, to dry solids suitable for ultimate storage. Based on compression tests, solids of good durability can be prepared in this manner from Sulfex and Zirflex decladding wastes.

The solids produced from Sulfex decladding waste had the following composition (parts by weight): decladding waste, 1.0; $Ca(OH)_2$, 0.26; sand, 0.26; cement, 0.55. After 27 days' curing, the compression test on the briquette was 3000 psi, the density was 1.33 g/cm^3, and the volume increase of the solid over the original liquid was 45%.

The solid produced from Zirflex decladding waste had the following composition (parts by weight): decladding waste, 1.0; $Ca(OH)_2$, 0.06; sand, 0.26; cement, 0.90. The waste solution was heated with $Ca(OH)_2$ to drive

Table 6.2. Thermogravimetric Analysis of Various Waste Components

Substance Heated	Temperature (°C)	Weight Loss (%)	Indication
$Fe(NO_3)_3 \cdot 9H_2O$	300	80	Fe_2O_3 formed
$Al(NO_3)_3 \cdot 9H_2O$	500	86	Al_2O_3 formed
$Fe_2(SO_4)_3 \cdot XH_2O$	400–700 800	23	$Fe_2(SO_4)_3$ formed Fe_2O_3 formed
$Ni(NO_3)_2 \cdot 6H_2O$	200–250 500	25	4 moles of H_2O lost NiO formed
$Sr(NO_3)_2$	675–950	50	SrO formed
$CsNO_3$	600–975	100	Decomposed; oxide sublimed
$Cr(NO_3)_3 \cdot 9H_2O$	500–1000	81	Cr_2O_3 formed
Na_2SO_4	1000	0	Stable at 1000°C
NH_4NO_3	350	100	Decomposes
$(NH_4)_2SO_4$	475	100	Decomposes
$NaNO_3$	850 1175	62 100	Na_2O formed Oxide sublimed
$FeSO_4 \cdot 7H_2O$	200–600 650–950	42 71	$FeSO_4$ formed Fe_2O_3 formed
$Al_2(SO_4)_3 \cdot 18H_2O$	400–600 800	46 86	$Al_2(SO_4)_3$ formed Al_2O_3 formed
$NiSO_4 \cdot 6H_2O$	500–750 950	41 71	$NiSO_4$ formed NiO formed
Cs_2SO_4	1000	0	Stable at 1000°C
$CaSO_4 \cdot 2H_2O$	200–1100	20	$CaSO_4$ formed (stable at 1100°C)
$MgSO_4$	1100	67	MgO formed
Na_2CO_3	1050	0	Stable to 1050°C

off NH_3 and reduce the volume before adding sand and cement. A 7-day-cured briquette collapsed under a pressure of 4200 psi. Its density was 1.85 g/cm^3, and the volume decrease of the solid over the original liquid was 23%.

Maritime Reactor Waste Disposal

Investigation of a procedure for the disposal of demineralizer resins by mixing with cement to form concrete blocks of low leachability has been

completed.[2] The results of sea disposal of both treated and untreated resins were studied. The untreated resins were rapidly eluted by sea water, while the resins fixed in concrete showed a much decreased rate of activity dispersion. For fixation of nuclear-reactor demineralizer resin in concrete, a mixture of two parts of Portland cement, one part of resin, and one part of water was optimum. A concrete block prepared in this manner lost only 0.44% of the gross gamma activity after 2540 hr of contact with simulated sea water. The data indicate that little or no further leaching will occur.

6.3 ION EXCHANGE TREATMENT OF LOW-RADIOACTIVITY-LEVEL WASTES

A flowsheet was demonstrated, on a laboratory scale, for decontaminating large volumes of low-radioactivity-level process-water wastes (Fig. 6.4). The wastes considered in the studies have a macrochemical composition not very different from tap water but contain more than the maximum permissible concentration of radioisotopes for unrestricted discharge to the environment. The process consists in adjusting the water to about pH 12 (making it about 0.01 M in NaOH, for most waters), clarifying it to remove solids, and passing it through a bed of phenolic cation exchange resin.

With typical ORNL low-radioactivity-level waste water, most of the calcium and magnesium in the water precipitate when the water is made alkaline, carrying down with them suspended solids and a substantial fraction of the radioactivity. Filtration then removes about 10% of the cesium, about 50% of the strontium, about 70% of the ruthenium and cobalt, and about 90% of the rare earths. The settled solids volume is about 1% of the original waste volume, and the filtered solids have a volume about 0.1% of the original waste volume and an even smaller volume after drying. The ion exchange step removes part of the residual ruthenium and cobalt, most of the residual rare earths, and nearly all the remaining cesium and strontium. For 1500 volumes passed through 1 volume of phenolic resin on a three-day loading cycle, the over-all process decontamination factors were 10 for ruthenium and cobalt, 100 for rare earths, and 1000 for cesium and strontium.

---

[2] R. R. Holcomb, Maritime Reactor Waste Disposal Studies: Solidification of Ion-Exchange Resin with Portland Cement for Radioactive Waste Disposal, ORNL-2899 (in press).

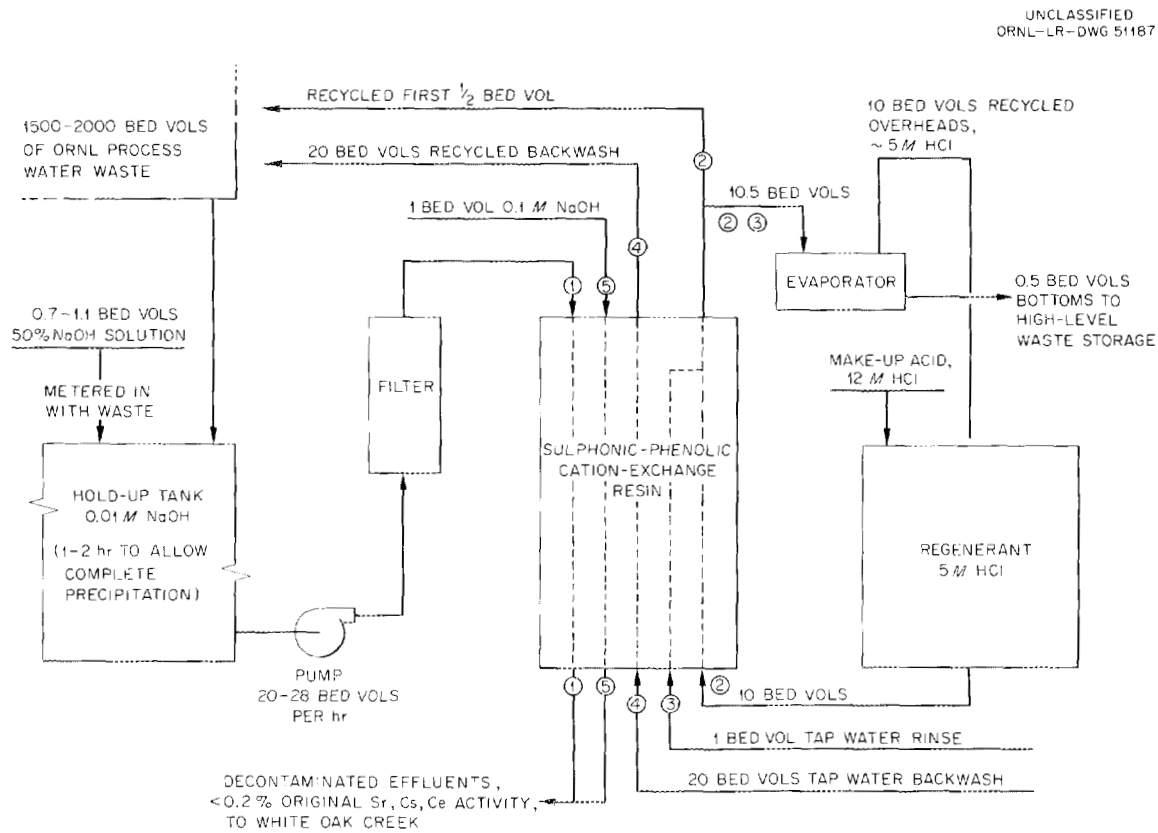

Fig. 6.4. Ion Exchange Process for the Treatment of ORNL Low-Level Process-Water Waste. Three-day sorption cycle, 8-hr regeneration cycle.

Duolite C-3, a phenolic-sulfonic resin, and Duolite CS-100, a phenolic-carboxylic resin, were about equally effective for cesium removal in the loading cycle. Both are also about as effective as the standard polystyrene-sulfonate resins (Dowex 50) for the polyvalent radioisotopes but are much more effective for cesium since the phenolic group, ionized only at high pH, is unusually selective for cesium in the presence of sodium and other cations. More than 99.9% of the cesium and strontium can be removed from Duolite C-3 by upflow regeneration with 10 volumes of 5 M HCl in 7 hr. Regeneration of Duolite CS-100 is the same except that only 1 M HCl need be used since it is a weak-acid resin. In either case, the 10 volumes of regenerant waste can be evaporated by a factor of 20, to give a volume reduction factor from original waste water to concentrated regenerant waste of about 3000. The condensate from the regenerant waste evaporation can be reused as regenerant after butting up to original strength with fresh acid. The use of sulfuric acid as regenerant is probably not

desirable because of the possibility of $CaSO_4$ precipitation in the resin bed during regeneration and because volume reduction factors on evaporation would be smaller. Regeneration with 5 M HNO_3 is precluded since it vigorously attacks phenolic resins; dilute nitric acid might be used to regenerate the CS-100 resin under carefully controlled conditions, but large volume changes between the acid and alkaline forms of this resin may lead to engineering problems.

6.4 ECONOMICS OF PERMANENT STORAGE OF LIQUID WASTES IN TANKS

The choice of disposal methods to be adopted by a nuclear power industry will depend on the allowable hazards involved and associated economics.[3] Although the costs of tank storage have been computed and analyzed for current production wastes, they have been based on only single tank lifetimes and reported in terms of cost per unit volume of tankage for government-owned installations. A study of the economics of permanent tank storage of power reactor fuel processing wastes indicates that the storage costs should average from 0.05 to 0.23 mill/kwhr of electricity produced (Table 6.3). Such costs cannot in themselves be considered exorbitant; however, they do not reflect the hazards of this practice that might be considered intolerable.

Two cases were considered in this study. Case 1 assumed that the waste-storage system was owned and operated by a chemical company without Government guarantees or subsidization. Under these circumstances, a 35% annual return on the investment was considered appropriate. Case 2 assumed Government-type financing. Here, a 10% return on the investment resulted in about a 3.6% return after taxes and expenses, which is near the current cost of money to the Government. In both cases the storage of chemical decladding wastes resulted in a significant contribution to the total costs. They ranged from 40% of the total for the thorium converters to as much as 83% for the zirconium-clad UO_2 converters; this is a clear-cut incentive for development of mechanical decladding methods.

---

[3] R. McKinney, Report of the Panel on the Impact of the Peaceful Uses of Atomic Energy to the Joint Committee on Atomic Energy 2, p 117–18, U.S.G.P.O., 1956 (secret).

Table 6.3. Summary of Waste Storage Costs from Fuel Processing of Various Reactor Types

Type of Waste	Volume Stored (gal/metric ton of U or Th)	Case 1: 35% Return on Investment		Case 2: 10% Return on Investment	
		($/gal)	(mills/kwhr, electrical)	($/gal)	(mills/kwhr, electrical)
Uranium converters					
Zr-clad UO_2					
Zirflex decladding waste	2120	3.14	0.1109	2.03	0.0717
Purex solvent-extraction raffinate	60	22.37	0.0224	12.21	0.0122
(Total)		(25.51)	(0.1333)	(14.24)	(0.0839)
Stainless-steel-clad UO_2					
Sulfex decladding waste	1100	3.84	0.0704	2.47	0.0453
Purex solvent-extraction raffinate	60	22.37	0.0224	12.21	0.0122
(Total)		(26.21)	(0.0928)	(14.68)	(0.0575)
Thorium converters					
Zr-clad ThO_2-UO_2					
Zirflex decladding waste	2120	3.14	0.0555	2.03	0.0358
Thorex solvent-extraction raffinate	640	15.60	0.0833	8.69	0.0464
(Total)		(18.74)	(0.1388)	(10.72)	(0.0822)
Fast breeders					
Stainless-steel-clad UO_2-PuO_2					
Sulfex decladding waste	1100	3.84	0.0857	2.47	0.0552
Purex solvent-extraction raffinate	60	22.37	0.0270	12.21	0.0148
(Total)		(26.21)	(0.1127)	(14.68)	(0.0700)
Thermal breeders					
Aqueous UO_2SO_4 solution					
Thorex solvent-extraction raffinate	640	15.60	0.2288	8.69	0.1275

7. FUEL CYCLE DEVELOPMENT

Fuel preparation and fabrication procedures adaptable to operation behind shielding are needed for recycling of irradiated Th-U^{233} fuels because of the presence of U^{232} and Th^{228} decay chains in recycled materials. Procedures now used in producing heterogeneous reactor fuel elements contain many steps and as a result are costly. Initial experimental studies were directed at developing simplified procedures for fabricating thorium oxide, uranium oxide, or mixed oxides into high-density metal-clad fuel elements. Vibratory compaction of oxide particles into cladding tubes was selected as a promising fabrication procedure, which has been reported[1] for UO_2 but not tested for ThO_2.

7.1 FABRICATION OF FUEL ELEMENTS

Effects of Equipment, Materials, and Procedures

Of the several types of pneumatic vibrators tested, the highest compacted densities were produced by the NAVCO "Bin Hopper" (1-1/4-in.-dia model) with the piston impacting directly against the housing at one end and air-cushioned at the other, giving a modified sawtooth wave form. A 2-in.-dia vibrator, air-cushioned at both ends of the piston housing, gave compacted densities ~1 g/cm^3 lower than the single-cushioned vibrator. The pneumatic vibrators were mounted beneath a spring-suspended base plate which also held the tube to be vibrated (Fig. 7.1). Inverting the piston in the 1-1/4-in.-dia vibrator changed the downward impact to upward with respect to the vibrating tube and produced a bulk density 0.2 to 0.3 g/cm^3 greater than that obtained when the piston delivered a downward impact.

The tube to be vibrated was vertically mounted in the tubing fitting of a Swagelok tubing-to-pipe connector screwed into the spring-suspended base plate. Originally the tubes were secured to the base plate by a holder which rigidly supported the entire tube length. Using the Swagelok connection which fastened only the bottom end of the tube, acceleration measurements, taken from a velocity pickup mounted on the top (free end) of a 2-ft tube, were 1.5 to 3 times those obtained from a similar tube

[1]Hanford Monthly Reports, e.g., HW-61575, Aug. 17, 1959; HW-63936, Feb. 10, 1960.

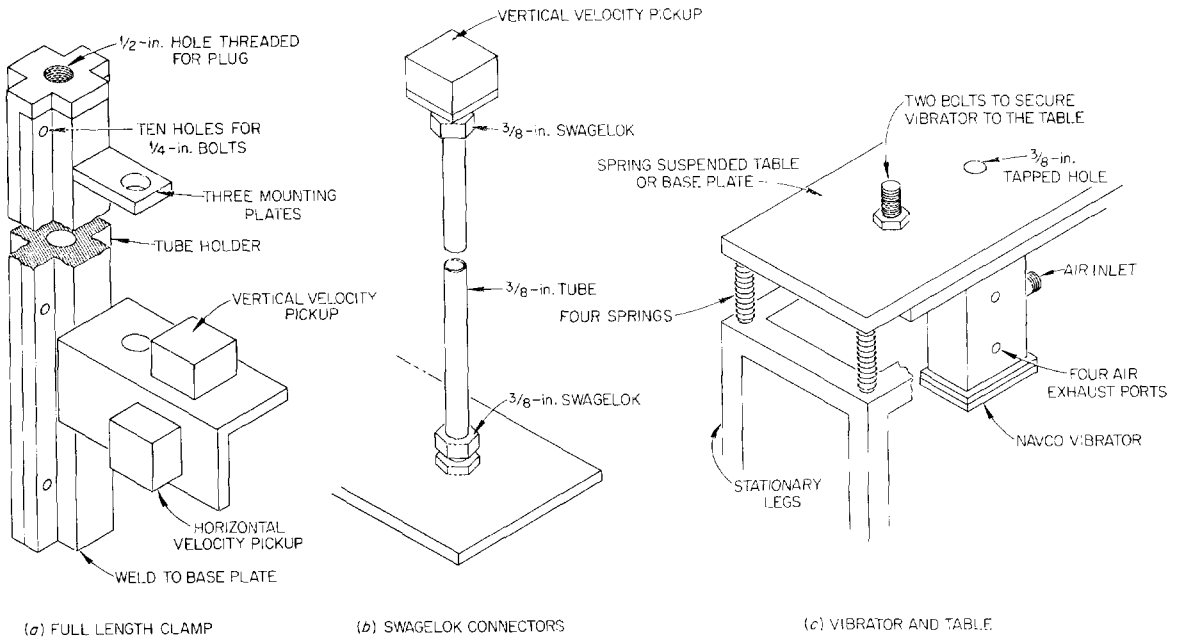

Fig. 7.1. Vibration Test Geometry.

clamped along its entire length. With the higher effective acceleration in the tube, vibratory compacted oxide densities were 0.3 to 0.5 g/cm^3 greater.

The majority of the vibratory compaction runs were made in 3/8-in.-dia stainless steel tubes, 2 ft long with 35-mil walls. With 200-g batches of mixed oxide powder, bulk densities were up to 89% of theoretical with pneumatic vibration (Table 7.1). A bulk density 87% of theoretical was obtained for 950 g of mixed oxide in a similar tube 8 ft long.

Using an electronic vibrator with a sine wave input, Hauth obtained bulk UO_2 densities 90–91% of theoretical in Zircaloy-2 tubes;[2] at Huntsville, Alabama, and Savannah River, South Carolina, attempts to achieve Hauth's results with mixed urania-thoria in stainless steel tubes were generally unsuccessful, bulk densities obtained at Savannah River being 0.5 to 0.6 g/cm^3 less than those reported by Hauth. The maximum bulk density of mixed oxide powders compacted in Lucite tubing at ORNL by pneumatic vibration was 81% of theoretical. The results might indicate a

[2] J. J. Hauth et al., Ceramic Fuels Development Operation of the Hanford Works, HW-64200 (to be published).

Table 7.1. Effects of Equipment and Materials on the Vibrated Bulk Density

Standard conditions
Vibrator: BH, 1-1/4-in. single impacting piston with impact on the upward stroke
Tube holder: Swagelok fitting (see Fig. 7.1)
Tube: 2-ft-long, 3/8-in.-dia stainless steel tubing, 35-mil wall
Oxide powder: Arc-fused ThO_2-UO_2 (3.4 wt % UO_2); 58 wt % −10 +16 mesh, 15 wt % −70 +100 mesh, and 27 wt % −200 mesh; 10.1 g/cm^3 density

Parameter Varied from Standard Conditions	Vibrated Bulk Density (% of theoretical)
None (standard conditions)	89
Vibrator: BH, 1-1/4-in. (piston impact on the downward stroke)	86
Vibrator: BH, 2-in. (piston air-cushioned at both ends of housing)	79
Tube holder: tube rigidly supported its entire length	84
Tube: 8-ft-long, 3/8-in.-dia stainless steel	87
Tube: 8-ft-long, 3/8-in.-dia aluminum tubing	86
Tube: 6-ft-long, 3/4-in.-dia Zircaloy-2 tubing	84
Tube: 2-ft-long, 3/8-in.-dia Lucite tubing	81
Oxide powder: arc-fused ThO_2	87
Oxide powder: hydro-thermally denitrated ThO_2	87
Oxide powder: hydro-thermally denitrated ThO_2-UO_2 (5.0 wt % UO_2)	85

relation between the vibrated bulk oxide density and the mechanical properties of the tubing material, although such a conclusion would be difficult to explain.

Four types of oxide powders were pneumatically vibrated to bulk densities > 85% of theoretical (Table 7.1). The oxide powders for compaction

were crushed and blended from three size fractions of the following approximate proportions and sizes: 58 wt % (−10 +16 mesh), 15 wt % (−70 +100 mesh), and 27 wt % (−200 mesh). Optimum powder packing was found to be dependent on many variables, but the greatest single effect was increased compacted densities as the coarse-to-fine diameter ratio increased. The rate of density increase became insignificant as the diameter ratio was increased to within a range of 30 to 50.

The most satisfactory procedure for filling the tubes was to pour the blended oxide powders through a funnel with the pneumatic vibrator running at decreased speed. At the end of the loading operation, the oxide was compacted to ~82% of theoretical density. Bulk densities were usually > 85% of theoretical after 3–5 min of continuous pneumatic vibration with the maximum available air pressure of 85 psig. Blending the different powder size fractions prior to filling the tube would be expected to be a necessary step in the loading procedure; however, a bulk density 84% of theoretical was obtained by vibrating fused ThO_2-UO_2 with no premixing of the three fractions.

Effects of Vibration Characteristics

The most significant characteristic of the vibration from pneumatic vibrators was the tube acceleration, which was between 80 and 150 G with the NAVCO 1-1/4-in.-dia vibrator. Acceleration was measured at the free end of a vibrating tube by a velocity pickup. The tube vibration produced by the 1-1/4-in.-dia vibrator when air-cushioned at one end showed between 15- and 20-mils vertical displacement and short periods of high accelerations. Air-cushioning the piston at both ends gave a sine wave displacement curve and poorer compaction.

Pulsing the vibrating frequency of the tube between 0 and 80 cps did not increase the bulk oxide density, and most of the pneumatic compaction studies were made at a frequency of 75–80 cps. The highest frequency attainable with standard commercial pneumatic vibrators is 200 cps. With an electronic vibrator, Hauth[2] achieved bulk urania densities between 90 and 91% of theoretical by pulsing the vibration frequency between 50 and 2000 cps; with these higher frequencies the results were obtained at an armature acceleration of approximately 10 G. With the electronic vibrator

at Savannah River and arc-fused ThO_2-UO_2, pulsing the frequency of vibration between 50 and 2000 cps in four runs gave bulk powder densities between 84 and 85% of theoretical. A fifth run at Savannah River with a saw-tooth wave input signal resulted in a bulk density 87% of theoretical.

In the Bin Hopper 1-1/4-in.-dia vibrator runs the 2-ft-long stainless steel tube and oxide powder weighed approximately 0.8 lb, and the vibrator housing plus mounting plate weighed 12 lb. With multiple tube bundles, the tubes plus the oxide powder would become a significant part of the vibrating load; however, larger vibrators are available for less than $100. A typical 3-in.-dia vibrator delivering a force of 21,000 lb at an air pressure of 40 psig (the frequency is 55 cps at this air pressure) should be capable of delivering an acceleration of 100 G to a vibrating load, tubes plus oxide, of 140 lb.

7.2 MEASUREMENT OF DENSITIES AND POROSITIES OF FUEL MATERIALS

Plots of pore volume vs nominal pore diameter (Fig. 7.2) are useful in selecting powders that will compact well. For example, powders that show essentially no voidage within the particles (curves D and E) are of interest in vibratory compaction. Powders with an appreciable volume of voids of $> 1\ \mu$ in diameter would not densify well by vibratory compaction (curve A). Where curves become essentially horizontal at higher void diameters (curves A and D), linear extrapolation to zero pore diameter gives density values agreeing well with experimental tap densities. The bimodal nature of curve B and known particle size ($1.7\ \mu$) suggest that this powder is bridged to weak agglomerates of roughly two size classes (3 and $15\ \mu$) and the inflection at $0.5\ \mu$ shows fine porosity within the particles. A sharp increase in void volume for some particular pore size followed by rapid leveling of the curve for larger sizes indicates uniformity in particle size. The shapes of curves B, C, and E suggest inflections beyond the range of the apparatus.

The curves in Fig. 7.2 were made by mercury porosimetry,[3] which provides for any solid mass a direct experimental measure of volume for any

[3] L. C. Drake and H. L. Ritter, "Pore Size Distribution in Porous Material," Anal. Chem. 17, 782 (1954).

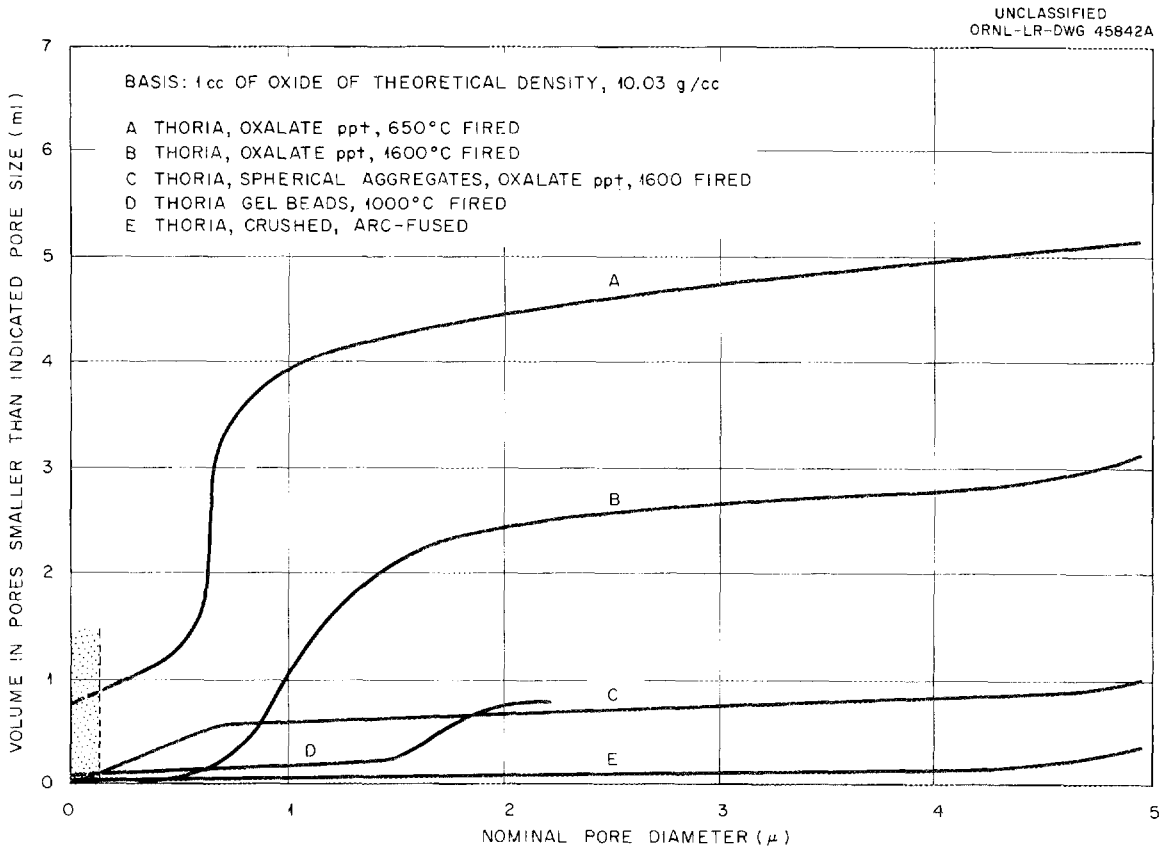

Fig. 7.2. Pore Volume as a Function of Pore Diameter for Thoria Powders.

pore size in its pressure range. For fuel materials, the measurement of ultimate particle density by mercury porosimetry is much more reliable than by conventional pycnometric methods. The size of pore filled by mercury is a function of pressure only, since mercury has an essentially constant nonwetting character for the material being tested. The size of pore filled by toluene or other conventional pycnometric fluid is dependent on contact angle, which in turn is a function of interfacial tension and may vary with different materials.

8. AMEX PROCESS

In the Amex process, the principles of anion resin exchange are applied on a liquid-liquid basis. The wide range of control obtainable through choice of reagent structure and diluent type is combined with the inherent advantages of liquid-liquid techniques. The amines, dissolved in hydrocarbon diluents, first react (during extraction from acidic liquors) to form alkylammonium salts. Subsequent extraction of metal or other ions follows closely the pattern for sorption with weak-base anion exchange resins and is assumed to occur by a mechanism analogous to anion exchange. The Amex process was originally designed for recovering uranium from ore leach liquors,[1] but has been shown to be useful for thorium, vanadium, molybdenum, and rare earths also. At present one Canadian, six American, and two Australian mills are using the Amex process for uranium recovery, and additional mills are being considered in the United States, France, Spain, and Sweden.

8.1 URANIUM RECOVERY

Carbonate and Nitrate Stripping Studies

An economical process was successfully demonstrated in bench-scale equipment for stripping uranium from amines with ammonium carbonate solution. By recycling the strip solution to allow buildup of the concentration of ammonium sulfate (formed in the stripping reactions) to 1–2 M, the solubility of uranium in the aqueous phase was limited to < 3 g/liter and ammonium uranyl tricarbonate (AUT) precipitated in the stripping system. The AUT, which settled and filtered rapidly, was readily converted to U_3O_8 by calcination at 500°C. The process has the advantage of producing a high assay (> 98% U_3O_8) product, virtually free of sodium, molybdenum, and vanadium, which should be highly amenable to the direct reduction-hydrofluorination-fluorination process for producing UF_6.

Operational feasibility of a nitrate stripping method which produces a relatively pure concentrated uranyl nitrate solution instead of the conventional solid uranium product was demonstrated in bench-scale continuous

---

[1] K. B. Brown and C. F. Coleman, Progr. in Nuclear Energy, Ser. III 2, 3 (1958).

tests (Fig. 8.1). Uranium-loaded tertiary amine (Amberlite XE-204) was contacted with 2.5 M calcium nitrate solution to precipitate sulfate and convert the uranium in the solvent to an amine nitrate–uranyl nitrate complex. The uranium was stripped with 0.2 M nitric acid and nitrate was recovered from the amine for recycle by contact with a lime slurry. The uranyl nitrate product solution could be shipped directly to the refinery or be used as a convenient starting point for preparation of pure UO_3 or UO_2 at the mill site.

UNCLASSIFIED
ORNL-LR-DWG 51080

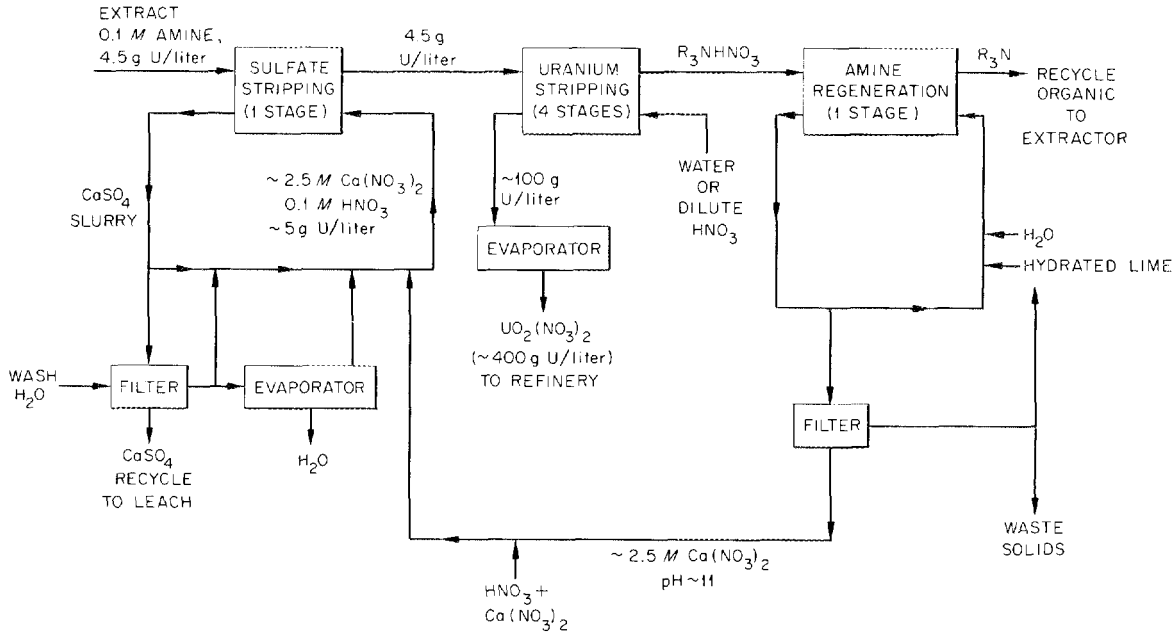

Fig. 8.1. Stripping Uranium from Tertiary Amines by the High Nitrate–Water Stripping Method.

Uranium Recovery from Carbonate Solutions

A flowsheet for recovering uranium from synthetic carbonate liquors by extraction with a quaternary ammonium compound (Aliquat 336) in kerosene-tridecanol and precipitation of uranium directly from the solvent with 0.5 M Na_2CO_3–1 M NaOH solution was demonstrated successfully. However, application of the flowsheet to an actual leach liquor from a western uranium mill gave poor results owing to interference of relatively large quantities of vanadium, molybdenum, sulfate, chloride, and organic matter.

It was concluded that solvent extraction is not competitive with the precipitation process currently used in mills employing the carbonate leach circuit.

8.2 THORIUM RECOVERY

Owing to the large variations in the relative extraction power of thorium and uranium by amines of different types and structure, the Amex process can be used for separate recovery of these two elements from sulfate solutions in which they coexist. Flowsheets have been described[2] for the treatment of Canadian Blind River ore leach liquors and monazite sulfuric acid digest liquors.

Amine Solubility

Further measurements of the solubility loss of Primene JM (a homologous mixture of primary amines) to aqueous solutions showed a continuous decrease in the loss rate even after the solvent had been contacted with 2000 volumes of aqueous phase. From these studies, the average loss rate is known to be much lower than indicated in earlier measurements. Consequently, Primene JM can be applied to treatment of liquors more dilute in thorium than had previously been considered economically practicable.

---

[2]D. J. Crouse, Jr., and K. B. Brown, Ind. Eng. Chem. 51, 1461 (1959).

9. THORIUM RECOVERY FROM GRANITIC ROCKS

Although thorium and uranium are relatively abundant elements, the reserves of high grade ores are extremely limited; therefore the greatest portion of these elements are found in very low grade, subcommercial deposits. It is apparent that, in the long-range future, fuel supplies for the production of nuclear power will depend completely on these low-grade sources. As a consequence, information on their extent and probable treatment costs can be an important factor in reactor-program planning.

As a result of considerable previous work on low-grade uranium ores such as shales and phosphates, fairly dependable information already exists on reserves and probable treatment costs of some of these materials. Equivalent information is not available, however, on low-grade thorium ores. For this reason studies have recently been initiated on the processing of granitic rocks, which are the major and most probable future low-grade source of thorium. These studies are an extension of preliminary tests on igneous rocks reported previously by Brown and Silver[1] of the California Institute of Technology.

9.1 SAMPLE COLLECTION AND SOURCE EVALUATION

Twelve samples of granitic rock ranging from 10 to 95 ppm in thorium concentration have been obtained from the USGS and Rice Institute. Owing to the large variations in mineralization that exist in granitic rock, these few samples do not give a good statistical representation of all rocks that might be available for processing. It is encouraging to note, however, that some of the samples contained thorium at concentrations considerably higher than the average of 12 ppm for igneous rocks in the earth's crust. At present, Rice Institute (under subcontract) is collecting additional samples in the field and will conduct sufficient sampling of some formations to permit a rough estimate of thorium reserves.

---

[1]H. Brown and L. T. Silver, Proc. Intern. Conf. Peaceful Uses Atomic Energy, Geneva, 1955, 8, 129 (1956).

9.2 LABORATORY PROCESSING STUDIES

In preliminary sulfuric acid leaching tests, thorium recoveries from the twelve granite samples ranged from 25 to 80%. The differences in recoveries were apparently due to variation in mineralization. Detailed mineralogical studies of the granite samples are currently being made at Rice Institute for correlation with the leaching results. Consumption of sulfuric acid during leaching was high, ranging from 40 to 100 lb/ton of granite. This compares with a consumption of 14 lb of H_2SO_4 per ton reported by Brown and Silver.[1] Filtration of the leached pulp was rapid after treatment with Separan 2610.

9.3 COST STUDIES

Detailed cost analyses of granite processing have been started in cooperation with A. H. Ross and Associates of Toronto, Canada. Based on analogies in the copper industry, direct costs for granite mining have been estimated at 45¢ per ton. Cost analyses of other process operations await development of further data. Rough preliminary estimates suggest that the thorium cost will be very high, perhaps as high as $400–500 per pound, from average grade refractory granites containing 12 ppm Th and yielding an over-all recovery of only 20%. More acceptable costs, for example, <$100 per pound, may be attainable from more easily leached, higher-grade granites. These estimates, however, are highly tentative and could change significantly as further, more reliable information becomes available.

10. GAS COOLED REACTOR COOLANT AND EQUIPMENT DECONTAMINATION

Experimental studies are in progress on systems for removal of chemical impurities from coolant gases and decontamination of equipment that has been exposed to coolant gases containing radioactivity released from fuel elements. This work has direct application to gas-cooled reactors.

10.1 COOLANT CLEANUP STUDIES

The anticipated nonradioactive gaseous contaminants in a helium coolant for a gas cooled reactor which will have to be maintained at a very low level are CO, H_2, CO_2, H_2O, and trace amounts of hydrocarbons. It is planned to remove these contaminants by oxidizing the CO, H_2, and hydrocarbons to H_2O and CO_2 and removing the CO_2 and H_2O by a sorption process. A test facility has been completed for evaluation of the oxidation and sorption steps (Fig. 10.1). The immediate experimental goal is to evaluate purification unit operations which fulfill the requirements for purification of the helium coolant in the EGCR. The design criteria for this system are:

	Impure Gas (vol %)	Desired Operating Concentration (vol %)
He	95.1	
CO	2.3	$\leq$ 0.1
H_2	2.3	$\leq$ 0.1
CO_2	0.2	nil
N_2	0.1	$\leq$ 0.1
H_2O and fission products	trace	trace

More advanced gas-cooled reactors will probably have stricter purity requirements.

In 12 experimental runs, CuO proved to be an excellent oxidizing agent for hydrogen. The tests were made in a 2-in.-dia oxidizer at 300 psia with bed temperatures of 396 to 540°C, total gas flow rates of 12.0 and 67.0 liters/min (STP), and inlet hydrogen concentrations of 0.66 to 3.50 vol %. Reagent grade CuO wire 0.017 in. in diameter averaging 0.034 in. in length was used. Conversion of H_2 to H_2O ranged from 56.7 to > 99.9%.

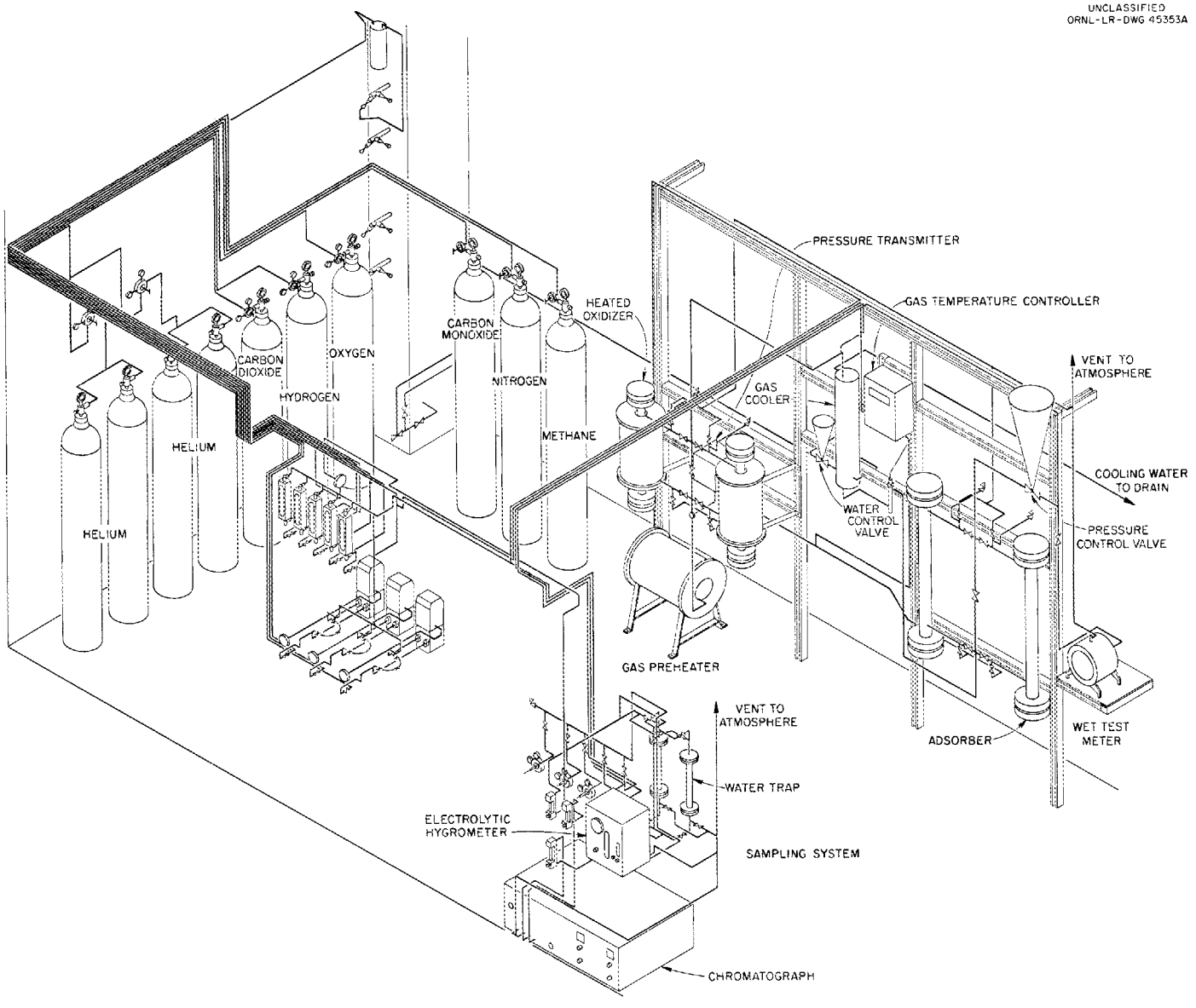

Fig. 10.1. GCR Helium Coolant Purification Test Facility.

The resulting design equation for a fixed bed oxidizer is

$$V = \frac{F}{K_1 \pi} \ln \frac{y_0}{y} + \frac{F y_0 \theta}{\rho} \quad ,$$

where

V = volume of CuO bed necessary to achieve design specifications, cm^3,

F = total feed rate of gas to reactor, g moles min^{-1},

y_0 = mole fraction of hydrogen in entering gas,

y = mole fraction of hydrogen in oxidizer off-gas,

K_1 = overall reaction rate constant, which is a function of temperature and mass flow rate of gas, g moles cm^{-3} min^{-1} atm^{-1},

π = total pressure of system, atm,

θ = operating time without regeneration of bed, min,

ρ = density of CuO in bed, g moles cm^{-3}.

The first term on the right in the design equation is the volume of CuO bed necessary to achieve the desired hydrogen concentration in the oxidizer off-gas and the second term is the volume of bed necessary for operation of time θ without regeneration.

The CuO oxidizer will be tested for use as an oxidizing agent for CO and combinations of H_2 and CO. These tests will include some extended tests in deep beds with alternate depletion and regeneration to test the feasibility of long-term operation. A platinum catalyst for oxidizing with O_2 will also be evaluated. The first sorption process to be tested will be co-sorption of H_2O and CO_2 on molecular sieves.

10.2 DECONTAMINATION OF EQUIPMENT

Development of satisfactory decontamination methods has been directed initially to the charge and service machines of the EGCR, which will be too large for filling with solutions and must be decontaminated by spraying techniques. The machines may be expected to become contaminated either by contact with the reactor coolant or from broken fuel elements. Since they are constructed of mild steel and contain precision parts, the procedure must be noncorrosive to this material.

The procedure developed for removing water-soluble and volatile fission products and UO_2 dust consists in spraying with hot nonfoaming detergent solution to dissolve, for example, cesium and iodine and to flush away some of the UO_2. If UO_2 still remains, as indicated by a broad spectrum of fission products when scanned by the remote probe of a scintillation γ spectrometer, the machines will then be sprayed with a peroxide—sodium oxalate solution to dissolve the UO_2. In experimental work, cesium and iodine deposited on mild steel from aqueous solutions were removed by hot water or steam by factors of 5000 for iodine and 250 for cesium. Ultrafine UO_2 dust, like that expected to be blown into the machines by the helium, was only about 50% removed by detergents but was dissolved in a few seconds by the peroxide solution, with decontamination factors from neutron-irradiated UO_2 of 100 to 1000.

The sodium oxalate—peroxide solution is the most attractive reagent tested to date. It both dissolves massive UO_2 rapidly and removes adsorbed fission products. This reagent has a useful life of at least 20 min at 95°C, as contrasted with 0.75 min for carbonate—peroxide studied earlier.

Tellurium, ruthenium, and cerium deposited on steel from carbonate solution and baked to the oxide were removed by a steam spray containing 10% Turco 4518, a proprietary compound containing inhibited oxalic acid, by factors of 155 (10 min boiling), 65 (10 min, 75°C), and 1.5×10^4 (20 min boiling). Yttrium and barium—lanthanum were removed by factors of 4000 and 360, respectively, in 30 min boiling. Ruthenium and cerium deposited on steel from aqueous solutions and strongly heated in air, were removed by factors of only 5 (30 min boiling) and 125 (20 min boiling). If ruthenium and cerium are not adequately decontaminated by inhibited oxalic acid in the charge and service machines, decontamination can be increased by factors of 50 to 100 by pretreatment with alkaline permanganate at 100°C and then re-treating with the oxalic acid.

11. HRP THORIA BLANKET DEVELOPMENT

The preparation of thoria blanket material for the HRP has been reported in the HRP Quarterly Progress reports. The pilot-plant-scale equipment for preparation of thoria and thoria-urania powders was moved to a new site specially built for thorium oxide preparation and placed in operation in July 1959. The layout of equipment and the methods of preparation are discussed in detail in a special report[1] and in the HRP Quarterly reports.[2–4]

Twenty-four experimental batches of ThO_2 and 19 of thorium-uranium oxide containing 0.5, 3.0, and 8.0 wt % U, ~ 150 lb per batch, were prepared during the year. The mean particle size requested covered the range < 1 to 10 μ, and the material prepared had an actual range of 1 to 7.9 μ. The firing temperature requested for various oxides ranged from 650 to 1600°C. Specifications for thoria were met with few exceptions; however, the mixed oxides were not satisfactory due to the lack of integrity of the particles. Since laboratory tests have not determined the reason for this, mixed-oxide preparation was suspended in December 1959. All operations were suspended on June 17, 1960, and the plant placed in stand-by status.

11.1 OXIDE PREPARATION DEVELOPMENT

Flame Denitration

Studies on the preparation of thoria particles by flame denitration of alcohol solutions of thorium nitrate were completed. Approximately 30 lb of thoria-urania prepared to give spherical particles with a U/Th mole ratio of 0.03 and containing 1.6 wt % Al_2O_3 were size-classified to remove particles > 10 μ in diameter and circulated as an aqueous slurry in a 100A

---

[1] K. O. Johnsson and R. H. Winget, Pilot Plant Preparation of Thorium and Thorium-Uranium Oxides, ORNL-2853 (Dec. 8, 1959).

[2] R. H. Winget, HRP Quar. Prog. Rep. Oct. 31, 1959, ORNL-2879, p 231–234.

[3] O. C. Dean et al., HRP Quar. Prog. Rep. Jan. 31, 1960, ORNL-2920, p 117–123.

[4] O. C. Dean et al., HRP Quar. Prog. Rep. Apr. 30, 1960, ORNL-2947, p 113–117.

loop. The results[5] at 250°C and an oxygen atmosphere show low corrosion-erosion attack rates, ≤ 0.1 mpy, at 20 fps and 0.2 to 1.3 mpy at 40 fps along with little particle degradation. The yield stresses of this 1.3-μ mean diameter material extrapolated to 1350 g of Th per kg of H_2O were 0.027 lb/ft^2 prerun and 0.072 lb/ft^2 postrun.

Rounded oxide particles of 1 to 3 μ dia were also prepared by addition of 3.5 wt % beryllia or of 0.5 to 5.0 wt % alumina or silica to methanol solutions of $Th(NO_3)_4$ or uranium-thorium nitrate up to 8 mole % uranium, followed by flame denitration.

Substitution of $Th(SO_4)_2$ for $Th(NO_3)_4$ and/or H_2O for CH_3OH in the feed solution and of N_2 for O_2-C_3H_8 as the atomizing gas, as well as increasing the size of feed solution droplets to the flame from 30 to 150 μ, failed to give the desired oxide average-particle-size increase of from 2 to 10 μ. Reduction of the temperature of the burner reflector from 1600 to 1000°C and doubling the mole concentration of metal nitrates in the feed increased the mean particle size from 2 to 2.9 μ.

Microspheres Preparation by Gel Technique

Spherical thorium oxide particles in the size range 0.5 to 30 μ were prepared by setting a thoria sol to gel spheres by spraying the sol and an isopropyl alcohol–water mixture simultaneously through an orifice, followed by slow drying and calcination to 1000°C. A typical product had a density of 6.8 g/cm^3, and a nitrogen surface area of 0.68 m^2/g. When the final calcination temperature was increased to 1600°C, the density was increased to ~ 8.3 g/cc, but the spheres tended to agglomerate. This method was developed in an effort to simplify the Houdry gel technique,[6] in which sols were prepared by peptization of ammonia-precipitated thoria with thorium nitrate to give a Th/NO_3 weight ratio of 4 and then were set by co-spraying with 1 M hexamethylenetetramine into a mineral oil–kerosene forming bath.

The use of 100% isopropyl alcohol for forming and washing resulted in a hollow "egg shell" structure. Increasing the water content of the system

[5]E. L. Compere et al., HRP Quar. Prog. Rep. Jan. 31, 1960, ORNL-2920, p 94–98.

[6]Houdry Process Corporation Final Report on Subcontract 904 Under W-7405 eng-26 (Dec. 30, 1958).

to > 23% caused dispersion of the beads. Since the solubility of ammonium nitrate in isopropyl alcohol increases eightfold as the water is increased to 15%, a saturated wash solution (17%) gave the best results. Washing was followed by slow drying to 250°C and then calcination at 1000°C. The maximum density, 8 g/cm^3, was obtained by firing at 1000°C. Decomposition of residual ammonium nitrate was the probable cause for porosity. Bead preparation is described in greater detail in quarterly reports.[7,8]

11.2 PREPARATION OF THORIA PELLETS FOR HR PEBBLE-BED BLANKET STUDIES

An aqueous homogeneous reactor with a pebble-bed blanket has been proposed, and preliminary studies of its feasibility are being made. Spheroidal thoria pellets, 0.13 to 0.25 in. in diameter, as resistant as possible to attrition by flowing 280°C water and hydraulic transport and to degradation by irradiation and thermal cycling, are required in approximately 5-kg batches for these studies. Certain additives for strengthening or enhancing resistance to attrition are permissible if they do not compete unduly with thorium for neutrons, promote corrosion of Zircaloy or stainless steel or are not leached excessively from the pebbles and deposited on surfaces at temperatures different from the pellets.

A tentative spouting-bed attrition test[9] similar to one developed and used by manufacturers of petroleum-cracking catalysts appears to approximate attrition conditions to which pellets will be exposed in the reactor. Only pellets whose minimum hourly weight loss in this test is less than 0.5% are of interest. Two general methods being investigated for preparation of the above pellets are press forming and sintering of thoria powders and forming and firing of thoria gel beads.

Press-Forming and Sintering of Thorium Powders

Thoria powder is treated with binders, such as polyalcohols and/or die lubricants, for example, kerosene or stearate soaps, and is then granulated by pressing and sieving. From this, powder pellets are formed by

---

[7]R. L. Pearson and A. T. Kleinsteuber, HRP Quar. Prog. Rep. Oct. 31, 1959, ORNL-2879, p 227–232.

[8]O. C. Dean and A. T. Kleinsteuber, HRP Quar. Prog. Rep. Jan. 31, 1960, ORNL-2920, p 117–123.

[9]E. L. Compere *et al.*, HRP Quar. Prog. Rep. Apr. 30, 1960, ORNL-2947, p 91–96.

pressing in a Stokes model E automatic tablet press fitted with a die having a slight taper and ball-face punches, and then the pellets are densified and strengthened by calcination at 1600 to 1750°C. A subcontract was negotiated with the Davison Chemical Company for the fabrication of 5 kg of strong, attrition-resistant, spherical pellets by the best techniques known to them. Efforts to prepare specification thoria spheres are also being made by the Ceramics Section of the Metallurgy Division at ORNL and by the Chemical Technology Division.

The Davison product, as delivered, was composed of nearly perfect spherical pellets, but they were weak, of low density, and had low resistance to attrition (Table 11.1). Soaking of batches in 2 M thorium nitrate, 1.7 M ammonia-neutralized thoria sol, or 5 M dibasic aluminum nitrate solution and refiring to 1750°C increased the density and decreased attrition losses. The effects of increasing the firing temperature were

Table 11.1. Fabrication Conditions and Properties of Davison Thoria Spheres

Formed from ceramic-grade oxalate-precipitated powder in a Stokes model E automatic tablet press. Binder-lubricant, 1% PVA plus 0.5% kerosene

Test Batch No.	Additive	Final Firing Temperature (°C)	Bulk Density (g/cm^3)	Attrition Loss (wt %/hr)
P-45	None	1450	5.05	21.5
P-46	None	1750	6.01	6.4
P-48	Diban*	1750	7.42	0.8
P-49	Thoria sol**	1200	5.61	24.3
P-50	Thoria sol	1750	6.74	1.8
P-51	2 M $Th(NO_3)_4$	1200	5.48	15.7
P-52	2 M $Th(NO_3)_4$	1750	6.62	3.5

*Dibasic aluminum nitrate solution, 5 M; NO_3/Al molar ratio, 1.2.
**Ammonia-neutralized to NH_3/Th mole ratio of 3; 1.7 M thorium.

similar. The diban-treated batch was of sufficient interest to be duplicated in a 4-kg batch for further testing.

The most significant variables in maximizing strength and density while minimizing attrition loss and cracking were: method of powder preparation, granulation pressures, additives, green density, and calcination temperatures. Conventional techniques that gave good results for cylindrical pellets produced spheres that had weaknesses at the junction of hemispheres which, in a significant percentage of pellets, resulted in cracks. Powders that gave spheres of highest integrity and density and lowest attrition loss were those prepared by oxalate precipitation, without digestion, under conditions that gave maximum particle size spread, followed by 1 to 4 hr calcination at 800 to 1000°C. Blends of low-temperature and high-temperature calcined powders showed some advantage for spheres, probably because strong granules are needed for making density adjustments when pressed in a spherical die, while yielding particles are needed to achieve the close packing necessary for optimum sintering.

In the use of an automatic tablet press, it is important that the powder flow uniformly into the die. Granules are prepared from the powder by treating with a binder, pressing, and sieving through a 20-mesh U.S. Standard sieve. Aluminum stearate (4% by weight) in isopropyl alcohol solution and 1% Carbowax in water were the most effective of the binder-die lubricants (Table 11.2). Optimum granulation pressure for binder-doped and dried powders was dependent on the prefiring temperature of powders and was 4,500 to 15,000 psi for powders fired to 650 to 1000°C. The best flowing powders had more than 75% particles greater than 100 mesh.

In press-forming pellets with the automatic tablet press, the optimum compaction pressure was indicated by the green density of the pellets. Die pressures were adjusted to give green strength sufficient for handling. Overpressing resulted in cracking during firing. Optimum green densities for powders prefired to 650 to 800°C were 4.5 to 4.9 g/cm^3, and for powders fired to 800 to 1000°C green densities were 5.0 to 5.6 g/cm^3.

Pellets were strengthened, densified, and increased in attrition resistance by calcination in air. In experiments with pellets from three powder preparations, calcinations were conducted at 1300°C for 20 hr, at

Table 11.2. Fabrication Conditions and Properties of Thoria Pellets

Powder: oxalate-precipitated, ceramic grade
Calcination conditions: 4 hr at 1750°C

Batch No.	Description of Powders Used	Binder-Lubricant	Bulk Density (g/cm^3)		Ultimate Attrition Loss (wt %/hr)
			As Pressed	As Fired	
1	Fired at 800°C for 1 hr	Al stearate, 5%*	4.5	9.7	0.25
2	A blend: 80% fired at 800°C for 1 hr, and 20% fired at 800°C for 4 hr	Al stearate, 5%	4.8	9.7	0.60
3	A blend: 30% fired at 650°C for 4 hr, and 70% fired at 1000°C for 1 hr	Al stearate, 5%	5.8	9.6	0.43
4	Fired at 800°C for 2 hr	Al stearate, 4%		9.5	0.21
5	A blend: 30% fired at 650°C for 4 hr, and 70% fired at 950°C for 2 hr	Carbowax, 1%**		8.65	0.31

*Aluminum stearate, 3.4% aluminum, prepared by reaction of aluminum chloride and 50% excess stearic acid in isopropyl alcohol. The purified salt was dissolved in isopropyl alcohol to the extents shown in the table (4 or 5%).

**The Carbowax was dissolved in water.

1600°C for 6 hr, and at 1750°C for 4 hr. In all cases, approximately 4-hr heatups and 8-hr cooldowns were allowed. Even with shorter times at higher temperatures, densification was increased and attrition rates were decreased by increased calcination temperature (Table 11.3). Both Al_2O_3 and CaO additives, up to 1.0 wt %, gave increased density, strength, and attrition resistance. In another calcination study for temperatures 1450°C or less, and the pellets being granulated with aluminum stearate, the greatest densification (9.37 g/cm^3) was obtained with a 75% N_2–25% CO atmosphere.

Table 11.3. Effects of Calcination Conditions on Density and Attrition Resistance of Spherical ThO_2 Pellets Prepared from Three Powders

Powders: ceramic grade, oxalate-precipitated ThO_2

Powder	Binder	Calcination Temperature (°C), and Time	Bulk Density (g/cm^3)	Attrition Loss (wt %/hr)
Single: 800°C-fired	4% Al stearate in isopropyl alcohol	1300, 20 hr	8.7	3.3
		1600, 6 hr	9.5	1.6
		1750, 4 hr	9.5	0.8
Blend: 20% 800°C-fired, 80% 950°C-fired	1% Carbowax in water	1300, 20 hr	7.4	3.3
		1600, 6 hr	8.1	2.6
		1750, 4 hr	8.7	1.6
Blend: 30% 800°C-fired, 70% 950°C-fired	1% Carbowax in water	1300, 20 hr	7.2	2.8
		1600, 6 hr	8.2	2.3
		1750, 4 hr	8.9	2.3

Gel Sphere Technique

The manufacturers of silica-alumina petroleum-cracking catalysts have developed an economical silica-alumina-gel bead forming technique which consists of forming spherical droplets of a fast setting sol in an oil bath, followed by drying and firing. Thoria spheres of 3 to 40 μ were also formed by this technique by the Houdry Process Corporation. The bulk density of beads of 3- to 10-μ size calcined to 1000°C was 9.9 g/cm^3. Houdry Process Corporation has agreed to produce 5 kg of beads of 0.125–0.25 in. diameter by this technique.

11.3 EVALUATION OF THORIA AND THORIA-URANIA POWDER PREPARATIONS FOR BLANKET SLURRIES

Jet Abrasion Testing

Previous testing with the jet abrasion tester[10] showed it to be capable of detecting the tendency of thoria or thoria-urania particles to be degraded when a slurry containing them was impinged on a metal foil. Further testing showed that, while the test distinguishes readily between a

[10] J. P. McBride et al., HRP Quar. Prog. Rep. July 31, 1957, ORNL-2379, p 150–151.

readily degraded (low-fired) oxide and one of high integrity (i.e., 1600°C-fired ThO_2), it cannot detect small (less than a factor of 2) changes in particle size. There was no clear evidence that difference in particle shape affected the abrasiveness of the powder.

Degradation and Clinker Formation in Thorium-Uranium Oxides

Slurries containing thoria plus 0.5 and 3 mole % urania in which the powders had been fired to temperatures of 1325 and 1100°C, respectively, were degraded severely in loop and toroid tests. Some of these slurries formed dilatant plugs in vertical sections. In jet abrasion tests of mixed oxides prepared by adsorption of UO_3 on ThO_2 containing 0.5 mole % urania fired at 1225°C, 3 mole % urania fired at 1100°C, and 8 mole % urania fired at 1050°C, particles were degraded by a factor of 2 or more. Oxides containing 0.5 and 8 mole % urania could be calcined at 1400°C without clinkering if prefired at 1000°C for 4 hr. An oxide containing 3% urania gave clinkers when calcined above 1200°C. Calcining of powders previously fired to only 650°C and heating directly at 1100°C or higher caused excessive clinkering in powders of all compositions. Prefiring of powders at 1000°C for 4 hr, then at higher temperatures, decreased clinker formation.

Properties of Thorium-Uranium Oxides[11]

Studies were made of properties of thorium-uranium oxides, prepared by deposition of uranium oxide on preformed thoria,[12] containing mole fractions of uranium varying from 0.0054 to 0.044 and fired in air or hydrogen at 1100°C for 4 to 24 hr. Lattice dimensions were calculated for these oxides from x-ray diffraction data and compared with those calculated from Vegard's law[13] for solid solutions having cubic structures, using lattice dimensions 5.5973 A for pure ThO_2 and 5.4691 A for pure UO_2.[14] The mixed oxides fired in hydrogen deviated more in lattice constants from Vegard's

---

[11] O. C. Dean and C. E. Schilling, HRP Quar. Prog. Rep. Oct. 31, 1959, ORNL-2879, p 220–225.

[12] J. P. McBride *et al.*, HRP Quar. Prog. Rep. Oct. 31, 1958, ORNL-2654, p 202–214.

[13] L. Vegard, Z. Physik 5, 17 (1921).

[14] R. E. Rundle *et al.*, J. Am. Chem. Soc. 70, 99–104 (1948); MDDC-1608.

law than did those fired in air, and the deviation increased with increasing uranium content. Surface area decreased more and crystallite size increased more in all thorium-uranium oxides when fired in air than when fired in hydrogen. Excess oxygen appears to promote sintering at the lower (1100°C) temperature. As the uranium content of the air-fired samples increased from 0.0054 to 0.044 mole fraction, the O/U ratio decreased from $UO_{2.67}$ to $UO_{2.2}$, which indicates that the capacity of the cubic thorium-uranium oxide lattice for interstitial oxygen is limited. For oxides fired in air, the fraction of uranium removed by leaching with 8 N HNO_3 decreased with increasing uranium content and was directly proportional to the surface area of the mixed oxide. Oxides fired in hydrogen showed a lower specific leaching effect.

11.4 GAS-RECOMBINATION CATALYST DEVELOPMENT

Further studies were carried out on the catalytic combination of hydrogen or deuterium and oxygen in aqueous reactor slurries containing a sol-prepared palladium-thoria catalyst.[15] The sol method of preparing the palladium catalyst, described below, has given the most active catalyst yet prepared and appears reproducible. Reasonable agreement was obtained between out-of-pile and in-pile tests, but all experiments showed that there were limits of hydrogen or oxygen overpressure or H_2/O_2 ratio under which catalytic activity was maintained. A slurry sample from a pumping-loop gas-recombination experiment showed a lower specific activity than did an unpumped slurry, and confirmed qualitatively the decline in activity observed in the loop. A new apparatus for carrying out the laboratory studies was developed in which measured quantities of hydrogen and oxygen could be injected at temperature into the autoclave containing the slurry catalyst system, simplifying and improving the experimental procedure.

Palladium Catalyst Development

The sol preparation method consisted of refluxing a 650°C-fired thorium oxide in an aqueous solution of palladium nitrate [0.5 g of $Pd(NO_3)_2$ to 10 g of ThO_2] to form a sol, and then reducing the sol with hydrogen.

[15] J. P. McBride and L. E. Morse, HRP Quar. Prog. Rep. Apr. 30, 1960, ORNL-2947, p 87–90.

Treatment with hydrogen (or deuterium for heavy water preparations) reduced the palladium, destroyed the bulk of the nitrate ion, and flocculated the sol. The catalyst preparation was a flocculated, slow-settling suspension, an aliquot of which was added to the slurry under test. Preparations were made in both ordinary water (P-23) and heavy water (P-28 A and P-28 B-C).

The sol-prepared catalyst was active in both thoria and thoria-urania slurries (Table 11.4). The data were usually evaluated in terms of a catalyst performance index, CPI, which relates catalytic activity (moles of D_2 per liter per hr) to reactor power density (w/ml) at an equilibrium partial pressure of 100 psi radiolytic D_2:

$$w/ml = \frac{\text{moles of } D_2 \text{ per liter per hr}}{(0.38)(G_{D_2})} ,$$

where G_{D_2} is the G value for D_2 production, 0.7.

Out-of-pile experiments with slurries of 1600°C-fired thoria, 1000°C-fired Th–8% U and Th–16% U oxide, and where the H_2/O_2 ratio of the partial pressure was ≤ 2, gave CPI's from 8 to 19 w/ml per millimolal Pd concentration at 280°C and a deuterium partial pressure of 100 psi (Table 11.4).[15] With slight excesses of H_2 over the stoichiometric $H_2 + 1/2\ O_2$ in the gas phase, specific catalytic activities were 30 to 40 times higher. In an in-pile test with a slurry of the Th–8% U oxide under excess O_2, CPI's of 20 to 30 w/ml per millimolal Pd concentration were observed.[16] In a similar in-pile test with Th–16% U oxide a CPI of only 0.3 w/ml was obtained, at variance with data obtained with the same oxide out-of-pile.[17] However, the limits of hydrogen or oxygen overpressure or pretreatment or the H_2/O_2 ratios under which catalytic activity is maintained have not been explored. There are indications that some limitations exist, and that activity is not maintained where a large excess of either oxygen or hydrogen is present. In the Th–8% U oxide in-pile test, 540 psi excess O_2 at 280°C was present; in the Th–16% U oxide test, 650 psi O_2 was used.

---

[16]In-pile tests conducted by E. L. Compere and L. F. Woo of the Reactor Experimental Engineering Division.

[17]E. L. Compere and L. F. Woo, HRP Quar. Prog. Rep. July 31, 1960 (to be published).

Table 11.4. Palladium Catalysis of Hydrogen-Oxygen Reaction in Thoria Slurries

Catalyst: sol-prepared
Temperature: 280°C

Catalyst Preparation	Slurry	Catalyst Concentration (ppm Pd, based on Th)	Pretreatment Gas or Gas in Excess	Reaction Rate, P_{H_2} = 100 psi (moles of H_2 per liter per hr)	CPI* at 0.001 m Pd, P_{H_2} = 100 psi (w/ml)
P-23	100 g Th per kg H_2O; 1600°C ThO_2	275	H_2	25	460
P-28 A	100 g Th per kg H_2O; 1600°C ThO_2	117	O_2	0.23	8
P-28 A	500 g Th per kg H_2O; 1600°C ThO_2	23.4	H_2	−50	−2000
P-28 A	100 g Th per kg H_2O; 1000°C Th−8% U oxide**	59.3	O_2	0.11	8
P-28 A		118.6	O_2	0.34	11
P-28 A		170	O_2	0.59	14
P-28 A	1080 g Th per kg H_2O; 1000°C Th−8% U oxide** (in LITR)	59.3	O_2		20−30
P-28 B-C	69.2 g Th per kg H_2O; 1000°C Th−16% U oxide**	133	O_2	0.42	19
P-28 B-C	820 g Th per kg H_2O; 1000°C Th−16% U oxide** (in LITR)	2500	O_2		0.3

*Catalyst performance index = $\frac{\text{reaction rate at 0.001 m Pd and } P_{H_2} \text{ of 100 psi}}{(0.38)(0.7)}$, where 0.7 is the G value.

**Thorium−8% uranium oxide and thorium−16% uranium oxide are equivalent to U/Th mole ratios of 0.08 and 0.16, respectively.

The order of the recombination reaction with respect to H_2 or O_2 has not been obtained. Random over-all apparent reaction orders of from 0 to 2, based on total gas pressure in excess of steam, have been observed.

Effect of Slurry Concentration

A series of 40 experiments was carried out in which the P-28A catalyst preparation was first added to a slurry of 1600°C-fired oxide (100 g of Th per kg H_2O) at a concentration of 117 ppm of Pd, based on thorium; the catalytic activity was measured, and then thoria was added to the suspension in 100-g-Th-per-kg-H_2O steps and the activity again measured.[15] Increasing the thoria content to 500 g of Th per kg of H_2O without adding any more palladium did not significantly change the specific activity of the catalyst at either 250 or 280°C, the two reaction temperatures investigated. Duplicating the final conditions (500 g of Th per kg of H_2O; 23.4 ppm Pd, based on Th) in a separate experiment resulted in only a 40% increase in specific activity. Hence it appears that the sol-prepared catalyst's specific activity is essentially independent of ThO_2 slurry concentration.

Effect of Pumping

The Slurry Corrosion Group of the Reactor Experimental Engineering Division has carried out gas-recombination tests in a pump loop at 280°C and 200 psi excess O_2 pressure with a Th–0.5% uranium oxide slurry containing the sol-prepared catalyst.[15] Specific activities in the loop appeared to be 10 to 20 times lower than those obtained in laboratory tests in autoclaves and, in addition, the specific activity dropped with time, with a several hundred hour halflife. Laboratory tests on a duplicate of the original charge and a loop sample confirmed the decline in activity. No explanation has been found for either the unusually low specific activities observed in the loop or the decline in activity.

Gas-Injection Apparatus for Catalyst Studies[18]

An apparatus that permits the injection of measured quantities of hydrogen and oxygen into an autoclave containing slurry at reaction temperature was developed for use in the catalyst development work. The arrangement of the apparatus permits, without dismantling the autoclave, removal

---

[18] J. P. McBride and L. E. Morse, HRP Quar. Prog. Rep. Oct. 31, 1959, ORNL-2879, p 175.

from the slurry of water that had been added as a result of the H_2-O_2 reaction. Addition of the gases at temperature eliminates the explosion hazard encountered when gases are charged at room temperature and heated to reaction temperature, and it also permits better control over the initial conditions of the combination reaction.

11.5 HYDROGEN AND OXYGEN SOLUBILITY IN AQUEOUS SLURRIES[19]

The solubility of hydrogen and oxygen was measured in water and in ThO_2 slurries containing 250, 500, and 1000 g of Th per kg of H_2O, at temperatures from 27 to 300°C. The ThO_2 was fired at 650°C and had a surface area of 32 m^2/g. Hydrogen and oxygen overpressures up to 700 psi were used. Good agreement was obtained with literature data on solubilities in water. The solubility of hydrogen in the slurry appeared to be no greater than could be accounted for by the solubility of hydrogen in the liquid phase of the slurry alone. Slurries of freshly prepared ThO_2 in water adsorbed up to 2.0 cm^3 (STP) of oxygen per gram of ThO_2 in an irreversible manner. After the initial exposure to oxygen, the apparent solubility of oxygen in the slurry at 250°C was 1.2 to 2.3 times as great as the solubility in water, increasing with slurry concentration. However, with a low-surface-area oxide, such as that recommended for reactor use, this increased solubility can probably be neglected.

The solubilities were determined by loading a known quantity of water or slurry into an autoclave and admitting a measured number of moles of gas at room temperature. The gas solubility was calculated from the pressure and volume data obtained at various temperatures, using the perfect-gas law.

11.6 THORIA POWDER IRRADIATIONS[20]

Radiation stability is a necessary condition for the successful use of oxide slurries in aqueous homogeneous reactors. No gross irradiation

---

[19] J. P. McBride and N. A. Krohn, HRP Quar. Prog. Rep. Jan. 31, 1960, ORNL-2920, p 91.

[20] J. P. McBride and N. A. Krohn, HRP Quar. Prog. Rep. Apr. 30, 1960, ORNL-2947, p 91.

effect on slurry behavior has been observed, but radiation-induced sintering observed in dry thoria powders and a possible similar effect in a settled slurry bed could influence the choice of oxide to be used in a reactor slurry.

Thoria powders fired at 650, 800, 900, 1100, and 1500°C were irradiated in aluminum capsules for 16 and 22 months in a lattice position of the Low Intensity Test Reactor (LITR) at a flux of 2×10^{13} neutrons cm^{-2} sec^{-1}. After irradiation the 650, 800, and 900°C-fired oxides were red, and the particles had agglomerated into hard, glossy clinkers (Fig. 11.1). The 1100 and 1500°C-fired oxides were powders of off-white and blue coloration (Fig. 11.2). Specific surface areas for all oxides except the 1500°C-fired samples were markedly decreased by the irradiation (Table 11.5) despite the fact that the estimated maximum temperature of the powders during irradiation was below 300°C. The decrease in surface area for all except the high-fired oxides suggests that irradiation produced about the same sintering effect as firing of an oxide at 1500°C.

The powders were canned in 1/2-in.-OD, 1/4-in.-ID aluminum capsules about 2.5 in. long. They were irradiated in such a way that the reactor cooling water flowed over the outside of the capsules. Cobalt and titanium flux monitors were included in the capsules.

Table 11.5. LITR Thoria Powder Irradiations

Thermal flux: $\sim 2 \times 10^{13}$ neutrons cm^{-2} sec^{-1}
Fast flux ($\sim$ 5 Mev): $\sim 1.5 \times 10^{3}$ neutrons cm^{-2} sec^{-1}
Estimated maximum temperature: 300°C

Oxide Firing Temp (°C)	Specific Surface Area (m^2/g)			Description of Irradiated Oxide
	Before Irradiation	After 16 Months of Irradiation	After 22 Months of Irradiation	
650	28.4	1.0	0.5	Red clinkers
800	15.2	0.5	0.5	Red clinkers
900	7.9	0.5	0.5	Red clinkers
1100	3.3	1.9	0.5	Off-white powder
1500	0.8	0.8	0.8	Blue powder

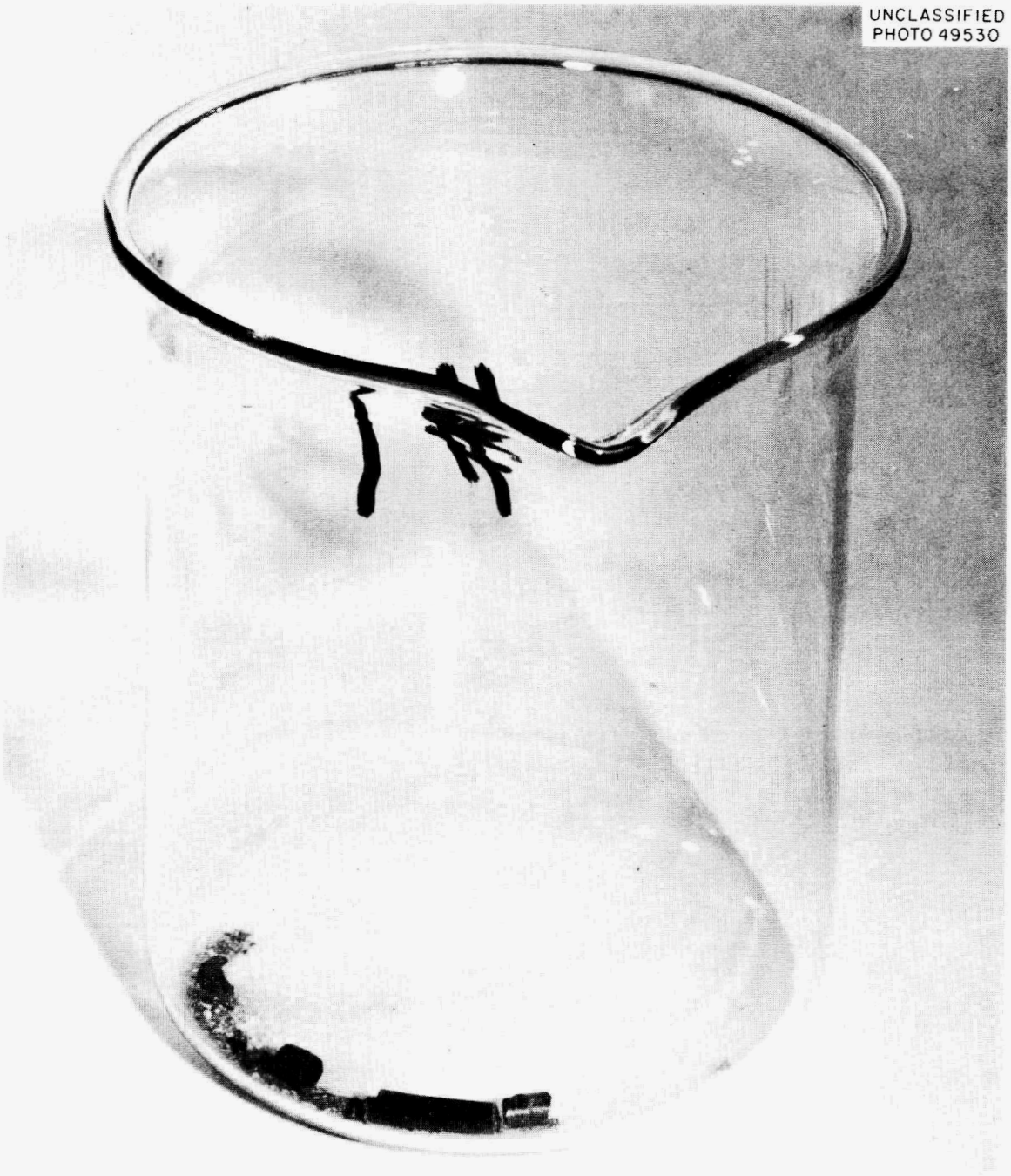

Fig. 11.1. Thorium Oxide Powder, 650°C Fired, After 16 Months Irradiation in the LITR. Flux, 2.5×10^{13} neutrons cm^{-2} sec^{-1}.

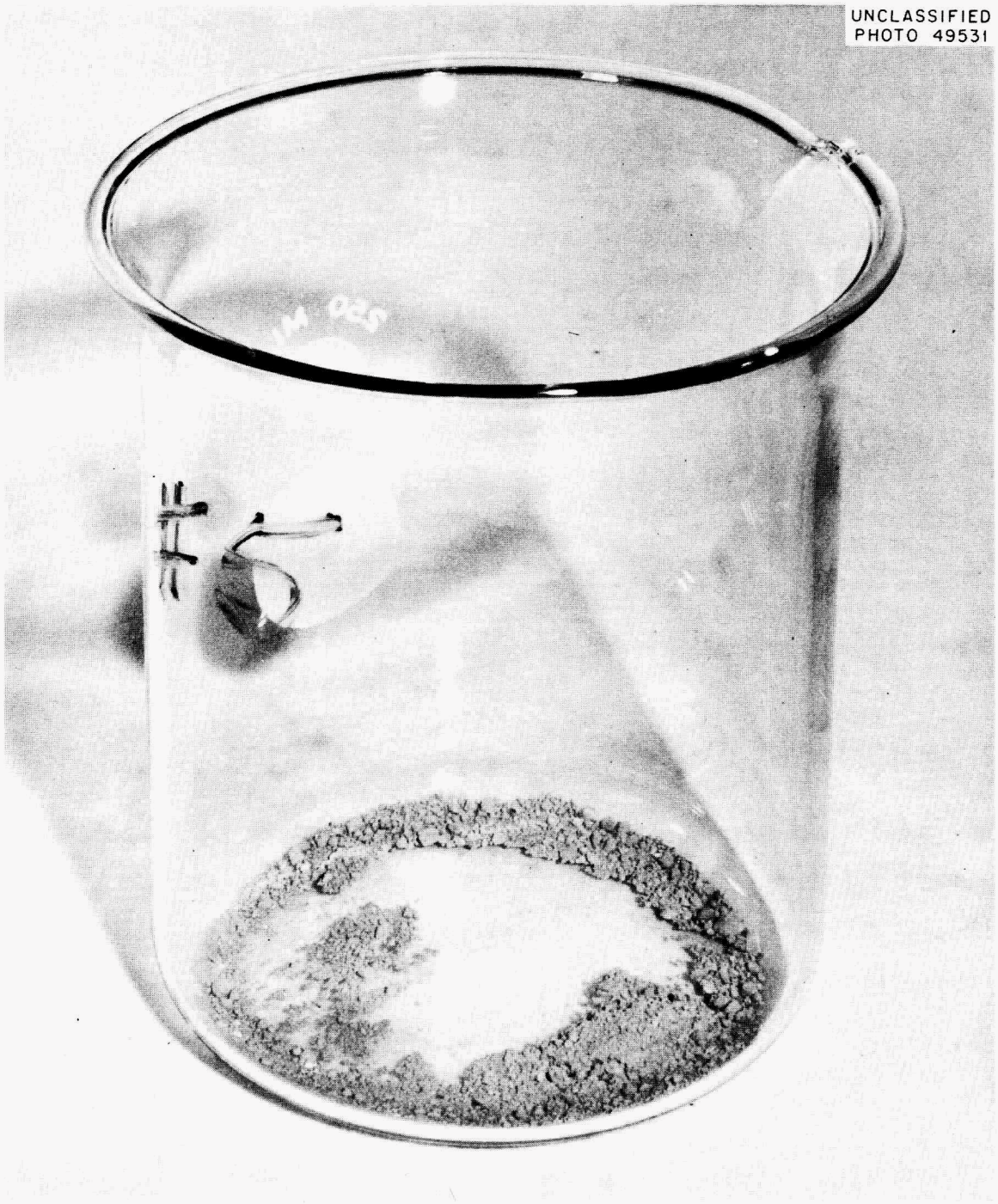

Fig. 11.2. Thorium Oxide Powder, 1500°C Fired, After 16 Months Irradiation in the LITR. Flux, 1.7×10^{13} neutrons cm^{-2} sec^{-1}.

11.7 THORIA SPRAY COATING

A 40-kw plasma jet was installed and used in preliminary investigations of the feasibility and possible advantages of spray coating ThO_2 breeder-blanket pellets with thin layers of metals and ceramics. Adherent coatings of Al_2O_3, nickel and chromium have been obtained. In the cases of the nickel and chromium coatings there appears to be a beneficial effect in admixing 5 to 10% hydrogen in the argon that is normally used as the plasma gas. The coatings are significantly more adherent when sprayed from the reducing hydrogen environment.

12. SURFACE CHEMISTRY

An objective of the Surface Chemistry Program is the preparation of a ThO_2 sample suitable for studying the equilibrium between a ThO_2 surface and an aqueous solution. It is commonly thought that a mobile layer of ions is often formed near the surface as a result of this equilibrium. If the ion concentration of this layer is determined as a function of solution concentration, ionic valence, and temperature, the surface potential can be calculated by Gouy-Chapman theory[1] and used to estimate[2] the peptization state of a suspension as a function of temperature, particle radius, valence of counter ion, electrolyte concentration, and suspension concentration.

An ideal material for surface adsorption should be solid particles of the order of 1000 A in diameter. The particles should be solid so that all the adsorption measured is on the external surface, since adsorption in fissures presumably can be much more complicated. They should be small enough to offer a significant amount of surface for study, but they should be appreciably larger than the effective thickness of the mobile layer to permit the necessary assumption of a flat mobile layer.

12.1 PREPARATION OF ThO_2 FOR SURFACE ADSORPTION MEASUREMENTS

Degradation of ThO_2 from Thorium Oxalate

The most successful method found for preparing solid ThO_2 particles was to separate the crystallites in ThO_2 particles produced by the thermal decomposition of thorium oxalate. In earlier experiments[3] a ThO_2 sample produced by firing thorium oxalate at a temperature of 650°C broke up into smaller particles when left in contact with dilute nitric acid for several days, the decrease in size being evidenced by an appreciably decreased settling rate. Apparently, the dilute acid dissolves the bridges holding

---

[1] J. Th. G. Overbeek, in Colloid Science, vol K, p 128–30, ed. by H. R. Kruyt, Elsevier, New York, 1952.

[2] F. H. Sweeton, Calculation of Suspension Peptization, ORNL-2791 (Mar. 16, 1960).

[3] F. H. Sweeton, HRP Quar. Prog. Rep. Apr. 30 and July 20, 1958, ORNL-2561, p 319.

the crystallites of one particle together. A sized ThO_2 sample for adsorption studies was prepared by digesting ThO_2 that had been fired at 1000°C, and had average particle diameters of 10^4 A, with 0.01 M HNO_3 for several days at a temperature below 100°C. The digested material was classified by seven cycles of centrifugal sedimentation-resuspension to remove particles settling slower than spheres 2000 A in diameter. The remainder was put through seven similar sedimentations timed for complete settling of particles equivalent to 3000-A spheres or larger. The final product (8 g) had an effective size range of 2000 to 3000 A. A ThO_2 preparation that had been fired at 1600°C and had crystallites > 2500 A in diameter was not broken up by this nitric acid treatment.

Thorium Peroxide Intermediate

A suggested method[4] for forming large crystallites of ThO_2 involves the formation of crystals of thorium peroxide, then decomposing them to ThO_2. In exploratory tests, the peroxide method gave larger crystallites, about 400 A, than did the homogeneous precipitation or the ion exchanger methods (see below), but reduction of the peroxide to ThO_2 was not attempted since the thorium oxalate method (see preceding paragraphs) being studied simultaneously had been found promising.

The peroxide procedure was to mix solutions of $Th(NO_3)_4$ of concentration varying between 0.03 and 0.5 M and containing enough nitric acid to give pH readings between 0.0 and 1.0. The H_2O_2 solutions varied between 0.02 and 2.0 M in concentration. The experiments were carried out at temperatures of 25 and 60°C. The average crystallite diameters, as determined by x-ray line broadening varied from 50 to 400 A. The x-ray diffraction pattern of one product changed when the sample was allowed to dry in air at room temperature.

Precipitation with Ion Exchanger

The use of ion exchangers for the precipitation of ThO_2 from $Th(NO_3)_4$ solutions gave materials about 100 A in diameter instead of the desired

[4]Gordon, Salutsky, and Willard, Precipitation from Homogeneous Solution, Wiley, New York, 1959.

1000 A. The pH of a $Th(NO_3)_4$ solution was adjusted until the solution was just saturated with respect to the precipitation of ThO_2, and then an ion exchanger that had been adjusted to be in equilibrium with a solution slightly more alkaline was added. The theory was that the ion exchanger should make the $Th(NO_3)_4$ solution more alkaline and therefore supersaturated with respect to ThO_2 but not enough supersaturated to form nuclei of ThO_2, allowing the slow formation of a few relatively large crystallites from a few small seed crystallites. Under the conditions used, the products were particles no larger than 100 A, and this method was abandoned.

Homogeneous Precipitation

The ThO_2 crystallites formed by the homogeneous reaction of $Th(NO_3)_4$ with the decomposition products of urea (Table 12.1) clumped together to form spherical aggregates (Fig. 12.1). It appeared impossible to cause the crystallites to grow to the desired diameter of an appreciable fraction of a micron when in this clumped state. The technique of homogeneous precipitation, developed for use in chemical analysis[4] involves the reaction of two chemicals in one solution, one of the chemicals being liberated within the homogeneous solution rather than being added as a separate phase. This method appears to offer the possibility of growing sizable crystallites, since slowly precipitating material should deposit on crystallites of the same material if such crystallites are present. Urea, the commonly used reagent for precipitating metallic oxides in aqueous solutions, hydrolyzes near the boiling point, liberating ammonia which decreases the acidity of the solution.

12.2 USE OF THE GLASS ELECTRODE IN MEASURING pH OF SLURRIES

Some workers with thoria slurries have obtained data indicating that the position of a glass electrode in a settled slurry appreciably affects its reading, but this should not be so if the supernatant and settled bed are in chemical equilibrium and if the glass electrode is reversible. The results of three tests indicated that absorption of atmospheric carbon dioxide affected the pH of slurries, presumably by changing the equilibrium between the supernatant and the settled bed. No significant dependence of the glass electrode reading on its position in a settled slurry protected from atmospheric contamination was found.

Table 12.1. Summary of Homogeneous Precipitation Runs

Test No.	Length of Test (hr)	Saturating Solution			pH of Suspension			Crystallite Size (A)		Particle Size (A)	
		Urea (mmole)	HNO_3 (mmole)	pH	Max	Min	Final	By X-Ray Diffraction	By N_2 Adsorption	By Settling Rate	By Electron Microscopy
1	1.7	20	0	3.4		*	6.2	47	*	*	*
2	3	7.5	0	3.4		2.6	6.9	50	*	*	*
4	15	7.5	3.8	2.5	2.5_5	2.4_7	3.5	90	76	600	800
5	11	7.5	3.9	2.4	2.5	2.4_0	2.6_2	62	66	*	500

*Not determined.

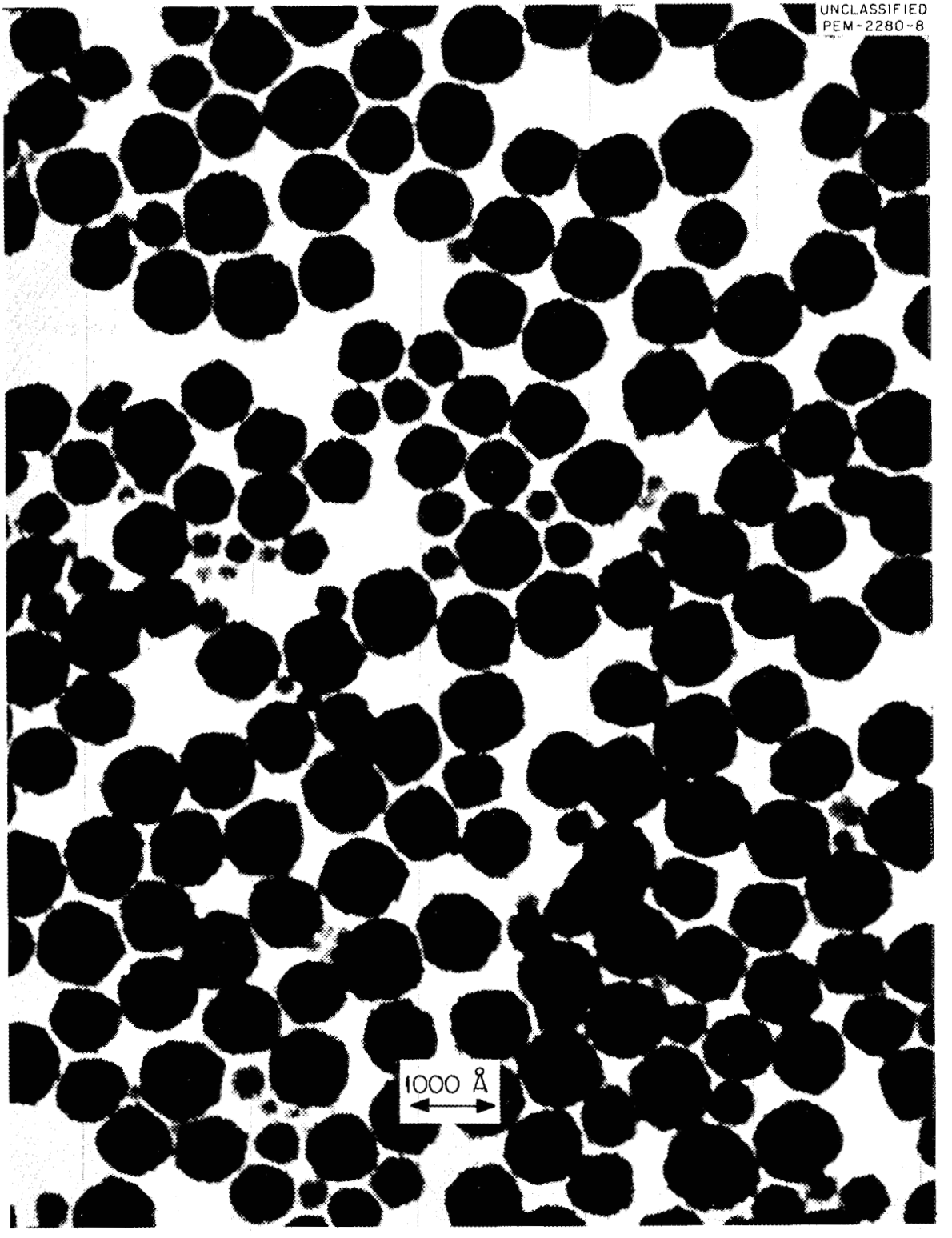

Fig. 12.1. Aggregated ThO_2 Formed by Homogeneous Precipitation.

The first test (see Fig. 12.2 for diagram of apparatus used) was made with a 500-g/liter thoria suspension, the supernatant of which had an initial pH of 6.7. The slurry was suspended thoroughly and then the indicated pH of the top electrode vs that of the bottom was followed for 67 hr. During this time, the two electrodes gave readings differing by 0.01

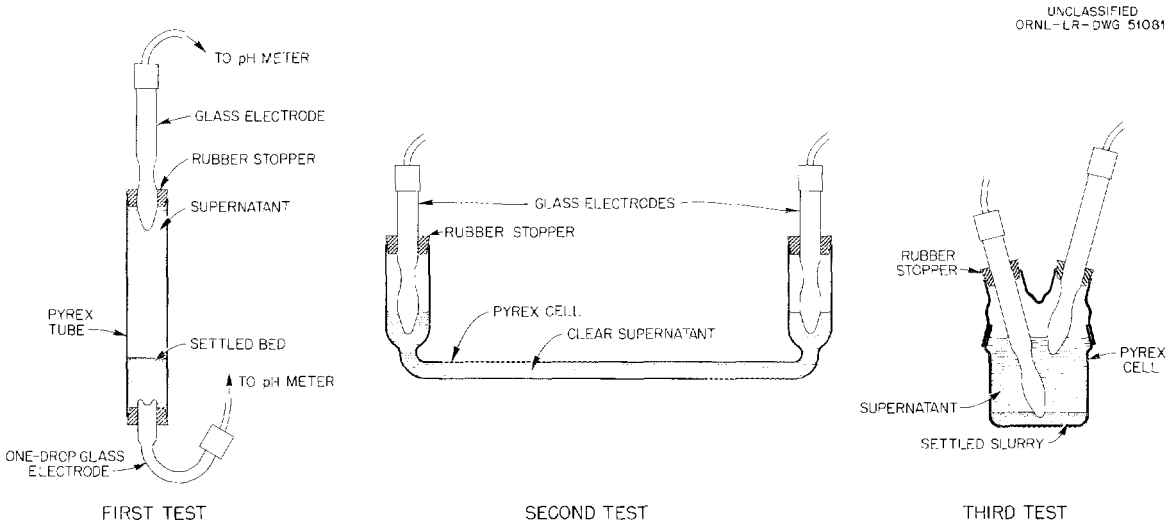

Fig. 12.2. Cells Used to Compare Glass Electrodes.

to 0.06. Then the seal at the top was broken so that air could make contact with the liquid surface. The measured difference in pH over the next 19 hr remained in the same range. Nitric acid was then added, bringing the pH of the supernatant down to 2.8. With the cell again sealed the measured difference in pH varied between 0.00 and 0.06 over the next 28 hr. It was concluded that the glass electrodes were not significantly affected in this case by whether the slurry was in a suspended or a settled state, or by whether or not the cell was open to the air.

A second test was made with a clear supernatant in the second cell and a different set of glass electrodes. The pH of the supernatant was 9.0. For an hour after the cell was sealed the measured pH difference was 0.02 or less. Then one side of the cell was opened to admit air. During the next 5 hr the measured pH of the open side relative to that of the other gradually dropped 0.5 unit; at 23 hr it had dropped 1.7 units. After resealing the cell and remixing the solution, the difference in pH was 0.07. This test showed that the pH of a supernatant can be lowered appreciably by prolonged contact with the air.

The third test was made on a 115-g/liter thoria suspension having a pH of 9.0. The electrodes of the previous test were used. The measured difference in pH of the top electrode relative to the bottom was +0.03, six days later. When the ground joint was opened to let outside air contact the sample, the pH at the top started dropping and read −0.3, 7 hr later. In the following two days this reading varied between −0.5 and −1.0. After sealing and remixing, the reading became 0.00 to 0.04. This test was another example in which the glass electrodes were not significantly affected by the settling of the slurry and, likewise, another example in which atmospheric contamination did affect the pH reading.

13. TRANSURANIUM STUDIES

The purpose of the Transuranium Studies Program is to develop separation processes for the transuranium elements, primarily those produced by long-term irradiation of Pu^{239}. Chemical process development was carried out on a laboratory scale, design work for the Transuranium Processing Facility was continued, equipment design for the Transuranium Facility was initiated, and irradiation of the initial 10 kg of Pu-Al alloy was started at Savannah River.

Transplutonium elements up to Cf^{252} can be produced by long-term neutron irradiation of Pu^{239} (Fig. 13.1). Because of the large amount of

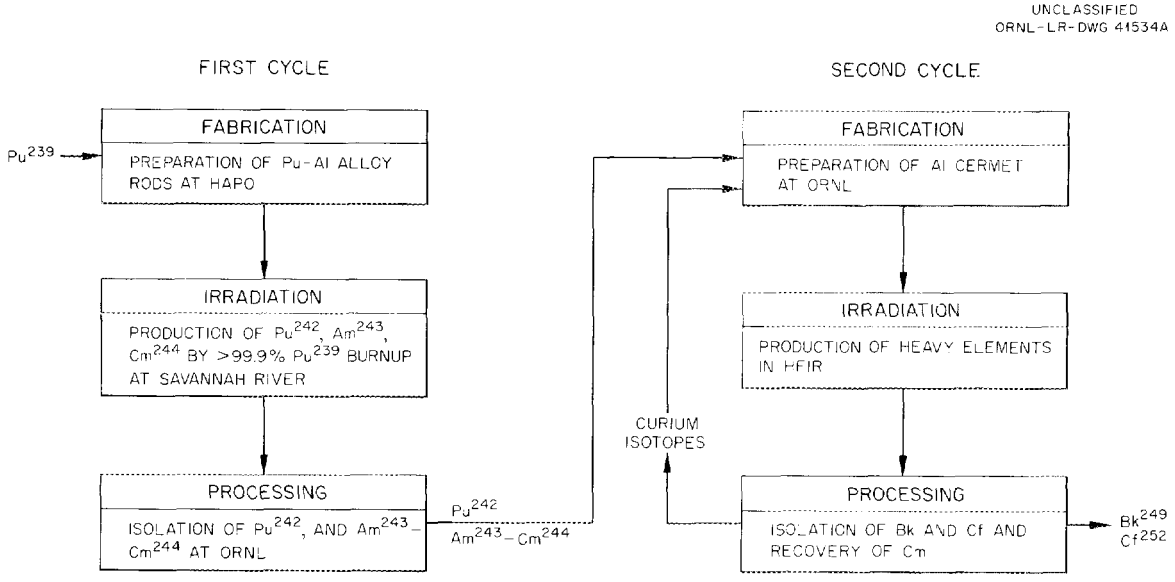

Fig. 13.1. Flowsheet for Transuranium Element Production.

heat generated during fission, the initial irradiation must be carried out at moderate neutron fluxes until all the fissionable plutonium (Pu^{239} and Pu^{241}) is consumed. The Pu^{242}, americium, and curium formed during this initial irradiation can then be irradiated at the highest neutron flux available for rapid formation of the higher isotopes. Chemical processing is required after each irradiation.

A flowsheet has been developed for processing the Pu-Al alloy after the first irradiation (Fig. 13.2). This process separates Pu^{242}, americium, and curium from the major neutron poisons and gross impurities.

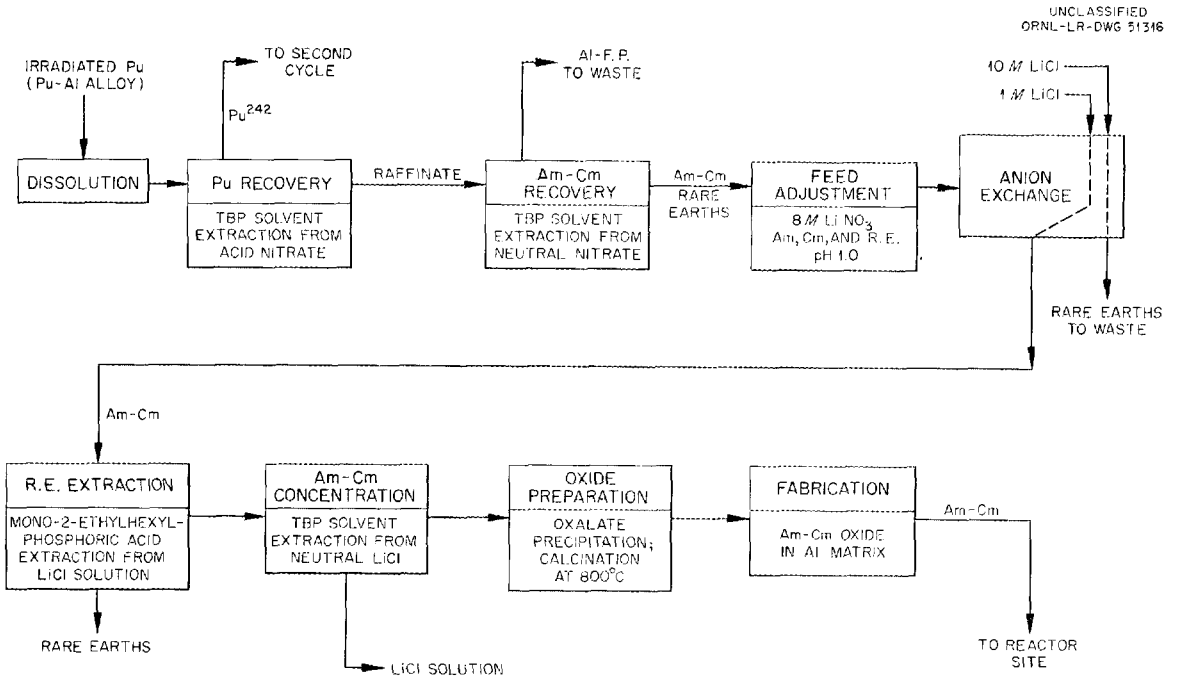

Fig. 13.2. Flowsheet for Processing Highly Irradiated Plutonium.

13.1 PLUTONIUM-242 AND AMERICIUM-CURIUM RECOVERY CYCLES

The Building 3019 pilot plant processed eight irradiated plutonium fuel rod assemblies, using approximate conditions proposed for first-cycle plutonium recovery and for the americium-curium recovery cycle. Conditions for these solvent extraction runs are described in Sec 1.7.

Plutonium recovery was successfully demonstrated with a decontamination factor from rare-earth beta activity of 2.2×10^4. Processing of the aqueous raffinate for americium, curium, and rare earths was interrupted due to mechanical difficulties, and analytical results indicate that equilibrium conditions for the process did not obtain. Analysis of flowing stream samples show that rare earth extraction increased from 0.04 to 36% after 6 hr of operation; this indicates that conditions necessary for a successful extraction were not far from being achieved. Ruthenium was quantitatively extracted with the product, and chemical development studies are planned to overcome this difficulty.

Fifteen liters of this americium-curium-rare-earth extraction product, which contains Cm^{242} to the extent of about 8×10^8 counts min^{-1} ml^{-1}, has

been saved to provide feed for actinide-lanthanide separation processes at high radiation levels.

13.2 ANION EXCHANGE SEPARATION OF ACTINIDES AND LANTHANIDES

The separation of americium and curium from rare earths by anion exchange based on selective chloride complexing was developed and tested on a laboratory scale, using tracer amounts of Am^{241} and Cm^{242} with macro amounts of mixed rare earths (Fig. 13.3). The product contained > 99.5%

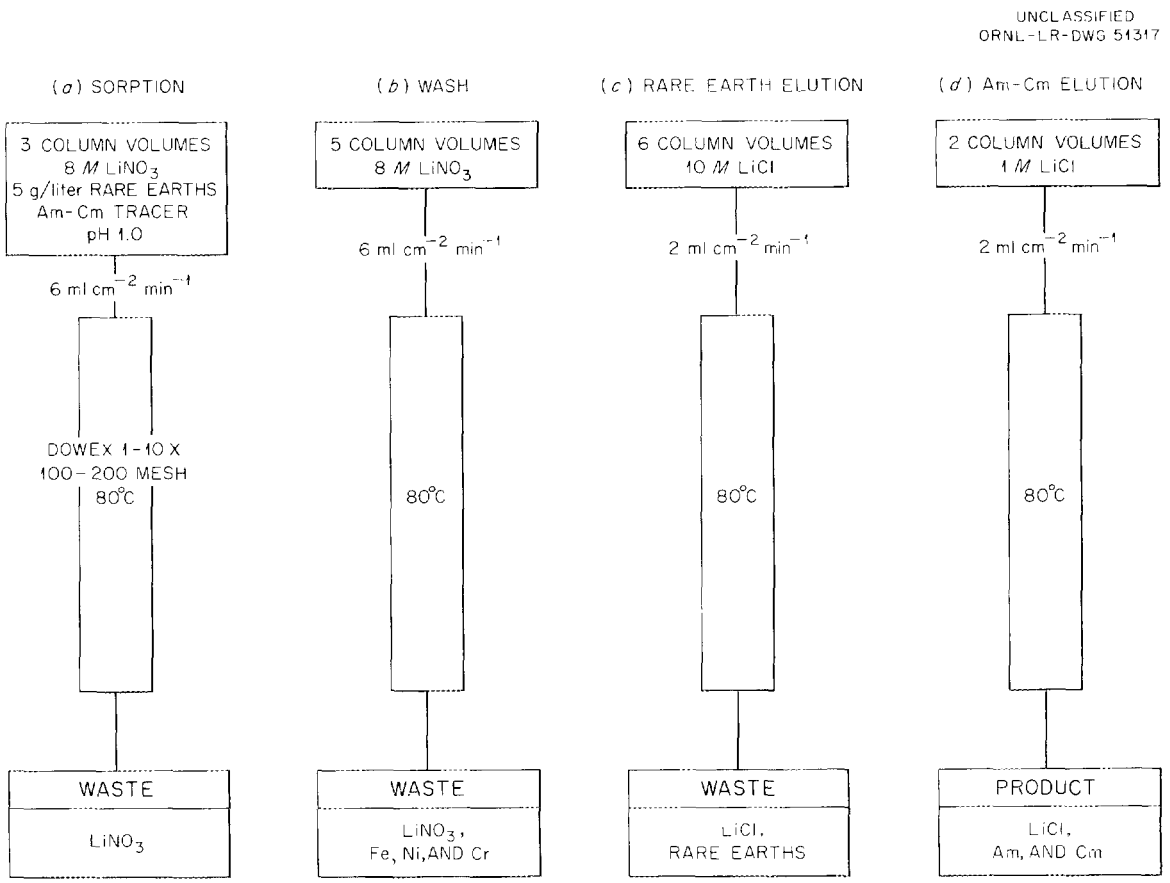

Fig. 13.3. Anion Exchange Flowsheet for Separating Am and Cm from Rare Earths.

of the americium and curium, with no rare earths detectable by oxalate precipitation. This represents a decontamination factor from rare earths of > 100. Runs at high activity levels are planned to determine the magnitude of the rare-earth decontamination factors that can be obtained. In the sorption cycle, 8 M $LiNO_3$, at pH 1.0, containing 5 g of rare earths per liter and tracer americium and curium is passed through a column of

Dowex 1-10X resin at 80°C. Washing at 80°C with 8 M $LiNO_3$ removes weakly sorbed materials such as iron, chromium, and nickel. Practically all the rare earths are then eluted at 80°C with 10 M LiCl, and americium and curium are completely removed by eluting at 80°C with 1 M LiCl.

This anion exchange procedure, based on data of Marcus and Nelson,[1] is a modification of that used at the University of California Radiation Laboratory[2] and at Argonne National Laboratory.[3] The principal difference is that sorption onto the anion resin is from lithium nitrate instead of lithium chloride solution. Its advantages are: (1) nitrate solutions from solvent extraction processes can be readily adjusted to feed conditions, (2) feed with lower rare-earth concentrations can be used because of the higher distribution coefficients from nitrate solutions, and (3) moderate amounts of impurities in the feed do not interfere.

Contaminants in the feed can vary considerably without affecting the separation of americium and curium from rare earths. Feeds containing 1 g of iron, 1 g of chromium, and 1 g of nickel per liter were satisfactorily processed, producing products completely free of these contaminants. Aluminum in the feed did not interfere. Separations from 6 M $LiNO_3$ and 1 M $Al(NO_3)_3$ were successful, and preliminary data indicate that it is possible to completely replace the lithium with aluminum.

Variation of $LiNO_3$ concentration between 8 and 10 M in the feed and of flow rates between 2 and 6 ml min^{-1} cm^{-2} had only a slight effect on sorption. The pH must be kept below 2.0 to prevent iron precipitation, but high acid concentration prevents sorption of actinides and lanthanides. Feed with acid concentrations as high as 0.2 M was satisfactory.

For the selective elution of rare earths, a LiCl concentration of 10 M was more effective than 11 M, and a flow rate of 2 ml min^{-1} cm^{-2} was much more effective than 6 ml min^{-1} cm^{-2}.

Column length is important. When a resin column 1 in. in diameter and 20 cm long was used, product free of rare earths contained only 88%

---

[1]Y. Marcus and F. Nelson, J. Phys. Chem. 63, 77 (1959).

[2]G. H. Higgins and W. W. T. Crane, Proc. UN Intern. Conf. Peaceful Uses Atomic Energy, 2nd, Geneva, 1958 17, 245 (1959).

[3]P. R. Fields, Argonne National Laboratory, personal communication.

of the americium. With a 40-cm-long column, the product free of rare earths contained 99.9% of the americium. Resin particle size is also important. Results were best with the smallest resin. Permutit SK or Dowex 21K resin is more stable to radiation than Dowex 1, but scouting tests with 20- to 60-mesh samples of these resins did not give satisfactory results; however, in a single scouting run with Dowex 21K (50–100 mesh) the decontamination factor of the rare earths from curium was 150, and curium recovery was 99.7%. Finer-mesh resins should produce even higher decontamination factors from rare earths.

13.3 RARE EARTH EXTRACTION INTO M-2EHPA

A flowsheet for separating americium from rare earths by rare earth extraction into mono-2-ethylhexyl orthophosphoric acid (M-2EHPA) was developed and tested on a laboratory scale. The feed solution is 10 M LiCl–0.5 M HCl containing up to 2.5 g of rare earths per liter and tracer americium. The scrub is 10 M LiCl–1.0 M HCl, and the solvent is 0.5 M M-2EHPA in xylene. Feed:scrub:solvent flow ratios are 1:1:3. Calculations based on distribution-coefficient data indicate that 8 scrub and 10 extraction stages will give > 99.9% americium recovery, containing 2% of the lanthanum and < 0.1% of the other lanthanides. In experimental runs in a laboratory mixer-settler with 7 scrub and 8 extraction stages used to verify this flowsheet, extractions of neodymium, cerium, and lanthanum were 99.9, 98, and 90%, respectively, and americium loss was 0.04%. Careful control of flow rates, acid concentrations, and operating characteristics of contactors was necessary. Theoretically the lanthanum can be completely separated also, but such close control of conditions is required that this separation would probably not be feasible.

Americium and curium were concentrated after the rare-earth extraction cycle by extraction into 100% TBP from an aqueous phase adjusted to contain 10 M LiCl–0.1 M HCl and 0.5 M $LiNO_3$. Distribution coefficients for americium and curium were of the order of 1000 for this system.

Process variables that were investigated include (1) acidity of the 10 M LiCl, (2) rare-earth concentration, (3) M-2EHPA concentration in xylene diluent, and (4) xylene vs hydrocarbon diluent. The addition of acid to 10 M LiCl depressed the distribution coefficients and slightly

increased the separation factors between americium-curium and the lanthanides (Fig. 13.4). Regulating the acid concentration in 10 M LiCl is therefore a convenient way to adjust conditions in multistage extraction contactors so that the lanthanide extraction factor is always greater than

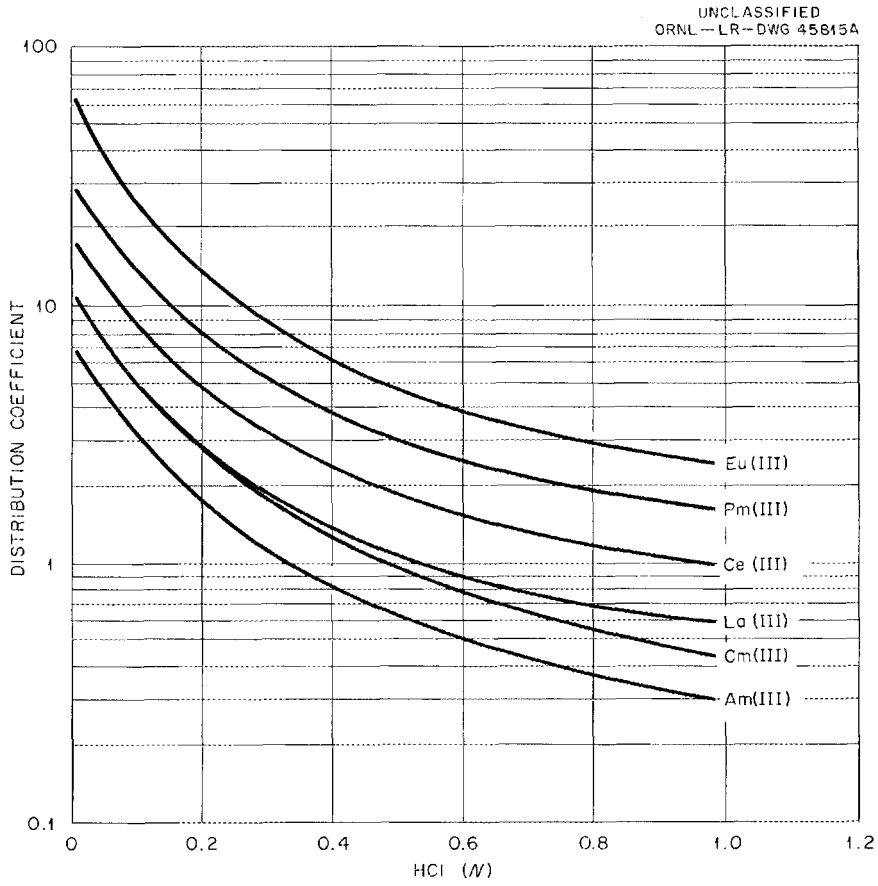

Fig. 13.4. Distribution Coefficients Between 10 *M* LiCl Containing Various Amounts of Free Acid and 0.5 *M* Mono-2-ethylhexyl Phosphoric Acid in Xylene Diluent.

1 and the americium and curium extraction factors are less than 1. Actinide and lanthanide distribution coefficients decreased with increased solvent loading. Increasing the rare-earth concentration from tracer amounts to 1 g/liter decreased the distribution coefficients about 15%, and with 5 g of rare earths per liter in the feed, distribution coefficients were only about half the value for tracer concentrations. The rate of decrease appears to be the same for americium and the lanthanides; hence, separation factors do not change with solvent loading.

Actinide and lanthanide distribution coefficients between 10 M LiCl–0.05 M HCl and M-2EHPA in xylene diluent were directly proportional to the M-2EHPA concentration. Scouting studies were made in order to determine the feasibility of using straight-chain hydrocarbons as diluents instead of cyclic aromatic compounds. When M-2EHPA was diluted with kerosene or n-heptane it gave distribution coefficients 30 to 50% greater than when diluted with toluene or xylene. However, when hydrocarbon diluents were used in contact with solutions of high acidity, a second organic phase formed. This did not occur when cyclic aromatic diluents were used.

13.4 OXIDE PREPARATION

The conversion of americium and curium to AmO_2 and Cm_2O_3 is a necessary step for americium-curium reactor target fabrication. Experience in AmO_2 preparation was provided by the necessity of converting americium chloride solution containing 170 g of americium to americium dioxide.

The process consisted in neutralizing the acid to 0.1 M followed by the addition of oxalic acid to 100% excess oxalate. Americium oxalate precipitated and was allowed to digest at 30°C for 1 hr, and was then filtered, washed with water, and allowed to air-dry. The partially dry oxalate was transferred to a platinum boat and calcined in temperature increments up to 800°C. Most of the conversion resulted in pure AmO_2, which assayed at the theoretical value of 88.3% americium per gram of oxide. Americium losses for the process, which were primarily due to oxalate solubility, were 0.1% of the total americium processed. No effort was made to control or measure the particle size of the AmO_2.

13.5 TARGET FABRICATION

A program to test the compatibility of plutonium and americium oxides in matrixes of aluminum, beryllium, and aluminum-beryllium mixtures is under way. Preliminary work is being done with CeO_2. To date there has been no thermite reaction between CeO_2 and aluminum during 200 hr of thermal cycling at temperatures as high as 400°C. Pellet growth has been 1 to 2%. Equipment is being set up for making similar tests with plutonium and americium oxides.

13.6 TRANSURANIUM PROCESSING FACILITY AND EQUIPMENT

Design work for an addition to the Isolation Building, which will provide laboratories for work with alpha-active materials and cells for work with alpha-, gamma-, and neutron-active materials, was continued. The Catalytic Construction Co. of Philadelphia, Pa., was selected as the architect-engineer. They have prepared conceptual designs and cost estimates for several concepts in order to arrive at an optimum design. Present plans call for construction to begin by September 1961, with completion scheduled for early 1963.

Equipment design for the Transuranium Facility was started. Design work for a cell mockup was completed and construction is in progress.

14. FISSION PRODUCT RECOVERY

The objective of this program is the development of processes for recovering megacurie quantities of fission products from reactor-fuel processing wastes. It is expected that large quantities of these elements may be required in the future for industrial applications. Relatively small amounts of these elements have been recovered in the past, principally by batch precipitation techniques. It is possible that solvent extraction and ion exchange may offer better methods for commercial application.

14.1 BY SOLVENT EXTRACTION

Strontium and Rare Earths

Based on laboratory-scale tests with simulated solutions, a possible process has been proposed (Fig. 14.1) for recovery of strontium and rare earths from Purex 1WW by extracting with a solvent containing di(2-ethylhexyl)phosphoric acid (D2EHPA), sodium di(2-ethylhexyl)phosphate (NaD2EHP), and tributylphosphate (TBP) in Amsco 125-82.[1-3] To prevent subsequent precipitation, the copious quantity of iron in the 1WW is initially complexed with tartrate, and the pH is adjusted to 6 with sodium hydroxide. In the first cycle, > 99% of the strontium and > 95% of the rare earths are extracted along with minor amounts of iron and other fission products. Strontium, rare earths, and sodium (from the NaD2EHP) are stripped from the solvent with 2 M HNO_3. Through this part of the process, the iron separation factor is $> 1.4 \times 10^3$, and decontamination factors from Ru, Zr-Nb, and Cs are 24, 9, and 26, respectively. In the second cycle, the strip solution from cycle 1 is adjusted to pH 2 and the rare earths are separated from strontium by extracting into the D2EHPA-NaD2EHP-TBP-Amsco solvent, scrubbing with 1.2 M $NaNO_3$, and stripping with 2 M HNO_3. The aqueous raffinate from the second cycle is adjusted to pH 6, and strontium is extracted in

---

[1] Chem. Tech. Div., Chem. Dev. Sec. C, Monthly Prog. Rep., Sept. 1959, ORNL CF-59-9-85.

[2] Chem. Tech. Div., Chem. Dev. Sec. C, Monthly Prog. Rep. Oct. 1959, ORNL CF-59-10-101.

[3] Chem. Tech. Div., Chem. Dev. Sec. C, Prog. Rep. Feb.-Mar. 1960, ORNL CF-60-3-136.

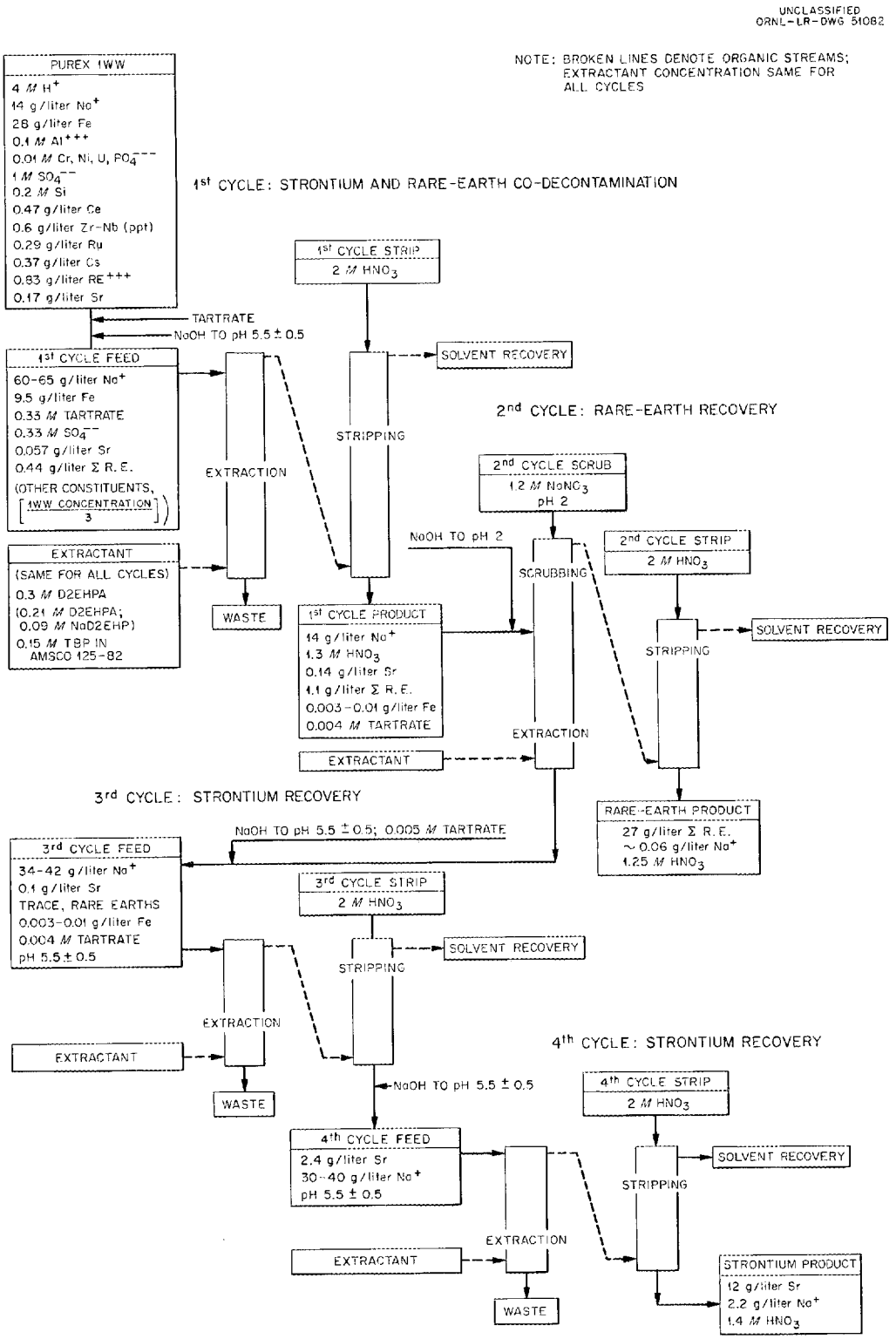

Fig. 14.1. Fission Product Recovery Flowsheet for Strontium and Rare Earths.

a third cycle by solvent of the same composition and stripped with 2 M HNO_3. In the fourth cycle, the strip solution from cycle 3 is again adjusted to pH 6 and the strontium re-extracted and subsequently stripped with 2 M HNO_3.

The rare-earth-product solution from cycle 2 contains ~27 g of total rare earths per liter and ~0.06 g of sodium per liter, representing a rare-earth concentration factor of about 20. The over-all separation factors from strontium and sodium are about 2.5×10^4 and 4.5×10^3, respectively. The strontium-product solution from the fourth cycle contains ~12 g of strontium and ~2 g of sodium per liter, representing a strontium concentration factor of about 70. The over-all separation factors from rare earths and sodium are about 2.5×10^3 and 6×10^2, respectively. Both the strontium and rare-earth products are in nitrate solution and are readily amenable to additional purification treatment.

Cesium

Two solvents, out of a number tested, have shown ability to extract cesium from Purex 1WW solutions.[4] With 0.5 M sodium tetraphenyl boron in hexone, cesium distribution coefficients of 30–35 were obtained from Purex waste adjusted to pH 5 with NaOH and containing tartrate to prevent precipitation of iron. Thus far, however, no acceptable way has been found to strip cesium from this solvent without converting the sodium tetraphenyl boron to a form which is ineffective for reuse. With dinonyl nephthalene sulfonic acid in Amsco 125-82, the extraction of cesium from the adjusted Purex waste was comparatively weak; the distribution coefficients ranged from 0.3 to 0.4. Process application of this reagent may be possible, however, if future tests show a very high selectivity for cesium over other components of the waste.

14.2 BY ION EXCHANGE RESIN

The quantity of fission products potentially recoverable from Purex process waste is calculated to be about 91 gram-equivalents (active plus inactive) per metric ton of uranium for a high-burnup (7620 Mwd per metric ton of uranium) reactor. An ion exchange scheme was developed for recover-

[4] Chem. Tech. Div., Chem. Dev. Sec. C, Prog. Rep. Apr.-May 1960, ORNL CF-60-5-114.

ing separately the radiosiotopes for which there is a current sizable demand, namely, Sr^{90} and the rare earths Ce^{144} and Pm^{147}. The Purex waste concentrate (1WW; see ref 5) is diluted by a factor of 10 and made 0.124 M in oxalic acid to complex iron and aluminum prior to pumping it through a column of hydrogen-form Dowex 50W X-8 (20–50 mesh) resin. Fifty per cent of the strontium (tracer Sr^{85}) breaks through after about 22 resin volumes of feed. About 10% rare-earth (tracer Ce^{144} + Pr^{144}) breakthrough is detectable after 67 resin volumes of feed have passed through. The strontium is eluted with 1 M HNO_3 and then sorbed on a second resin column, which is three times the volume of the first column (Fig. 14.2). Because of the dif-

[5]Synthetic 1WW composition: 6.1 M NO_3^-, 1.0 M SO_4^{--}, 4.6 M H^+, 0.6 M Na^+, 0.5 M Fe^{+++}, 0.1 M Al^{+++}, 0.01 M Cr^{+++}, 0.01 M Ni^{++}, 0.01 M UO_2^{++}, plus stable elements equivalent to 3.75 g of gross fission products per liter, and radioactive tracers.

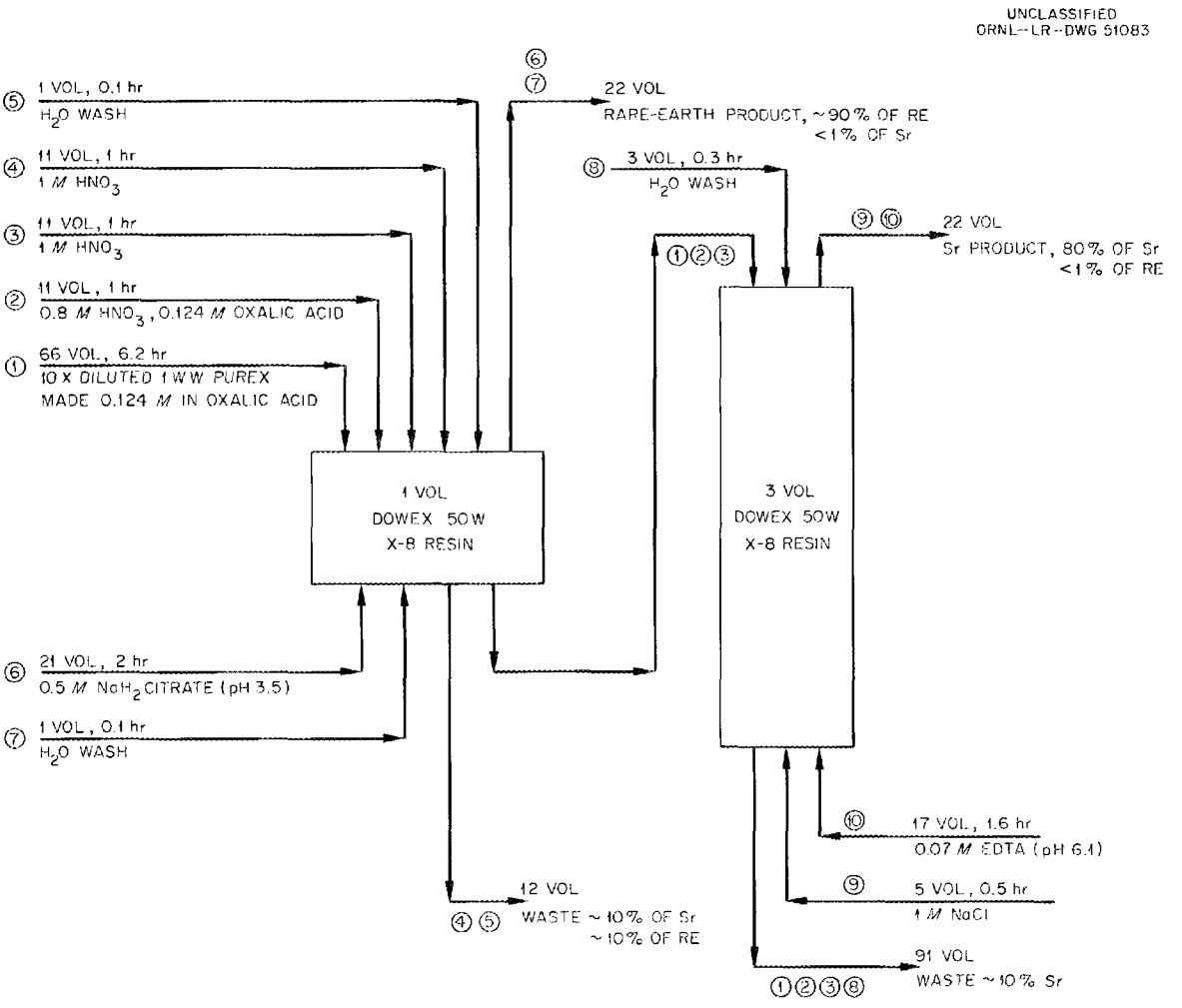

Fig. 14.2 Proposed Flowsheet for the Recovery of Rare Earths and Strontium from 1WW Purex Waste.

ference in the distribution coefficient (DC_{Sr} = 22, DC_{RE} = > 67) it is possible to transfer practically all the strontium to the second column, leaving the rare earths sorbed on the original column. The strontium is recovered by adjusting the column pH with 5 resin volumes of 1 M NaCl and then eluting with 0.07 M sodium Versenate (pH 6.1). The rare earths are eluted from the first column with 0.5 M monosodium citrate (pH 3.5).

15. SOLVENT EXTRACTION TECHNOLOGY

New solvent extraction agents and solvent extraction chemistry pertinent to the general AEC program are being developed. Solvent extraction is a unit operation of considerable importance and utility, particularly in remote-control operations. However, the technology used thus far has been limited to a small group of solvents which are useful over a narrow range of aqueous compositions. Wider application of solvent extraction should be possible through a wider choice of solvent extraction reagents. In the ORNL raw materials program (see Secs 8 and 9) a number of new solvents have been developed and are commercially used for extracting uranium and other metals from acid ore-leach liquors. Some of the solvents extract uranium by cation or anion exchange, offering a new technology that uses the principles of ion exchange on a liquid-liquid basis, with the inherent engineering advantages of liquid-liquid systems. Other solvents extract a large number of metals from a wide variety of different aqueous compositions, with considerable control of extraction properties being possible through choice of reagent structure.

15.1 URANIUM-THORIUM SEPARATION

Comparisons[1] of di-*sec*-butyl phenylphosphonate (DSBPP) with tri-*n*-butyl phosphate (TBP) as a uranium process extractant indicated advantages for DSBPP of higher radiation stability, stronger uranium and plutonium extraction, and better selectivity. Uranium separation from thorium with DSBPP is 34-fold that with TBP. Comparison of 1 *M* DSBPP in xylene vs 1 *M* TBP in Amsco extraction from an aqueous phase of 4 *M* HNO_3, 0.002 *M* U, and 0.002 *M* Th showed respective uranium E_a^o's of 60 and 36, thorium E_a^o's of 0.26 and 3.4, and/or uranium separation factors from thorium of 370 and 11.

In continuing work, DSBPP was investigated as the extractant for a final U^{233} purification cycle in the Thorex process. An aqueous U^{233} product concentrate which would represent the feed to such a cycle would probably be a 1 *M* HNO_3 solution containing about 150 g of uranium and 1.0 g of thorium per liter. With such a feed, an aqueous scrub solution of 1.0 *M*

---

[1] Chem. Tech. Ann. Prog. Rep. Aug. 31, 1959, ORNL-2788, p 91.

HNO_3, an organic extractant of 1 M DSBPP in Solvesso 100, and F/S/O flow ratios of 1.0/0.5/1.6, a tentative extraction cycle was demonstrated in laboratory batch countercurrent tests. Uranium recovery was complete and decontamination factors from thorium were > 250.

15.2 URANIUM-PLUTONIUM EXTRACTION

Uranium-Plutonium Separation and Decontamination

The DSBPP complexes of $UO_2(NO_3)_2$ and $Th(NO_3)_4$ have been found[1] to be incompletely soluble in Amsco 125-82, but soluble in commercial aromatic diluents, for example, Solvesso 100, Solvesso 150, and sec-butyl benzene, and in CCl_4. From the uranium and thorium data it was predicted that DSBPP-CCl_4 might be a useful extractant in final plutonium purification cycles where the less radiation-stable TBP-CCl_4 extractant is now used.

In fission product extraction and decontamination studies, TBP diluted with the aromatic Solvesso 100 gave higher uranium extraction and uranium-fission product separation factors than when diluted with the aliphatic Amsco 125-82 (Table 15.1). The extractant DSBPP-Solvesso 100 was only slightly better than TBP-Solvesso 100 with respect to uranium-fission product (U/FP) separation. Separative advantages of these two extractants over TBP-Amsco 125-82 were maximum at approximately 0.7 M reagent concentration.

A "nitrite-acetone" digestion head-end treatment of a synthetic aqueous Purex process feed solution increased the decontamination factors in the subsequent extraction cycle by an order of magnitude (Table 15.2). The treatment consisted in adjusting the ~ 2 M $UO_2(NO_3)_2$ dissolver solution to 0.3 M HNO_3 deficiency and 0.05 M $NaNO_2$ and digesting at room temperature for > 1 hr. This solution was then adjusted to 0.3 M HNO_3, 1 vol % acetone was added, and the mixture was digested at 90°C for > 1 hr and finally adjusted to the specified aqueous feed composition.

Plutonium Extraction Coefficients

In continued systematic study of plutonium extraction from acid nitrate solutions, extremely high Pu(IV) extraction coefficients were measured with dialkylphosphoric acids, and usable extractions from some reduced

Table 15.1. Distribution Coefficients in TBP-Amsco, TBP-Solvesso 100, and DSBPP-Solvesso 100

Aqueous phase: 3 N HNO_3, 10.1 g U per liter, 10 g Th per liter, FP spike

Organic phase: DSBPP at varying concentrations in Solvesso 100, o/a = 1.0

Reagent	Element			
	U	Ru	Zr-Nb	TRE
Distribution Coefficients, o/a				
0.698 M TBP-Amsco	11.8	0.0108	0.0072	0.0074
0.707 M TBP-Solvesso	15.8	0.0026	0.0022	0.0021
0.712 M DSBPP-Solvesso	21.4	0.0023	0.0023	0.0015
1.37 M TBP-Amsco	21.0	0.0471	0.0190	0.0220
1.37 M TBP-Solvesso	29.6	0.0173	0.0122	0.0130
1.33 M DSBPP-Solvesso	39.4	0.0238	0.0122	0.0110
Separation Factors				
0.698 M TBP-Amsco		1090	1635	1590
0.707 M TBP-Solvesso		5980	7310	7900
0.712 M DSBPP-Solvesso		9460	9340	14300
1.37 M TBP-Amsco		446	1105	954
1.37 M TBP-Solvesso		1710	2420	2280
1.33 M DSBPP-Solvesso		1650	3230	3580

solutions were found with tertiary amines. Emphasis was on di-n-butyl and di-sec-butylphenyl phosphonates (DNBPP and DSBPP), two reagents which show potential advantages over TBP in Thorex- and Purex-type processes.

The log-log plots of the plutonium extraction coefficient vs nitric acid concentration for DNBPP, DSBPP, and TBP gave nearly straight lines, which were closely parallel, from ~ 2 M HNO_3 down to at least 0.4 M HNO_3, with slopes close to 2.5 (Fig. 15.1). The coefficients with DSBPP were close to those with TBP, while those with DNBPP were a factor of 1.5 higher. These curves are steeper and straighter than those given by TBP

Table 15.2. Effect of Nitrite-Acetone Aqueous Feed Treatment Procedures on Fission Product Extraction and Decontamination

Countercurrent extraction with 1 M TBP or 1 M DSBPP in Solvesso 100

Aqueous feed: 427 g U per liter, 2 N HNO_3, 0.005 M $NaNO_2$, FP spike

Aqueous scrub: 2 N HNO_3, F/S/O = 1/0.75/4.75

Countercurrent Stage	1 M TBP		1 M DSBPP	
	Untreated Feed	Treated Feed	Untreated Feed	Treated Feed
	Zr^{95}–Nb^{95} Extraction Factors			
6S	4.3	1.73	1.2	0.85
2S	0.12	0.04	0.092	0.012
1E	0.012	0.0005	0.011	0.0004
5E	0.018	0.0019	0.012	0.0026
(Over-all DF's)	(1130)	(11,900)	(566)	(23,400)
	Ru Extraction Factors			
6S	2.05	1.48	0.965	1.18
2S	0.343	0.047	0.189	0.032
1E	0.0173	0.0008	0.0067	0.001
5E	0.177	0.0009	0.125	0.0074
(Over-all DF's)	(640)	(13,000)	(480)	(11,000)

extraction data from the literature,[2] with extraction coefficients close to agreement at ~ 1 M HNO_3 but lower by a factor of ~ 5 at 0.2 M HNO_3. The reason for this discrepancy has not been found. Comparison of back-extraction with direct-extraction equilibrations ruled out the possibility that the new values might have been erroneously low because of nonequilibrium formation of inextractable hydrolytic plutonium species, at least at acidities down to 0.4 M HNO_3. At the same time, the literature data[2] are well supported by internal agreement of macro and trace extractions.

[2]G. F. Best, H. A. C. McKay, and P. R. Woodgate, J. Inorg. Nuclear Chem. 4, 315 (1957).

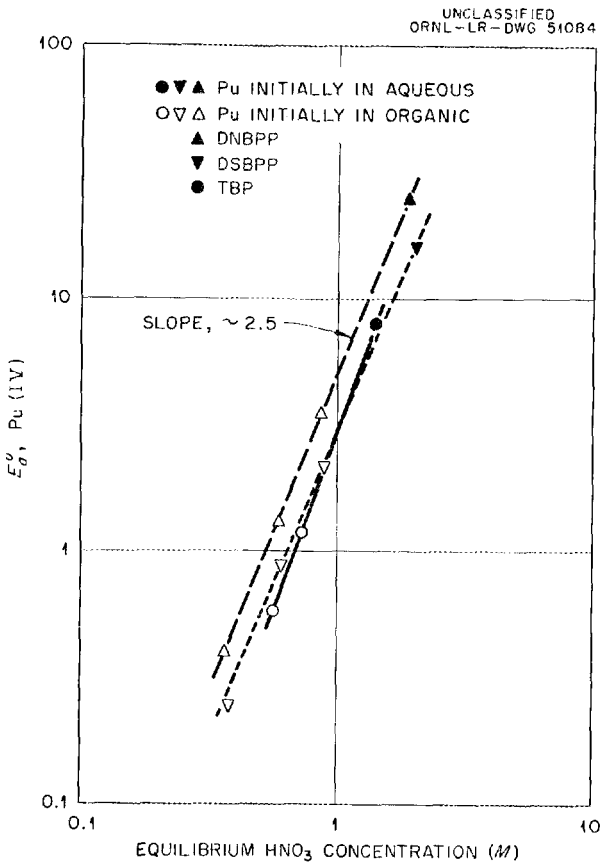

Fig. 15.1. Plutonium(IV) Extraction from Nitric Acid Solution by 1 *M* Di-*n*-butylphenyl Phosphonate, Di-*sec*-butylphenyl Phosphonate, and Tributyl Phosphate. Xylene diluent.

Surprisingly, with both TBP and phosphonates, back-extraction data agreed closely with direct extractions at aqueous acidities $\lesssim$ 0.4 M, but plutonium retention was considerable in back extractions at acidities below 0.4 M but still above the acidities where plutonium polymerization would be expected.[3]

Plutonium(IV) is extracted from dilute nitric acid solutions much more strongly by di(2-ethylhexyl)phosphoric acid (D2EHPA) than by either amines or phosphine oxides, for example, E_a^o(Pu) $\approx$ 5000 with 0.01 M D2EHPA from 0.3 M HNO_3. As expected for cation exchange, the extraction coefficients decreased with increasing acidity over most of the range (0.3 to 10 M HNO_3), but in closer inverse proportion to the square than to the

[3]A. Brunstad, Ind. Eng. Chem. 51, 38 (1959).

fourth power, which would be expected for exchange of 4 H^+ for Pu^{4+}. Addition of sodium nitrate had little effect. The extraction coefficient varied with the square of the uncomplexed D2EHPA concentration (Fig. 15.2), calculated on the basis of four D2EHPA's complexed per plutonium. Since

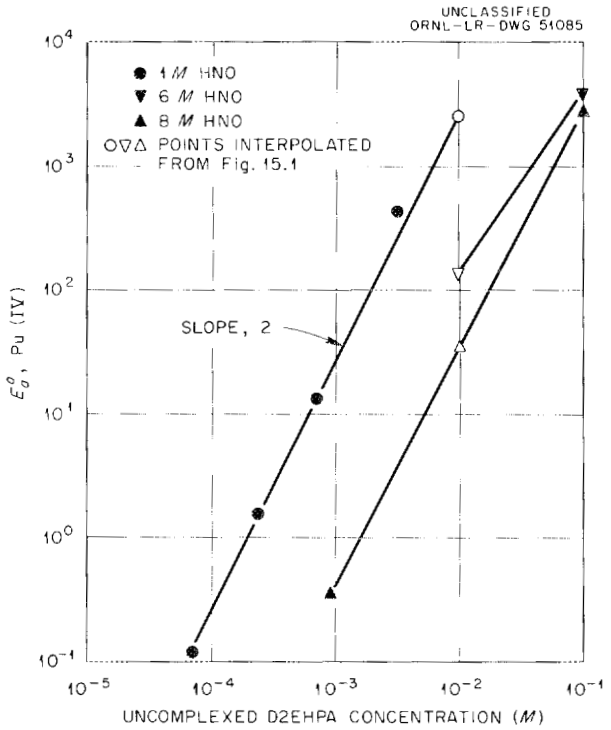

Fig. 15.2. Variation of Pu(IV) Extraction Coefficient from Nitric Acid Solutions by Di(2-ethylhexyl)phosphoric Acid with Change in Extractant Concentration. Amsco 125-82 diluent; ~ 10 mg of Pu per liter in aqueous initially.

D2EHPA is dimeric in hydrocarbon solution, these results suggest that the extraction reaction is

$$M^{++} + \underset{\cdots\cdots}{2(HX)_2} \rightleftharpoons \underset{\cdots\cdots}{MX_4H_2} + 2H^+$$

where X represents the dialkylphosphate anion and M^{++} is probably PuO^{++}, or possibly $Pu(NO_3)_2^{++}$, etc. This is analogous to the previously proposed[4] formulations $UO_2X_4H_2$, $Fe(OH)X_4H_2$, and ThX_8H_4. Plutonium(VI) extraction coefficients with D2EHPA were lower than Pu(IV) coefficients by several

[4]C. A. Blake et al., Proc. U.N. Intern. Conf. Peaceful Uses Atomic Energy, 2nd, Geneva, 1958 28, 289 (1959).

orders of magnitude, for example, ~ 10 with 0.1 M D2EHPA from 4 M HNO_3. They were slightly lower than U(VI) coefficients and fairly closely parallel to them, including impairment on addition of alcohol and synergistic enhancement on addition of phosphine oxide to the hydrocarbon diluent. Plutonium(III) extraction with D2EHPA is still lower, but could not be measured accurately because of variations attributed to enhanced oxidation to (IV), in spite of the use of holding reductants and an inert atmosphere (see below).

While the extraction of Pu(III) from nitric acid solutions was low with all classes of amines, tertiary amines gave high extraction coefficients for reduced plutonium from aluminum nitrate solutions at low acidity (Fig. 15.3). This is of interest for, as an example, the simultaneous extraction of plutonium with neptunium, which must be reduced to (IV) for best extraction. It was not established whether the Pu(III) was extracted as such or was oxidized to the more extractable Pu(IV) before or during transfer. If transferred as Pu(III), it appeared to be rapidly oxidized

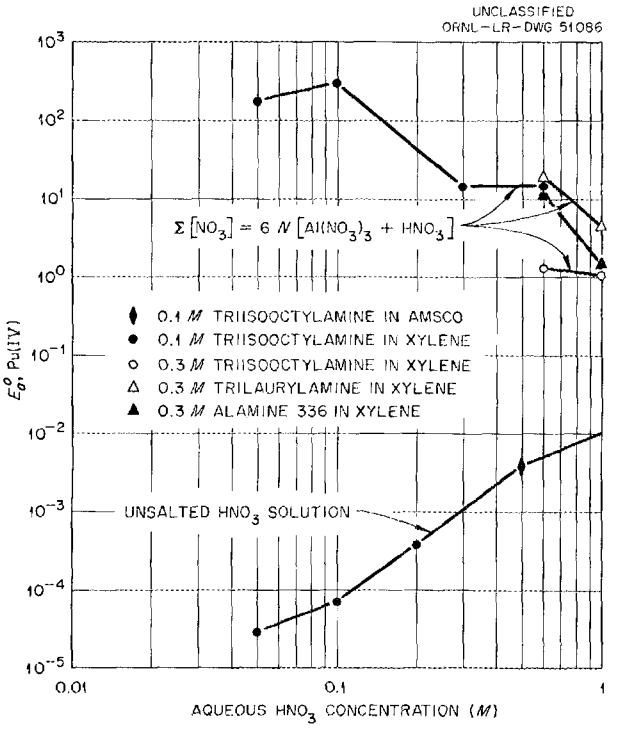

Fig. 15.3. Extraction of Pu(III) by Tertiary Amines from Nitric Acid Solutions With and Without Aluminum Nitrate Salting.

after extraction (in spite of the inert atmosphere), since a 2 M HNO_3–0.1 M NH_2SO_3H scrub removed only a small amount.

Scavenging from Sulfex Decladding Wastes

Laboratory-scale process development on solvent extraction methods to recover plutonium and uranium lost to sulfuric acid stainless steel cladding solutions was completed.[5] Consecutive extraction of U(IV) and Pu(III) or (IV) by 0.1–0.3 M primary amine in hydrocarbon-alcohol diluent appeared promising, and chemical flowsheets were demonstrated in laboratory-scale continuous countercurrent extraction. Extraction of U(VI) with a dialkylphosphoric acid appeared promising when plutonium recovery is not needed. Recovery is also chemically feasible by extraction of U(VI) and Pu(IV) with an N-benzyl secondary alkyl amine or a trialkylphosphine oxide. The amine extracts are stripped with nitric acid, giving a sulfate-nitrate product solution. The organophosphorus extractants permit elimination of the sulfate but require sodium carbonate for stripping.

15.3 METAL NITRATE EXTRACTIONS BY AMINES[6]

A study is in progress on the amine extraction characteristics of a range of fission-product and corrosion-product metals of interest in radiochemical nitrate systems. The study is directed primarily toward the descriptive chemistry of the extractions — the magnitude of the extraction coefficients and their dependences on some of the major variables. Molybdenum, zirconium, ruthenium, and samarium have been examined in nitric acid and in acidified sodium nitrate solutions, using a straight-chain quaternary, straight-chain tertiary, highly branched secondary, slightly branched secondary, and highly branched primary amine [respectively, Aliquat 336, trilaurylamine, bis(1-isobutyl-3,5-dimethylhexyl)amine, ditridecylamine, and Primene JM-T].

---

[5]D. E. Horner and C. F. Coleman, Recovery of Uranium and Plutonium from Sulfuric Acid Decladding Solutions, ORNL-2830 (Nov. 11, 1959).

[6]Work done by the Department of Nuclear Engineering, MIT, under subcontract.

Molybdenum(VI)[7] extraction coefficients with 0.1 M amines in toluene were of the order of 100 and higher at nitric acid concentrations below 0.1 M, dropping rapidly to $\sim 10^{-4}$ at 2–8 M HNO_3 and to $< 10^{-5}$ at 10 M HNO_3. They were appreciably higher at 6 M than at 2 or 8 M HNO_3, but still near 10^{-4}. Apparently, over most of the acidity range, the molybdenum was extracted as molybdate in direct competition with nitric acid, with extraction of a nitrate complex becoming barely discernable at ~ 6 M HNO_3. Differences between extraction coefficients with the different amines were small in comparison with their variation with acidity. At low loading, the extraction coefficients from 0.1 M HNO_3 increased with increasing molybdenum concentration. At high molybdenum concentrations the molybdenum/amine mole ratio rose rapidly to 1/1 and then more gradually to $\sim 2/1$. Both these observations indicate considerable polymerization of the molybdenum.

Zirconium (ref 8) extraction coefficients were very low from dilute nitric acid. They increased rapidly with increasing nitric acid concentration, in proportion to about the fourth power, but still were only ~ 0.01 from 10 M HNO_3 with 0.3 M amine. The results over the entire range were rather well summarized by

$$E_a^o(Zr) = K(\underline{M}_{amine})^2 \ (\underline{M}_{H^+})^2 \ (\underline{M}_{NO_3^-})^2 \quad ,$$

with K around 6×10^{-6} for trilaurylamine and for Primene JM-T, and around 2×10^{-5} for Aliquat 336, in toluene diluent. The extraction coefficients were slightly higher when the diluent was Amsco Odorless Solvent containing 10–20% decanol.

Ruthenium (ref 9) extraction coefficients rose rapidly with contact time, for example, from 0.03 at 0.5 hr to 0.05 at 1 hr, 0.08 at 24 hr,

---

[7]Ammonium molybdate dissolved in the desired nitric acid or nitric acid–sodium nitrate solution.

[8]Zirconyl nitrate dissolved in 8 M HNO_3, refluxed 15 hr, and then adjusted to the desired nitrate concentration. Extraction results were the same after aging for several months (8 M HNO_3) as when fresh.

[9]Nitrosylruthenium nitrate prepared by fusing ruthenium metal in sodium peroxide, dissolution, precipitation of RuO_2 with methanol, redissolution in refluxing 8 M HNO_3, treatment with nitrogen oxides, and drying to solid under vacuum at room temperature. The solutions were prepared by dissolving this solid in the desired nitrate solution for use either immediately or after aging.

and 0.1 at 4 days in extraction with 0.4 M trilaurylamine in toluene from (aged) 2 M HNO_3 solution. As measured at 24 hr, the extraction coefficients were directly proportional to the amine concentration and inversely proportional to the nitric acid concentration. It has not yet been determined whether the extracted ruthenium has any tendency to resist removal by scrubbing from the amines, as it does from TBP.

Extraction coefficients for samarium (ref 10), taken as a representative trivalent rare-earth ion, were all below $\sim 10^{-4}$ with 0.3 M amines in toluene. There was no obvious systematic change with either nitric acid concentration (2–9 M) or amine class.

The results so far from this program suggest that ruthenium is more likely than zirconium or rare earths to be the first limitation reached in using amine extraction for high decontamination of, for example, plutonium. Work is continuing on further extraction variables and on extension to niobium, cerium, and stainless steel metals.

15.4 TECHNETIUM-NEPTUNIUM-URANIUM RECOVERY

An important potential source of technetium and neptunium is uranium fluorination plant residues. In routine operation these are processed for recovery and recycle of the uranium, and technetium and neptunium, when present, are dissolved along with the uranium in the acidified aluminum nitrate leach. A TBP extraction process for the recovery of both uranium and neptunium has been developed.[11] Thus, any process designed for technetium recovery should be compatible with or satisfactorily replace existing uranium and neptunium processes. After investigation of amine vs TBP extraction, and separate vs co-recovery, a single-cycle process was designed for coextraction by tertiary amine of uranium, neptunium, and technetium, and separation by consecutive stripping (Fig. 15.4).

Technetium Extraction Coefficients

Technetium(VII) is extracted by amines from acidified nitrate solution by anion exchange in direct competition with nitric acid (Fig. 15.5).

---

[10] Solutions prepared from Lindsay Chemical 99.9% samarium oxide.

[11] Chem. Tech. Ann. Prog. Rep. Aug. 31, 1958, ORNL-2576, p 61.

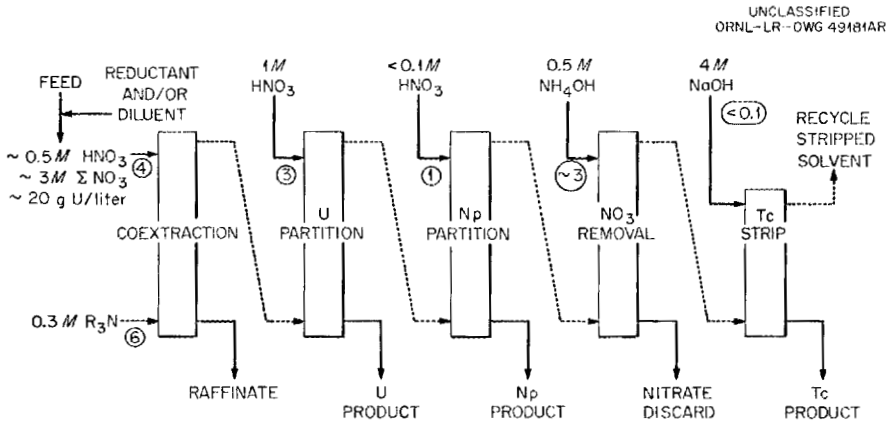

Fig. 15.4. Technetium-Neptunium-Uranium Recovery Process. Circled numbers indicate flow ratios.

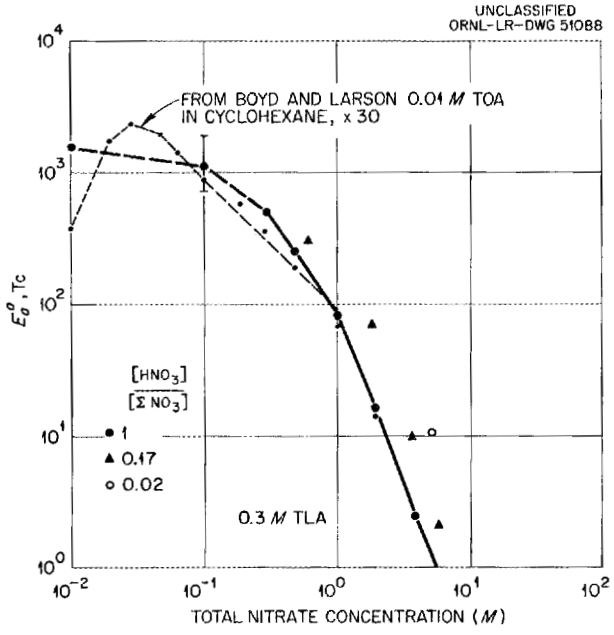

Fig. 15.5. Technetium Extraction by Tertiary Amines from Nitrate Solutions.

The extraction coefficients are directly proportional to the amine concentration, and our results with 0.3 M trilaurylamine in Amsco 125-82 agree well with the 0.01 M triisooctylamine data, multiplied by 30, of Boyd and Larson.[12] Aluminum nitrate impaired the technetium extraction nearly as much as the equivalent amount of nitric acid. Addition of an

[12]G. E. Boyd and Q. V. Larson, "Solvent Extraction of Heptavalent Technetium," J. Phys. Chem. 64, p 988–96 (1960).

alcohol (to prevent third-phase formation and improve the physical performance) lowered the extraction coefficients, for example, ~ 50% with 5–10% tridecanol. Neither fluoride nor ferrous sulfamate (neptunium reductant) impaired technetium extraction.

Chemical Flowsheet

A feed solution of ~ 3 M total nitrate, of which a fairly small part (~ 0.5 M) is nitric acid, permits usefully high extraction coefficients for both technetium and uranium with 0.3 M tertiary amine and a still higher coefficient for neptunium(IV) (see ref 13). This composition can be obtained from a typical leach solution (Table 15.3) by simple dilution. Since uranium is the only extractable component at a major concentration,

[13] B. Weaver and D. E. Horner, "Distribution Behavior of Neptunium and Plutonium Between Acid Solutions and Some Organic Reagents," J. Chem. Eng. Data, 5, p 260–65 (1960).

Table 15.3. Typical Feed Composition

Plant solution No. 1

Specific gravity: 1.4
Gross β: ~ 10^5 counts min^{-1} ml^{-1}, 10% geometry
Gross γ: ~ 10^4 counts min^{-1} ml^{-1}, 25% efficiency

Constituent	Amount Present	
	g/liter	M
Tc	0.08	
Np	0.06	
U	40	
Th	1	
Al	50	
SS metals	5	
H^+		0.74
NO_3^-		6
F^-		0.3
SO_4^{--}		< 0.003

the system will follow the uranium extraction isotherm (Fig. 15.6). After details of the flowsheet were established with simulated feed and Tc^{95m} tracer, a demonstration run was made with actual plant leach solution in a 24-stage mixer-settler bank. Flow ratios (Table 15.4) set for uranium loading at ~ 15 g/liter of 0.3 M amine gave essentially complete uranium extraction in the first four stages and left sufficient amine free for complete neptunium and technetium extraction in the first three stages.

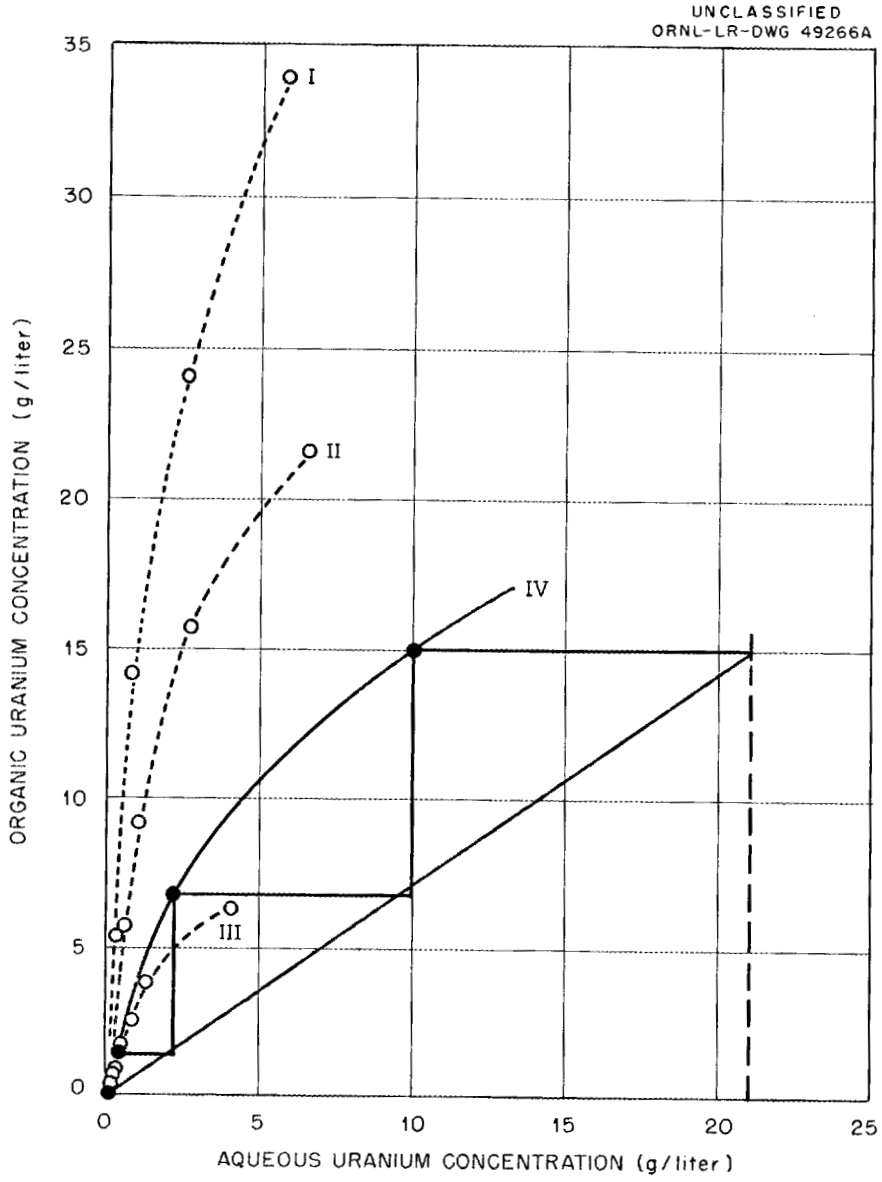

Fig. 15.6. Uranium Extraction Isotherms with Tertiary Amines from Nitrate Solutions. (I) 0.5 *M* TLA, 10% TDA; (II) 0.3 *M* TLA, 6% TDA; (III) 0.1 *M* TLA, 2% TDA, in batch extractions from 1.0 *N* HNO_3–5.0 *N* $Al(NO_3)_3$ solutions; (IV) 0.3 *M* Alamine 336, 10% TDA, in continuous countercurrent extraction from plant solution.

Table 15.4. Operating Conditions for Continuous Countercurrent Test with Plant Feed

Flowsheet: see Fig. 15.4

24-stage mixer-settler bank

Step	In			Out	
	Stage No.	Stream	Volume (ml/hr)	Stage No.	Stream
Coextraction	1	Solvent, 0.3 M Alamine 336 (free-base form) in 90% Amsco 125-82, 10% tridecanol	300		
	1	2 N HNO_3[a]	~ 15	1	Raffinate
	7	Adjusted feed,[b] ~ 0.5 M HNO_3, ~ 0.83 M $Al(NO_3)_3$	200		
U partitioning	13	1 M HNO_3	150	8	U product
Np partitioning	19	0.05 M HNO_3[c]	50	14	Np product
NO_3^- removal	23	0.5 M NH_4OH[d]	160	20	NO_3^- discard
Tc stripping	24	Initially 4 M NaOH	Static[e]	24	Tc product
				24	Stripped solvent to recycle

[a]At the flow ratio set for the desired uranium loading, the recycled amine required more acid than was available from the feed. The additional acid was added to the raffinate stage in preference to the feed.

[b]Plant solution No. 1 (see Table 15.3) made 0.1 M in ferrous sulfamate and diluted to twice its original volume.

[c]During a part of this run, 1% H_2O_2 was added to the 0.05 M HNO_3 neptunium strip solution.

[d]A tendency toward emulsification in the nitrate removal section was eliminated by adding 5 ppm of Victawet 12 to the 0.5 M NH_4OH.

[e]The technetium strip solution, 160 ml, was recycled continuously from the settler back to the mixer in stage 24. After processing of 8.3 liters of the adjusted feed, ~ 80% of the sodium hydroxide had been neutralized and the technetium concentration had reached 1.87 g/liter.

Table 15.5. Distribution of Uranium, Neptunium, and Technetium

	Amount (% of feed[a])		
	Tc	Np	U
Raffinate	< 0.2[b]	< 0.1[b]	0.003
U product	2	6	104
Np product	0.1	95	0.05
NO_3^- discard	0.3	0.3	0.002
Tc product	104	< 0.1[b,c]	< 0.001

[a]Not adjusted for material balances, which were 107, 103, and 104%, respectively, for technetium, neptunium, and uranium.

[b]Below analytical limits.

[c]Less than 0.1% of the neptunium reported to the technetium product when H_2O_2 was used in the neptunium strip solution, and ~ 1% when H_2O_2 was not used.

The uranium was effectively stripped with 1 M HNO_3 in six stages, carrying with it 1% of the technetium and 6% of the neptunium (Table 15.5). A higher nitric acid concentration in the uranium strip solution would have decreased this neptunium leakage, but at the cost of increased technetium leakage and impaired uranium stripping. Moreover, this neptunium should not be lost, but recycled through the fluorination plant with the uranium. The neptunium was stripped moderately well with 0.05 M HNO_3 and, alternatively, very efficiently with 0.05 M HNO_3 plus 1% H_2O_2. The technetium was effectively stripped with a small excess of either sodium or ammonium hydroxide. The technetium was effectively stripped with a small excess of either sodium or ammonium hydroxide. The technetium/nitrate ratio, and hence the attainable technetium product concentration, was improved by prior fractional stripping of ~ 80% of the nitrate from the extract; 90–95% recovery for the organic in the strip cycle appeared feasible.

The uranium product stream (Table 15.6) is suitable for evaporation, denitration, and recycle to the fluorination plant. The neptunium product stream, < 0.1 M HNO_3, is suitable for evaporation and final purification

Table 15.6. Product Solution Analyses

Product	Amount (g/liter)				Concentration (M)			Activity (counts min^{-1} ml^{-1})[e]	
	Tc	Np	U	Th	HNO_3	$NaNO_3$	NaOH	Gross β	Gross γ
Tc[a]	1.87	0.007	0.002			3.2	0.8[d]	3×10^6	10^4
Np[b]	0.001	0.09	0.04	1.2	0.05			1.5×10^4	5×10^4
U[c]	0.001	0.002	29	0.6	1			5×10^3	4×10^3

[a]Product fraction collected after 16th hr of 58-hr run.

[b]Product fraction collected for last 12 hr of run.

[c]Product collected for entire run.

[d]NaOH remaining unconsumed at arbitrary termination of test. In plant operation essentially complete consumption of the NaOH would be expected.

[e]Beta counts at ~ 10% geometry, gamma counts at ~ 25% efficiency.

by amine extraction[14] or other means. Its major contaminant is thorium. The technetium product stream contains ~ 2 g/liter (~ 5 g/liter probably attainable) as pertechnetate, well separated from contaminants, in ~ 4 M sodium or ammonium nitrate solution.

15.5 SEPARATION OF TRANSPLUTONIUM ELEMENTS FROM LANTHANONS

The extraction of americium and some of the lanthanons by several amines and neutral organophosphorus compounds was studied in a search for new methods of separating the transplutonium elements from fission product rare earths. The lanthanons were represented by Ce^{144} and Eu^{152}, which bracket almost the whole fission product lanthanon range. Some data were obtained with Nd^{147}, Pm^{148}, Lu^{177}, and Y^{91}.

The most promising separation observed thus far is extraction with tributyl phosphate (TBP) from slightly acid, highly concentrated lithium chloride solution. Separations with diamyl amylphosphonate (DAAP) and dibutyl butylphosphonate (DBBP) were slightly less favorable, and the results with dibutyl phenylphosphate (DBPP) were variable. The amines[15]

[14]Chem. Tech. Ann. Prog. Rep. Aug. 31, 1958, ORNL-2576, p 106.

[15]A primary amine, Primene JM-T, 0.4 M, from dilute sulfuric acid, 0.3 M trilaurylamine from 8 M $LiNO_3$–0.1 M HNO_3, 0.1 M tetra-n-heptylammonium from 8 M $LiNO_3$–0.1 M HNO_3 and 10 M LiCl–0.01 M HCl.

tested were not suitable for this separation since they all extracted americium with factors between those of cerium and europium (Fig. 15.7).

Single-stage extraction coefficients for Ce^{144}, Eu^{152}, and Am^{241} by 1 M TBP in Amsco 125-82 from 9.9 M LiCl–0.1 M HCl were 0.20, 0.38, and 1.35, respectively. A 12-stage batch countercurrent separation of americium from europium showed, after 125 cycles, 98% of the Am^{241} leaving the system in the organic stream and 87% of the Eu^{152} leaving in the aqueous. The over-all separation factor of 310 was 0.2 of the predicted factor. There were variations in coefficients in different parts of the cascade. A still more favorable separation of the heavier transplutonics from the fission product lanthanons would be expected.

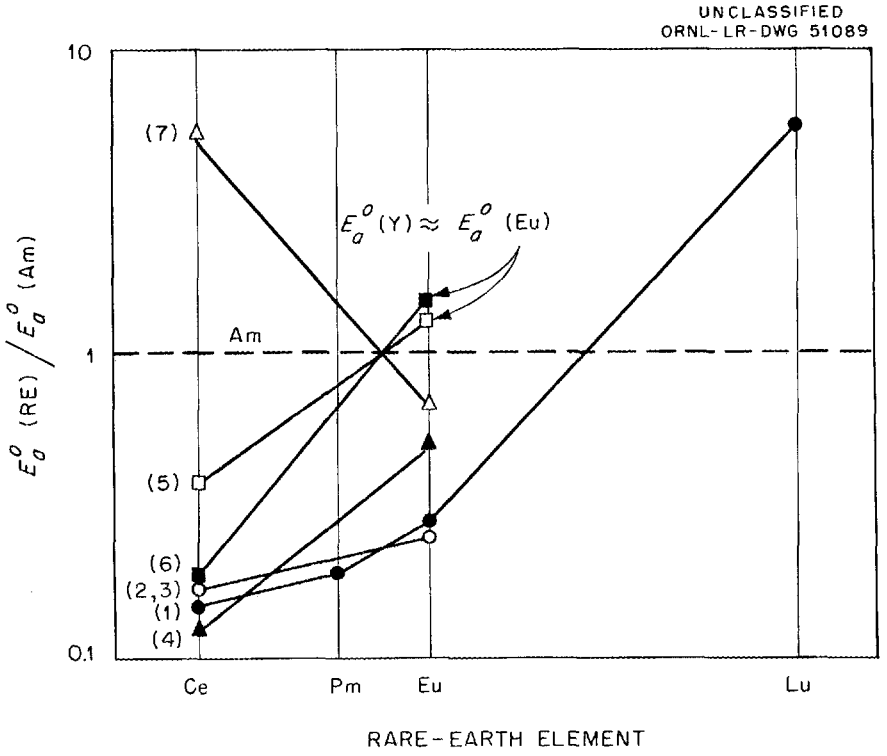

	Organic	Aqueous
(1)	Tributyl phosphate	10 *N* LiCl–0.1 *N* HCl
(2)	Dibutyl butylphosphonate	10 *N* LiCl–0.1 *N* HCl
(3)	Diamyl amylphosphonate	10 *N* LiCl–0.1 *N* HCl
(4)	Dibutyl phenylphosphonate	10 *N* LiCl–0.1 *N* HCl
(5)	Tetraheptylammonium	10 *N* LiCl–0.01 *N* HCl
(6)	Tetraheptylammonium	8 *N* $LiNO_3$–0.1 *N* HNO_3
(7)	Trilaurylamine	8 *N* $LiNO_3$–0.1 *N* HNO_3

Fig. 15.7. Relative Extractabilities of Rare Earths in Comparison with Americium.

Single-stage extractions of europium and yttrium were nearly equal. Lutetium was extracted preferentially to europium by a factor of at least 20, indicating an unusual case of greater differences between successive elements in the heavier part of the lanthanide series than in the lighter part.

15.6 EXTRACTION PERFORMANCE AND CLEANUP OF DEGRADED PROCESS EXTRACTANTS

TBP–Amsco 125-82 solutions were degraded chemically with nitric acid and radiolytically by Co^{60} gamma irradiation as a first approximation to the degradation encountered in radiochemical processing. The extent of degradation and the effectiveness of solvent cleanup treatments were assessed by measuring the extraction and stripping of Zr^{95}-Nb^{95} and of Ru^{106}.

Zr^{95}-Nb^{95} Extraction

The extraction coefficients for zirconium and niobium from 2 M nitric acid with 1 M TBP in Amsco 125-82 ($E_a^oZr = 0.04$, $E_a^oNb = 0.009$) increased rapidly with degradation, typical examples being a 25-fold increase after treatment of a 1 M TBP solution for 4 hr with 2 M HNO_3 at 107°C, or subjecting it to ~ 100 whr/liter of Co^{60} gamma irradiation, and a hundredfold increase when the TBP-Amsco solution contained 0.25 M HNO_3 during irradiation. Such factors varied widely with the source and pretreatment of both diluent and TBP.

Extraction was primarily by degradation products soluble in dilute alkaline scrub solutions (e.g., 0.2 M Na_2CO_3), presumably low-molecular-weight acids such as dibutylphosphoric formed by hydrolysis of TBP. Such scrubbing decreased subsequent Zr^{95}-Nb^{95} extraction by 80–90%. Products not removed by alkaline scrub solutions, for example, polymeric compounds and nitrated diluent molecules, extracted much less Zr^{95}-Nb^{95} but held that small amount so strongly that even concentrated acids failed to strip it.

Ru^{106} Extraction

The response of Ru^{106} extraction (as the nitrate nitrosylruthenium complexes) to variations in the treatment of the solvent was tested in a

manner similar to that used for Zr^{95}-Nb^{95}. In contrast, the Ru^{106} extraction properties of fresh TBP in fresh Amsco (E_a^o = 0.08 from 2 M HNO_3 with 1 M TBP) were not significantly altered by chemical degradation of the diluent, by simulated degradation of the TBP (addition of its principal hydrolysis product), or by irradiation of the complete solvent. Only when the Ru^{106} was extracted into degraded solvent and then aged for several days did simple scrubbing with acid or alkaline solutions fail to remove it completely.

Solvent Cleanup

Solvent cleanup methods involving a combination of alkaline and acid washes (sometimes in conjunction with alkaline permanganate) effectively removed the acid- and radiation-degradation products of the extractant but not all the degradation products of the diluent. The proportion of the latter increased with degradation. Since different diluents are in use at different processing sites, and each can vary from batch to batch, there is wide variation in the degree of degradation of the total solvent that can be tolerated before special cleanup methods are required. The most effective cleanup studied was by sorption on activated alumina, although the quantities required may be excessive for plant use.

Compounds known to contain nitrogen were isolated from degraded Amsco 125-82 and showed chemical and extraction properties similar to those of the degraded diluent. Synthetic nitrohydrocarbons, demonstrating the same properties, have been used as prototypes for the constituents of degraded diluent, and cleanup investigations have been directed toward exploitation of their known chemical properties, for example, conversion by salt formation or by further degradation to forms that are soluble in liquid scrub solutions, thus eliminating the need for the liquid-solid contact and separation. Treatment with low-molecular-weight amines such as ethanolamine has been promising.

15.7 SOLVENT EXTRACTION EQUILIBRIA

Amine Extraction of Thorium Sulfate

In a detailed study of the extraction of thorium sulfate from acidified sulfate aqueous solutions by di-n-decylamine sulfate in benzene, distribution data obtained under three specific sets of experimental conditions permitted evaluation of (1) the composition of the organic-thorium complex, (2) an equilibrium constant for the over-all extraction reaction, and (3) Debye-Hückel corrected formation constants for the thorium tri- and tetrasulfate complexes in the aqueous phase.

The first of these results was obtained on the basis of the same assumptions made in the corresponding uranium studies;[16] that is, the amine sulfate--metal sulfate complex contains no bisulfate, and the presence of the complex does not alter the equilibrium between the aqueous sulfuric acid and the sulfate-bisulfate ratio in the uncomplexed amine salt species. The equilibrium for the extraction of thorium sulfate by the di-n-decylamine sulfate—bisulfate mixture can be written

$$nxRH_2SO_4 + \frac{n}{2}(1 - x)\, R_2H_2SO_4 + Th(SO_4)_2 = R_nH_nTh(SO_4)_{n/2+2} + \left(\frac{nx}{2}\right) H_2SO_4 \quad (1)$$

where

$$R = (C_{10}H_{21})_2NH, \text{ and } x = \frac{[RH_2SO_4]}{[RH_2SO_4] + 2[R_2H_2SO_4]},$$

the equivalent fraction of bisulfate present.

For each mole of thorium extracted, this equation predicts the transfer of nx/2 moles of sulfuric acid back into the aqueous phase. Since x is known from acid extractions in the absence of thorium, careful measurements of the acidity changes accompanying the transfer of known amounts of thorium permit calculation of n, the number of equivalents of amine per mole of thorium in the complex. The results obtained on extracting constant amounts of thorium at varying sulfuric acid and organic bisulfate

---

[16] K. A. Allen, J. Am. Chem. Soc. 80, 4133 (1958); W. J. McDowell and C. F. Baes, Jr., J. Phys. Chem. 62, 777 (1958).

levels by both the usual vigorous agitation and the new quiescent-interface[17] techniques are shown in Table 15.7. These n values are in good agreement with those obtained from the isotherm plateaus, and their internal consistency indicates that this equilibrium is not markedly affected by violence of agitation during equilibration.

Extraction data taken at constant aqueous sulfate ion concentration but with varying sulfuric acid activity are shown in Table 15.8. From an equilibrium-constant expression for the reaction shown in Eq. 1, by making reasonable substitutions for the activities of the various species,

---

[17]K. A. Allen and W. J. McDowell, J. Phys. Chem. 64, 877 (1960).

Table 15.7. Amine Sulfate–Thorium Sulfate Complex Composition According to Acid-Transfer Measurements

Vigorous Agitation			Gentle Agitation		
x	$\Delta[H^+]_{aq}$	n	x	$\Delta[H^+]_{aq}$	n
0.229	0.0121	5.28	0.180	0.0096	5.33
0.309	0.0166	5.37	0.228	0.0117	5.13
0.348	0.0195	5.60	0.311	0.0157	5.05
0.384	0.0211	5.49	0.350	0.0198	5.66
0.416	0.0222	5.34	0.382	0.0210	5.53

Table 15.8. Thorium Extraction Coefficient as a Function of Sulfuric Acid Concentration at Constant Total-Sulfate-Ion Molarity

$[Na_2SO_4]_{aq}$	$[H_2SO_4]_{aq}$	$[H_2SO_4]_{org}$	$E = [Th]_{org}/[Th]_{aq}$
0.315	0.035	0.0570	326
0.323	0.057	0.0600	240
0.328	0.082	0.0629	144
0.330	0.110	0.0656	95
0.343	0.147	0.0684	67
0.351	0.189	0.0703	47

the following equation may be derived:

$$y + ax = k + nz \quad , \tag{2}$$

where x is the equivalent fraction of uncomplexed amine in the bisulfate form; y is the logarithm of the thorium extraction coefficient E; z is one-half the logarithm of the equivalent fraction of uncomplexed amine in the normal sulfate form; and a, k, and n are constants representing, respectively, the amine sulfate-bisulfate equilibrium, the equilibrium constant for the over-all reaction (Eq. 1), and the number of equivalents of amine sulfate per mole of thorium in the complex. A simultaneous least-squares analysis of the data in Table 15.8 gave a = 1.3, k = 2, and n = 7. Of these three numbers, the only one subject to comparison with other evaluations is n; the agreement here is considered remarkable, in view of the involved series of deductions necessary in getting from Eq. 1 to Eq. 2.

At constant composition of the organic phase (i.e., constant amine molarity, constant organic thorium concentration, and constant sulfuric acid activity) but with various amounts of aqueous sulfate ion concentration, the equilibrium aqueous thorium molarities shown in Fig. 15.8 were obtained. On making single-parameter Debye-Hückel corrections for the ionic-strength effects (using 2 as a fixed distance term) and then attributing the remaining deviations from ideality to mononuclear thorium sulfate complexes, it is possible to obtain the following values for the formation constants of these complexes (see Fig. 15.8):

$$K_{23} = \frac{[Th(SO_4)_3^{--}]}{[Th(SO_4)_2]\ [SO_4^{--}]} = 6 \quad ,$$

$$K_{34} = \frac{[Th(SO_4)_4^{4-}]}{[Th(SO_4)_3^{--}]\ [SO_4^{--}]} = 0.005 \quad .$$

Both these constants are for zero ionic strength, as a result of the Debye-Hückel corrections. Under the present experimental conditions no evidence appeared for the presence of the species Th^{4+} or $ThSO_4^{++}$, and back calculations from constants reported elsewhere for the lower complexes[18] indicated that the positively charged species should be negligible at the present sulfate levels.

[18] E. L. Zebroski, H. W. Alter, and F. K. Heumann, J. Am. Chem. Soc. 73, 5646 (1951); A. J. Zielen, ibid., 81, 5022 (1959).

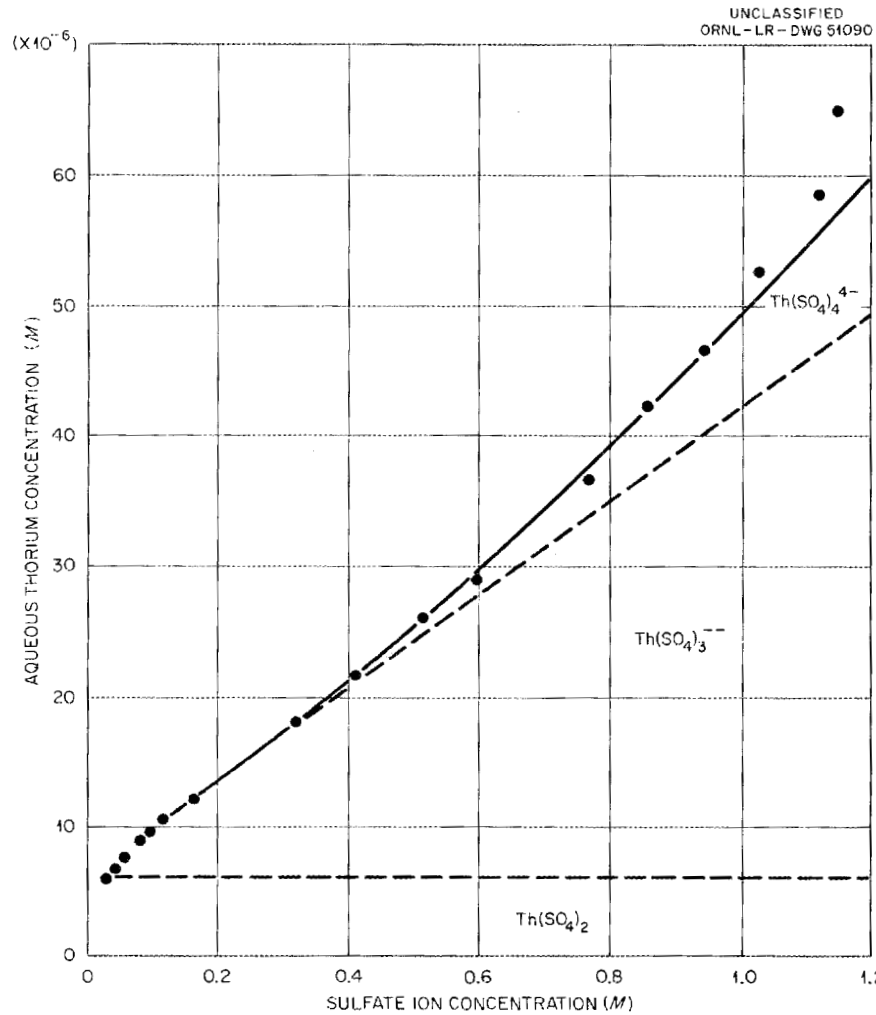

Fig. 15.8. Total Aqueous Thorium as a Function of Sulfate Ion Molarity at Constant Thorium Sulfate Activity and Constant Sulfuric Acid Activity. The solid line was computed from the formation constants $K_{23} = 6$ and $K_{34} = 0.005$ for the thorium tri- and tetrasulfate complexes. The areas separated by dashed lines indicate the relative quantities of $Th(SO_4)_3^{--}$ and $Th(SO_4)_4^{4-}$ at the various sulfate ion levels.

Anomalous Equilibria in Solvent Extraction Systems

In the di-n-decylamine sulfate and tri-n-octylamine sulfate (TOAS) extraction systems, the uranium distribution-coefficient dependence on organic reagent concentration has been found to be anomalously affected by the method of equilibration.[18]

In continued search for anomalous equilibria in systems other than these two, the extraction-coefficient dependence on reagent concentration

by vigorous and by gentle equilibration was determined for several other reagents. Both thorium extraction by di-n-decylamine sulfate (DDAS) and uranium extraction by 1,3-ethylpentyl-4-ethyloctylamine sulfate (EPOS) showed definite evidence of anomalous behavior. In the former, severe scatter of the experimental points precluded interpretation of the slopes, but the differences between the results of the two methods of equilibration were consistent and reproducible (Fig. 15.9). The latter system was

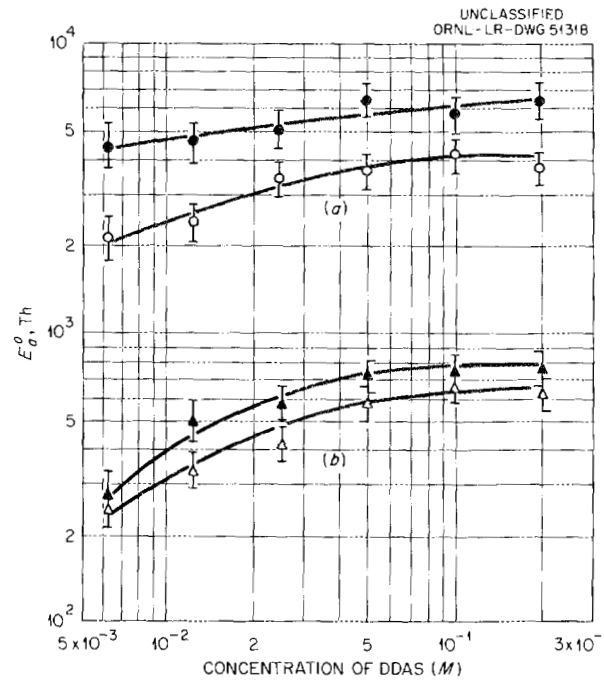

Fig. 15.9. Extraction of Thorium from (a) 0.005 M H_2SO_4 and (b) 0.005 M H_2SO_4–0.995 M Na_2SO_4 by DDAS in Benzene with Vigorous (Open Points) and Gentle (Solid Points) Equilibration.

the first so far examined which has shown anomalous behavior over the entire concentration range of interest. Whereas in the case of TOAS the results from the two equilibrations coincided at low concentrations, while with DDAS there was agreement at higher concentrations, it is apparent according to Fig. 15.10 that in the case of EPOS, since the lines cross, the disparities between the two methods continue to become even more pronounced at both ends of the concentration range.

Anomalous solvent extraction equilibria due to vigorous agitation during equilibration are apparently not widespread. However, it has been

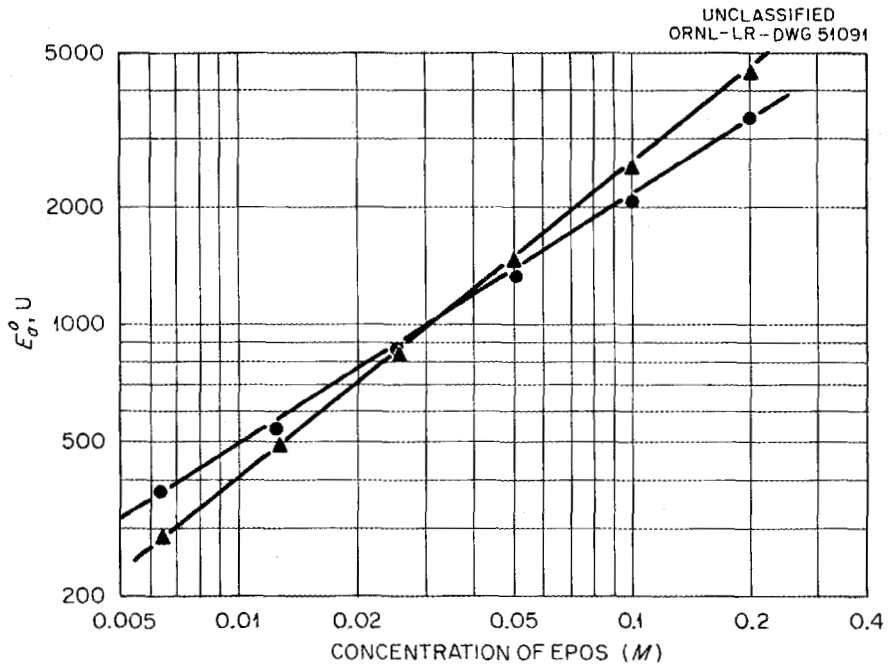

Fig. 15.10. Extraction of Uranium from 0.005 M H_2SO_4 by EPOS in Benzene with Vigorous (●) and Gentle (▲) Equilibration.

definitely established in a sufficient number of cases that any extractant system must be considered to possess this potential anomalous behavior potential until proved otherwise.

Activities in Solvent Extraction Systems

In interpreting the equilibration behavior of the organonitrogen and organophosphorus extractants, it has become increasingly apparent that serious limitations are imposed by a lack of accurately determined activity coefficients for the organic solutes. An apparatus constructed for obtaining accurate vapor pressure data has two magnetically stirred flasks, one for solvent and the other for solution, connected to a special U-tube mercury manometer. The valves and most of the associated tubing are of metal. Except for four Teflon O-rings, the vapors come in contact with only metal and glass. A special feature of the manometer is the reading device: a stainless steel pointer is driven down into one arm by a metric micrometer operating through a stainless steel bellows. The point of contact with the mercury is observed with a low-power binocular microscope. A practiced operator can easily obtain a series of readings whose average

deviation from the mean is 1 μ or less. Thus, since the total pressure difference is twice the change on one side of the U-tube, the over-all error in the pressure is about ±2 μ. The two arms of the manometer are of 1-in.-ID precision bore tubing, which provides a planar reading surface and ensures that twice the change on one side will be the true total pressure difference.

Operation of the apparatus with 99 mole % n-hexane in both receivers, and using the usual outgassing steps (several pumpdowns at −77°C, followed by room-temperature expansions into a 2-liter bulb), gave differences varying by tens of microns, far greater than the manometer reading error. This was attributed to the presence of small amounts of volatile impurities (e.g., pentane, heptane) in the solvent which were only partially and unequally removed during the outgassing. A procedure consisting of several such pumpdowns, followed by several distillations back and forth of about half the solvent in each flask, and then, omitting the cold pumpdowns, several room-temperature expansions into the evacuated 2-liter bulb, gave negligible vapor pressure differences between the two flasks.

16. EXTRACTION REAGENT PERFORMANCE

During the processing of spent nuclear fuels by solvent extraction, radiation causes partial decomposition of both extractant and diluent to products that have various deleterious effects. Tributyl phosphate (TBP) is partially decomposed by acid dealkylation[1] and radiation[2] to, among other products, di- and monobutyl phosphoric acids. These acids form compounds with uranium, plutonium, thorium, and fission product cations which affect the degree of recovery of valuable materials, change decontamination factors,[2,3] and might result in precipitation of solids in extraction columns. Further experiments were made on the products of TBP hydrolysis under simulated process conditions and on methods for recovering solvent for re-use.

16.1 RADIATION DAMAGE TO SOLVENTS

Tributyl Phosphate—Amsco 125-82 Systems[4]

Previous studies[5] of the radiolysis of TBP, which were conducted primarily in the anhydrous state, were extended to water-saturated systems and to systems containing nitric acid. Water-saturated systems, containing 0 to 100% TBP in Amsco, were irradiated to 330–400 whr/liter and subsequently analyzed for acid degradation products; in addition, the gas formation rate was measured. At concentrations of TBP below ~250 g/liter, the yield of dibutyl plus monobutyl phosphoric acids, G(HDBP + H_2MBP),[6]

---

[1]L. L. Burger, "The Decomposition Reactions of Tributyl Phosphate and Its Diluents and Their Effect on Uranium Recovery Processes," chap. 7-5 in Process Chemistry (ed. by F. R. Bruce et al.), Pergamon Press, New York, 1958.

[2]T. Rigg and W. Wild, "Radiation Effects in Solvent Extraction Processes," chap. 7-6 in Process Chemistry (ed. by F. R. Bruce et al.), Pergamon Press, New York, 1958.

[3]E. K. Dukes, The Formation and Effects of Dibutyl Phosphate in Solvent Extraction, DP-250 (November 1957).

[4]Work performed at Stanford Research Institute under subcontract; reported by R. M. Wagner and R. Farrand, "Radiation Stability of Organic Liquids," Stanford Research Institute Semiann. Rep. 6 on Subcontract 1081 (Jan. 5, 1960).

[5]Chem. Tech. Ann. Prog. Rep. Aug. 31, 1959, Sec 18, ORNL-2788.

[6]G = molecules of product formed per 100 ev of irradiation.

probably is somewhat greater in the water-saturated than in the anhydrous system. At higher concentrations of TBP in the diluent, the reverse is true (Fig. 16.1). The lower value of G(HDBP + H_2MBP) = 1.5 for the water-saturated TBP vs 2.3 for anhydrous TBP is in qualitative agreement with the results summarized by Rigg and Wild.[2] Yields of gases formed during these studies were in the range 2.2 ≦ G(gas) ≦ 3.8 for both systems.

Variables studied included (1) temperature, the solutions being heated to 70–80°C in two experiments but at 25–35°C in all others, (2) radiation exposure from 45 to 418 whr/liter, (3) the concentration of nitric acid

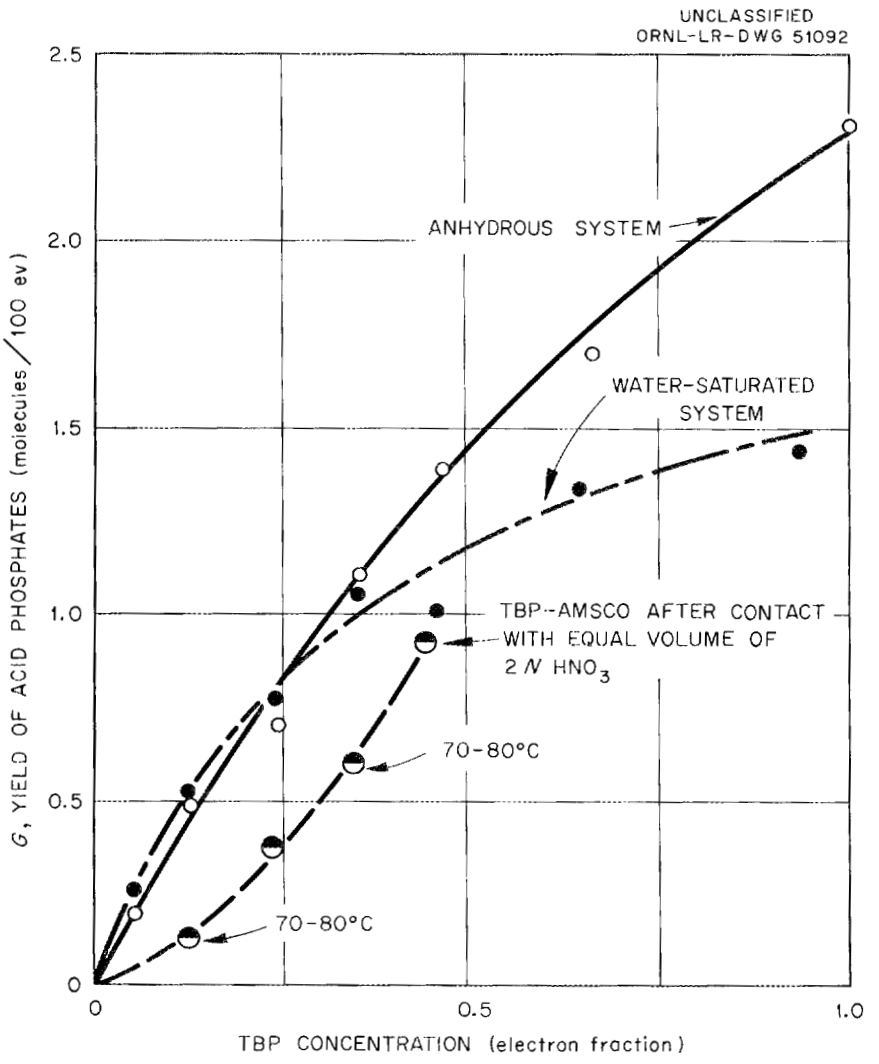

Fig. 16.1. Yield of Acid Phosphates from TBP–Amsco 125-82 Solutions as a Function of TBP Concentration. Temperature, 25–35°C except as noted; irradiation, 10^{22} ev/g or 300–400 whr/liter. Electron fraction ≈ weight fraction.

with which these solutions were contacted prior to irradiation of the organic phase, 0.3 to 7 N HNO_3, and (4) TBP concentration in the initial TBP-Amsco solution, from 0.376 to 1.505 M TBP or 13.15 to 47.65 wt %. At a constant dose of 10^{22} ev/g, corresponding to 300 to 400 whr/liter, increasing the temperature from 25 to 80°C had little effect on the production of di- and monobutyl phosphoric acids (Fig. 16.1). However, there was a considerable increase in discoloration of the solution at 80°C over that observed at 25°C, and the nitric acid in the solutions was completely destroyed at the higher temperatures.

A series of solutions of ~1 M TBP in Amsco was contacted with equal volumes of 0.3 to 7 N HNO_3 and then irradiated to levels of 45 to 418 whr/liter. In about half of these experiments the HNO_3 was completely destroyed. The value of $G(-HNO_3)$ is probably in the range 2.5 to 5.5 molecules HNO_3 destroyed per 100 ev of energy absorbed by the solution. Nitric acid contributed only 1 to 6% to the total electron density of these solutions, in which case values of $G(-HNO_3)$ in the range 0.03 to 0.2 might have been expected. The larger experimental values suggest that nitric acid serves as an energy sink or that it is decomposed by a very efficient chain mechanism.

Other Extractants and Diluents

Many acidic, basic, and neutral extractants have been investigated[5] for potential use in reactor fuel processing operations. Of these, di-sec-butylphenylphosphonate (DSBPP) has a radiolytic yield of monobasic acid, G(mono acid), of about 0.5, contrasted with a value of ~2.1 for TBP. Since DSBPP also has certain attractive features with respect to separation of elements, its radiation stability was studied in more detail. The aromatic diluent Solvesso-100 was used in some tests because aromatic diluents are necessary to achieve sufficient organic phase solubilities of uranium-organophosphorus complexes.

Comparative studies with nominal 1-Mev electron and Co^{60} gamma radiation showed appreciably lower values of G(acid) for 1 M DSBPP in Amsco 125-82 or Solvesso-100 than for 1 M TBP in Amsco (Table 16.1). The difference was largely eliminated when TBP was used in Solvesso diluent.

Table 16.1. Acids Produced in TBP and DSBPP Systems by Irradiation

Irradiated Material	Dose (whr/liter)	G (molecules/100 ev)		
		Mono Acid	Di Acid	Total Acid
Irradiation by 1-Mev Electrons				
1 M TBP–Amsco	~400*	0.87	0.11	
1 M DSBPP–Amsco	~400*	0.27		
1 M TBP–Solvesso-100	~400*	0.30	0.04	
1 M DSBPP–Solvesso-100	~400*	0.23		
	400	0.19		
	135	0.46		
	45	0.58		
Irradiation by Co^{60} Gamma				
1 M TBP–Amsco	259			0.72
	86			0.81
	29			0.76
	10			0.70
1 M TBP–Solvesso-100	237			0.33
	79			0.29
	26			0.30
	9			0.30
1 M DSBPP–Solvesso-100	205			0.24
	68			0.27
	23			0.29
	8			0.18

*The dose was 1.08×10^{22} ev/g, which corresponds to about 400 whr/liter.

The aromatic diluent acts as a protective agent for TBP during acid formation. The effect of total dose on acid formed in DSBPP–Solvesso-100 systems is in some doubt. With the nominal 1-Mev electron source used at Stanford Research Institute, the acid yield increased with decreasing dose. In the range ~8 to ~200 whr/liter (Co^{60} gamma) the yield of acid formation was found at ORNL to be approximately constant at 0.2 to 0.3 molecule/100 ev. The origin of these differences is not known at present, but the same effect of dose shown in Table 16.1 (irradiation by 1-Mev

electrons; see ref 7) was also observed with solutions of 1 M DSBPP in Solvesso-100 irradiated after contact with equal volumes of 0.3 or 1 M HNO_3.

16.2 SOLUBILITIES OF DI- AND MONOBUTYL PHOSPHATES IN PROCESS SOLUTIONS

Further information on these butyl phosphates is being obtained by measurement of their solubilities in various aqueous and TBP–Amsco 125-82 solutions. Several dibutyl or monobutyl phosphates were prepared as nearly pure compounds by reacting aqueous solutions of metal nitrates with aqueous solutions of the sodium salts of the acids and subsequently washing the precipitates. Compounds so prepared include a zirconium dibutyl phosphate,[8] uranyl dibutyl phosphate, uranyl monobutyl phosphate, iron(III) dibutyl phosphate, and iron(III) monobutyl phosphate. Solubilities are being determined separately in aqueous solutions of HNO_3 and $UO_2(NO_3)_2$ and the 1.13 M TBP solutions in Amsco 125-82 that are in equilibrium with the aqueous solutions.

Solubilities (Fig. 16.2) of the compounds studied to date varied from 4×10^{-6} M zirconium dibutyl phosphate[9] in water to about 0.7 M uranyl dibutyl phosphate in the 1.13 M TBP–Amsco solution in equilibrium with aqueous 3 M HNO_3. Uranyl dibutyl and monobutyl phosphates and zirconium dibutyl phosphate were all more soluble in the organic than in the aqueous phases. The first two will therefore affect the solvent extraction process by being difficult to strip back into an aqueous phase, while the zirconium compound will show undesirable extractability into the organic phase rather than reporting to the extraction-column raffinate.

Solubilities of the iron(III) dibutyl phosphate in the organic phases were below the limit of detection, 1×10^{-5} M, but ranged from $< 1 \times 10^{-5}$

---

[7] L. H. Towle and R. S. Farrand, "Radiation Stability of Organic Liquids," Stanford Research Institute Semiann. Rep. 7 on Subcontract 1081 (June 15, 1960).

[8] Work performed at Ga. Inst. of Tech. under subcontract; reported by F. Sicilio, T. H. Goodgame, and B. Wilkins, Jr., Distillational Purification of Irradiated Tributyl Phosphate in Kerosene-Type Diluent, final report on subcontract 1374 (Jan. 31, 1960).

[9] W. Davis, Jr., and H. H. Carmichael, Solubility of Zirconium Dibutyl Phosphate in Solvent Extraction Solutions, ORNL-2857 (Jan. 6, 1960).

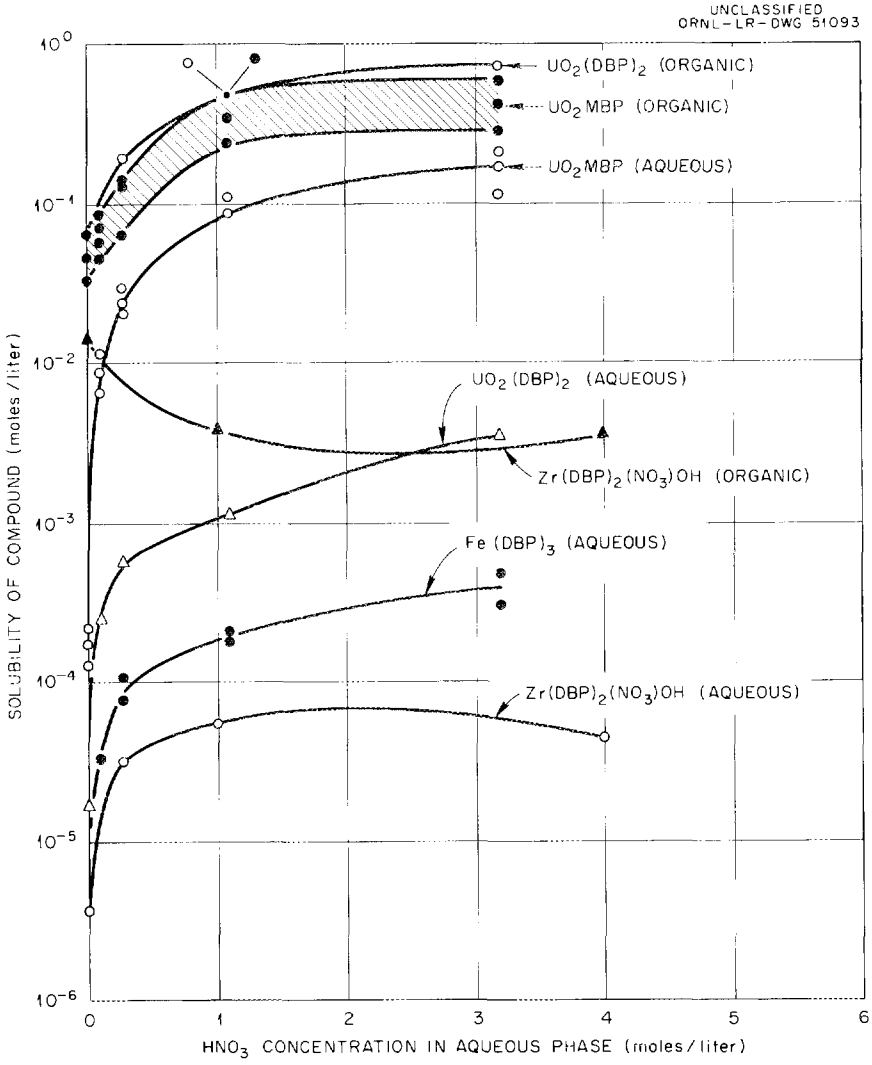

Fig. 16.2. Solubilities of Fission Product Complexes with TBP Degradation Products in Aqueous and Organic Phases. Basis: aqueous HNO_3 in equilibrium with 30% TBP in Amsco; phases studied separately.

M in water to ~4×10^{-4} M in 3.2 M HNO_3. These data suggest that the amount of dibutyl phosphoric acid produced by acid dealkylation of TBP in an extraction column will be sufficient to initiate precipitation of this iron compound if the iron concentration exceeds 50 to 100 ppm.

16.3 PURIFICATION OF DEGRADED SOLVENT BY DISTILLATION

In preliminary laboratory tests both low-pressure and molecular distillation appeared suitable for purifying solutions of TBP in Amsco 125-82 that had been degraded by radiation or by use in the Building 3019 (Purex)

pilot plant. The radiation degradation was produced by exposing 30% TBP in Amsco solution to Co^{60} gamma radiation to a level of ~120 whr/liter and simultaneously agitating it with an aqueous solution containing 1.3 M U(VI) and 1.84 M HNO_3, which represents a composite of feed and scrub streams of a Purex process described by Irish and Reas.[10] Uranium was stripped from the organic phase with 0.01 M HNO_3 and then either distilled or stripped further with aqueous sodium carbonate solution and then distilled. Distillate fractions were tested for the degree to which they extracted and could be stripped of ruthenium, uranium, or zirconium.

Low-Pressure Distillation of Irradiated 30% TBP in Amsco 125-82[8]

Nearly all of more than 50 fractions of Amsco and TBP taken during column distillation at 20 to 50 mm Hg of radiation-degraded solvent showed extraction, scrubbing, and stripping properties similar to those of similarly distilled as-received materials with respect to ruthenium and uranium tracers. However, in order to distill degraded solvent in a fractionating column it was first necessary to separate the solution into its two major components, Amsco and TBP, by a rapid volatilization process at ~0.5 mm Hg. Without this preliminary step most of the TBP and some of the diluent were converted to a black residue; with this step the TBP fraction started to decompose only after about 80% of it had been distilled. Considerably smaller losses would be expected in larger-scale operations.

After the degraded solution had been separated into its two major fractions, each was distilled at 20 to 50 mm Hg in a column of ~42 theoretical plates from which 7 to 24 fractions were withdrawn. Each fraction was used to make a solution of 30% TBP, by adding as-received TBP to fractions from the Amsco distillation or by adding as-received Amsco to TBP fractions. These solutions were used in either extraction-scrub or extraction-strip studies to determine how effectively extracted ruthenium or uranium could be removed by scrubbing, with 4 M HNO_3, or by stripping, with 0.01 M HNO_3. Aqueous solutions used in the extraction step contained tracer quantities of $Ru\text{-}Rh^{106}$ and U^{233}. The aqueous solutions used in

[10] E. R. Irish and W. H. Reas, "The Purex Process-A Solvent Extraction Method for Irradiated Uranium," Book 1, Session 1 in Symposium on the Reprocessing of Irradiated Fuels, Brussels, Belgium, May 20-25, 1957, TID-7534.

extraction-scrub studies also contained 4.86 M HNO_3, while those used in extraction-strip studies contained 4.47 M HNO_3.

Molecular Distillation

Molecular distillation of 30% TBP–Amsco solutions degraded by Co^{60} gamma radiation or by use in the Building 3019 pilot plant produced diluent and TBP fractions that were equal or superior to as-received materials with respect to extraction-stripping tests with zirconium tracer. In each case the diluent fraction was removed with a pot temperature $\leq$ 35°C, while TBP fractions were taken with the pot temperature $\leq$ 70°C, corresponding to a pressure of $\leq$ 0.2 mm Hg. From the radiation-degraded sample about 99% recovery of diluent and TBP as clear liquids was achieved; the residual 1%, of orange-red color, was found by infrared analysis to contain large quantities of nitro compounds. Tests with distillates from badly degraded pilot-plant solvent with respect to zirconium-niobium extraction and stripping may be summarized as follows: (1) the diluent was very similar to as-received Amsco 125-82; (2) 80% of the TBP was recovered as material that was equal or superior to as-received TBP.

17. RADIATION EFFECTS ON CATALYSTS

Work was initiated on a study of the effects of preirradiation and of incorporated radioisotopes on catalysts. Initial work was on $MgSO_4$-Na_2SO_4 and promoted Cr_2O_3-Al_2O_3 catalysts. A nearly twofold increase in the rate of dehydration of cyclohexanol to cyclohexene at 400°C in the presence of the $MgSO_4$-Na_2SO_4 catalyst was observed when 25.9 mc of S^{35} per gram was incorporated in the catalyst preparation. No increase in the rate of dehydration was observed when the catalyst was preirradiated in air with Co^{60} radiation at a dose rate of 5.9×10^8 ergs g^{-1} hr^{-1} to an integrated dose of 10^{11} ergs/g. The rate of dehydrogenation of methylcyclohexane to toluene at 460°C increased 30% when the promoted Cr_2O_3-Al_2O_3 catalyst was preirradiated in air at a rate of 5.5×10^8 ergs g^{-1} hr^{-1} to an integrated dose of 1.8×10^{11} ergs/g. Dehydrogenation experiments carried out with catalyst containing up to 168 mc of Pm^{147} per gram were inconclusive with regard to the effect of incorporated radioisotopes.

17.1. DEHYDRATION OF CYCLOHEXANOL ON $MgSO_4$-Na_2SO_4 CATALYSTS

The alcohol cyclohexanol may be dehydrated to cyclohexene at 300–425°C over an $MgSO_4$-Na_2SO_4 catalyst. It has been reported[1,2] that when small amounts of radioactive S^{35}, as $Na_2S^{35}O_4$, are incorporated into the catalyst, large changes in catalytic activity occur. For example, 9.2 mc/g increased the percentage conversion of the alcohol 90%, while the presence of 105.2 mc/g increased it 180%. Work was initiated to verify this extraordinary effect and to extend its investigation if verified.

The results of initial experiments indicate that on fresh catalyst surfaces there is no difference in the activity of the radioactive and nonradioactive catalysts, but that when aged by use at 400–410°C for 3–4 hr, the radioactive catalyst is more active by a factor of 2 at 390°C. Arrhenius plots made by treating the percentage conversion as a rate constant (this is justifiable since the conversions were all < 20%) showed

---

[1]A. A. Balandine et al., Doklady Nauk. SSSR 121, 495 (1958).

[2]A. A. Balandine et al., Paper No. 68, Second International Conference on Catalysis, Paris, July 1960.

apparent activation energies of -25.7 ± 1.5 and -32.8 ± 1.9 kcal/mole for the aged radioactive and aged nonradioactive catalysts, respectively.

Co^{60} irradiation of the nonradioactive catalyst at 5.9×10^8 ergs g^{-1} hr^{-1} to a total dose of 10^{11} ergs/g had no apparent effect on the conversion.

The $MgSO_4$-Na_2SO_4 catalysts were prepared by mixing solutions of the chemically pure salts, evaporating slowly to dryness, and heating the resulting cake overnight at 410°C. The cake was ground and sieved, and the 30–40 mesh fraction was used in most of the experiments. The radioactive catalyst was prepared similarly, but a small amount of $Na_2S^{35}O_4$ solution was added prior to the evaporation. Properties of the catalyst are given in Table 17.1.

Table 17.1. Properties of $MgSO_4$-Na_2SO_4 Catalysts

Catalyst	Specific Activity (mc/g)	Surface Area (m^2/g)	Amount (%)		
			Mg	Na	SO_4
Nonradioactive	0	3.1	18.64	1.55	76.9
Radioactive	25.9	3.3	18.48	1.51	75.7

The activity of the catalysts was determined in a flow reactor using 0.1500 g of catalyst and a cyclohexanol feed rate of 0.31 ml/min.

The reaction tube was mounted in an inclined furnace tube, with a heated section of glass beads serving as a vaporizer. The products were condensed and collected in a graduated receiver. The percentage conversion of the alcohol to cyclohexene was determined by refractive index measurements and by determination of the bromine number (ASTM method D1158-57T).

17.2 DEHYDROGENATION OF METHYLCYCLOHEXANE ON PROMOTED CHROMIA-ALUMINA CATALYSTS

Methylcyclohexane may be dehydrogenated to toluene (methylbenzene) at 340–550°C on a promoted Cr_2O_3-Al_2O_3 catalyst. Work has been reported on the effect on this and similar dehydrogenation reactions of catalyst

preparation and composition variations[3,4] and on the effect of promotors.[5] No work on the effect of irradiation of the catalyst has been reported. Investigation of the effect on this reaction of Co^{60} gamma irradiation of the catalyst was initiated. Preliminary investigation was made of the effect of adding Pm^{147} to the catalyst preparation.

Batches of catalyst were irradiated in air in a Co^{60} gamma-ray source at a dose rate of 5.5×10^8 ergs g^{-1} hr^{-1} to total doses of 1.25×10^{11} and 1.81×10^{11} ergs/g. At the lower dose, an Arrhenius plot of irradiated catalyst activity was not significantly different from that of the control over the temperature range 440–485°C. At the higher dose, catalytic activity enhancement amounted to 34% at 485°C. The apparent activation energy is -43.7 ± 8.7 kcal/mole for both irradiated catalyst and control, to within experimental accuracy.

The results of methylcyclohexane dehydrogenation experiments with catalyst containing up to 168 mc of Pm^{147} per gram were inconclusive. Further work along these lines is planned.

Catalysts containing 8–9% chromium and about 1% each of cerium and potassium promotors were prepared by impregnating washed and ignited Al_2O_3 successively with aqueous solutions containing CrO_3 and $Ce(NO_3)_3$ plus KNO_3. The impregnated alumina was air-dried after both impregnations. Heating the air-dried catalyst in air at 500°C for 4.5 hr denitrated and dried it to about a 13% weight loss, measured after air equilibration. Reduction in hydrogen at 500°C for 4 hr resulted in another about 1% weight loss, measured as before. Typical catalyst properties are:

Particle diameter	0.84–1.19 mm
Surface area	69 m^2/g
Chromium	8.77%
Cerium	0.98%
Potassium	1.09%

---

[3]R. C. Archibald and B. S. Greensfelder, Ind. and Eng. Chem. 37, 356 (1945).

[4]A. H. Rubinstein et al., Paper No. 100, Second International Conference on Catalysis, Paris, July 1960.

[5]B. S. Greensfelder, R. C. Archibald, and D. L. Fuller, Chem. Eng. Prog. 43, 561 (1947).

As with the $MgSO_4$-Na_2SO_4 catalyst, catalytic activity was determined in a flow reactor. Catalyst weights varied from 1.16 to 1.40 g. Bulk densities were about 0.89 g/cc. The feed rate was 1.55 mmoles/min. The reaction tube was a 1-cm-ID quartz tube mounted vertically in a tube furnace and filled with glass beads both before and after the catalyst bed. The extent of reaction was determined continuously by hydrogen-volume measurement, using a wet test meter. The nonvolatile reactant composition was followed by periodic sampling and gas chromatographic analysis. Decomposition of organic compounds and resultant catalyst caking and surface area diminution made it desirable to use initial reaction rates as a measure of catalyst activity, and to use a given catalyst sample only once.

18. ION EXCHANGE TECHNOLOGY

The Ion Exchange Technology Program has included work on properties of resins and kinetics of ion exchange reactions, and applications to specific problems, for example, waste disposal (Sec 6) and fission product recovery by both solid and liquid ion exchange processes (Sec 14).

18.1 RADIATION DAMAGE TO ION EXCHANGE RESIN

For irradiated Dowex 50 resin, both Higgins and Wedemeyer[1] have reported a 10–20% capacity loss per whr of energy absorbed per dry gram of resin. However, resin which had been exposed to a calculated dose of 12.5 whr per dry gram was found to have retained most of its salt-splitting capacity. This is significant in that the published data would have predicted a complete loss in resin capacity. The irradiated Dowex 50W X-12 (100–200 mesh) resin was analyzed for moisture, capacity, and sulfur content, and the results compared with results of similar analyses obtained for unirradiated resin. Moisture content values, as determined by conventional oven-drying, were not closely reproducible; however, the increase noted in the irradiated resin from about 40 to about 70% moisture corresponds roughly to a decrease in crosslinking from 12 to about 4%.

Capacity determinations, made by adding excess NaCl and titrating with 1 M NaOH to pH 7, indicated that the resin had, in addition to retaining its salt-splitting capacity, acquired some weak acid capacity. Typical of preliminary results obtained were 4.84 meq per gram of dry resin total capacity for the new resin and 4.68 meq per gram of salt-splitting capacity and 5.02 meq per gram of total capacity for the irradiated resin. New resin samples could be titrated to very sharp end points, but a steady-state end point was difficult to reach with irradiated resin.

The irradiated resin analyzed had been used by the Isotopes Division for obtaining pure Pm^{147}. The dose of ~ 12.5 whr per gram of dry resin was calculated on the basis of a total energy dose of 2780 whr to a resin

[1] G. W. Parker, I. R. Higgins, and J. T. Roberts, in Ion Exchange Technology (ed. by F. C. Nachod and J. Schubert), p 144, Academic Press, New York, 1956.

bed volume of 500 ml. Because of a limited knowledge of the previous history of the resin, the resin bed volume and the corresponding radiation dosage figures should be considered estimates only.

Determination of sulfur in resin samples by the Paar method was to be used as a check on the salt-splitting capacity as determined by titration, that is, the concentration of active sulfonic acid groups on the resin. Results have not been reproducible due to incomplete combustion of the resin samples.

18.2 KINETICS OF URANYL SULFATE ANION EXCHANGE

In an effort to obtain a better understanding of ion exchange process and column behavior, uranyl sulfate anion exchange with Dowex 21K, a strong base resin, is being studied in detail. Rate studies made by a single-bead technique have shown the rates of exchange can be described reasonably well by apparent uranium diffusion coefficients measured for the particular ion exchange step studied (Figs. 18.1 and 18.2). The studies were made with a single-bead technique which involved contacting individual beads with a rapidly stirred bath of electrolyte solution and determining the uranium gained or lost by counting the beads in a gamma spectrometer for the 0.2-Mev gamma emission from U^{235}. The results are described reasonably well by the curves predicted by Fick diffusion into a sphere; however, the diffusion coefficient observed is determined by all the ions involved in the process, not just a uranium ion. The poorest fit of the data occurred with samples having a short contact time with the solution. Although counter-diffusion of two or more ions should not be expected to follow exactly the curves predicted by a constant apparent-diffusion coefficient, the deviation at low loadings is believed to arise largely because of changes in the resin diameter with loading and the fact that the fraction of equilibrium loading is based on diameters measured at various loadings. Attempts are being made to determine the variation of resin diameter with uranium loading and confirm if this effect will adequately predict the deviations in the loading curve.

For the same resin size, the apparent uranium diffusion coefficient for uranyl ion loading on nitrate-equilibrated Dowex 21K was greater than

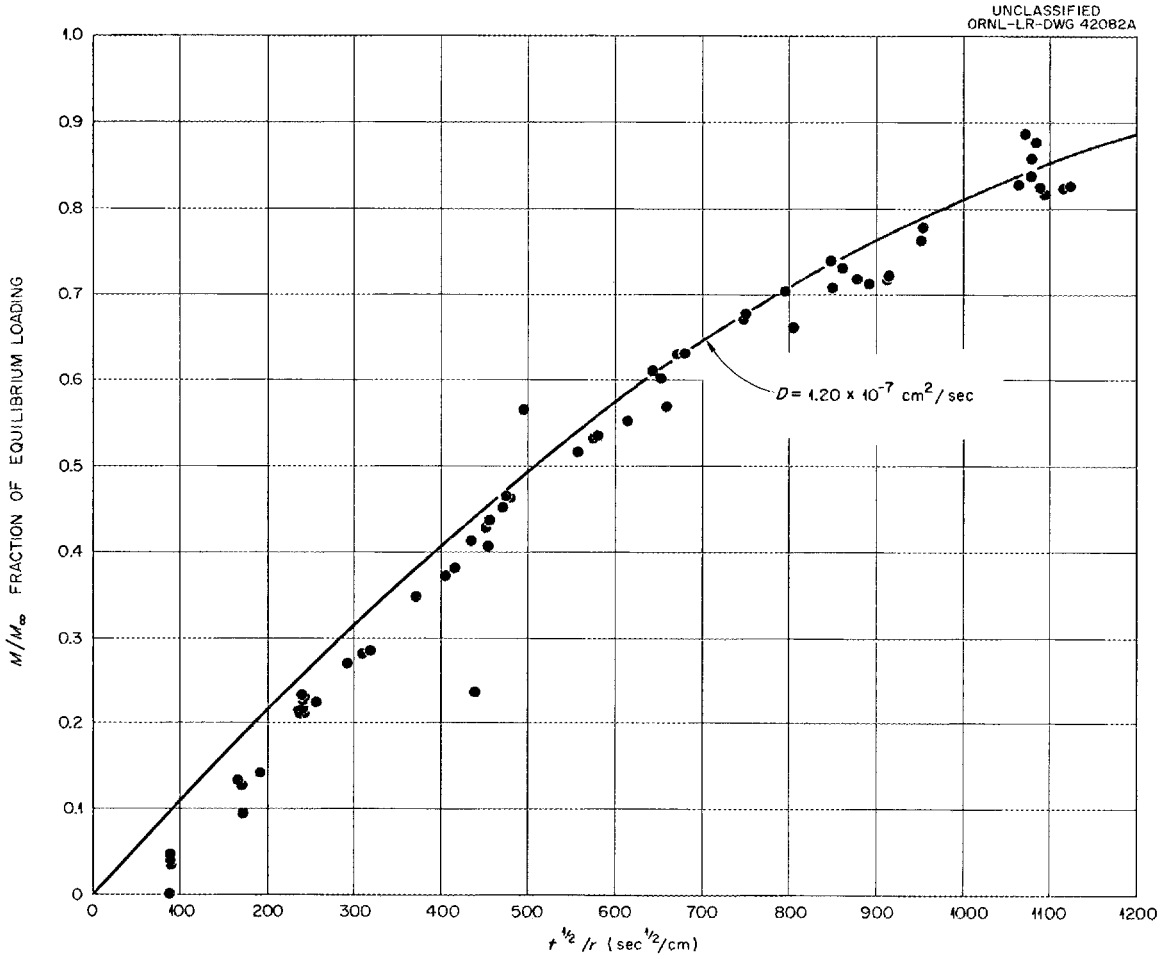

Fig. 18.1. The Rate of Uranium Sorption on Sulfate-Equilibrated 1200-μ Dowex 21K from a 0.004 *M* Uranyl Sulfate Solution 0.024 *M* in Total Sulfate.

for sulfate-equilibrated (Table 18.1). The table shows the effects of counter-diffusion of different ions. These values were relatively independent of the loading solutions concentration, but greatly dependent on resin size. The sulfate self-diffusion coefficient varied similarly with resin size, indicating that the diffusive properties of the resin vary with the particle size. The single-bead technique was used in this study, with S^{35} as the tracer and counted with either a liquid scintillant or a thin-walled G-M counter. Beads were equilibrated with a "spiked" 1 M Na_2SO_4 solution, and the rate of elution of activity from the resin by an identical "cold" solution was determined.

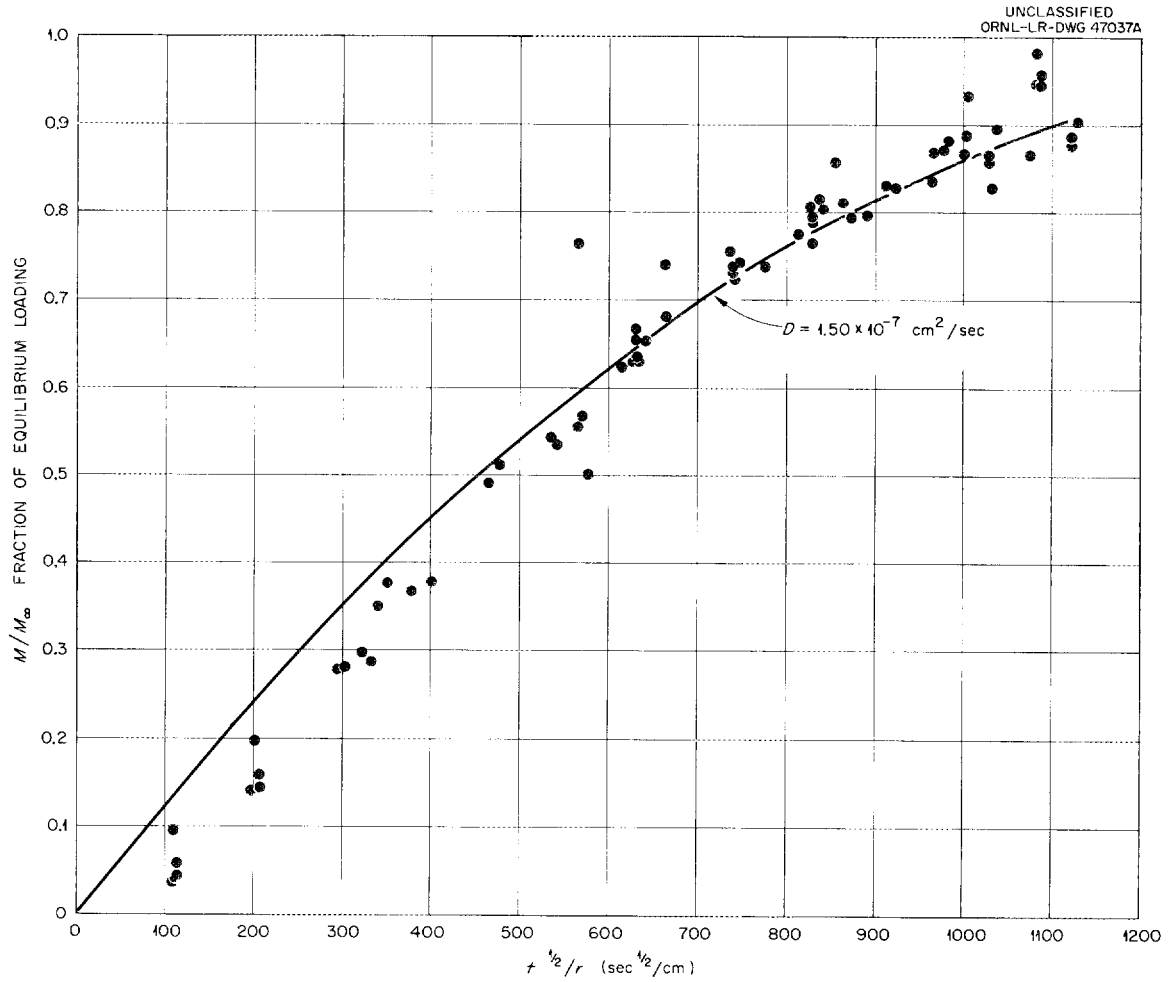

Fig. 18.2. The Rate of Uranium Sorption on Nitrate-Equilibrated 1200-μ Dowex 21K from a 0.005 *M* Uranyl Sulfate Solution 0.025 *M* in Total Sulfate.

Table 18.1. Comparison of Diffusion Coefficients

Resin Size, μ	Diffusion Coefficient (cm^2/sec)		
	Apparent Diffusion		Sulfate Self-Diffusion
	On Sulfate-Equilibrated Resin	On Nitrate-Equilibrated Resin	
1200	1.3×10^{-7}	1.5×10^{-7}	$(1.27 \pm 0.25) \times 10^{-6}$
960	0.76×10^{-7}	0.9×10^{-7}	$(0.60 \pm 0.18) \times 10^{-6}$
820	0.49×10^{-7}	0.9×10^{-7}	$(0.75 \pm 0.17) \times 10^{-6}$

The single-bead technique could not be used to study uranyl sulfate self-diffusion or elution by nitrate and chloride solutions because variations in the capacity of the individual beads caused considerable uncertainties in the results. To overcome these difficulties, a resin-solution contactor was designed to contact a resin sample of several beads (Fig. 18.3). This device is essentially a submerged centrifugal pump with a rapidly removable resin holder located at the pump outlet. The solution flow

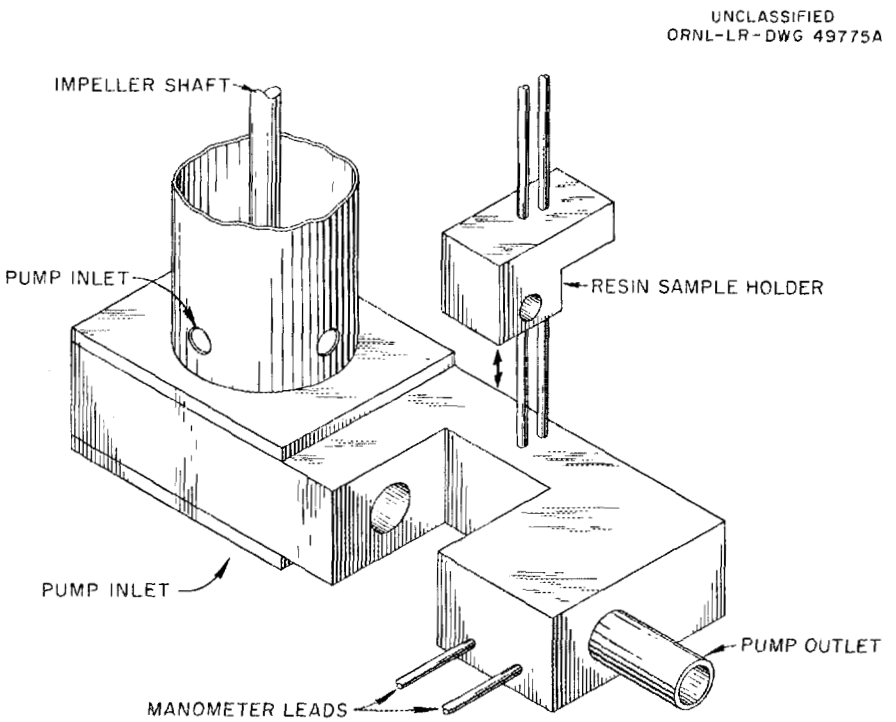

Fig. 18.3. Submerged Pump Contactor.

rate past the resin sample is measured by an orifice just downstream from the samples. The use of this device to measure uranyl sulfate elution and self-diffusion rates has given considerable improvement in the data scatter (Figs. 18.4 and 18.5). The uranyl sulfate self-diffusion coefficient is approximately 4.42×10^{-8} cm^2/sec at all solution flow rates greater than 11 cm/sec, indicating that under those conditions film resistance is negligible. The apparent uranium diffusion coefficients observed during nitrate and chloride elution from 1200-μ Dowex 21K are 1.8×10^{-7} and 2.38×10^{-7} cm^2/sec, respectively.

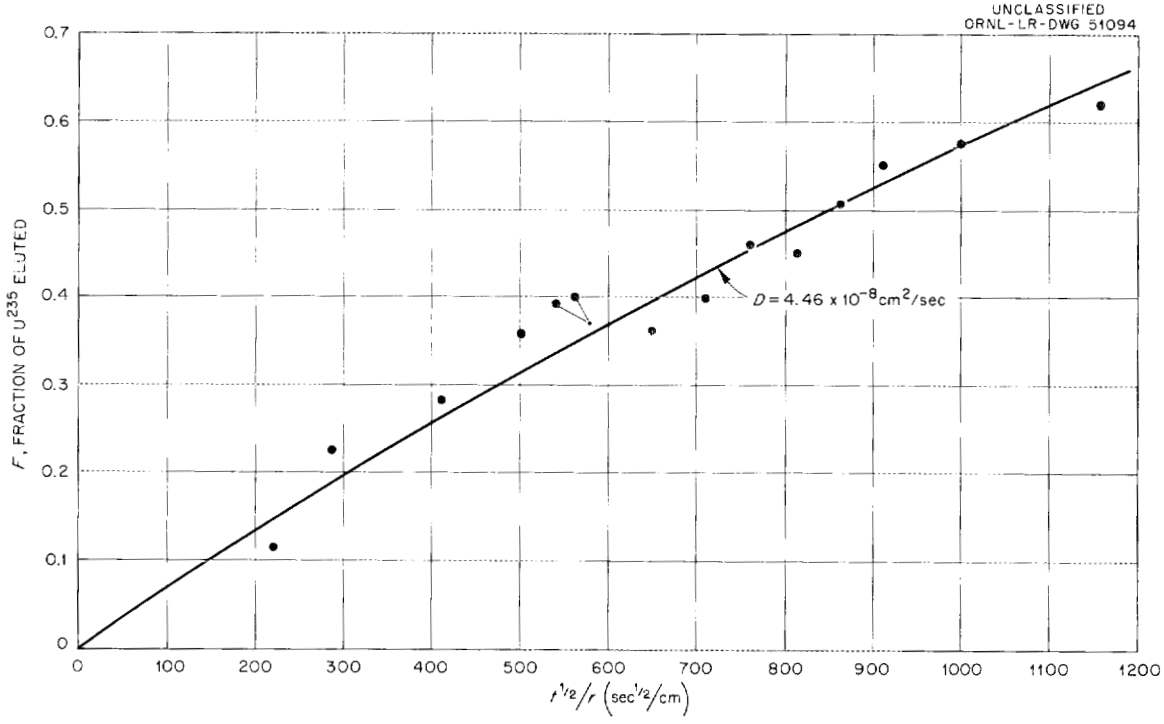

Fig. 18.4. Uranium Self-Diffusion from 1200-μ Dowex 21K with a Solution Flow Rate of 16.6 cm/sec.

From these rate data, attempts are being made to get a more complete understanding of the uranyl sulfate anion exchange processes. A machine code has been written and is being "debugged" which will attempt to predict the observed apparent uranium diffusion coefficients from self-diffusion measurements.

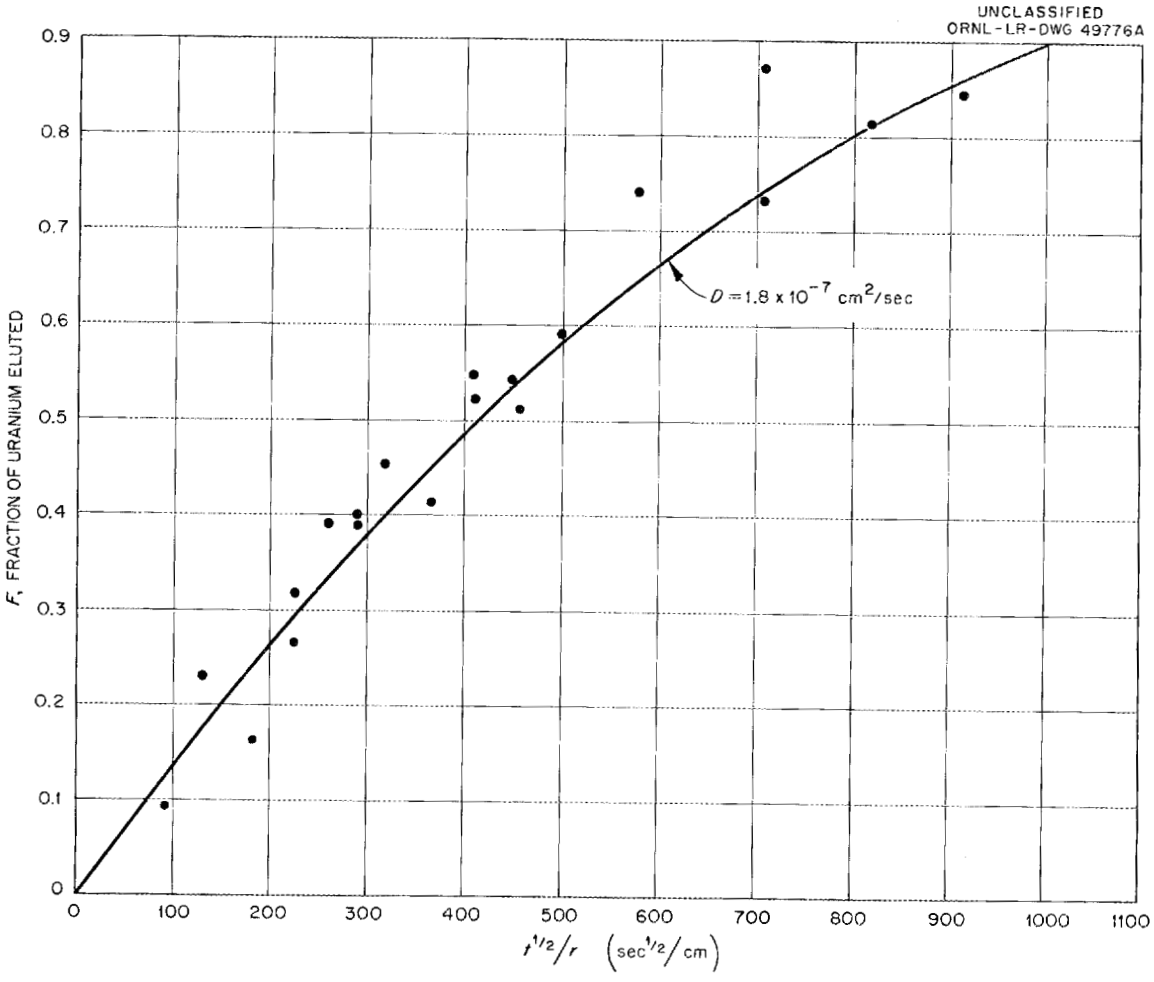

Fig. 18.5. The Rate of Uranyl Sulfate Elution from 1200-μ Dowex 21K with a 1 *M* $NaNO_3$ Solution Flowing at 25 cm/sec.

19. CHEMICAL ENGINEERING RESEARCH

Chemical engineering research has been concerned primarily with a solvent extraction contactor made up of hydroclones stacked each above the other, which has a high efficiency and low organic holdup per stage and thus decreased radiation damage to solvent in liquid-liquid extractions; the characteristics of a resonant steam pulser, which could be used to pulse an extraction column; and the mechanism of transfer of uranyl ion across a water-TBP interface in liquid-liquid extraction.

19.1 STACKED-HYDROCLONE CONTACTOR

A five-stage 3/4-in.-dia stacked-hydroclone contactor (Fig. 19.1) with the kerosene (Supersol or Amsco)–0.08 M HNO_3 benzoic acid system showed countercurrent capacities for both phases of 1.0–2.2 liters/min. Solvent retention time per mechanical stage was 2.5–10 sec with Supersol and 5–10 sec with Amsco, over the region of normal operation. Comparable times in a pulsed column contactor, for example, are 30–60 sec. Stage efficiencies with Supersol were 20–75; incomplete data with Amsco showed comparable efficiencies over a range of aqueous to organic flow rates from 0.23 to 4.75. Mechanically and hydraulically the stacked clones are capable of operation with flow ratios (A/O) as high as 300.

In this contactor the stage recycle pumps handle mostly aqueous and cause a forced vortex in the associated stage (Fig. 19.2). The light phase concentrates in a central dispersed core. The stage recycle flow, of itself, produces no interstage flow. The countercurrent interstage flow, which represents throughput, is driven by the induced underflow effect; that is, there is a relative low-pressure area, which induces solvent in the center, and a relative high-pressure area, which expels aqueous at the wall of the underflow port.

When no provision was made at the bottom outlet of the apparatus for coalescence (a simple pipe connection approximately equal to the hydroclone underflow diameter was used) the Amsco system showed 0–2% entrainment of solvent with the aqueous phase, depending on the flow rates; the Supersol system showed negligible entrainment over the region studied. However,

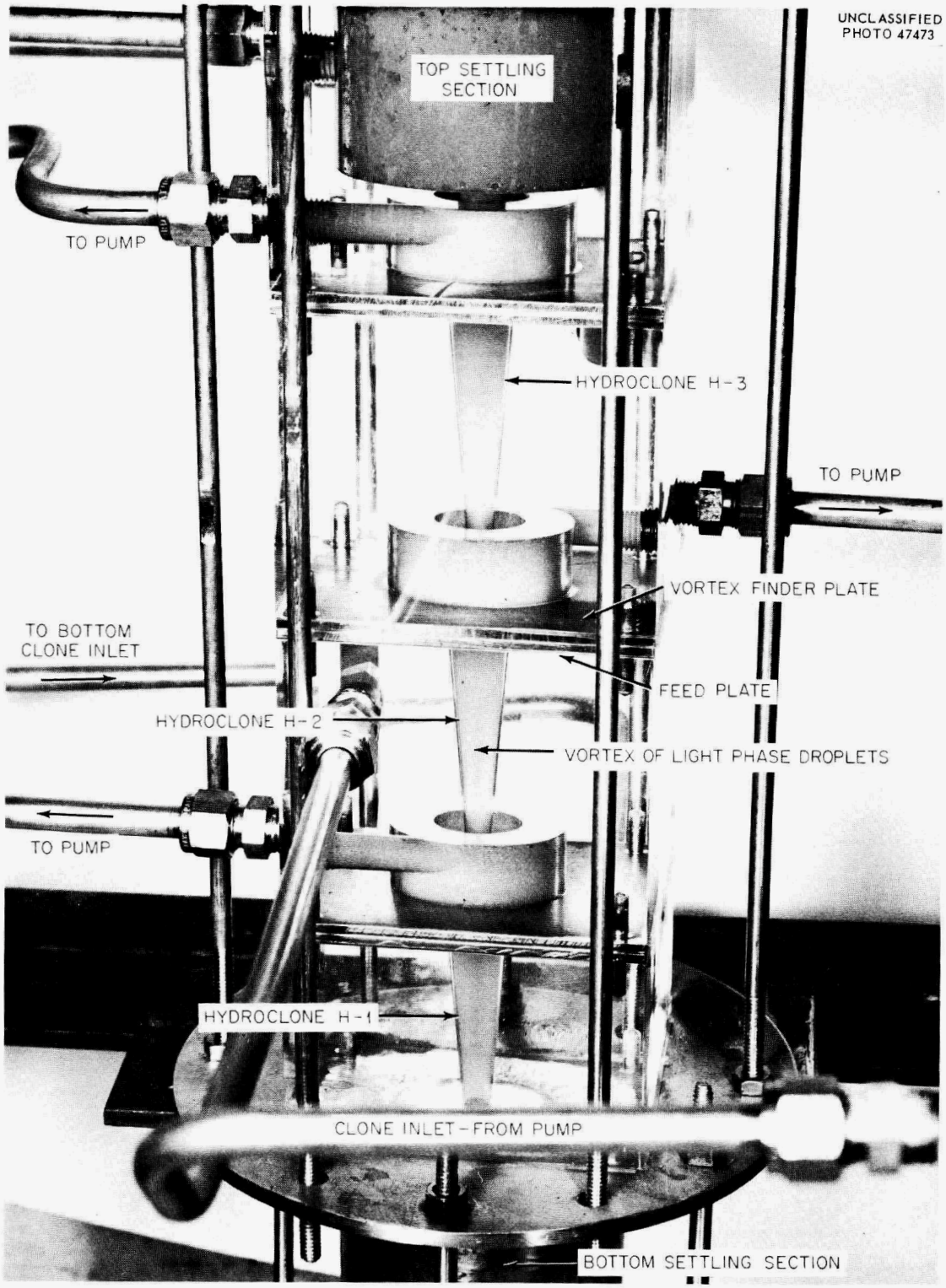

Fig. 19.1. High-Speed Contactor Column.

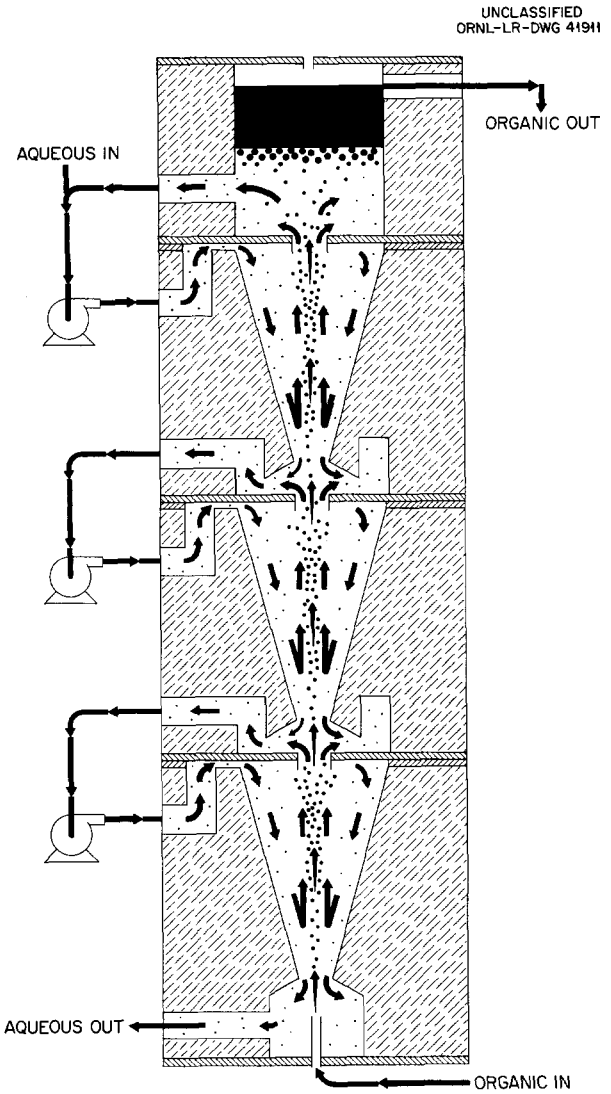

Fig. 19.2. Flow Diagram of Three-Stage High-Speed Contactor.

the provision of one clone polishing stage below the organic feed point decreased Amsco entrainment by an order of magnitude. With four polishing stages below the organic feed point, entrainment was negligible over the operable range of the device.

19.2 IMPEDANCE MATCHING OF A PISTON PULSER TO A PULSED COLUMN BY A RESONANT TRANSFER LINE AND AIR CAVITY

A study of the characteristics of the transfer line and vapor cavity of the resonant steam pulser was made with a piston pump to provide a pulse of known wave form. Unexpected advantages in pulse volume and pressure

smoothing accrue when the transfer line and air cavity are tuned and used as an impedance matching network to couple a low-resistance high-volume load (column) to a high-pressure low-volume driver (pump). The practical significance of the tuned network for a mechanical pulser is that the size of the pulser required would be decreased about 30% and diaphragm life should be extended by the cushioning effect of the air cavity. Plots of the ratio of pulse volume to piston displacement vs pulse frequency show 30 to 70% enhancement of pulse volume and a decrease in resonant frequency with increased air volume (capacitance) for a hydraulic resistance typical of a sieve plate cartridge. At low resistance a subharmonic mode of oscillation exists where the pulser makes two strokes for each pulse in the column.

The mathematical description of the system was approximated by writing the differential equations for the system and rounding off fractional powers of fluid velocity. This system of equations when solved with an analog computer predicted the enhanced pulse volume and the subharmonic mode that were observed experimentally.

19.3 TRANSFER OF URANYL ION ACROSS A WATER-TBP INTERFACE

The steady-state transfer of uranyl nitrate across a quiescent interface between water and tri-n-butyl phosphate in kerosene was studied in an attempt to elucidate the mechanism of transfer in solvent extraction operations. It was concluded that uranium transfer is controlled by the physical processes of eddy and molecular diffusion. Deviation from equilibrium values of the concentrations at the interface was smaller than the sensitivity of the experiment. This means that the equivalent resistance of the interface is less than that of 20 μ of organic solvent, the estimated limit of detectability. Assuming a molecular diffusivity of 10^{-6} cm^2 sec^{-1}, the heterogeneous rate constant is greater than 5×10^{-4} cm sec^{-1}. If we assume that the reaction occurs within 50 A of the interface, the homogeneous rate constant is greater than 1000 sec^{-1}; that is, the reaction would have a half time much less than 1 msec.

The experiment was repeated with a surface active agent (10 ppm of Tide) in the solutions. No increase in interfacial resistance to mass

transfer was observed. This supports the observation of other experimenters that the reduction in mass transfer to falling drops when a surface active agent is added is due to change in the hydrodynamic properties of the system rather than to formation of an impermeable membrane at the interface. The effect of a surface active agent may be to reduce the interface turbulence caused by concentration and temperature gradients along the interface itself; it is known that surface active agents increase the two-dimensional viscosity of the interface, thus powerfully hindering the beneficial distortions of the interphase boundary.

The steady-state profile and consequent molecular flux were established in a 2-mm square cross section vertical column of liquid contained in a specially designed cell. The bottom of the column was maintained at saturation by the presence of a slowly dissolving crystal of uranyl nitrate. The aqueous-organic interface was about halfway up the 12-mm-long column, in a plane normal to the column. The organic phase was a 30% solution of TBP in Amsco. The uranyl concentration at the top was maintained at essentially zero by pumping fresh organic across the top of the column. Photographic photometry of concentration profiles in both phases permitted point analyses up to within 100 μ of the interface. Extrapolation of the steady-state profile to the interface showed the two phases to have the same concentration ratio as that obtained by batch equilibration.

19.4 THERMAL DIFFUSION

Thermal diffusion of electrolytes is being studied to advance the basic understanding of this relatively new chemical engineering unit operation.[1] An improved cell for measuring Soret coefficients with an accuracy of 1% was constructed. The Soret coefficients of $CuSO_4$ and $CoSO_4$ were determined in the improved cell and related to temperature by the following empirical dimensional equations:

$$\sigma_{CoSO_4} = 4.00 \times 10^{-3} + 0.116 \times 10^{-3}\ t \quad ,$$

$$\sigma_{CuSO_4} = 2.00 \times 10^{-3} + 0.110 \times 10^{-3}\ t \quad ,$$

[1]By University of Tennessee, under subcontract.

where σ is the Soret coefficient, in reciprocal degrees centigrade, and t is temperature in degrees centigrade. The Soret coefficient relates the concentration gradient of the ionic species to the temperature gradient.

The horizontal membrane thermal diffusion column described in ORNL-2788 was run at finite reflux ratios in preliminary experiments with the following results:

Cold Side Flow Rate (ml/hr)	Reflux Ratio	HTU, $CuSO_4$ (ft)	HTU, $CoSO_4$ (ft)	Separation Factor Cu/Co
2.1	2.0	0.67	0.77	1.05
3.1	8.6	1.16	1.37	1.05

Studies of Soret coefficients and column HTU's are being extended to the UO_2-SO_4-H_2O system and to the Zr-HF system.

19.5 TRANSIENT RESPONSE OF THE CELL VENTILATION SYSTEM IN BUILDING 3019 TO IMPULSE AND RAMP PRESSURE PERTURBATIONS

As an adjunct to the redesign of the ventilating systems of several cells and buildings in which experimentation and processing of radioactive materials are carried out by the Chemical Technology Division, the transient behavior of the newly designed ventilating systems (Fig. 19.3) is being analyzed. Specifically of interest is the length of time during which a building or cell would remain at a pressure above atmospheric after an impulse pressure increase, as might be caused by an explosion, and after a ramp pressure increase, as might be caused by the breakage of a gas cylinder.

Of the seven cells in the building, two are used for the Volatility Process Pilot Plant and five for the Power Reactor Fuel Processing Pilot Plant. The pressure perturbations were assumed to occur in one of the PRFP cells. The flow from the Volatility Process cells 1A and 2, the pipe tunnel, and one PRFP cell, which was assumed to have its top removed at the time of the incident, can be handled in the calculations as a single stream because each of these streams is within 0.1 to 0.2 in. H_2O of atmospheric pressure and enters the off-gas header through a single orifice

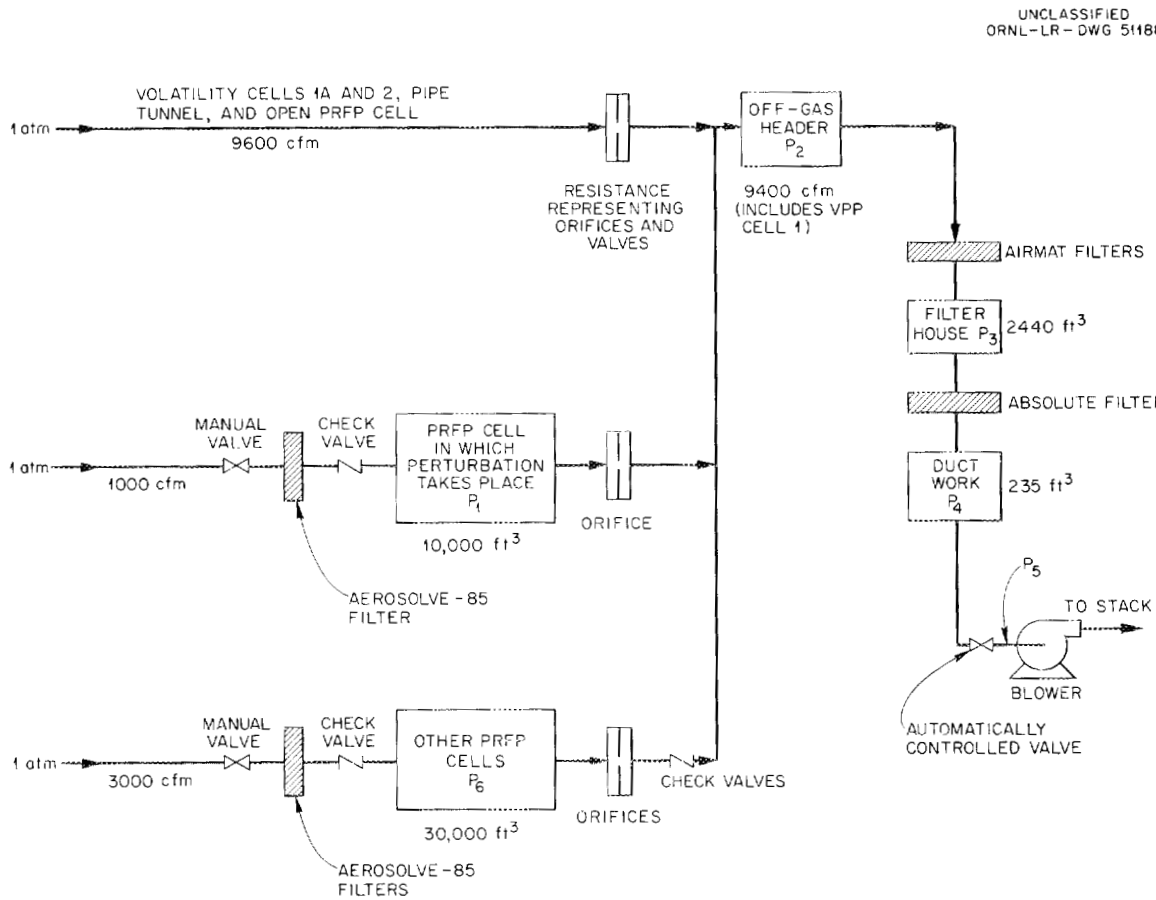

Fig. 19.3. Schematic of Cell Ventilation System in Building 3019.

or manual valve. Similarly, the PRFP cells, which were assumed to be operating normally, were treated as a single unit since they have an identical set of resistances and capacitances in parallel. The resistances of the Aerosolve-85 filters in the inlet lines to the cells were negligible compared to the resistances of the manual valves.

Equating accumulation rate to the difference of input and output rate for each capacitance gave the following set of simultaneous equations:

$$\frac{dP_1}{dt} = 0.545\sqrt{-P_1} - 2.52\sqrt{P_1 - P_2} \quad , \tag{1}$$

$$\frac{dP_6}{dt} = 0.545\sqrt{-P_6} - 2.52\sqrt{P_6 - P_2} \quad , \tag{2}$$

$$\frac{dP_2}{dt} = 5.57\sqrt{-P_2} + 2.67\sqrt{P_1} - P_2 + 8.02\sqrt{P_6} - P_2 - 3.25(P_2 - P_3) \quad , \tag{3}$$

$$\frac{dP_3}{dt} = 125(P_2 - P_3) - 49.4(P_3 - P_4) \quad , \tag{4}$$

$$\frac{dP_4}{dt} = 511(P_3 - P_4) - 106.7\sqrt{P_4 - P_5} \quad , \tag{5}$$

$$\sqrt{P_4} - P_5 = 11.8 - 2.05\sqrt{-P_5} \quad . \tag{6}$$

The more important assumptions were: (1) no pressure drop in the duct work (justified by pressure drop calculations), (2) no capacitance effect associated with P_5 due to the small volume of about 20 ft^3, and (3) no change in the resistance of the automatic control valve located at the blower inlet. The third assumption was necessary because the control valve had not been designed; however, it appears to have been a good assumption in the light of the results of the calculations, showing that the perturbations had negligible effect on the portion of the system from the off-gas header to the stack.

Since the set of simultaneous equations included several nonlinear differential equations, solutions were obtained on an analog computer, using the circuit diagram in Fig. 19.4. Switch F-1 was used to determine the effect of the check valve in the inlet to the cell in which the perturbations took place. Switch F-2 and potentiometer 19 were used to introduce the ramp perturbations. The automatic switching circuit at the bottom of the diagram was used to simulate the check valve between P_6 and the off-gas header.

For an impulse rise to 8.5 in. H_2O above atmospheric pressure, 1.3 sec would be required for the cell to return to atmospheric pressure, assuming that the check valve in the inlet line did not seat, and 1.5 sec if the check valve did seat (Table 19.1). Corresponding times for an impulse rise to 4.25 in. H_2O were 0.9 and 1.0 sec. A constant input (ramp perturbation) of 3 in. of H_2O per sec increased the steady-state cell pressure from the design value of −1.5 in. H_2O to atmospheric pressure. Ramp inputs of 7 and 10 in. of H_2O per sec raised the cell pressure to 4.0 in. H_2O in 3.8 and 1.6 sec, respectively.

The recovery of this system from the perturbations studied appears to be reasonably rapid.

UNCLASSIFIED
ORNL-LR-DWG 51189

POT. NO.	SETTING
1	0.1000
2	0.1570
3	0.1000
5	0.0160
6	0.0842
7	VARIABLE
9	0.3160
10	0.0795
11	0.1000
12	0.0176
14	0.1000
15	0.1000
16	0.3250
17	0.0545
18	0.1250
19	VARIABLE
20	0.0187
21	0.5110
22	0.4940
24	0.0262
26	0.1180
27	0.1000
32	0.6700
34	0.0150
36	0.0172
37	0.1000
39	0.1067
40	0.0030
52	0.0252
53	0.3160

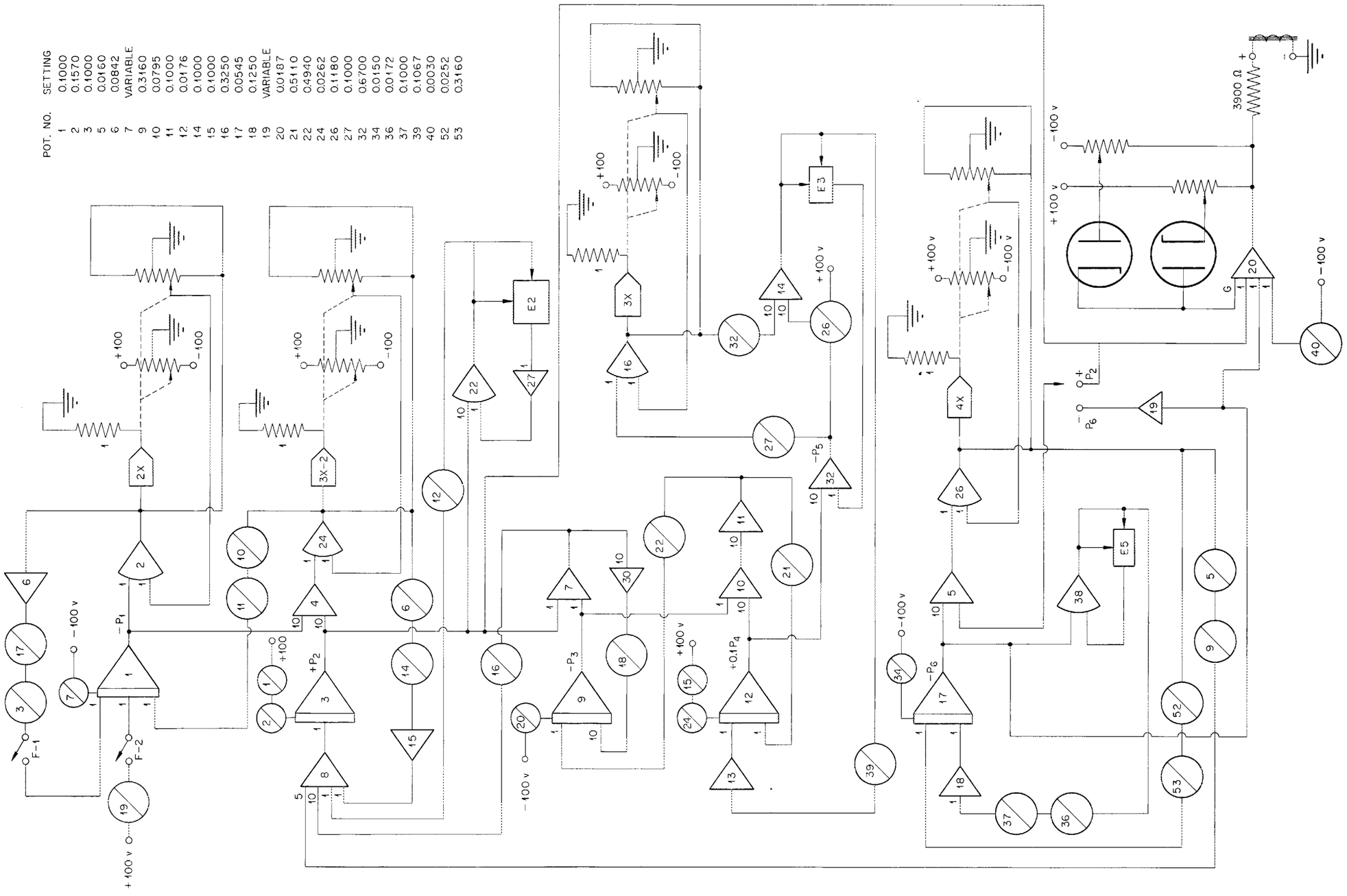

Fig. 19.4. Analog Computer Circuit for Building 3019 Cell Ventilation Problem.

Table 19.1. Time Cell Is Above Atmospheric Pressure Following Various Pressure Perturbations

Nature of Perturbation	Length of Time Cell Pressure Above Atmospheric (sec)	Comments
Impulse rise to +8.5 in. H_2O	1.3	Inlet to cell open
Impulse rise to +8.5 in. H_2O	1.5	Inlet to cell closed
Impulse rise to +4.25 in. H_2O	0.9	Inlet open
Impulse rise to +4.25 in. H_2O	1.0	Inlet closed
Ramp input of 10 in. H_2O per sec for 3.8 sec	4.9	Maximum pressure +8.0 in. H_2O; inlet open
Ramp input of 10 in. H_2O per sec for 2.2 sec	3.1	Maximum pressure +6.0 in. H_2O; inlet open
Ramp input of 10 in. H_2O per sec for 1.1 sec	1.6	Maximum pressure +4.0 in. H_2O; inlet open
Ramp input of 7 in. H_2O per sec for 3.4 sec	3.8	Maximum pressure +4.0 in. H_2O; inlet open
Ramp input of 7 in. H_2O per sec for 2.3 sec	2.7	Maximum pressure +3.0 in. H_2O; inlet open
Ramp input of 7 in. H_2O per sec for 1.0 sec	1.1	Maximum pressure +2.0 in. H_2O; inlet open

19.6 INSTRUMENTATION

A sensitive method for continuous gas density measurement using absorption of Tc^{97} monoenergetic beta rays was devised. The method is based on the highly sensitive response of Tc^{97} beta-ray absorption to absorber thickness in a range of practical utility. The range of highest sensitivity as well as near-linear absorption as a function of absorber thickness is from about 5 to less than 0.5 mg/cm^2. Obvious possible applications are to process control where a variable mixture of two gases of different molecular weights at known temperature and pressure is to be monitored, and to gas temperature measurement of gases of known pressure and composition.

20. CHEMICAL APPLICATIONS OF NUCLEAR EXPLOSIONS

The purpose of this program is to study the chemical reactions of isotopes produced by nuclear explosions. Only completely contained nuclear explosions are considered for this purpose, where air contamination is eliminated and the hazard of ground water contamination is minimum.[1,2] The type of containment medium will govern the dispersal and chemical states of the isotopes produced. Rock salt is generally considered the best medium in which to produce isotopes and power. The principal impurities in rock salt are sulfates which exist as anhydrite ($CaSO_4$) and polyhalite ($K_2SO_4 \cdot MgSO_4 \cdot 2CaSO_4 \cdot 2H_2O$).

The chemical reactions of hydrogen under the conditions expected from nuclear explosions were studied. Hydrogen was chosen since it is a convenient reference point for oxidation-reduction reactions, and its isotopic exchange is easy to measure. These studies included the exchange reaction of tritium from tritiated water to molecular hydrogen in the presence of $CaSO_4$, the reactions of hydrogen with $CaSO_4$ and $MgSO_4$, and evaluation of the exploding-wire technique as a method for studying reactions at the temperature of nuclear explosions.

20.1 HYDROGEN ISOTOPIC EXCHANGE

Studies of the isotopic exchange of tritium between tritiated water (as steam) and molecular hydrogen passing over calcium sulfate showed 0.19, 5.4, and 8.5% exchange at temperatures of 380, 600, and 700°C, respectively, after 40 min. The flow rates of H_2 and H_2O were 9×10^{-3} and 4.5×10^{-4} mole/min. The quantity of $CaSO_4$ was 2.8 g and the specific activity of the tritiated water was 2.74 mc/mole.

20.2 REDUCTION OF $CaSO_4$ AND $MgSO_4$ BY H_2

Calcium sulfate is reduced to CaS by hydrogen. The reduction proceeded readily in the 800–900°C range. At 800°C, the reduction rate was

---

[1] G. W. Johnson and C. E. Violet, Phenomenology of Contained Nuclear Explosions, UCRL-5124 Rev. I (December 1958).

[2] G. H. Higgins, Evaluation of the Ground Water Contamination Hazard from Underground Nuclear Explosions, UCRL-5538 (Apr. 8, 1959).

0.6 g of $CaSO_4$ per liter of H_2 per hr. The rate decreased by a factor of 1.2 to 1.7 when $CaSO_4$ was dissolved in molten NaCl. Magnesium sulfate was reduced to MgO rather than MgS. The reduction proceeded readily above 700°C, at a rate of 1.1 g of $CaSO_4$ per liter of H_2 per hr. The gaseous reduction products were H_2O, H_2S, and S. The solid reduction products of both reactions were determined by direct weight loss, x-ray diffraction analyses, and chemical analyses.

A study of the rate of reduction of $CaSO_4$ under flow conditions using a recording thermogravimetric balance indicated that the reaction was controlled by bed diffusion. Under static conditions, the reduction rate is apparently independent of hydrogen pressure in the 200–600 mm range.

20.3 WIRE EXPLOSIONS

Uranium wire explosions by condenser discharge were investigated as a means for simulating nuclear explosions contained in rock salt. After explosion of the wire, microscopic examination of the salt showed melting on the edges of only a few salt crystals, although temperatures produced by the wire were $>10^4$°K.

Temperatures were estimated from the available energy of the condenser bank and the maximum size of the fireball. Calculations of the average temperature of the exploding wire from the available energy of the condenser discharge, mass of uranium wire, and appropriate heat capacity data gave 5×10^4°K, assuming no ionization of uranium and uniform dissipation of energy in the wire. The rate of fireball growth was also used to calculate the temperature. The estimated average radius of the fireball was 5 cm at 1 μsec. If complete ionization of the uranium is assumed, the calculated temperature was 1.1×10^4°K. Since some ionization undoubtedly occurred, the true temperature must have been between these values and it is reasonable to assume a fireball temperature of $1–5 \times 10^4$°K.

The physical damage to compacted salt from exploding wires within the salt depended on the strength and rigidity of the material used to encase the salt. The salt specimens used were solid cylinders (1-in. dia and 1.5-in. length), 85% of theoretical density. Intimate contact between

the wire and salt interface was obtained by pressing the salt into cylinders around the wire at 10,000 to 12,000 psi. Explosions were conducted with salt cylinders having no encasement and with cylinders encased in Lucite and in stainless steel. The greatest damage and radial distribution of the wire were with no encasement, and the least damage was with encasement in stainless steel. Unencased samples were completely shattered at 20 cal/cm length of wire and Lucite-encased samples at 40 cal/cm. Stainless-steel-encased samples were not completely shattered at the maximum energy tested (80 cal/cm), and the radial distribution of the exploded wire was independent of explosion energy above 30 cal/cm. Microscopic examination showed a very small amount of melted salt. No chemical effects could be studied since all the energy for raising the temperature went into the wire and very little into the salt.

Measurement of the sound intensity from exploding wires in air gave shock energy values which varied by a factor of 3. In three duplicate experiments the measured sound intensities were 129, 130, and 134 db at an explosion energy of 22 cal/cm length of wire. An intensity of 130 db corresponds to an energy of 10^3 $\mu w/cm^2$.

20.4 PLASMA-JET CHEMISTRY

The degree of ionization and enthalpy for temperatures up to 20,000°K were calculated for argon, hydrogen, and nitrogen.[3] Studies are under way for temperature measurement from the broadening of the hydrogen Balmer lines by the technique of Dickerman.[4]

---

[3]W. D. Bond, Calculated Thermal Ionization and Enthalpy of Hydrogen, Nitrogen, and Argon in the 298–20,000°K Range, ORNL CF-60-1-96, Rev. I (June 2, 1960).

[4]P. Dickerman, "The Determination of the Equilibrium Temperature of a Plasma," in Conference on Extremely High Temperatures, Wiley, New York, 1958.

21. OXYGEN-17 SEPARATION PILOT PLANT

Assistance is being given the Chemistry Division in the design[1] and construction of an O^{17} pilot plant. The facility is designed to produce about 2 g of 98% O^{18} and 70 mg of 50% O^{17} per day.

The initial separation of the heavier oxygen isotopes from O^{16} will be made in a water system in a six-column tapered distillation cascade. Packed columns will be used, with column diameters ranging from 5.3 to 0.5 in. Each column will be provided with a constant temperature hot water jacket, in which water will be at the same temperature as the column, to provide nearly adiabatic conditions. The cascade will be operated at or near atmospheric pressure and at essentially the same temperature throughout the entire six-column set.

A side stream from the distillation cascade will be electrolyzed. The oxygen obtained, containing about 4% O^{17}, will be fed to a five-column thermal diffusion cascade. Here it will be separated into two fractions, one consisting mainly of O^{16} and O^{17} and the other consisting mainly of O^{17} and O^{18}. Each of these fractions will be fed to four-column diffusion cascades, where the O^{17} will be separated from the other isotope.

Each thermal diffusion column consists of a 30-ft length of water-jacketed copper pipe about 0.5 in. in diameter with a hot platinum wire down the center. The wire must be precisely vertical, absolutely straight, and exactly in the center of the pipe and the pipe walls must be precisely vertical or convection currents will be set up that will destroy the separation gradient. The columns will be operated at or near atmospheric pressure.

The equilibrium time of the distillation cascade will be about 18 months; equilibrium time of the thermal diffusion cascade will be about two months.

Because these already long equilibrium times would be lenghtened still further by any shutdown, considerable effort has been directed to ensure uninterrupted operation. A cooling water system and a steam system separate from the plant systems are being provided to eliminate any necessity for shutting down because of temporary interruption of these services. A diesel

[1] Oak Ridge National Laboratory Status and Progress Report, February 1960, ORNL-2922, p 26; Oak Ridge National Laboratory Status and Progress Report, April 1960, ORNL-2945, p 22.

generator is being provided for emergency electrical service. An emergency supply of instrument air is provided.

The design, procurement, fabrication, and installation of the water distillation cascade is complete. The design, procurement, and fabrication of the thermal diffusion cascade is complete, and installation is 80% complete.

22. REACTOR EVALUATION STUDIES

22.1 ECONOMIC GUIDES TO FUEL MATERIAL SELECTION FOR PRESSURIZED-WATER REACTORS

Nuclear and economic optimization calculations made for a pressurized-water reactor have been used to correlate the effect of fuel material parameters with fuel cycle cost. These correlations can serve as a guide to predict which of the many possible uranium fuel materials may show economic promise.

The nuclear calculations are based on a pressurized-water reactor having the same core size, thermal efficiency, and cladding as the Yankee Atomic Reactor.[1] Core reactivity lives were calculated as a function of fuel enrichment, fuel density, diluent poison, and fuel geometry, using an IBM-704 code[2] based on a spatially uniform flux model in which the flux changes over the core life.

Figure 22.1 shows the results of the calculations after the fuel cycle costs have been optimized for enrichment and fuel geometry; reactivity life was assumed to be the only limit to fuel life. The effect of the uranium density in the fuel material on optimum fuel cycle costs, using a limited cladding heat transfer rate (87,000 Btu hr^{-1} ft^{-2}, average) and variable fabrication costs, is shown in Fig. 22.1a. The cladding heat-transfer limit requires that the lower-density fuels which optimize at a larger diameter have a higher allowable $\int k d\theta$. (The fuel thermal conductivity is represented by k; θ is the temperature in excess of the fuel surface temperature; the limits of integration are from the surface to the center of the fuel; $\int k d\theta$ is proportional to the heat release rate per unit length of fuel element.[3] The limiting value is a function of fuel properties.) The effect of the $\int k d\theta$ limit on optimum fuel costs as a function of fuel density and fabrication cost is shown in Fig. 22.1b. A correlation

---

[1] Nuclear Power Plant Data, vol 1, Power Reactors 1959, American Society of Mechanical Engineers, McGraw-Hill, New York (1959).

[2] S. Jaye, M. P. Lietzke, and R. D. Cheverton, Reactivity Lifetime and Fuel Cost Calculations, ORNL (unpublished).

[3] J. A. L. Robertson, $\int k d\theta$ in Fuel Irradiations, CRFD-835 (1959).

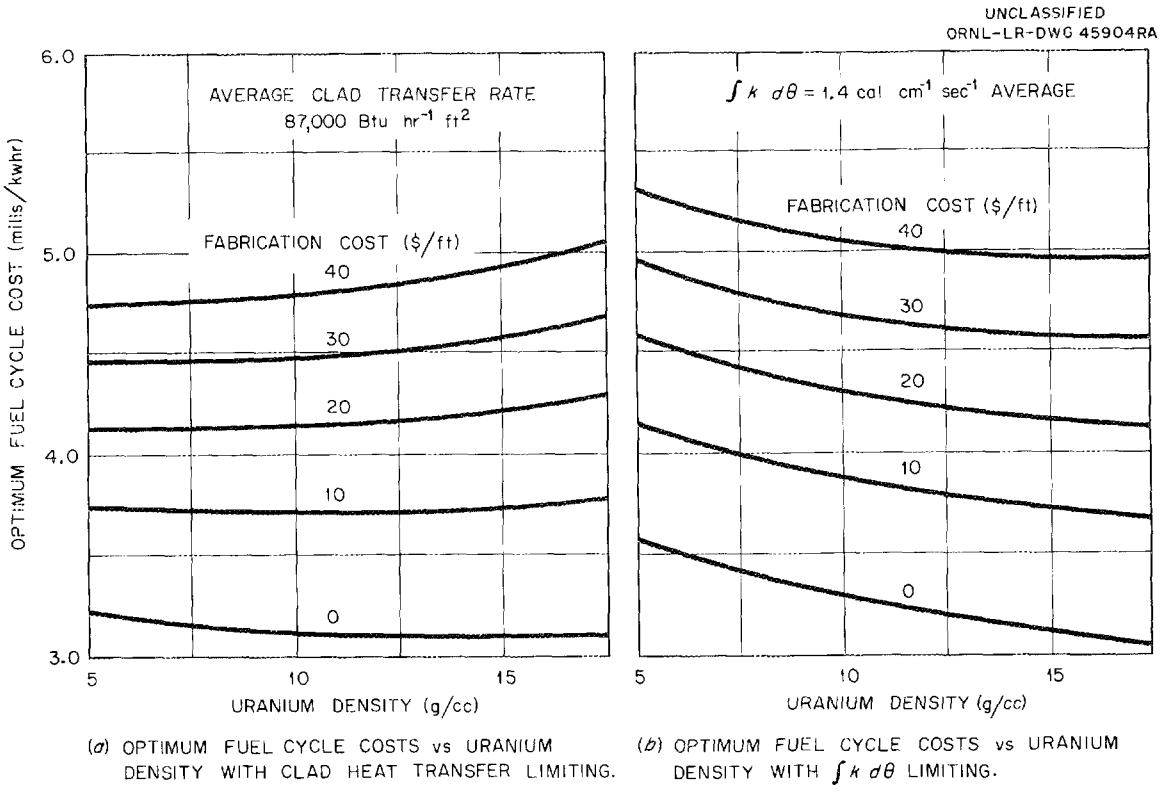

(a) OPTIMUM FUEL CYCLE COSTS vs URANIUM DENSITY WITH CLAD HEAT TRANSFER LIMITING.

(b) OPTIMUM FUEL CYCLE COSTS vs URANIUM DENSITY WITH $\int k\, d\theta$ LIMITING.

Fig. 22.1. Optimum Fuel Cycle Costs in a Pressurized-Water Reactor.

of the data has been made so that the optimum fuel cycle cost can be estimated for any set of conditions, as follows:

$$\text{optimum cycle cost, mills/kwhr}$$

$$= A + \frac{B}{\int k d\theta} + C\,\frac{(\text{fabrication cost, \$/ft of fuel element})^{0.785}}{(\int k d\theta)^{\alpha}}$$

where A, B, C, and α are functions of the fuel uranium density (Fig. 22.2), and $\int k d\theta$ in fuel = average over reactor (cal cm^{-1} sec^{-1}).

The effect of diluent poisons up to 2 barns per uranium atom on optimum fuel cycle costs was also investigated as a function of fuel density and fabrication cost, with fuel-cladding heat transfer limiting. The increase in cycle costs was found to be proportional to the poison per uranium atom at a constant density and fabrication cost. The increase in optimum cycle cost per barn per uranium atom vs the fuel uranium density is shown in Fig. 22.3. The fabrication cost is used again as a parameter.

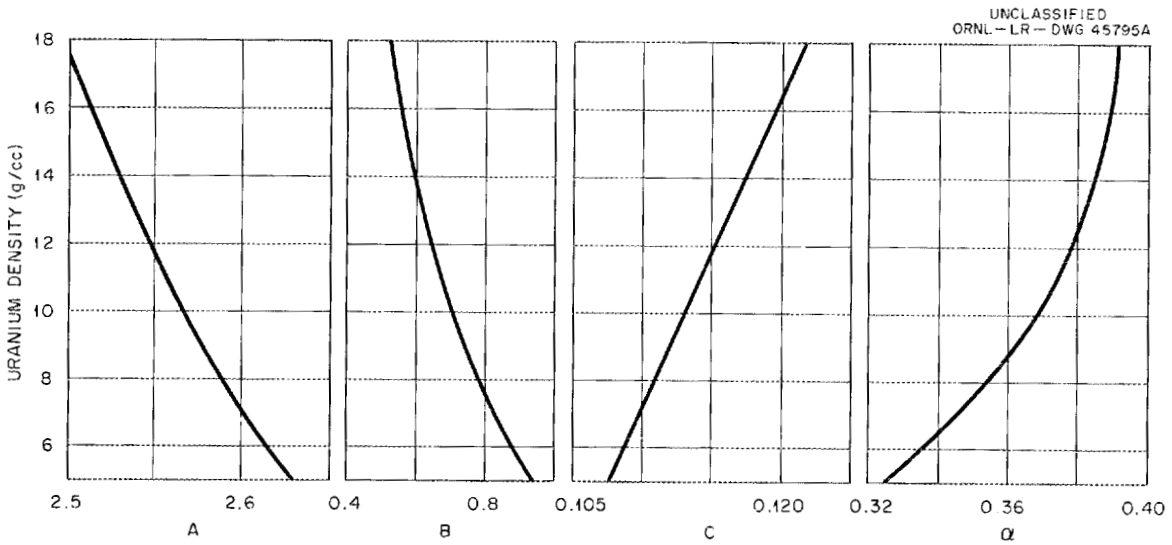

Fig. 22.2. Constants for Optimum Fuel Cycle Cost Correlation.

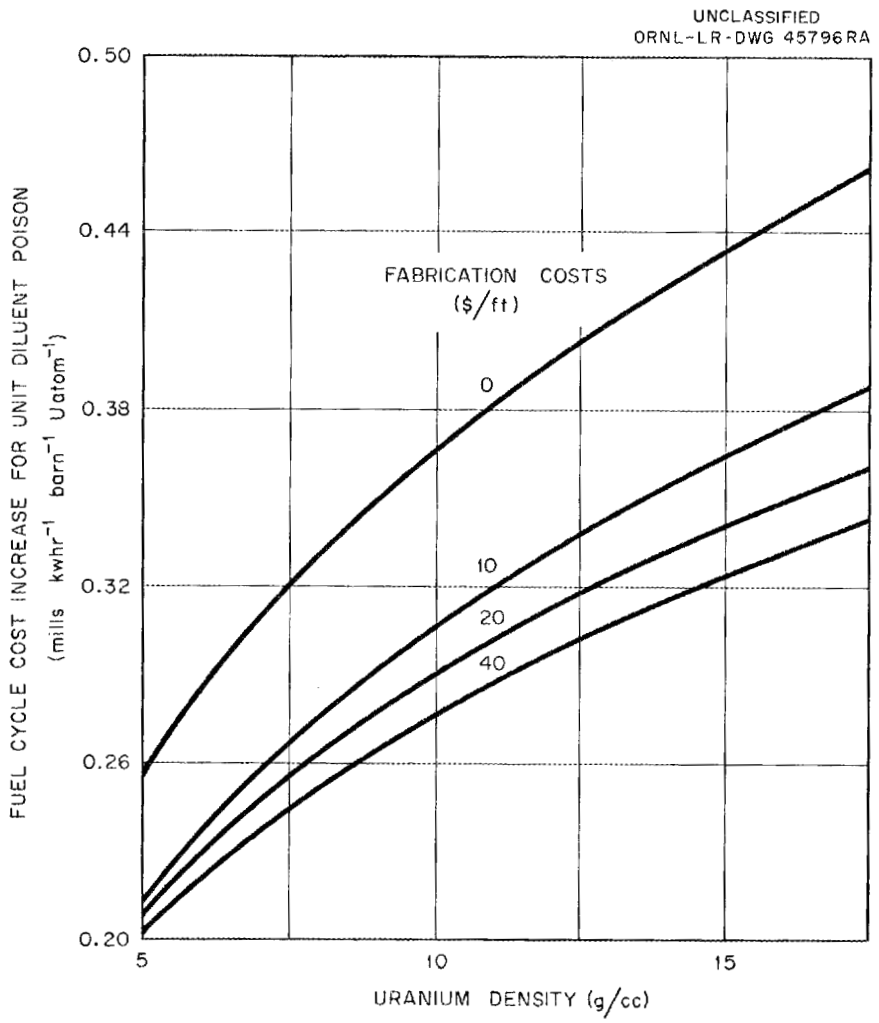

Fig. 22.3. Effect of Diluent Poison on Optimum Fuel Cycle Costs.

An example of the use of the correlations to compare the economics of alternative fuel element materials with UO_2 is presented in Table 22.1. It is unlikely that UN or USi_3 would be competitive with UO_2 in a reactor with an 87,000 Btu hr^{-1} ft^{-2} heat transfer limit; however, USi_3 might be competitive if full advantage could be taken of its higher allowable $\int k d\theta$ by increasing the cladding heat-transfer rate.

22.2 COST AND HAZARDS OF TRANSPORTING SPENT FUELS

Shipment of the highly irradiated fuels from a civilian power complex poses significant problems of radiation hazards and heat removal during shipment and their effects on shipping costs. These problems directly affect carrier design and the economics of the fuel cycle.

A study is in progress on shipments of radioactive fuel elements from the reactor operator to the processing sites. Criticality and shielding problems have been studied, but do not appear to present the difficulties that heat dissipation does. Shipments are covered by federal, state, and local regulations which emphasize problems associated with carrier design, public safety, and transportation economics. Carriers must be designed to give adequate radiation shielding, to contain radioactivity under accident conditions, and to conform with governmental regulations and economic feasibility.

None of the material shipped, which includes fuel elements, built-in poisons, and the cask construction materials, should be allowed to approach closer than 180°F to their melting points. Since, in the case of a serious accident, it is extremely difficult to guarantee the containment integrity of any internal coolants, it should be assumed in designs that the damaged carrier will be dry and air filled.

The surface temperature of the carrier (or barrier around the carrier, if one is used) should remain under 180°F. If a barrier is used, then the surface temperature of the carrier may be allowed to go higher than 180°F but should be kept below 440°F if a lead carrier is used (180°F below the melting point of lead).

The thermal conductivity of lead decreases about 50% as it melts, which would probably ensure complete melting once it started, and it expands 3.6% of the solid volume, which would almost certainly rupture the

Table 22.1. Comparison of Alternative Fuel Materials to UO_2

Compound	U Density (g/cm^3)	Poison (barns/U atom)	Case 1 Cladding Heat Transfer Limiting (87,000 Btu hr^{-1} ft^{-2}, Average)	Case 2 $\int kd\theta$ Limiting	
			Optimum Cycle Cost at \$20/ft Fabrication Cost (mills/kwhr)	$\int kd\theta$ Limit, Based on ~10% of Maximum (cal cm^{-1} sec^{-1})	Optimum Cycle Cost at \$20/ft Fabrication Cost (mills/kwhr)
UO_2	9.66	0.0004	4.14	1.45	4.14
USi_3	6.02	0.39	4.21	4.5	3.57
UN	13.5	1.9	4.81	2.5	4.25

carrier and allow loss of shielding. Therefore, if it is possible for high temperatures to be encountered during shipment, it may be necessary to consider steel, iron, or uranium for shielding material.

An example of the controlling nature of heat removal is shown in Fig. 22.4. Average Consolidated Edison fuel elements were considered (since

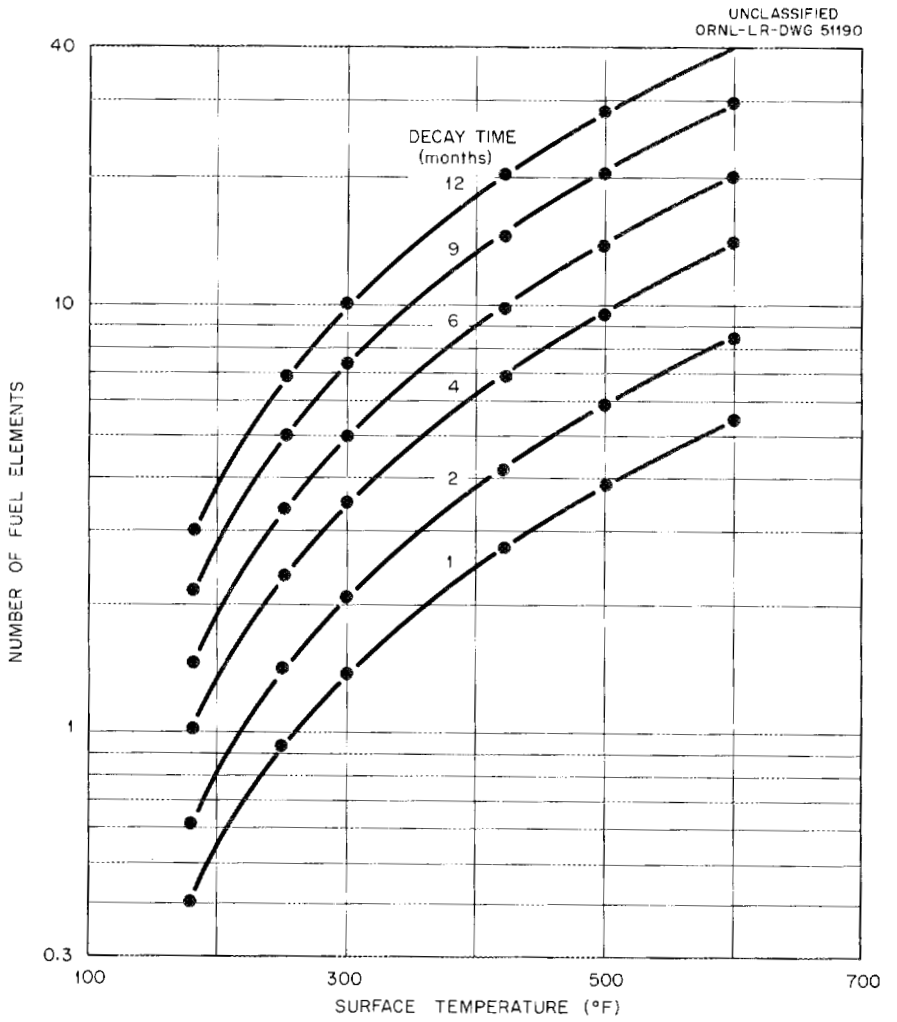

Fig. 22.4. Allowable Fuel Elements Shipped vs Carrier Surface Temperature. Carrier, 34 in. ID; maximum number of fuel elements, 12; ambient air temperature, 100° F; shielding, 7 in. of lead.

this fuel is at present more highly irradiated than any proposed for shipment), each of which had a decay heat generation rate of 11,400 Btu/hr after 4 months' decay. All heat was removed by convection and radiation from the unfinned surface. If it is necessary to keep the carrier surface temperature at 180°F, one element may be shipped after four months'

decay or three after 12 months' decay. The radiation level at the carrier surface through 9 in. of lead shielding for the former case was calculated to be 14 mr/hr and for the latter, 7 mr/hr.

22.3 MISCELLANEOUS IBM-704 CODES

Several codes which pertain to many different phases of activity of the Chemical Technology Division have been completed, or are being written, for the IBM-704 (or 7090). These codes are described below.

1. 25-Th Reactor System. Determines reactivity lifetimes and discharge isotopic concentration for well-moderated thorium-U^{235}-fueled reactors. (Completed).
2. Pu-Th Reactor System. Same as 1 except for Th-plutonium fueled reactors. (Completed).
3. Special Plutonium Code. Calculate discharged isotopic composition for irradiation of uranium in either mixed fuel or seed and blanket reactors. (Completed).
4. Leak Tight. Code for use in calculating the downwind hazard following an explosive-type accident in a processing cell. Code considers building design, safety features, and atmospheric parameters. (In "debugging" stage).
5. Special Thorium Code. Similar to 3 except thorium is substituted for U^{238}. Computational part is much more extensive since many more irradiation chains are considered. (In "debugging" stage).
6. Shielding Calculations. Code designed to determine the required shield thickness for any of 10 source geometries and 11 shield materials. As many as 12 gamma energy groups can be considered. (Code has been approximately one-third completed).
7. TRUFIZ. Special code for calculation buildup of fission products and transuranium elements, using the IBM-7090.

Since future power reactor fuels will be subjected to very high burnups, the fission product spectrum will differ considerably from that of pure U^{235}. Large concentrations of the transuranium isotopes will also be produced. Previous calculations of fission product and transuranium isotope levels in irradiated fuel have been based on pure U^{235} and/or constant flux operation. In this study, a flexible program is proposed which will allow any combination of isotopes, any effective reactor cross section for all isotopes, and any combination of outputs. In addition, all concentrations will be computed for constant power operation.

The input-output information used in this program will be more complex than that given by Blomeke and Todd,[4] due to consideration of other fissionable isotopes in the same system. Since this is the case, the calculational methods for fission products and the number of chains used by the above-mentioned authors will be simplified in order to limit the total generated output. In the proposed program, except for special cases, only fission products having half lives greater than one day, yields greater than 0.01%, and/or cross sections greater than 1 barn (for poison considerations) will be considered. Also, decay periods of less than one day will not be considered. (Development of mathematical models has just begun. No part of this problem has been coded.)

---

[4]J. O. Blomeke and Mary F. Todd, Uranium-235 Fission Product Production as a Function of Thermal Neutron Flux, Irradiation Time, and Decay Time, ORNL-2127 (Aug. 19, 1957).

23. EUROCHEMIC ASSISTANCE PROGRAM

The USAEC is assisting in the construction of a fuel processing plant at Mol, Belgium. ORNL's contribution to the program consisted of the full-time loan of one technical consultant, short-term visits of several technical consultants, the full-time assignment of one technical co-ordinator in the United States, and the review and exchange of technical data pertinent to the radiochemical processing of irradiated fuels. Approximately 1050 USAEC-originated documents, including 30 specially prepared for Eurochemic, and 600 drawings and items of miscellaneous information have been transmitted to Eurochemic since the program began.

The fourth preliminary design and the cost estimate (Project IV) within the budget framework specified through 1963 ($\$21.77 \times 10^6$) were completed. The design capacity is 350 kg of natural uranium per day or 250 kg of up to 5% enriched uranium per day. Head-end processes being considered are Sulfex for stainless-steel-clad fuels, Zirflex for Zircaloy-clad fuels, dilute sulfuric acid for magnesium-clad fuels, and sodium hydroxide for aluminum-clad fuels. The solvent extraction system will consist of a co-decontamination cycle and a second uranium cycle. The second plutonium cycle and anion exchange tail-end step have been eliminated, with an amine extraction cycle being considered as a replacement.

Plant layout and auxiliary equipment design are in the preliminary stage. The austerity program has resulted in combining the analytical laboratory for the plant with the research analytical laboratory. Two or possibly three heavily shielded radioactive cells will be used for sample receipt, storage, dilution, and high-activity analytical work. Samples will be taken and transported by a modified ORNL Thorex sampling system.

Negotiations are under way with the St. Gobian company of France on the engineering contract terms for the main plant. The first phase will probably be a 6-month preproject study by St. Gobian, which will be a detailed preliminary project proposal. Presumably, it will include engineering flowsheets, process and laboratory building layouts, preliminary specifications, and a cost estimate. The preproject is to be prepared so the detailed design work may be split into three to five parts to permit companies from different countries to participate in the work. Two other

major engineering groups may also participate. One may be the Swiss-Danish-Spanish group for the design of the research laboratory and a Belgian company for the waste disposal system design.

The Eurochemic charter has been ratified by all participating countries except Italy and Sweden. Spain has joined the organization, bringing the total participating countries to 13. The company was formally organized in July 1959, with E. Svenke of Sweden as Chairman and B. Goldschmidt of France as Vice-Chairman of the Board of Directors. E. Pohland of Germany was appointed General Manager of the company. Seven people associated with Eurochemic visited four USAEC sites during a three-week tour in October 1959. Process engineering and chemistry were discussed along with associated fields of health physics, criticality, analytical work, and building design.

24. PUBLICATIONS AND ORAL PRESENTATIONS

POWER REACTOR FUEL PROCESSING

Blanco, R. E., L. M. Ferris, J. R. Flanary, F. G. Kitts, R. H. Rainey, and J. T. Roberts, "Chemical Processing of Power and Research Reactor Fuels at Oak Ridge National Laboratory," TID-7583 (CF 59-12-70).

Clark, W. E., and S. Peterson, "Electrolytic Disintegration of Zircaloy-2 in Nitric Acid Solutions," ORNL-2824 (Nov. 13, 1959).

Ferris, L. M., "Process for Dissolution of Borax IV Reactor Fuel: Laboratory Development," ORNL-2821 (Jan. 19, 1960).

Ferris, L. M., "Decladding of Consolidated Edison Power Reactor Fuel by Sulfex and Darex Processes: Cyclic Dissolution Experiments," ORNL-2822 (Jan. 14, 1960).

Ferris, L. M., and A. H. Kibbey, "Laboratory Development of the Sulfex Process for the Dissolution of Consolidated Edison Power Reactor Fuel," ORNL-2714 (Oct. 16, 1959).

Gens, T. A., "Sulfex Process: Depassivation of Stainless Steel," ORNL-2785 (Nov. 6, 1959).

Gens, T. A., "New Developments in Uranium Alloy Fuel Reprocessing," presented at the American Nuclear Society Meeting, Washington, D.C., Nov. 4–6, 1959 (CF 59-10-102).

Gens, T. A., and F. G. Baird, "Modified Zirflex Process for Dilution of Zirconium- and Niobium-Bearing Nuclear Fuels in Aqueous Fluoride Solutions: Laboratory Development," ORNL-2713 (Dec. 8, 1959).

Gens, T. A., "Modified Zirflex Process for Dissolution of 1–10% U-Zr Alloy Fuels in Aqueous NH_4F-NH_4NO_3-H_2O_2: Laboratory Development," ORNL-2905 (March 4, 1960).

Goeller, H. E., "Fuel Processing Facilities at ORNL," TID-7583 (CF 59-12-70).

Holmes, J. M., "Power Reactor Fuel Aqueous Processing at ORNL," presented at the Tennessee Academy of Sciences Meeting, Nashville, Tenn., Dec. 11, 1959 (CF 59-11-51).

Horner, D. E., and C. F. Coleman, "Recovery of Uranium and Plutonium from Sulfuric Acid Decladding Solutions," ORNL-2830 (Nov. 11, 1959).

Irvine, A. R., "Special Problems in Chemical Processing at ORNL," TID-7583 (CF 59-12-70).

McDuffee, W. T., "Accountability of Special Nuclear Material at Oak Ridge National Laboratory," TID-7583 (CF 59-12-70).

Ullmann, J. W., "Reactor Fuel Element Types," Third Conference on Analytical Chemistry, Gatlinburg, Tennessee, Oct. 26–28, 1960 (CF 59-9-73).

HOMOGENEOUS REACTOR FUEL PROCESSING

Haas, P. A., "Solids Separation by a Hydraulic Cyclone with a Batch Underflow Receiver," ORNL-2876 (March 4, 1960).

Rom, A. M., and H. O. Weeren, "Design of Chemical Processing Plant for Homogeneous Reactor Test," ORNL-2784 (Oct. 7, 1959).

Weeren, H. O., "Tantalum Withstands Boiling H_2SO_4 and 400°F Mercury," Corrosionomics, Vol. 4, No. 3 (1959).

Youngblood, E. L., "Development of an Electrolytic Cell for Removal of Nickel from HRT Fuel Solutions," ORNL-2923 (May 5, 1960).

WASTE TREATMENT AND DISPOSAL

Bruce, F. R., "The Origin and Nature of Radioactive Wastes in the Atomic Energy Program," presented at the Conference on Land and Sea Disposal of Radioactive Wastes, Principality of Monaco, Nov. 16–21, 1959 (CF 59-11-6).

Godbee, H. W., and J. T. Roberts, "Survey on the Measurement of Thermal Conductivity of Solids Produced by Evaporation and Calcination of Synthetic Fuel Reprocessing Solutions," ORNL-2769 (Aug. 10, 1959).

Holcomb, R. R., "Maritime Reactor Waste Disposal Studies: Solidification on Ion-Exchange Resin with Portland Cement for Radioactive Waste Disposal," ORNL-2899 (Aug. 10, 1960).

Lacy, W. J., F. M. Empson, and I. R. Higgins, "Physical and Chemical Properties of Nuclear Power Reactor Waste Solutions," Ind. and Eng. Chem. 51, No. 10 (1959).

Oliver, J. R., and J. R. Meriwether, "Disposal of Nuclear Reactor Waste by Fixation in Aluminosilicate Systems," presented at the American Chemical Society Regional Meeting, Baton Rouge, La., Dec. 5, 1959 (work done under subcontract at ORNL).

Perona, J. J., and M. E. Whatley, "Calculation of Temperature Rise in Deeply Buried Radioactive Cylinders," ORNL-2812 (Feb. 3, 1960).

HEAD-END AND SOLVENT EXTRACTION PROCESSING

Bradley, M. J., and L. M. Ferris, "Reprocessing of Rover Fuel: Laboratory Development Progress to April 1, 1959," ORNL-2741 (Oct. 19, 1959) (secret).

Bradley, M. J., and L. M. Ferris, "Recovery of Uranium and Thorium from Graphite Fuels. I. Laboratory Development of a Grind-Leach Process, ORNL-2761 (March 17, 1960).

Davis, W., "Radiation Densities and TBP Radiolysis During Thorex Short Decay Runs," ORNL-2764 (Aug. 6, 1959).

Dean, O. C., A. F. Messing, and H. C. Forsberg, "Use of Mercury in Reprocessing Nuclear Fuels," presented at the Annual Meeting of the Metallurgical Society of the American Institute of Mining Engineers, New York, February 1960 (CF 60-2-3).

Forsberg, H. C., "Thermodynamic Properties of the Uranium Mercurides," ORNL-2885 (Feb. 15, 1960).

Messing, A. F., and O. C. Dean, "Processing of High-Fired Uranium Dioxide by a Reduction-Mercury Extraction-Oxidation Process," ORNL-2909 (July 26, 1960).

Messing, A. F., and O. C. Dean, "Solubilities of Selected Metals in Mercury: Hermex Process," ORNL-2871 (June 15, 1960).

Moore, J. G., and R. H. Rainey, "Chemical Feasibility of Homogeneous Neutron Poisons for Criticality Controls in Consolidated Edison Fuel Processing Solutions," ORNL-2854 (March 25, 1960).

Watson, C. D., J. B. Adams, G. K. Ellis, G. A. West, F. L. Hannon, W. F. Schaffer, and B. B. Klima, "Mechanical Processing of Spent Power Reactor Fuel at Oak Ridge National Laboratory," TID-7583 (CF 59-12-70).

West, G. A., and C. D. Watson, "Decontamination Testing of Highly Contaminated Protective Coatings," ORNL-2811 (Nov. 18, 1959).

FUSED SALT-FLUORIDE VOLATILITY PROCESS

Cathers, G. I., R. L. Jolley, and E. C. Moncrief, "Tests of the Fused Salt Volatility Process with High Burnup Fuel in a Hot Cell Facility," presented at the American Nuclear Society Meeting, Chicago, Illinois, June 12–15, 1960 (CF 60-3-11).

McNeese, L. E., "UF_6-NaF Sorption," presented at UCC Mass Transfer Meeting Held in Buffalo, New York, April 1960 (CF 60-3-118).

Whitmarsh, C. L., and W. H. Carr, "Fused Salt Fuel Processing in the ORNL Volatility Pilot Plant," ORNL-2918 (May 6, 1960).

MOLTEN-SALT REACTOR FUEL PROCESSING

Campbell, D. O., and G. I. Cathers, "Processing of Molten Salt Power Reactor Fuel," Ind. Eng. Chem., 52: 41–44 (January 1960).

FUEL CYCLE

Guthrie, C. E., and L. J. King, "Economic Guides to Fuel Material Selection for Pressurized Water Reactors," presented at the American Nuclear Society Meeting, Chicago, Illinois, June 12–15, 1960 (CF 60-3-2).

RAW MATERIALS

Baes, C. F., and H. T. Baker, "The Extraction of Iron(III) from Acid Perchlorate Solutions by Di(2-ethylhexyl)phosphoric Acid in n-Octane," J. Phys. Chem. 64, No. 1, 89 (1960).

Crouse, D. J., and K. B. Brown, "Solvent Extraction Recovery of Vanadium (and Uranium) from Acid Liquors with Di(2-ethylhexyl)phosphoric Acid," ORNL-2820 (Nov. 11, 1959).

Crouse, D. J., and K. B. Brown, "The Amex Process for Extracting Thorium Ores with Alkyl Amines," Ind. and Eng. Chem. 51, 1461–1464 (December 1959).

Crouse, D. J., "Controlled pH Stripping of Uranium from Amines," ORNL-2941 (May 31, 1960).

Hurst, F. J., and D. J. Crouse, "Recovery of Uranium from Di(2-ethylhexyl)phosphoric Acid (Dapex) Extractant with Ammonium Carbonate," ORNL-2952 (June 30, 1960).

Ryon, A. D., F. L. Daley, and R. S. Lowrie, "Scaleup of Mixer-Settlers," Chem. Eng. Prog. 55:70 (1959).

Ryon, A. D., F. L. Daley, and R. S. Lowrie, "Design and Scaleup of Mixer-Settlers for the Dapex Solvent Extraction Process," ORNL-2951 (in press).

GAS-COOLED REACTOR COOLANT AND EQUIPMENT DECONTAMINATION

Lane, J. A., L. L. Bennett, H. N. Culver, L. J. King, J. P. Sanders, J. L. Scott, W. E. Unger, "A Study of Problems Associated with Release of Fission Products from Ceramic Fuels in Gas-Cooled Reactors," ORNL-2851 (Oct. 27, 1959).

HRP THORIA BLANKET DEVELOPMENT

Clinton, S. D., "Comparison of a Fluidized-Bed and an Agitated-Trough Chemical Reactor for Producing ThO_2 from $Th(NO_3)_4$," ORNL-2875 (Jan. 29, 1960).

Haws, C. C., "Flame Ceramics: A Means of Producing Particulate Thoria for Use as a Slurry in Nuclear Reactors," Supplement to an International Symposium on High Temperature Technology, Asilomar Conference Grounds, Calif., 61–62. (Presented at International Symposium on High Temperature Technology, Stanford Research Institute, Menlo Park, Calif., Oct. 6–9, 1959) (CF 59-9-86).

Johnsson, K. O., and R. H. Winget, "Pilot Plant Preparation of Thorium- and Thorium-Uranium Oxides," ORNL-2853 (Dec. 8, 1959).

Krohn, N. A., "The Catalysis of the Hydrogen-Oxygen Reaction by Aqueous Slurries of Thorium Oxide and Thorium-Uranium Oxide," ORNL-2878 (Jan. 20, 1960).

TRANSURANIUM STUDIES

Baybarz, R. D., and R. E. Leuze, "Separation of Transplutonic and Rare Earth Elements by Liquid-Liquid Extraction," presented at the American Nuclear Society Meeting, Chicago, Illinois, June 12–15, 1960 (CF 60-3-22).

Lloyd, M. H., and R. E. Leuze, "Anion Exchange Separation of Trivalent Actinides and Lanthanides," presented at the American Nuclear Society Meeting, Chicago, Illinois, June 12–15, 1960 (CF 60-3-23).

FISSION PRODUCT RECOVERY

Weaver, B., and F. A. Kappelmann, "Purification of Promethium by Liquid Extraction," ORNL-2863 (Jan. 29, 1960); also CF 59-7-6, presented at AIChE Meeting, San Francisco, Calif., December 1959.

Weaver, B., and F. A. Kappelmann, "Separation of Rare Earths by Liquid-Liquid Extraction," presented at the Annual Meeting of the Metallurgical Society of the American Institute of Mining Engineers: New York, February 1960 (CF 60-1-78).

SOLVENT EXTRACTION TECHNOLOGY

Allen, K. A., "Some New Solvent Extraction Equilibria," presented at the Tennessee Academy of Sciences Meeting, Nashville, Tennessee, Dec. 11, 1959 (CF 59-11-52).

Allen, K. A., "The Relative Effects of the Uranyl Sulfate Complexes on the Rate of Extraction of Uranium from Acidic Aqueous Sulfate Solutions," J. Phys. Chem. 64: 667 (May 1960).

Allen, K. A., and W. J. McDowell, "Anomalous Solvent Extraction Equilibria Due to Violence of Agitation," J. Phys. Chem. 64: 877 (July 1960).

Blake, C. A., Jr., A. T. Gresky, J. M. Schmitt, and R. G. Mansfield, "Uranium and Thorium Separation with Di(sec-butyl) Phenylphosphonate and Other Reagents," presented at the American Nuclear Society Meeting, Chicago, Illinois, June 12–15, 1960 (CF 60-3-25).

Coleman, C. F., F. A. Kappelmann, and B. Weaver, "Solvent Extraction Recovery of Technetium and Neptunium from Fluorination Plant Residues," presented at the American Nuclear Society Meeting, Chicago, Illinois, June 12–15, 1960 (CF 60-3-26).

Weaver, B., and D. E. Horner, "Distribution Behavior of Neptunium and Plutonium Between Acid Solutions and Some Organic Extractants," J. Chem. and Eng. Data (July 1960).

EXTRACTION REAGENT PERFORMANCE

Davis, W., Jr., "Tributyl Phosphate-Hydrocarbon Diluent Repurification in Radiochemical Processing at ORNL: Status Summary," ORNL-2848 (March 7, 1960).

Davis, W., Jr., and H. H. Carmichael, "Solubility of Zirconium Dibutyl Phosphate in Solvent Extraction Solutions," ORNL-2857 (Jan. 6, 1960).

ION EXCHANGE TECHNOLOGY

Watson, J. S., "The Kinetics of Uranyl Sulfate Anion Exchange," presented at the UCC Mass Transfer Meeting, Buffalo, New York, April 1960 (CF 60-3-120).

CHEMICAL ENGINEERING RESEARCH

Chester, C. V., "Transfer of Uranyl Ion Across a Water-TBP Interface," presented at the UCC Mass Transfer Meeting, Buffalo, New York, April 1960 (CF 60-3-119).

CANE

Bond, W. D., and W. E. Clark, "Leaching of Tamalpais Debris," ORNL-2810 (Jan. 13, 1960).

Bond, W. D., and W. E. Clark, "Reduction of Cupric Oxide by Hydrogen. I. Fundamental Kinetics," ORNL-2815 (Feb. 4, 1960).

Bond, W. D., and W. E. Clark, "Reduction of Cupric Oxide by Hydrogen. II. Conversion of Hydrogen to Water over Fixed Beds," ORNL-2816 (Jan. 29, 1960).

Landry, J. W., "Oak Ridge National Laboratory Sampler for the Tamalpais Underground Nuclear Detonation Experiment," ORNL-2881 (June 30, 1960).

USES OF DEPLETED URANIUM

Bresee, J. C., et al., "Nonnuclear Uses for Depleted Uranium," ORNL-2889 (Feb. 17, 1960).

IN-LINE INSTRUMENTATION

Landry, J. W., "In-Line Instrumentation: Gamma Monitor, Uranium Colorimeter," ORNL-2978 (in press).

EXCER PROCESS

Ferris, L. M., and F. G. Baird, "Decomposition of Uranyl Fluoride Between 700 and 900°C," J. Elect. Soc., 107, 305 (1960).

GENERAL

Culler, F. L., et al., "Chemical Technology Division Annual Progress Report for Period Ending August 31, 1959," ORNL-2788 (Sept. 11, 1959).

Gresky, A. T., "Universal Units of Magnetism, Mechanics, and Temperature," J. Franklin Inst., Vol. 268, p. 388 (November 1959).

Gresky, A. T., "A Simple Unified Field Equation," J. Franklin Inst., Vol. 269, p. 105 (February 1960).

CHEMICAL TECHNOLOGY DIVISION

P. L. CULLER, DIRECTOR
VIRGINIA WELLS, SECRETARY
NANCY CULLISON, SECRETARY
W. K. DISTER, TECHNICAL ASSISTANT
LUCRETIA REED, SECRETARY
MARTHA GERBARD, REPORTS EDITOR

LONG RANGE PLANNING COMMITTEE

A. T. GRESKY*
E. D. ARNOLD
C. E. GUTHRIE
J. W. ULLMANN
FRANCES QUILLEN, SECRETARY

C. W. SCHERSTEN, ADMINISTRATIVE ASSISTANT TO DIRECTOR
RUTH HAMPLIN, SECRETARY
H. B. GRAHAM, ADMINISTRATIVE ASSISTANT
LUCILLE KUYKENDALL, SECRETARY
W. D. GREEVER, PROCUREMENT
J. W. CLARK, PROCUREMENT

APPLIED RESEARCH GROUP

K. G. WYMER
N. A. KROHN

TECHNICIAN
D. M. HELTON

CHEMICAL DEVELOPMENT SECTION A

D. E. FERGUSON, SECTION CHIEF
JOANNE MAYES, SECRETARY
INOGENE LOOPE, SECRETARY
C. F. KECK, TECHNICIAN

SURFACE CHEMISTRY

C. H. SECOY, GROUP LEADER
H. F. HOLMES
F. H. SWEETON

TECHNICIAN
H. F. SOARD

THORIUM OXIDE STUDIES

J. P. McBRIDE, GROUP LEADER
L. E. MORSE

TECHNICIANS
P. P. HAYDON
W. L. PATTISON

ALPHA-ACTIVE MATERIALS PROCESSING

R. E. LEUZE, GROUP LEADER
R. O. BAYBARZ, PROBLEM LEADER, *TRANSURANICS*
M. H. LLOYD

TECHNICIANS
R. L. HICKEY
O. K. TALLENT

EQUIPMENT DECONTAMINATION

A. B. MESERVEY, PROBLEM LEADER
J. M. CHILTON

TECHNICIAN
D. H. NEWMAN

FLUORIDE VOLATILITY PROCESSING

G. I. CATHERS, GROUP LEADER
S. S. KIRSLIS
R. L. JOLLEY, PROBLEM LEADER, *HOT CELL OPERATIONS*
D. O. CAMPBELL, PROBLEM LEADER, *NGR PROCESSING*
M. R. BENNETT

TECHNICIANS
T. E. CRABTREE
C. J. SHIPMAN

FUEL CYCLE STUDIES AND THORIUM BLANKET STUDIES

O. C. DEAN,* GROUP LEADER
A. T. KLEINSTEUEER
K. H. McCORKLE
C. E. SCHILLING

TECHNICIAN
C. W. GREENE

CHEMICAL DEVELOPMENT SECTION B

R. E. BLANCO, SECTION CHIEF
RUTH WILLIAMS, SECRETARY
PHYLLIS MARKS, SECRETARY
J. E. FARMER, DRAFTSMAN
J. A. McLAREN, SPECIAL ASSIGNMENT

FEED MATERIALS PROCESSING, HERMEX

O. C. DEAN,* PROBLEM LEADER
A. F. MESSING

TECHNICIAN
E. R. JOHNS

ION EXCHANGE TECHNOLOGY, WASTE TREATMENT

J. T. ROBERTS, PROBLEM LEADER
H. W. GOODBEE
L. L. ENNIS
W. E. TOMLIN
W. C. YEE
R. R. HOLCOMB, *MARITIME REACTOR WASTE DISPOSAL*
KARL ESCHLE[2]

TECHNICIAN
W. E. SHOCKLEY

POWER REACTOR FUEL PROCESSING

W. E. CLARK, PROBLEM LEADER, *CORROSION, CANF*
W. D. BOND

TECHNICIAN
J. F. TALLEY

L. M. FERRIS, PROBLEM LEADER, *SULFEX, ZIRFLEX, CERAMIC, AND GRAPHITE FUEL DISSOLUTION*
M. J. BRADLEY
T. A. GENS
A. N. KIBBEY
K. S. WARREN
J. D. VAUGHAN[1]

TECHNICIAN
J. F. LAND

J. R. FLANARY, PROBLEM LEADER, *FLOWSHEET DEMONSTRATION ON IRRADIATED FUELS*
J. H. GOODE
C. P. JOHNSTON

TECHNICIANS
L. A. BYRD
R. C. SHIPWASH
G. E. WOODALL

R. H. RAINEY, PROBLEM LEADER, *SOLVENT EXTRACTION OF THORIUM FUELS*
J. G. MOORE

TECHNICIAN
R. C. LOVELACE

W. DAVIS, PROBLEM LEADER, *MECHANISMS OF SEPARATION METHODS*
E. SCHONFELD[3]

TECHNICIAN
C. T. THOMPSON

CHEMICAL DEVELOPMENT SECTION C

K. B. BROWN, SECTION CHIEF
KATIE SPARKS, SECRETARY
VIRGINIA MORRIS, SECRETARY
C. F. COLEMAN, SPECIAL ASSIGNMENTS

RAW MATERIALS PROCESSING, AMEX PROCESS AND THORIUM RECOVERY

D. J. CROUSE, GROUP LEADER, *PROCESS DEVELOPMENT*
W. D. ARNOLD
R. J. HURST
F. G. SEELEY

SOLVENT EXTRACTION TECHNOLOGY

K. A. ALLEN, GROUP LEADER, *FUNDAMENTAL CHEMISTRY*
W. J. McDOWELL
A. L. MYERS[3]

TECHNICIAN
G. N. CASE

C. A. BLAKE, A. T. GRESKY,* GROUP LEADERS, *U, Th, Pu PROCESSING*
J. M. SCHMITT
R. G. MANSFIELD

TECHNICIAN
W. E. OXENDINE

B. S. WEAVER, GROUP LEADER, *SEPARATIONS CHEMISTRY AND REAGENTS*
F. A. KAPPELMANN

TECHNICIANS
J. P. EUBANKS
J. A. COLLINS

FISSION PRODUCT RECOVERY

R. P. WISCHOW, GROUP LEADER, *FISSION PRODUCT RECOVERY*
D. E. HORNER

TECHNICIANS
M. J. DERNAM
W. B. HOWERTON

UNIT OPERATIONS SECTION

M. E. WHATLEY, SECTION CHIEF
MARY MARGARET SNOYER, SECRETARY
MARTHA DAWSON, SECRETARY
PAULA MAYS, SECRETARY
MILDRED SWANN, SECRETARY
J. T. LONG, TEXTBOOK PREPARATION

FUEL CYCLE STUDIES

P. A. HAAS,* GROUP LEADER
J. W. SNIDER

TECHNICIAN
R. D. ARTHUR

HOMOGENEOUS REACTOR BLANKET STUDIES AND MRT-CP SUPPORT

P. A. HAAS,* GROUP LEADER
S. D. CLINTON
C. C. HAAS, JR.

TECHNICIAN
V. L. FOWLER

TRANSURANIUM ELEMENTS

P. A. HAAS,* GROUP LEADER
G. K. ELLIS

FUSED SALT – FLUORIDE VOLATILITY PROCESS

R. W. HORTON, GROUP LEADER
F. R. GROVES[1]
R. J. McNAMEE
L. E. McNEESE
S. H. STAINKER

TECHNICIANS
J. BEAMS
F. H. MCLAIN

CHEMICAL ENGINEERING RESEARCH

A. D. RYON,* GROUP LEADER
C. V. CHESTER

SOLVENT EXTRACTION DEVELOPMENT

A. D. RYON,* GROUP LEADER
F. L. DALEY
R. S. LOWRIE
W. M. WOODS

TECHNICIANS
G. JONES, JR.
F. G. KILPATRICK
K. LAND
R. D. PAYNE
C. H. TIPTON

GAS COOLED REACTOR PURIFICATION STUDIES

J. C. SUDDATH,* GROUP LEADER
C. D. SCOTT

TECHNICIAN
W. G. SISSON

ION EXCHANGE

J. C. SUDDATH,* GROUP LEADER
S. H. JURY[4]
J. S. WATSON

TECHNICIAN
D. A. McWHIRTER

WASTE PROCESSING STUDIES

J. C. SUDDATH,* GROUP LEADER
C. W. HANCHER
J. J. PERONA

TECHNICIANS
J. C. ROSE
J. S. TAYLOR

POWER REACTOR FUEL PROCESSING

C. D. WATSON, GROUP LEADER
J. B. ADAMS, *MECHANICAL PROCESSING*
G. A. WEST

TECHNICIANS
T. D. NAPIER
D. E. WILLIS

F. G. KITTS, *CHEMICAL HEAD-END*
B. C. FINNEY
R. A. HANNAFORD
H. F. JOHNSON[4]

TECHNICIANS
G. B. DINSMORE
F. L. ROGERS

PROCESS DESIGN SECTION

H. E. GOELLER, SECTION CHIEF
W. E. UNGER,* ASSISTANT SECTION CHIEF
A. M. ROM, *BOOK PREPARATION*
E. L. NICHOLSON, *EUROCHEMIC ASSISTANCE*
E. M. SHANK
J. W. LANDRY, *CANE PROJECT*
H. O. WEEREN* | O[17] *PILOT PLANT*
B. B. KLIMA*
MAY PEPPER, SECRETARY
NELLINE ROSS, SECRETARY
ALICE McWILLIAMS, SECRETARY
SANDRA GRAHAM, SECRETARY
JEAN HURD, SECRETARY
K. F. STOCKSBURY, CLERK

POWER REACTOR FUEL PROCESSING

A. R. IRVINE, PROBLEM LEADER, *CHEMICAL PROCESSING*
J. M. HOLMES*
J. P. NICHOLS
A. C. SCHAFFER
L. B. SHAPPERT

TECHNICIAN
J. S. NEWMAN

W. F. SCHAFFER, PROBLEM LEADER, *MECHANICAL PROCESSING*
B. B. KLIMA*

FLUORIDE VOLATILITY PROCESS

R. P. MILFORD, PROBLEM LEADER

TECHNICIAN
W. E. DUNN

TRANSURANIUM PROGRAM AND HOMOGENEOUS REACTOR FUEL PROCESSING

W. E. UNGER,* GROUP LEADER
T. A. ARBHART, *HOT CELL FACILITIES*
E. J. FREDERICK, *TRANSURANICS*
W. R. WINSBRO, *BUILDING 3019 CONTAINMENT*
R. V. FOLTZ
P. E. HARRINGTON, *BUILDING 3019 PROCESS CHANGES*
G. B. BERRY

ECONOMIC STUDIES

W. G. STOCKDALE

WASTE STUDIES

J. D. BLOMEKE, PROBLEM LEADER
J. M. HOLMES,* *BUILDING CALCULATION STUDIES*
F. N. BROWDER
F. C. McCULLOUGH
H. O. WEEREN*

PROJECT ENGINEERING

B. F. BOTTENFIELD, PROBLEM LEADER
P. L. ROBERTSON

DRAFTSMEN
J. H. HANNEY, CHIEF

EVELYN BRIDGES	R. R. MANGOLD
J. W. DAY	A. B. OLDHAM
J. D. CUPP	F. L. PEISHEL
W. L. ELLISON	J. D. PHILLIPS
H. W. FALLON	J. H. THOMPSON
L. F. FLOWERS	J. N. WHEELER
L. C. HUBBARD	R. L. KNIPPING

PILOT PLANT SECTION

J. C. BRESEE, SECTION CHIEF
W. H. LEWIS,* ASSISTANT SECTION CHIEF
BOBBIE HOYLE, SECRETARY
LORETTA JOHNSON, SECRETARY
P. G. PARKER, CLERK
R. S. WATERS, DRAFTSMAN

HOMOGENEOUS REACTOR FUEL PROCESSING

W. D. RUNCH, GROUP LEADER, *MRT CHEMICAL PLANT*
J. R. ENGEL
O. O. YARBRO
R. J. SHANNON

TECHNICIANS
W. T. BOSTIC
E. W. BROWN

THORIUM OXIDE SLURRY DEVELOPMENT

R. B. LINDAUER,* GROUP LEADER, *ThO₂ PREPARATION*
R. H. WINGET, PROBLEM LEADER
K. O. JOHNSSON

TECHNICIAN
W. A. LINDSEY

OPERATORS
J. P. CULP
J. R. EBLEN
C. H. JONES
F. H. WATSON

POWER REACTOR FUEL PROCESSING

W. H. LEWIS,* GROUP LEADER
J. L. MATHERNE, PROBLEM LEADER, *ENGINEERING*
C. D. HYLTON
T. S. MACKEY
R. H. VAUGHAN
W. R. WHITSON

TECHNICIANS
R. L. PURKEY
W. M. SPROULE
J. H. WALKER

W. T. McDUFFEE, PROBLEM LEADER, *DATA*
G. S. SADOWSKI
J. R. PARROTT, PROBLEM LEADER, *BUILDING 3019 FACILITY*
W. T. McCARLEY, *OPERATIONS*
W. A. SHANNON
D. E. SPANGLER
B. J. STRADER
D. H. SUMMERS
C. E. WADDELL
R. L. BROOKSBANK, PROBLEM LEADER, *BUILDING 3505 FACILITY*
G. D. DAVIS
J. F. LOCKMILLER
S. A. McCOSH
J. T. WIGGINS

OPERATORS

J. C. BACON	A. J. FARMER
C. W. BOATMAN	J. M. GLASGOW
E. C. BRANTLEY	W. K. GOODMAN
J. H. BROCK	G. W. MARTIN
J. V. BROCK	J. W. MEADE
W. J. BRYAN	M. PAYNE
H. S. CALDWELL	C. T. RANKIN
J. R. COLLINS	J. W. REECE
H. D. CROSS	J. A. ROBERTS
B. G. DEVALL	C. L. SHEPHERD
W. DUNCAN	G. R. THOMPSON

FLUORIDE VOLATILITY PROCESS

R. B. LINDAUER,* GROUP LEADER
W. H. CARR, PROBLEM LEADER
S. MANN
F. W. MILES
R. G. NICHOL
J. B. RUCH
C. L. WHITMARSH
E. L. YOUNGBLOOD

TECHNICIANS
H. C. THOMPSON
V. R. YOUNG

OPERATORS

R. M. DUFF	W. T. HENRY
J. N. GIBSON	Z. R. McNUTT
M. C. HILL	A. V. WILDER

TOTAL PERSONNEL

TECHNICAL	161
SCIENTIFIC	101
ADMINISTRATIVE AND CLERICAL	30
TOTAL	292
SUMMER EMPLOYEES	9

*DUAL CAPACITY
[1]RESEARCH PARTICIPANT
[2]FOREIGN RESEARCH PARTICIPANT
[3]EMPLOYEE OF RADIATION APPLICATIONS, INC.
[4]CONSULTANT, U.T.

ORNL-2993
UC-10 — Chemistry-Separation Processes
for Plutonium and Uranium
TID-4500 (15th ed.)

INTERNAL DISTRIBUTION

1. C. E. Center
2. Biology Library
3. Health Physics Library
4-6. Central Research Library
7. Reactor Experimental Engineering Library
8-62. Laboratory Records Department
63. Laboratory Records, ORNL R.C.
64. A. M. Weinberg
65. L. B. Emlet (K-25)
66. J. P. Murray (Y-12)
67. J. A. Swartout
68. E. D. Shipley
69. M. L. Nelson
70-71. F. L. Culler
72. W. H. Jordan
73. A. H. Snell
74. A. Hollaender
75. R. A. Charpie
76. K. Z. Morgan
77. T. A. Lincoln
78. C. S. Harrill
79. C. E. Winters
80. H. E. Seagren
81. W. K. Eister
82. F. R. Bruce
83. M. E. Whatley
84. R. S. Livingston
85. C. D. Susano
86. C. P. Keim
87. H. E. Goeller
88. R. N. Lyon
89. R. B. Briggs
90. C. W. Hancher
91. P. M. Reyling
92. G. C. Williams
93. R. E. Blanco
94. W. E. Unger
95. D. E. Ferguson
96. A. T. Gresky
97. G. E. Boyd
98. J. L. Gabbard
99. M. J. Skinner
100. J. S. Drury
101. E. D. Arnold
102. C. E. Guthrie
103. J. W. Ullmann
104. K. B. Brown
105. R. S. Cockreham
106. J. C. Bresee
107. E. P. Wigner (consultant)
108. J. H. Rushton (consultant)
109. D. L. Katz (consultant)
110. I. Perlman (consultant)
111. H. Worthington (consultant)
112. C. E. Larson (consultant)
113-114. ORNL — Y-12 Technical Library, Document Reference Section

EXTERNAL DISTRIBUTION

115. Sylvania Electric Products, Inc.
116. Division of Research and Development, AEC, ORO
117-630. Given distribution as shown in TID-4500 (15th ed.) under Chemistry-Separation Processes for Plutonium and Uranium category (75 copies — OTS)

Reports previously issued in this series are as follows:

ORNL-268	Period Ending May 31, 1949
ORNL-467	Period Ending August 31, 1949
ORNL-530	Period Ending November 30, 1949
ORNL-663	Period Ending February 28, 1950
ORNL-763	Period Ending May 31, 1950
ORNL-846	Period Ending August 31, 1950
ORNL-936	Period Ending November 20, 1950
ORNL-1000	Period Ending February 20, 1951
ORNL-1061	Period Ending May 20, 1951
ORNL-1141	Period Ending August 20, 1951
ORNL-1311	Period Ending February 10, 1952
ORNL-1328	Period Ending May 20, 1952
ORNL-1385	Period Ending August 20, 1952
ORNL-1448	Period Ending November 20, 1952
ORNL-1494	Period Ending February 20, 1953
ORNL-1561	Period Ending September 30, 1953
ORNL-1708	Period Ending March 31, 1954
ORNL-1800	Period Ending September 30, 1954
ORNL-1881	Period Ending March 31, 1955
ORNL-2000	Period Ending September 30, 1955
ORNL-2079	Period Ending March 31, 1956
ORNL-2169	Period Ending August 31, 1956
ORNL-2392	Period Ending August 31, 1957
ORNL-2576	Period Ending August 31, 1958
ORNL-2788	Period Ending August 31, 1959